

---

**DEVELOPMENT OF AGRO-WASTES  
BASED UNFIRED EARTH BLOCKS  
TO IMPROVE INDOOR THERMAL  
COMFORT IN TROPICS**

---

**NUSRAT JANNAT**

A thesis submitted in partial fulfilment of the requirements  
of Liverpool John Moores University for the degree of  
Doctor of Philosophy

**April 2023**

---

## **Supervisory Team**

---

**Dr Rafal Latif Al-Mufti (Lead Supervisor)**

School of Civil Engineering & Built Environment, Liverpool John Moores University,  
Liverpool, United Kingdom

**Dr Badr Abdullah (Co-supervisor)**

School of Civil Engineering & Built Environment, Liverpool John Moores University,  
Liverpool, United Kingdom

**Prof Alison Cotgrave (Co-supervisor)**

School of Civil Engineering & Built Environment, Liverpool John Moores University,  
Liverpool, United Kingdom

**Dr Aseel Hussien (Co-supervisor-External)**

Department of Architectural Engineering, University of Sharjah, Sharjah, United Arab Emirate

---

## **Declaration**

---

I declare that this thesis is my original work, and it has not been submitted in part or whole for any other degree or qualification.

Name: **Nusrat Jannat**

Signature:



Date: 02/04/2023

---

## Abstract

---

This research aims to develop agro-waste based unfired earth blocks that are suitable for tropical climate. The samples were produced using eggshell (10, 20, 30, 40, and 50wt.%), sawdust (2.5, 5, 7.5, and 10wt.%), coconut husk (2.5, 5, 7.5, and 10wt.%), and walnut shell (5, 10, 15, and 20wt.%) separately and in combination. In this study, several physico-mechanical, durability, and thermal properties tests were conducted. Moreover, numerical computer simulation analyses on the thermal performance of the developed materials were performed. Additionally, the effect of three different particle sizes of sawdust ( $212 \mu\text{m} < x < 300 \mu\text{m}$ ,  $425 \mu\text{m} < x < 600 \mu\text{m}$ , and  $1.18 \text{ mm} < x < 2.00 \text{ mm}$ ) was investigated. The results of physico-mechanical properties tests showed that the density of the samples gradually decreased with increasing agro-wastes percentages in the mixture. Besides, eggshell and walnut shell addition reduced the linear shrinkage and capillary water absorption, whereas finer sawdust particles and coconut husk incorporation increased both. The individual inclusion of eggshell, sawdust, and coconut husk improved the strength of clay blocks; however, walnut shell had a negative impact on the strength. On the other hand, combining eggshell with other agro-wastes did not contribute to improving the strength. The highest compressive strength (CS) and flexural strength (FS) of air-dried samples were obtained when 40% eggshell (CS: 5.68 MPa, FS: 2.24 MPa), 2.5% coconut husk (CS: 4.78 MPa, FS: 2.14 MPa), and 2.5% sawdust (CS: 4.74 MPa, FS: 2.00 MPa) were individually used. The compressive strength of eggshell, coconut husk, and sawdust samples improved by around 40%, 18%, and 17%, respectively, while the flexural strength enhanced about 47%, 41%, and 32% over the reference sample. The investigation of durability tests revealed that when agro-wastes were added, erosion resistance improved compared to the reference sample. According to the thermal properties tests, thermal conductivity and volumetric heat capacity decreased with the addition of agro-wastes. The lowest conductivity was obtained for the 10% coconut husk sample (0.172 W/mK), followed by the 10% sawdust (0.185 W/mK) and the 50% eggshell (0.299 W/mK) samples. Furthermore, in the wall scale test, the sample walls made of coconut husk, sawdust, and eggshell outperformed the reference sample wall in terms of thermal resistance, with

improvements of around 48%, 35%, and 16%, respectively. This result was also supported by the numerical thermal simulation analyses, where the findings showed that coconut husk wall construction had a relatively lower (14.90 MWh) yearly energy consumption than sawdust (15.10 MWh), eggshell (17.70 MWh), and reference (18.90 MWh) walls. The overall findings of this study suggest that the incorporation of agro-wastes into clay blocks improved their properties, making them suitable for use as building construction material.

---

## Acknowledgements

---

First and foremost, I would like to praise and thank Allah, the Almighty, for the countless blessings He has showered upon me throughout my PhD journey. My heartfelt gratitude goes to my supervisors, Dr Rafal Latif Al-Mufti, Dr Aseel Hussien, Dr Badr Abdullah, and Prof. Alison Cotgrave for their constant support, consistent guidance, and advice during this research work. I would also like to thank all the technical staff, specially Tonny and Mal from the School of Civil Engineering and Built Environment, Liverpool John Moores University, for their invaluable assistance in manufacturing equipment and purchasing materials. Moreover, I would like to express my appreciation to Dr Alan Simm, Robert Allen, Nicola Browning, and Paul Gibbons from the Faculty of Science, Liverpool John Moores University, for all their help. Also, I would like to acknowledge the invaluable suggestions and support from Steve Wynn and Dr Muhammad Waseem Ahmad in accessing and learning IES software during the COVID-19 pandemic. Thank you so much, Dr Jeff Cullen and my lab mate, Karyono Karyono; without your great assistance, I would not have been able to complete the setup for my thermal test.

Finally, I would like to give special thanks to my entire family and friends for their encouragement and continuous support throughout the completion of this research work.

I thank them all from the heart.

---

## Table of Contents

---

<b>DECLARATION .....</b>	<b>I</b>
<b>ABSTRACT .....</b>	<b>II</b>
<b>ACKNOWLEDGEMENTS .....</b>	<b>IV</b>
<b>TABLE OF CONTENTS .....</b>	<b>V</b>
<b>LIST OF FIGURES .....</b>	<b>VIII</b>
<b>LIST OF TABLES .....</b>	<b>XII</b>
<b>LIST OF ABBREVIATIONS .....</b>	<b>XIII</b>
<b>NOMENCLATURES.....</b>	<b>XIV</b>
<b>LIST OF APPENDICES .....</b>	<b>XV</b>
<b>DISSEMINATION .....</b>	<b>XVI</b>
<b><i>Chapter 1</i> INTRODUCTION.....</b>	<b>1</b>
1.1 Introduction .....	1
1.2 Background .....	1
1.3 Problem Statement.....	6
1.4 Aim and Objectives .....	9
1.5 Impact of the Research .....	9
1.6 Structure of the Thesis.....	11
1.7 Summary of the Chapter.....	14
<b><i>Chapter 2</i> LITERATURE REVIEW.....</b>	<b>15</b>
2.1 Introduction .....	15
2.2 Earthen Construction.....	15
2.2.1 Unfired Earth Blocks .....	15
2.2.2 Earth/Soil Stabilisation.....	17
2.3 Agricultural wastes/Agro-wastes.....	19
2.3.1 Agro-wastes in Unfired Earth Blocks.....	20
2.3.1.1 Agro-waste Fibre .....	20
2.3.1.2 Agro-waste Powder .....	32
2.3.1.3 Others (Neither Fibre nor Powder) .....	36
2.3.1.4 Summary.....	38
2.4 Thermal Performances of Building Materials .....	69
2.4.1 Heat Transfer Through the Walls .....	69
2.4.2 Thermophysical Properties of the Building Materials.....	71
2.4.3 Thermal Performance Assessment of the Building .....	73
2.4.4 Previous Numerical Simulation Investigations on Building Wall Materials....	75
2.5 Tropical Climate Context .....	77
2.6 Research Gap and Contribution to the Novelty.....	78
<b><i>Chapter 3</i> RESEARCH METHODOLOGY AND MATERIALS.....</b>	<b>81</b>

3.1	Introduction .....	81
3.2	Research Methodology Outline.....	81
	3.2.1 Laboratory Tests.....	83
	3.2.2 Numerical Simulation.....	85
3.3	Materials.....	88
	3.3.3 Clay .....	90
	3.3.4 Eggshell.....	94
	3.3.5 Sawdust .....	97
	3.3.6 Coconut Husk.....	101
	3.3.7 Walnut Shell .....	104
3.4	Summary of the Chapter.....	108
<b>Chapter 4 EXPERIMENTAL EVALUATION (PART A-PHYSICO-MECHANICAL PROPERTIES TESTS) .....</b>		<b>110</b>
4.1	Introduction .....	110
4.2	Sample Preparation.....	110
4.3	Tests.....	113
	4.3.1 Density.....	113
	4.3.2 Linear Shrinkage .....	114
	4.3.3 Flexural Strength .....	114
	4.3.4 Compressive Strength.....	115
	4.3.5 Capillary Water Absorption .....	116
4.4	Results and Discussions (Phase 1) .....	117
	4.4.1 Density.....	117
	4.4.2 Linear Shrinkage .....	119
	4.4.3 Compressive and Flexural Strength.....	121
	4.4.4 Capillary Water Absorption .....	127
4.5	Results and Discussions (Phase 2) .....	129
4.6	Summary of the Chapter.....	135
<b>Chapter 5 EXPERIMENTAL EVALUATION (PART B-DURABILITY PROPERTIES TESTS) .....</b>		<b>138</b>
5.1	Introduction .....	138
5.2	Sample Preparation.....	138
5.3	Tests.....	139
	5.3.1 Ultrasonic Pulse Velocity (UPV) .....	139
	5.3.2 Geelong Drip .....	140
	5.3.3 Water Spray (Pressure Spray Method) .....	142
5.4	Results and Discussions .....	143
	5.4.1 UPV .....	143
	5.4.2 Geelong Drip .....	147
	5.4.3 Water Spray .....	149
5.5	Summary of the Chapter.....	152
<b>Chapter 6 EXPERIMENTAL EVALUATION (PART C-THERMAL PROPERTIES</b>		

<b>TESTS).....</b>	<b>153</b>
6.1 Introduction .....	153
6.2 Tests.....	153
6.2.1 Phase 1 (Thermophysical Properties of Individual Samples).....	153
6.2.2 Phase 2 (Thermal Properties of Wall Samples).....	154
6.3 Results and Discussions .....	159
6.3.1 Phase 1 (Thermophysical Properties of Individual Samples).....	159
6.3.2 Phase 2 (Thermal Properties of Wall Samples).....	163
6.4 Summary of the Chapter.....	172
<b>Chapter 7 EVALUATION OF INDOOR THERMAL COMFORT (NUMERICAL SIMULATION).....</b>	<b>173</b>
7.1 Introduction .....	173
7.2 Integrated Environmental Solutions Virtual Environment (IES-VE) Software .....	173
7.3 Physical Model and Simulation Conditions .....	176
7.4 Simulation Phases.....	178
7.4.1 Phase 01: Different Wall Materials .....	178
7.4.2 Phase 02: Different Thicknesses of the Wall.....	179
7.5 Results and Discussions .....	179
7.5.3 Effects of Materials' Thermophysical Properties .....	179
7.5.4 Effects of Wall Thickness Variation .....	183
7.6 Summary of the Chapter.....	186
<b>Chapter 8 CONCLUSIONS AND FUTURE WORK .....</b>	<b>188</b>
8.1 Introduction .....	188
8.2 Conclusions .....	188
8.3 Limitations of Research.....	190
8.4 Future Work .....	191
<b>REFERENCES.....</b>	<b>192</b>
<b>APPENDICES .....</b>	<b>222</b>

---

## List of Figures

---

<b>Figure 1.1:</b> Areas of earthen architecture distribution across the world (Auroville Earth Institute, 2009).....	3
<b>Figure 1.2:</b> An overview of the research objectives with links to the thesis chapters. ....	13
<b>Figure 2.1:</b> Cradle-to-cradle life cycle diagram of the earthen building materials [edited from Schroeder (2012)]. ....	16
<b>Figure 2.2:</b> Techniques for unfired earth blocks production: (a) cut blocks (b) adobe blocks and (c) compressed earth blocks (Auroville Earth Institute, 2009). ....	17
<b>Figure 2.3:</b> Different procedures for soil reinforcement (Hejazi et al., 2012). ....	18
<b>Figure 2.4:</b> Classification of agricultural waste (Pattanaik et al., 2019). ....	19
<b>Figure 2.5:</b> Heat transfer process across: (a) solid wall (Nayak and Prajapati, 2006) and (b) composite wall (Paraschiv et al., 2020). ....	71
<b>Figure 2.6:</b> Heatwave propagation through an opaque wall and representation of TL and DF. ....	75
<b>Figure 2.7:</b> Tropical climate zone (Feeley and Stroud, 2018). ....	78
<b>Figure 3.1:</b> Research plan flow chart. ....	87
<b>Figure 3.2:</b> XRF analyser machine, EDX-720 Shimadzu. ....	89
<b>Figure 3.3:</b> XRD instrument, Rigaku MiniFlex. ....	89
<b>Figure 3.4:</b> FEI Inspect S SEM. ....	89
<b>Figure 3.5:</b> Measurement of the thermal properties of the raw materials. ....	90
<b>Figure 3.6:</b> (a) Photograph and (b) SEM micrograph of RCP. ....	90
<b>Figure 3.7:</b> Compaction curve to determine the maximum dry density and optimum moisture content of RCP. ....	91
<b>Figure 3.8:</b> Particle size distribution curve of RCP. ....	92
<b>Figure 3.9:</b> XRD spectrum of RCP. ....	92
<b>Figure 3.10:</b> Global poultry egg-producing countries (FAO, 2020). ....	95
<b>Figure 3.11:</b> XRD spectrum of ESP. ....	96
<b>Figure 3.12:</b> (a) Photograph and (b) SEM micrograph of ESP. ....	97
<b>Figure 3.13:</b> Global wood harvest (FAO, 2020). ....	99
<b>Figure 3.14:</b> XRD spectrum of SDP. ....	99

<b>Figure 3.15:</b> (a) Photograph and (b) SEM micrograph of SDP. ....	101
<b>Figure 3.16:</b> Global coconut producing countries (FAO, 2020). ....	102
<b>Figure 3.17:</b> XRD spectrum of CHP. ....	103
<b>Figure 3.18:</b> (a) Photograph and (b) SEM micrograph of CHP. ....	104
<b>Figure 3.19:</b> Global walnut producing countries (FAO, 2020). ....	106
<b>Figure 3.20:</b> XRD spectrum of WSG. ....	107
<b>Figure 3.21:</b> (a) Photograph and (b) SEM micrograph of WSG. ....	107
<b>Figure 4.1:</b> Reference samples: (a) Prism samples in 40 mm × 40 mm × 160 mm mould and (b) Full prism samples after demoulding. ....	112
<b>Figure 4.2:</b> Sample preparation: (a) dry mixing and (b) wet mixing. ....	113
<b>Figure 4.3:</b> Flexural strength test: (a) schematic and (b) experimental. ....	115
<b>Figure 4.4:</b> Compressive strength test: (a) schematic and (b) experimental. ....	116
<b>Figure 4.5:</b> Capillary water absorption test: (a) schematic and (b) experimental. ....	117
<b>Figure 4.6:</b> Density test results (Phase 1). ....	118
<b>Figure 4.7:</b> Linear shrinkage test results (Phase 1). ....	120
<b>Figure 4.8:</b> Compressive strength (CS) and flexural strength (FS) test results (Phase 1). ....	122
<b>Figure 4.9:</b> XRD analysis: (a) ESP samples, (b) SDP samples, (c) CHP samples and (d) WSG samples. ....	124
<b>Figure 4.10:</b> Interaction between natural fibre and soil (Ghavami et al., 1999; Hejazi et al., 2012). ....	125
<b>Figure 4.11:</b> Percentage increase/decrease in Compressive strength (CS) and flexural strength (FS) compared to the reference sample (Phase 1). ....	127
<b>Figure 4.12:</b> Capillary water absorption results (Phase 1). ....	129
<b>Figure 4.13:</b> XRD analysis of ES samples. ....	130
<b>Figure 4.14:</b> XRD analysis of EC samples. ....	131
<b>Figure 4.15:</b> XRD analysis of EW samples. ....	131
<b>Figure 4.16:</b> Density results (Phase 2). ....	133
<b>Figure 4.17:</b> Linear shrinkage results (Phase 2). ....	133
<b>Figure 4.18:</b> Capillary water absorption results (Phase 2). ....	134

<b>Figure 4.19:</b> Compressive strength (CS) and flexural strength (FS) test results (Phase 2).....	134
<b>Figure 4.20:</b> Percentage increase/decrease in Compressive strength (CS) and flexural strength (FS) compared to the reference sample (Phase 2).....	135
<b>Figure 5.1:</b> Samples: (a) 100 mm × 100 mm × 100 mm and (b) 215 mm × 102 mm × 65 mm. ....	139
<b>Figure 5.2:</b> UPV test: (a) schematic and (b) experimental.....	140
<b>Figure 5.3:</b> Drip test: (a) schematic and (b) experimental.....	141
<b>Figure 5.4:</b> Water spray test: (a) schematic and (b) experimental. ....	142
<b>Figure 5.5:</b> UPV test results of stabilised clay blocks.....	144
<b>Figure 5.6:</b> UPV vs Compressive strength (CS): (a) ESP samples, (b) SDP samples, (c) CHP samples, (d) ES samples and (e) EC samples. ....	147
<b>Figure 5.7:</b> Samples after water spray test. ....	151
<b>Figure 6.1:</b> Thermal test: (a) 100 mm × 100 mm × 100 mm sample and (b) 215 mm × 100 mm × 100 mm. ....	154
<b>Figure 6.2:</b> Test setup for thermal transmittance measurement. ....	156
<b>Figure 6.3:</b> Configuration of the sample wall and position of the sensors.....	157
<b>Figure 6.4:</b> Correlation between thermal conductivity and density. ....	161
<b>Figure 6.5:</b> Thermographs of different wall surfaces: (a) Reference wall, (b) SDP wall, (c) CHP wall and (d) ESP wall. ....	164
<b>Figure 6.6:</b> Wall surface temperature profiles (72 hours): (a) hot side and (b) cold side. ....	166
<b>Figure 6.7:</b> Relative humidity measured (72 hours): (a) hot chamber and (b) cold chamber. .	168
<b>Figure 6.8:</b> Heat fluxes measured across all wall samples (72 hours). ....	170
<b>Figure 6.9:</b> Comparison of thermal properties of different walls with literature. ....	171
<b>Figure 7.1:</b> Building geometry.....	177
<b>Figure 7.2:</b> 10-year (2005-2015) average of maximum, mean, and minimum monthly air temperatures of the capital city of Bangladesh, Dhaka (Bangladesh Meteorological Department, 2018). ....	177
<b>Figure 7.3:</b> 10-year (2005-2015) average relative humidity and rainfall of the capital city of Bangladesh, Dhaka (Bangladesh Meteorological Department, 2018). ....	178

<b>Figure 7.4:</b> Outdoor and indoor temperatures for four different wall material constructions: (a) summer day and (b) winter day.....	181
<b>Figure 7.5:</b> Time lag for different wall constructions (summer day).....	182
<b>Figure 7.6:</b> Yearly energy consumption and DF of different wall constructions.....	183
<b>Figure 7.7:</b> TL for different thicknesses of C-7.5 wall construction (summer day). ....	184
<b>Figure 7.8:</b> Outdoor and indoor temperatures for different thicknesses of C-7.5 wall construction: a) summer day and (b) winter day.....	185

---

## List of Tables

---

<b>Table 2.1:</b> Different agro-waste additives for the production of unfired earth blocks. ....	41
<b>Table 2.2:</b> Tests carried out in previous research. ....	45
<b>Table 2.3:</b> Types of binders/chemical solutions used in previous research. ....	53
<b>Table 2.4:</b> Overview of research on agro-waste additives for the production of unfired earth blocks. ....	55
<b>Table 3.1:</b> Properties of RCP. ....	93
<b>Table 3.2:</b> Properties of ESP. ....	96
<b>Table 3.3:</b> Properties of SDP. ....	100
<b>Table 3.4:</b> Properties of CHP. ....	103
<b>Table 3.5:</b> Properties of WSG. ....	106
<b>Table 4.1:</b> Mix details (Phase 1). ....	111
<b>Table 4.2:</b> Mix details (Phase 2). ....	130
<b>Table 5.1:</b> Scale of assessment for Drip test. ....	141
<b>Table 5.2:</b> Erodibility indices for pressure spray erosion test. ....	143
<b>Table 5.3:</b> Drip test results of stabilised clay blocks. ....	148
<b>Table 5.4:</b> Water spray test results of stabilised clay blocks. ....	150
<b>Table 6.1:</b> Equipment used for thermal transmittance test setup and measurement. ....	157
<b>Table 6.2:</b> Average values and coefficient of variation (% in parenthesis) of thermophysical properties of sample blocks. ....	160
<b>Table 6.3:</b> Last 24 hours average test results and coefficient of variation (% in parenthesis) of the different wall samples. ....	169
<b>Table 6.4:</b> Calculated U-values and R-values of the different wall samples. ....	170
<b>Table 7.1:</b> Average values and coefficient of variation (% in parenthesis) of thermophysical properties of different materials used for simulation. ....	179
<b>Table 7.2:</b> Derived thermal properties and yearly energy consumption of different wall thicknesses of C-7.5 wall construction. ....	184

---

## List of Abbreviations

---

<b>ASTM</b>	American Society for Testing and Materials
<b>BS</b>	British Standard
<b>BS EN</b>	British Standard European Norm
<b>CHP</b>	Coconut Husk Powder
<b>CV</b>	Coefficient of Variation
<b>DF</b>	Decrement Factor
<b>ESP</b>	Eggshell Powder
<b>FAO</b>	Food and Agricultural Organisation
<b>GHG</b>	Greenhouse Gas
<b>HVAC</b>	Heating, Ventilation, and Air Conditioning
<b>IEQ</b>	Indoor Environmental Quality
<b>IES-VE</b>	Integrated Environmental Solutions Virtual Environment
<b>IS</b>	Indian Standards
<b>ISO</b>	International Organisation for Standardisation
<b>NZS</b>	Standards New Zealand
<b>RCP</b>	Red Clay Powder
<b>SD</b>	Standard Deviation
<b>SDP</b>	Sawdust Powder
<b>SEM</b>	Scanning Electron Microscope
<b>SLS</b>	Sri Lanka Standards Institution
<b>TL</b>	Time Lag/Thermal Lag
<b>TS</b>	Turkish Standards Institution
<b>UPV</b>	Ultrasonic Pulse Velocity
<b>WSG</b>	Walnut Shell Grit
<b>XRD</b>	X-Ray Diffraction
<b>XRF</b>	X-Ray Fluorescence

---

---

## Nomenclatures

---

$\alpha$	Thermal Diffusivity	$m^2/s$
$\lambda$	Thermal Conductivity	$W/mK$
$\rho$	Density	$kg/m^3$
$\rho C_p$	Volumetric heat capacity	$J/m^3K$
$\tau$	Thermal Effusivity	$Ws^{1/2}/m^2K$
$C$	Compressive Strength	$MPa$
$C_p$	Specific heat capacity	$J/kgK$
$C_w$	Capillary Water Absorption Coefficient	$kg/(m^2 \times min^{0.5})$
$f$	Flexural Strength	$MPa$
$F$	Ultimate Load	$N$
$M$	Mass	$kg$
$q$	Heat flux	$W/m^2$
$R$	Thermal Resistance	$m^2K/W$
$S_d$	Linear Shrinkage	$\%$
$U$	Thermal Transmittance	$W/m^2K$
$V$	Volume	$m^3$

---

---

## **List of Appendices**

---

<b>Appendix A:</b> Physical properties tests results of stabilised clay blocks. ....	222
<b>Appendix B:</b> Mechanical properties tests results of stabilised clay blocks. ....	228
<b>Appendix C:</b> UPV test results of stabilised clay blocks. ....	234
<b>Appendix D:</b> Water spray test results of stabilised clay blocks. ....	236
<b>Appendix E:</b> Thermal properties tests results of stabilised clay blocks.....	237
<b>Appendix F:</b> Posters on the development of agro-wastes incorporated unfired earthen material to improve indoor thermal comfort in tropics. ....	238
<b>Appendix G:</b> Peer-reviewed published journal papers. ....	242

---

## Dissemination

---

### Peer-reviewed published journal papers

- [1] **Jannat, N.**, Jeff, C., Abdullah, B., Latif Al-Mufti, R., Karyono, K. (2022) Thermophysical Properties of Sawdust and Coconut Coir Dust Incorporated Unfired Clay Blocks. *Construction Materials*, 2(4), 234-257. <https://doi.org/10.3390/constrmater2040016>
- [2] **Jannat, N.**, Latif Al-Mufti, R., Hussien, A. (2022) Eggshell and Walnut Shell in Unburnt Clay Blocks. *CivilEng*, 3(2), 263-276. <https://doi.org/10.3390/civileng3020016>
- [3] **Jannat, N.**, Latif Al-Mufti, R., Hussien, A., Abdullah, B. and Cotgrave, A. (2022) Influences of agro-wastes on the physico-mechanical and durability properties of unfired clay blocks. *Construction and Building Materials*, 318. <https://doi.org/10.1016/j.conbuildmat.2021.126011>
- [4] **Jannat, N.**, Latif Al-Mufti, R., Hussien, A., Abdullah, B. and Cotgrave, A. (2021) Influence of Sawdust Particle Sizes on the Physico-Mechanical Properties of Unfired Clay Blocks. *Designs*, 5(3). <https://doi.org/10.3390/designs5030057>
- [5] **Jannat, N.**, Latif Al-Mufti, R., Hussien, A., Abdullah, B. and Cotgrave, A. (2021) Utilisation of nut shell wastes in Brick, Mortar and Concrete: A review. *Construction and Building Materials*, 293. <https://doi.org/10.1016/j.conbuildmat.2021.123546>
- [6] **Jannat, N.**, Hussien, A., Abdullah, B. and Cotgrave, A. (2020) A comparative simulation study of the thermal performances of the building envelope wall materials in the tropics. *Sustainability*, 12(12). <https://doi.org/10.3390/su12124892>
- [7] **Jannat, N.**, Hussien, A., Abdullah, B. and Cotgrave, A. (2020) Application of agro and non-agro waste materials for unfired earth blocks construction: A review. *Construction and Building Materials*, 254. <https://doi.org/10.1016/j.conbuildmat.2020.119346>

## **Prizes won at Liverpool John Moores University**

- [1] Poster Competition Winner (mid and later-stage PGR category) at Postgraduate Research Festival 2022, Liverpool John Moores University.
- [2] Poster Competition Winner (mid and later-stage PGR category) at Postgraduate Research Festival 2021, Liverpool John Moores University.
- [3] The Best Potential Impact: First Place at Postgraduate Research Day 2021, Faculty of Engineering & Technology, Liverpool John Moores University.

## *Chapter 1*    **INTRODUCTION**

### **1.1 Introduction**

This chapter outlines the problem statement, research background, aim, and objectives of the study. Besides, the impact of the research is explained. The chapter ends with a brief overview of the structure of the thesis.

### **1.2 Background**

The Brundtland Report, published in 1987 by the World Commission on Environment and Development (WCED), underlined the importance of sustainable development as a key solution to critical global environmental problems. In the report, the term “sustainable development” was defined as “the development that meets the needs of the present without compromising the ability of future generations to meet their own needs” (Brundtland, 1987). Under this wide concept, the construction industry has the potential to play a significant role in addressing the three dimensions of sustainability, which include environmental, economic, and social issues (Glass, 2012; Gou and Xie, 2017; Goh et al., 2020). In light of this, sustainable buildings can be characterised as eco-innovative constructions that are both environmentally and economically sound while also fulfilling the social needs of people to improve their quality of life (Adamczyk and Dylewski, 2017). Currently, buildings are responsible for 30-40% of total global energy consumption and one-third of total greenhouse gas (GHG) emissions, which is closely related to their embodied energy and operational energy consumption (Chel and Kaushik, 2018; Omer and Noguchi, 2020). The energy used to produce building materials is referred to as embodied energy, whereas operational energy is the energy required to run a building’s heating, cooling, lighting, and other integrated systems (Dixit et al., 2010; Ramesh et al., 2010; Chastas et al., 2016). Though operational energy accounts for a larger portion of a building’s overall life cycle energy than embedded energy, researchers have acknowledged the importance of giving attention to embodied energy as well when implementing energy-efficient building design (Thormark, 2006; Dixit et al., 2013;

Monteiro et al., 2016). In the manufacturing process, materials with a high embodied energy consume more energy compared to materials with a low embodied energy, resulting in higher GHG emissions, particularly carbon dioxide (CO<sub>2</sub>) (Cabeza et al., 2013; Ding, 2014). Hence, the appropriate selection of materials may significantly contribute to decreasing the energy consumption of the building construction sector (González and Navarro, 2006; Thormark, 2006; Pacheco-Torgal and Jalali, 2012). Consequently, the development of sustainable building materials has emerged as the key research emphasis in order to lessen the environmental impact of the construction industry and achieve the goal of sustainable construction. Materials that are natural, environmentally friendly, energy-efficient, and not harmful to human health are recognised as sustainable materials in construction (Franzoni, 2011; Windapo and Ogunsanmi, 2014; Sahlol et al., 2021). Recently, following the philosophy of sustainable development, the concept of “green buildings” has evolved, intending to employ environmentally responsible natural materials that can reduce the energy consumption of the buildings (Spiegel and Meadows, 2010; Zuo and Zhao, 2014; Latha et al., 2015; Nowotna et al., 2019). In this context, the application of locally available vernacular materials and techniques in building construction is considered one of the prospective ways to support sustainable development both in rural and urban housing sectors (Fernandes et al., 2014; Dayaratne, 2018; Mazraeh and Pazhouhanfar, 2018; Kulshreshtha et al., 2020). Nevertheless, it is important to ensure the thermal efficiency of these materials by assessing their thermal properties (thermal conductivity, thermal diffusivity, specific heat capacity, thermal resistance, etc.) before using them in the building envelope. Moreover, mechanical strength and durability need to be evaluated to determine their suitability as load-bearing elements under unfavourable climate conditions.

Earth is one of the oldest and most traditional construction materials in our world, dating back to 8000 B.C. (Blondet and Garcia, 2004). The construction of earthen buildings is still common in some of the most hazardous regions in the world, including Africa, Latin America, the Middle East, the Indian subcontinent, and other parts of Asia and Southern Europe. Statistics from the United Nations Commission on Human Settlements (UNCHS) show that around 40% of the world’s population lives in buildings made of earth, and in developing countries, the number is even higher (Figure 1.1) (Auroville

Earth Institute, 2009). In developing countries, nearly half the population lives in earthen dwellings, where at least 30% of the population is in rural areas and the others are in urban or suburban areas (Vyncke et al., 2018).

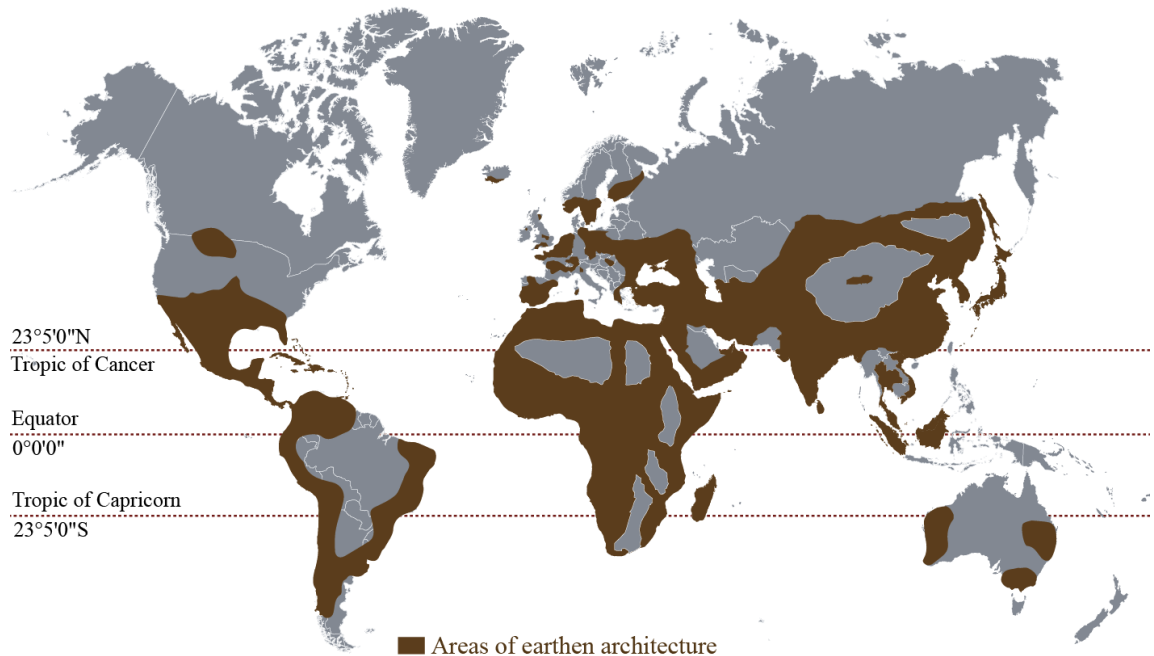


**Figure 1.1:** Areas of earthen architecture distribution across the world (Auroville Earth Institute, 2009).

Earth is considered an environmentally friendly choice due to its low carbon emission, low thermal conductivity, and good hygroscopic characteristics. There are also many other advantages of using unfired earthen building materials, such as regionally available resources, ease of construction, low cost, and ease of recycling with minimum environmental impacts (Chauhan et al., 2019; Valero et al., 2019; Kulshreshtha et al., 2020; Muheise-Araalia and Pavia, 2021). Besides, unfired bricks provide many advantages in comparison to traditional fired bricks and concrete masonry in terms of environmental effects. The energy-intensive processes of conventional fired brick and concrete masonry production lead to high levels of CO<sub>2</sub> emissions (Latawiec et al., 2018; Nath et al., 2018). One of the key sources of global CO<sub>2</sub> emissions (around 6-7%) is reported as cement production (Aprianti S, 2017; Sousa and Bogas, 2021; Wojtacha-Rychter et al., 2021), which contributes to 60% of global warming (Rashad, 2015) along with other GHG. The mean energy consumed per tonne of fired bricks is calculated at

706 kWh, and CO<sub>2</sub> emission per tonne is estimated at 0.15 tonne (Zhang et al., 2018b). On the other hand, unfired brick requires approximately 99% less energy for the manufacturing process compared to concrete (Zak et al., 2016) and has less embodied energy (0.45 MJ/kg) than fired brick (3 MJ/kg) (Heath et al., 2009). However, some of the disadvantages of earthen construction are the lack of strength, durability, and vulnerability to erosion by rain (Arooz and Halwatura, 2018; Costa et al., 2018; Anysz and Narloch, 2019; Kulshreshtha et al., 2020; Lin et al., 2021). Due to these drawbacks, the use of earthen building materials in the modern construction sector has been ignored for many years (Danja et al., 2017; Kulshreshtha et al., 2020). Although it is important to recognise the contribution that modern clay brick manufacturing and other modern earthen construction materials make to improve the overall properties of earthen structures, the environmental effects of these methods are equally important to consider. Currently, in order to meet the comfort standards needed today, building construction with earth is regaining its prominence in industrialised countries as well and becoming an integral part of “green thinking” (Lekshmi et al., 2017). Therefore, comprehensive articles on this issue have been published over the last decades. Many studies have presented that due to its popularity and cost-effectiveness, improving earthen building materials for large usage would seem to be a technique more likely to succeed than replacing them with new modern materials or using costly and inefficient methods (Goodbun, 2016; Van Damme and Houben, 2018; Kulshreshtha et al., 2020). One possible solution that has been tried over the decades to overcome the drawbacks of earthen materials is the “stabilisation method” which involves the use of additives to improve their properties. Fibrous material such as straw has long been used by local home brick manufacturers to enhance the strength of mud bricks (Odeyemi et al., 2017). However, they were unable to conduct basic experimental research on the optimisation and balance of materials. Hence, researchers have developed various additives and stabilisation methods to increase its performances like strength, aggregate stability, and resistance to water absorption (Laborel-Preneron et al., 2016; Al-Fakih et al., 2019; Shubbar et al., 2019; Gupta et al., 2020; Jannat et al., 2020). Different stabilisers have diverse impacts on the strength and durability of earthen materials depending on their chemical compositions and properties. Researchers have suggested several types of man-made stabilisers such as cement, lime, plastic waste, synthetic fibre, etc. to enhance the

properties of the earthen material (Onyelowe and Okafor, 2012; Danso et al., 2015a; Van Damme and Houben, 2018; Jesudass et al., 2021; Karrech et al., 2021). Though cement is a source of CO<sub>2</sub> emissions from these stabilisers, it is the most commonly used one (Jayasinghe and Kamaladasa, 2007; Barcelo et al., 2014; Guettatfi et al., 2021). The use of man-made stabilisers, however, lessens the “green” attributes of earthen materials as it increases levels of embodied energy and reduces the possibility of recycling the demolished waste. To overcome this, the utilisation of natural materials for earth stabilisation is becoming widespread among researchers (Vilane, 2010; Udawattha et al., 2018; Subramanian et al., 2021; Turco et al., 2021).

On the other hand, agricultural waste management has become one of the most important global environmental concerns. Agricultural wastes or agro-wastes are the residues generated from the production and processing of raw agricultural products such as crops, fruits, poultry, dairy products, etc. (Obi et al., 2016). In many developing countries, large quantities of agricultural waste are not efficiently managed and utilised, which eventually poses a threat to the environment (Broitman et al., 2018; He et al., 2019). However, several recent studies have presented that these agro-wastes have a high potential for application in the manufacture of building construction materials on account of their good physico-mechanical properties (Ogah and James, 2018; Paul et al., 2019), but there has been little work carried out to utilise these agro-wastes in the production of building materials, particularly in earthen matrix (Laborel-Preneron et al., 2016; Al-Fakih et al., 2019; Jannat et al., 2020). As alternative material studies are now clearly a priority for lowering energy consumption and minimising waste management difficulties, several studies have shown that materials manufactured using agro-wastes can meet this environmental challenge (Amziane and Sonebi, 2016; Pickering et al., 2016; Peñaloza, 2017; Muthuraj et al., 2019). Agro-waste materials are sustainable, primarily processed locally, and have the ability to act as an effective means of CO<sub>2</sub> processing (Martinez, 2017; Silva et al., 2018; Sinka et al., 2018). Hence, the application of these materials in the building industry has gained global significance (Jones and Brischke, 2017; Brunklaus and Riise, 2018; Sandak et al., 2019). Moreover, their use in the building construction sector can lead to a large decrease in waste production. Consequently, the proposed research work aims to utilise agro-wastes to produce environmentally friendly

unfired earth blocks with improved thermal properties for rural housing in the tropics, which ultimately reduce energy consumption. Additionally, the presence of agro-wastes in the blocks improves their other physico-mechanical and durability properties. Furthermore, the development of waste-incorporated unfired earth blocks is expected to support the commercial manufacturing potential of economically viable building materials for low-cost housing that could provide a sustainable replacement for conventional materials (concrete, fired bricks, etc.). Because of the use of agro-wastes as the key stabilising agent, the manufacturing cost of unfired earth blocks is likely to be lower than the other comparable building materials. Also, these agro-wastes incorporated unfired earth blocks could be pulverised and mixed with new biomass at the end of life to produce new unfired earth blocks instead of ending up in landfills. Therefore, the added environmental benefits of using agro-wastes would further improve its regional sustainability profile, as sustainability can only be accomplished when the building construction sector uses renewable or recycled materials from construction wastes (Serrano et al., 2016).

### **1.3 Problem Statement**

Indoor environmental quality (IEQ) is one of the major health concerns in the world, as people spend about 80–90% of their time at home or in other public indoor environments (Šujanová et al., 2019). Among various variables of IEQ, thermal comfort is a key component that is influenced by design techniques and materials used in buildings (Gou et al., 2018; Radivojević and Đukanović, 2018). Hence, it has become a priority to find ways to improve IEQ by using safe building materials with low environmental impact. Depending on how materials respond to climate, the human settlement environment on earth can be divided into two areas: the heat preservation priority climate zone and the heat insulation priority climate zone. In the heat preservation priority climate, building materials are used to prevent internal heat dissipation (cold zone) or the acquisition of external heat (dry hot zone), as there is a great difference in temperature between indoors and outdoors. The heat insulation priority climate zone refers to the tropical and subtropical regions where high humidity, temperatures, and solar radiation are the major stresses. Therefore, the materials in these regions are mainly used to solve sun shading

and heat insulation issues (Zhang et al., 2017; Nguyen et al., 2019). According to the State of the Tropics survey, half of the world's population will live in tropical areas by 2050, and consequently, the demand for indoor thermal comfort in these areas is significantly rising due to the proliferation of residents (Rodriguez and D'Alessandro, 2019). Rodriguez and D'Alessandro (2019) presented that the scientific literature on indoor thermal comfort in buildings is mostly conducted in Tropical Asia, with the majority of studies focusing on Singapore and Malaysia. But there is very little research available in highly populated countries such as India, Bangladesh, Indonesia, the Philippines, Vietnam, and Ethiopia. Studies on tropical regions revealed that dwellings constructed with vernacular materials such as stone, earth, wood, bamboo, straw, etc. perform better than modern materials in terms of thermal comfort (Rijal et al., 2010; Samuel et al., 2017; Dayaratne, 2018). Vernacular materials are locally available materials that are common in rural areas due to their availability and affordability. These materials require a less energy-intensive and transport-free manufacturing process, resulting in lower CO<sub>2</sub> emissions. Also, they are often renewable and biodegradable organic materials with a “cradle-to-cradle” life cycle (Fernandes et al., 2014; Sayigh, 2019). Some authors concluded that vernacular materials should be improved to meet certain conditions, such as exposure to subsidence, water intrusion, etc. (Dong et al., 2015; Motealleh et al., 2018; Benslimane and Biara, 2019). Hence, recently, a higher priority has been given to the durability issues of these materials. For example, modern technology has been used over time to improve the strength of raw earthen materials by transforming them into compact blocks. Additionally, water resistance is further improved by mixing cement with earth during the manufacturing process. Such compressed mud blocks generate 3-5 times less energy than traditional fired bricks. However, they are reduced in thickness compared to the typical mud block, eventually limiting their thermal insulation properties. Rammed earth and mud brick both have low insulation values, and they rely on 300 mm or more thicknesses to increase thermal lag (Auroville Earth Institute, 2009; Soebarto, 2009). Some researchers have presented that modern construction using local materials performs better than modern materials in terms of economy, energy use, and environmental quality (Mohebbi and Kazemi, 2014; Muazu and Alibaba, 2017; Jörchel, 2019).

The energy efficiency of buildings has become a key component of global sustainable

housing development, guiding researchers to develop novel building materials. Earth is an ideal available natural material that can cyclically regulate the relative humidity of indoor air by adsorbing additional humidity and releasing it when the temperature rises and the air becomes drier. Because of this excellent hygroscopic behaviour, earthen materials can function as natural air conditioners (Madhumathi et al., 2014; Fouchal et al., 2015; Chauhan et al., 2019). Despite the advantages, nowadays, earthen materials are being replaced by modern materials (fired brick and concrete) in rural areas due to some issues with earthen construction, such as lack of strength, durability and massive wall thickness, as well as the influence of modernity and status issues in the social hierarchy (Pacheco-Torgal and Jalali, 2012; Kulshreshtha et al., 2020). Hence, the question arises of how to achieve a comfortable indoor environment in rural housing. Several research projects have determined the properties of earthen masonry using various stabilisers to address some of these issues. However, limited study has been conducted on using natural stabilisers with earthen masonry to improve their thermal properties (Danso et al., 2015a; Laborel-Preneron et al., 2016; Al-Fakih et al., 2019; Jannat et al., 2020). Therefore, rigorous investigations are required to assess the potential utilisation of natural stabilisers to develop novel unfired earthen materials in order to save earthen building construction practices and for the betterment of the health of rural inhabitants.

In summary, the research problems are as follows:

- Rejection of traditional earthen building construction and acceptance of modern building materials in rural housing, resulting in negative environmental impacts.
- Inadequate investigation on building construction materials and indoor environmental comfort in tropical rural housing.
- A lack of research on the utilisation of agro-wastes for the production of thermally improved earthen building construction materials.

The following research question was formulated based on the research problems:

**“Which agro-wastes incorporated earthen materials are most efficient at providing indoor thermal comfort in tropical rural housing?”**

## 1.4 Aim and Objectives

The following aim was devised to answer the research question:

*“To investigate the properties of unfired earth blocks incorporating agro-wastes to produce thermally enhanced materials for sustainable rural housing construction in the tropics.”*

In order to achieve the aforementioned aim, the following objectives were set:

1. Identify the available vernacular building materials in the tropics.
2. Assess the characteristics of agro-wastes that have the potential to be used in the production of building materials.
3. Investigate the physico-mechanical, durability, and thermal properties of agro-wastes blended unfired earth blocks in the laboratory at the individual sample level.
4. Examine the thermal transmittance and resistance of small walls constructed with well-performing samples from the physico-mechanical, durability, and thermal properties tests using an adapted hot box method in the laboratory.
5. Analyse the thermal performance of agro-wastes incorporated unfired earth blocks (developed in the laboratory) under tropical climate conditions using simulation software.
6. Evaluate the optimum agro-waste quantity in the earthen matrix by analysing the laboratory and numerical simulation results and propose the most potential agro-waste incorporated unfired earth block that complies with current building material design specifications.

## 1.5 Impact of the Research

This present research would be supportive of particular groups, including building materials manufacturers, building and housing providers (housing associations, agencies, private companies, individuals, etc.), agricultural industries, and academic communities.

- This research will guide manufacturers of building materials to produce clay blocks with agro-wastes at a low cost in compliance with standard requirements by the way of comprehensive analysis. This research gives details on the procedure of manufacturing the agro-wastes incorporated clay blocks. Besides, it provides information on the optimal mix ratio for developing thermally improved clay blocks, which the manufacturer may employ.
- This work will be helpful to agricultural industries because their residues and by-products will be consumed and utilised to produce value-added materials. Consequently, this will significantly reduce waste generation and provide an effective solution to the waste management problem.
- The outcome of this study will be highly beneficial to building and housing providers (housing associations, agencies, private companies, individuals, etc.) as they will have technically developed low-cost materials as an alternative to expensive conventional materials. This will assist them in providing more affordable, low-cost housing to the people, especially those with low income.
- This study will be useful for academics who are interested in the field of building materials and construction by serving as a reference, particularly for agro-waste-based unfired clay block production. This will also guide them to investigate further in the area of low-cost and environmentally friendly building material production. Besides, this work may motivate prospective researchers to identify other potential agro-wastes that can be employed in the manufacture of unfired clay blocks.

The manufacturing of unfired earth blocks with agro-wastes requires no firing or traditional costly binders (cement, lime, etc.), making it a cheaper building material, and the utilisation of agro-wastes/by-products from local sources provides environmental advantages. This work thus holds significant technical, socio-economic, and environmental value.

## 1.6 Structure of the Thesis

The detailed structures of the thesis are as follows:

- **Chapter 1** introduces the problem statement and discusses the background of the research on which it is based. It further outlines the aim, objectives, and impacts of the research. The chapter ends with a brief overview of the structure of the entire thesis.
- **Chapter 2** aims to present a comprehensive review of the current “state of knowledge” on unfired earth block production utilising agro-wastes in order to identify research gaps. This chapter also summarises information on the production of unfired earth blocks, soil stabilisation, thermophysical properties, and thermal behaviour of building materials.
- **Chapter 3** outlines the research methodology and methods used in this study. Additionally, it gives a detailed description of the basic characterisation (physical properties, chemical compositions, mineralogical phases, and surface morphology) of the raw materials (clay and agro-wastes) used in this work.
- **Chapter 4** describes the experimental programme for determining the physico-mechanical properties (density, linear shrinkage, capillary water absorption, flexural strength, and compressive strength) of the produced clay samples. It also includes details of the mix proportions and sample preparation. Moreover, this chapter provides a comprehensive discussion of the test results.
- **Chapter 5** presents the durability tests carried out on the agro-wastes stabilised samples. It explains the results of durability against water tests such as the Geelong drip test and water spray test, as well as the non-destructive UPV test.
- **Chapter 6** reports the thermal experiments conducted on the various clay samples to compare the thermal performance of the best-performing samples from each agro-waste type. This chapter discusses all the test methods and findings for both individual and wall samples.
- **Chapter 7** details the numerical computer simulation analyses performed for

different types of materials under tropical climate conditions (Dhaka, Bangladesh) using the Integrated Environmental Solutions Virtual Environment (IES-VE) programme. The physical modelling of the space, simulation conditions, and data used as simulation inputs are provided in this chapter. Besides, it contains the findings of the simulation analyses on how to reduce indoor temperature fluctuation and energy consumption of the space.

- **Chapter 8** is the final chapter of the thesis, which summarises the major findings of the investigations and the limitations of the research. In addition, this chapter recommends areas where further research should be conducted in the future.

Figure 1.2 illustrates an overview of the research objectives linked to the structure of the work.

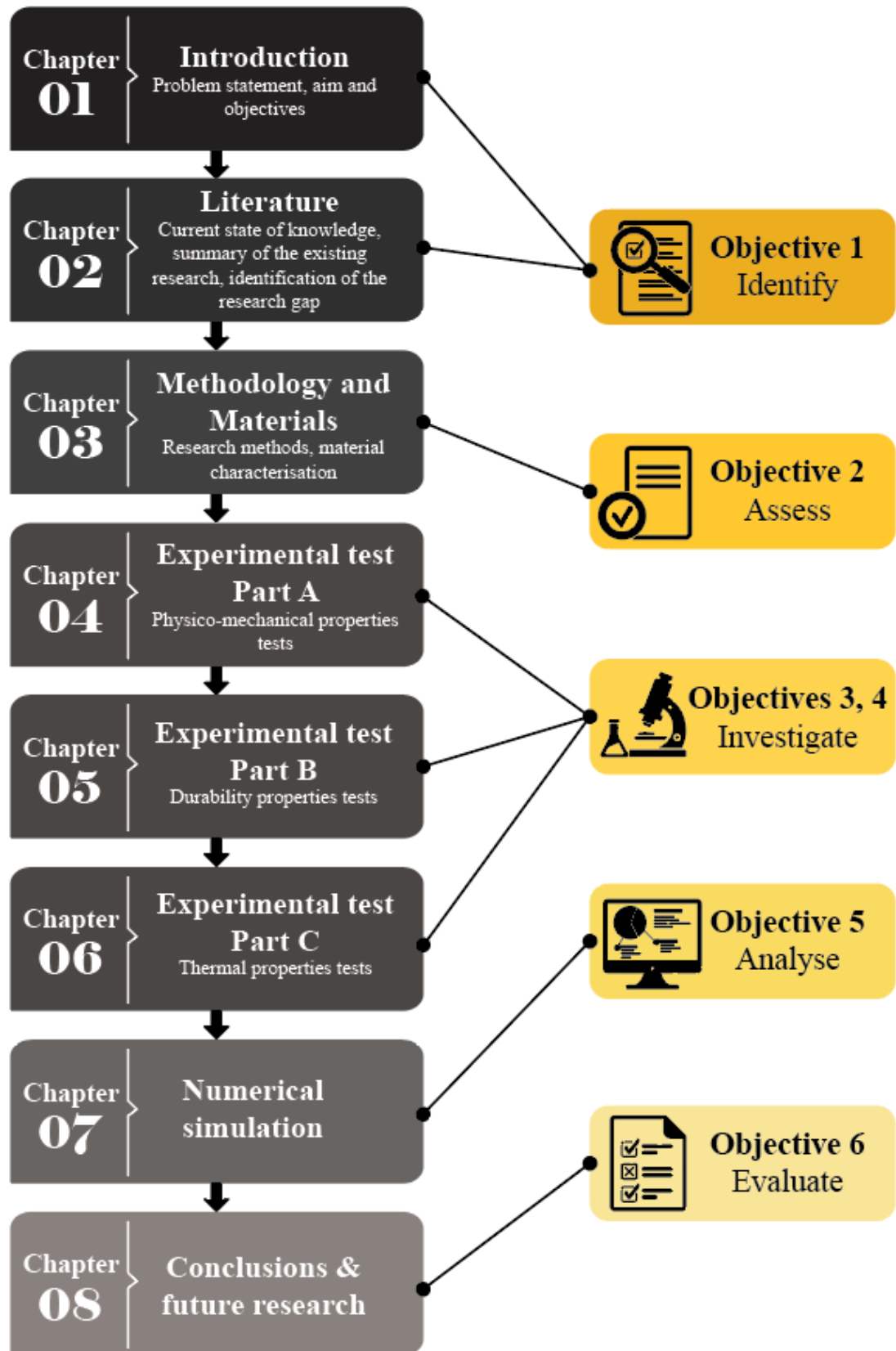


**Figure 1.2:** An overview of the research objectives with links to the thesis chapters.

## **1.7 Summary of the Chapter**

This chapter of the thesis first introduced the background and the problem statement of the study. It further discussed the aim, objectives, impact, and structure of the thesis. The background to the study explained the overall context in which the research is centred, and the problem statement defined the importance of the study. This research aimed to contribute to the knowledge in the field of building materials construction by investigating the different physico-mechanical, durability, and thermal properties of the laboratory-based agro-wastes blended unfired earth blocks. Finally, the entire framework of the thesis was defined in order to explain the courses of the analysis.

## *Chapter 2*    **LITERATURE REVIEW**

### **2.1 Introduction**

This chapter highlights a review of the existing volume of work on the production of unfired earth blocks incorporating different agro-wastes. Besides, it addresses current research thinking and knowledge to build the theoretical background of this study. This chapter also contains a source of knowledge for the production of unfired earth blocks, soil stabilisation, thermophysical properties, and thermal behaviour of building materials. This review, consequently, aims to provide a comprehensive understanding of the current “state of knowledge” and identify the research gap before developing the concept of this current study.

### **2.2 Earthen Construction**

#### ***2.2.1 Unfired Earth Blocks***

Buildings use energy in the form of embodied and operational energy during various phases of their life cycle (production, construction, use, and demolition). Operational energy is required to keep buildings comfortable through running systems such as heating, cooling, lighting, ventilation, and other appliances, and it is directly related to the energy consumption patterns of the inhabitants. On the other hand, embodied energy is associated with the production of building materials. Operational energy use can be minimised by improving the building design and efficiency of the systems. However, adopting this approach to reduce operational energy can lead to a considerable increase in embodied energy. This is due to the fact that actions like adding insulating materials to limit heat gain or loss, installing internal or exterior shading systems to block out undesirable solar heat gain, etc. increase material use in the building, consequently increasing overall embodied energy. However, embodied energy can be reduced by using materials with lower embodied carbon, recycled or reusable materials, and locally sourced materials (Ibn-Mohammed et al., 2013; Karimpour et al., 2014; Praseeda et al.,

2016; Amaral et al., 2020). In this context, earthen materials can be an excellent choice since they provide several advantages in terms of sustainability, including minimal need for transportation because of their local availability and less energy requirement in processing, resulting in lower embodied energy and CO<sub>2</sub> emissions. Additionally, they are renewable and biodegradable natural materials that may significantly improve a building's environmental performance by employing a “cradle-to-cradle” life cycle approach (Figure 2.1) (Schroeder, 2012).

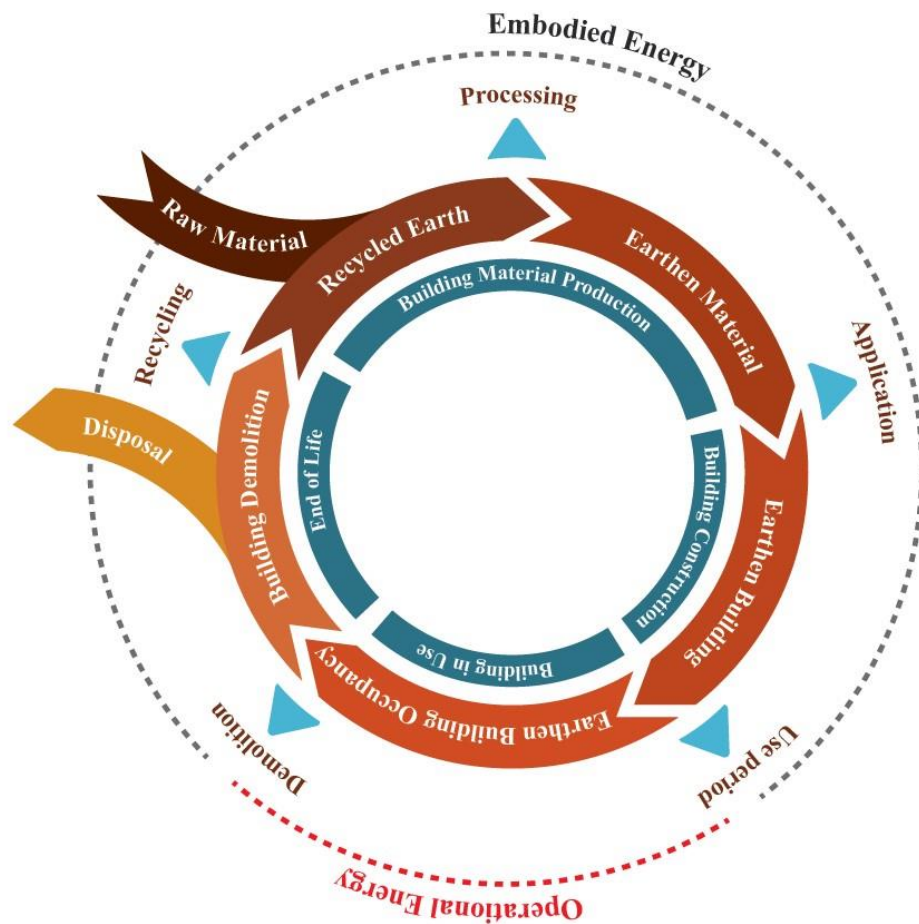


**Figure 2.1:** Cradle-to-cradle life cycle diagram of the earthen building materials [edited from Schroeder (2012)].

The Auroville Earth Institute (2009) reports that earthen building construction techniques have been the predominant mode of construction since the beginning of human history. It is an abundant natural resource that can be used flexibly. A building can be constructed of earth in whole or in part and can be monolithic or made of different elements such as blocks, infills, renders, etc. Unfired earth blocks are made of earthen materials and are

also referred to as earth masonry. These blocks are similar to other masonry systems, which are air-dried after manufacturing to minimise shrinkage and improve strength. Unfired earth blocks can be classified into three categories, “adobe blocks”, “compressed earth blocks”, and “cut blocks” based on the method used to shape the blocks (Figure 2.2).

**Adobe blocks:** Traditionally, adobe mud blocks are hand-shaped or made in wooden moulds and left to dry under the sun after casting. In order to improve the mechanical properties, straw, dung, and lime are frequently used as binders in the blocks. In South America, Africa, Eastern Europe, and Asia, buildings built with adobe blocks are popular.

**Compressed earth blocks:** Compressed earth blocks are made using a manual or motorised press. The method includes moistening the soil with water or stabilisers and then pouring it into a compacting steel press for compaction.

**Cut blocks:** These blocks are made by cutting earth and are used like bricks in areas where the soil is cohesive and has carbonate concretions. These examples are typically found in tropical areas with abundant laterite soils.

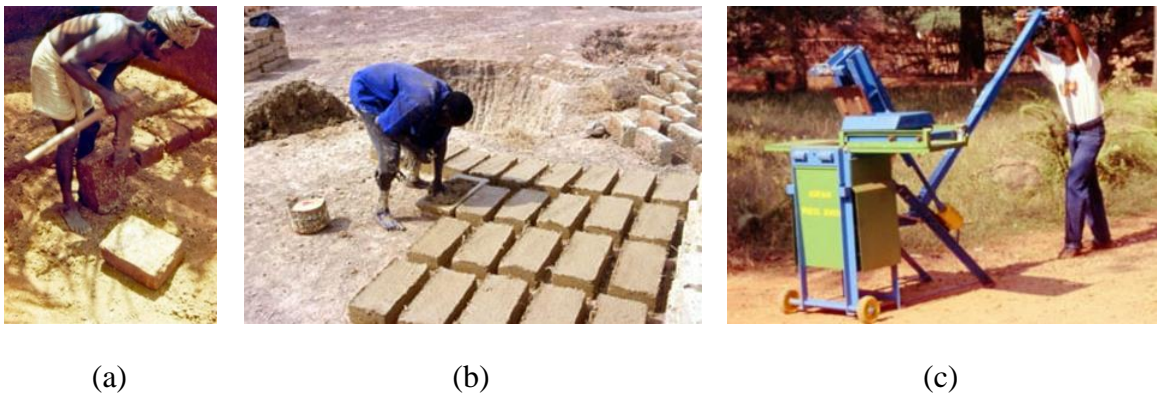


**Figure 2.2:** Techniques for unfired earth blocks production: (a) cut blocks (b) adobe blocks and (c) compressed earth blocks (Auroville Earth Institute, 2009).

### 2.2.2 *Earth/Soil Stabilisation*

Earth/soil stabilisation refers to the method used to enhance the properties of soil with natural or synthetic additives. The techniques of soil stabilisation have been carried out

for thousands of years. The Mesopotamians and Romans distinctly revealed that the capacity of roads to carry more traffic could be enhanced by combining the poor or soft soils with a stabiliser (pulverised limestone or calcium) (Masuka et al., 2018). On the other hand, the presence of arbitrarily oriented plant roots in the soil could improve the strength and stability of natural slopes (Morgan and Rickson, 2003; Gowthaman et al., 2018). It is evident from the Bible (Exodus chapter 5, verses 6-9) that the fibre reinforcement perception was recognised, dating back to the fifth and fourth millennia B.C. (Rawal et al., 2010). The Great Wall of China and the Ziggurats of Babylon are the two earliest examples of earthen structures using branches of trees, straws, and reeds as tensile elements for reinforcement (Moorey, 1999). Hence, in modern history, attempts have been made to use plant aggregates for soil stabilisation as an imitation of the past. Soil stabilisation methods which can be classified into several categories (Figure 2.3) based on reinforcing performance and the utilisation of natural stabilisers have attracted the growing attention of researchers due to their low environmental impact (Hejazi et al., 2012).

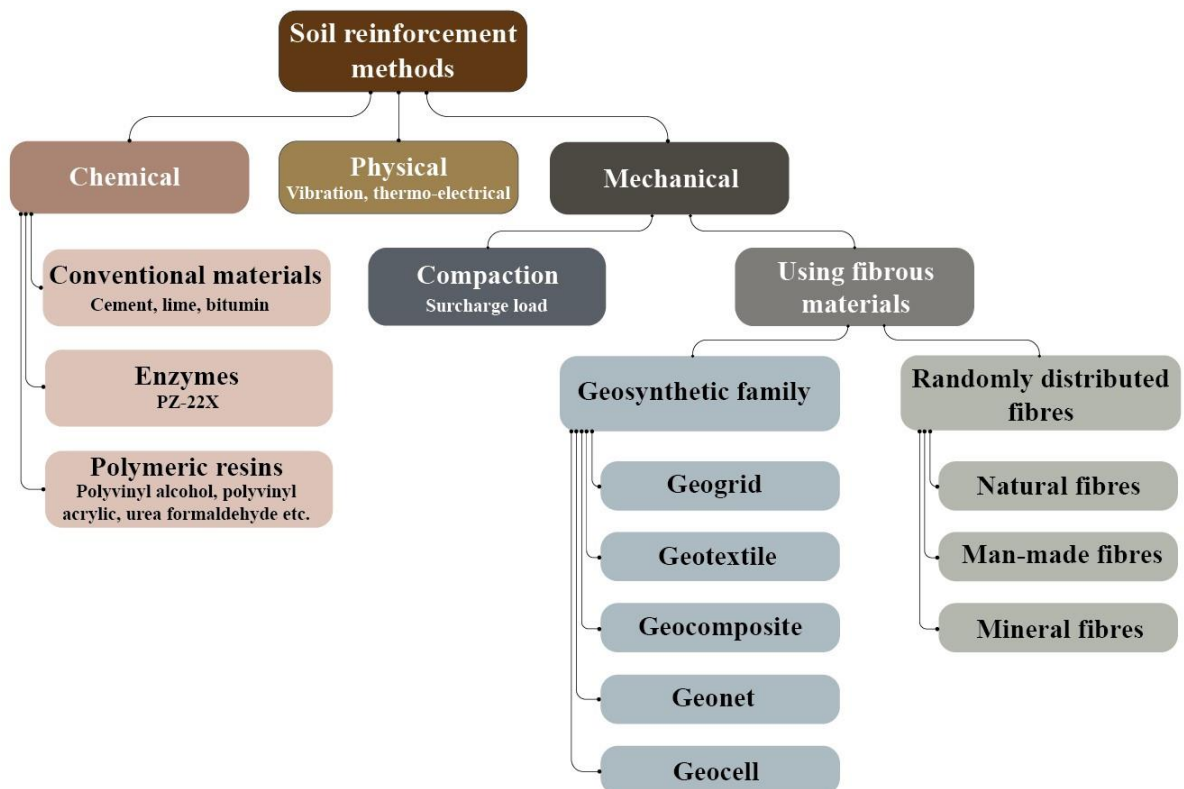


**Figure 2.3:** Different procedures for soil reinforcement (Hejazi et al., 2012).

### 2.3 Agricultural wastes/Agro-wastes

The residues from the cultivation and processing of raw farm products, including fruits, vegetables, meat, poultry, dairy products, and crops are known as “agricultural wastes” or “agro-wastes”. In other words, all undesirable materials generated by agricultural activities are known as agro-wastes. Their composition depends on the method and type of farming and can be in liquid, slurry, or solid form. Broadly, agricultural wastes can be divided into four categories: crop residues, agro-industry wastes, livestock wastes, and food wastes (Figure 2.4). It is projected that approximately 998 million tonnes of agro-waste are generated annually (Agamuthu, 2009). Improper disposal of these materials may result in undesirable environmental and health impacts. Therefore, currently, the proper management of these agro-wastes and by-products is a crucial necessity for the benefit of the environment.

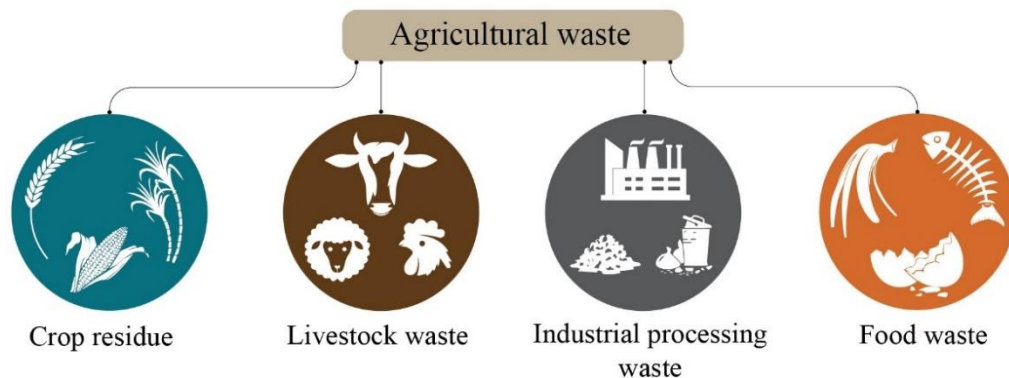


**Figure 2.4:** Classification of agricultural waste (Pattanaik et al., 2019).

Agricultural wastes consist of lignocellulosic composition. They are popular for use in reinforcement in composite materials because of their good mechanical properties and lower density compared to other inorganic materials. However, the hydrophilic nature of these wastes is one of the barriers to specific applications (Petroudy, 2017). These agro-wastes are also used for fertiliser application, anaerobic digestion, adsorbents in the elimination of heavy metals, pyrolysis, animal feed, and direct combustion (Obi et al., 2016). As the increasing need for sustainable development has driven researchers to focus their work on the use of waste or recycled materials in the construction sector, it is, therefore, worthwhile and necessary to investigate the concept of utilising potential agro-

wastes for the manufacture of building materials.

### ***2.3.1 Agro-wastes in Unfired Earth Blocks***

This section reviews the previous studies on agro-wastes incorporated unfired earth blocks and highlights five different properties (density, water absorption, compressive strength, flexural strength, and thermal conductivity) that were tested in most of the studies to evaluate their suitability for construction purposes. The findings from the literature review are very important since they could assist in determining the expected performance of agro-wastes incorporated samples. Table 2.1 lists all the articles included in this review as well as the types of waste materials, sources, and research locations. Besides, Table 2.2 specifies the different tests, Table 2.3 identifies the type of binders used in the previous research, and Table 2.4 details the results of the different tests. The agro-waste materials studied in the literature are categorised into three groups: agro waste fibre, agro waste powder and others (neither fibre nor powder).

#### **2.3.1.1 Agro-waste Fibre**

Binici et al. (2005), Vega et al. (2011), Ashour et al. (2015), Parisi et al. (2015), Abanto et al. (2017), Türkmen et al. (2017), El Azhary et al. (2017), Statuto et al. (2018), Wang et al. (2019), Mohamed (2013), De Castrillo et al. (2021), and Koutous and Hilali (2021) evaluated the impact of straw fibre incorporation on the engineering properties of unfired earth bricks. Various percentages and lengths of straw that were incorporated to produce the earth blocks were as follows: 2.5wt% (Binici et al., 2005), 25 and 33.3vol% (Vega et al., 2011), 3wt% (Ashour et al., 2015), 0.64wt% (Parisi et al., 2015), 1.5-3.7wt% (Abanto et al., 2017), 1mass% (Türkmen et al., 2017), 2-5wt% (El Azhary et al., 2017), 3wt% (Statuto et al., 2018), 5, 10 and 15wt% (Wang et al., 2019), 0.5, 1, 1.5wt% (Mohamed, 2013), 0.75% (Koutous and Hilali, 2021), 30, 40, 50, 60, 70 vol% (De Castrillo et al., 2021). Fibre length: 2-3 mm (Wang et al., 2019), lower than 10 mm (Parisi et al., 2015), 20 mm (El Azhary et al., 2017; Türkmen et al., 2017), 40 mm (Ashour et al., 2015), 50-100 mm (Vega et al., 2011), 15-25 mm (Mohamed, 2013). The analysis illustrated that the compressive strength, density, and thermal conductivity of the unfired samples decreased with the increased amount of straw fibre (Ashour et al., 2015; Abanto et al.,

2017; El Azhary et al., 2017; De Castrillo et al., 2021). However, Koutous and Hilali (2021) found the compressive strength of the stabilised sample was higher (2.74 MPa) than the unstabilised samples (2.03 MPa). The test results of Mohamed (2013) indicated that the water absorption, swelling potential, maximum dry density, and shrinkage limit of the samples decreased (up to 1% fibre), while the shear strength as well as the tensile strength increased with the addition of hay fibre. The maximum tensile strength was 0.07 kg/cm<sup>2</sup> (1% hay fibre), representing a 30% increase in strength compared to the fibre-free sample. Binici et al. (2005) found that at 3% fibre content wheat (0.30 W/mK) and barley straw (0.31 W/mK) had the lowest thermal conductivity. Other studies presented the lowest thermal conductivity of 0.25 W/mK (2.5% fibre) (Abanto et al., 2017) and 0.26 W/mK (5% fibre) (El Azhary et al., 2017), 0.20 W/mK (70vol% fibre) (De Castrillo et al., 2021). Vega et al. (2011) showed that maximum compressive strength (3.99 MPa for 33.3vol% fibre) was achieved with the highest amount of straw, while maximum flexural strength (0.82 MPa for 25vol% fibre) was obtained with the lowest fibre content. Wang et al. (2019) used cement (10, 15, and 20%) with straw and reported that the addition of cement prolonged the curing time and increased the compressive strength (11.70 MPa for 20% cement and 5% fibre). Other studies found the optimum compressive strengths to be 5.80 MPa (Binici et al., 2005), 2.69 MPa (De Castrillo et al., 2021), 0.46 MPa (Parisi et al., 2015), 4.58 MPa (Türkmen et al., 2017), and 1.86 MPa (Statuto et al., 2018). Parisi et al. (2015) measured peak tensile strength as 0.56 MPa (0.64% fibre). The density of the samples ranged from 1544.98 kg/m<sup>3</sup> to 1827.58 kg/m<sup>3</sup> (El Azhary et al., 2017), 1400 kg/m<sup>3</sup> to 1470 kg/m<sup>3</sup> (Türkmen et al., 2017), 1628.70 kg/m<sup>3</sup> to 1766.20 kg/m<sup>3</sup> (Abanto et al., 2017), 922 kg/m<sup>3</sup> to 1479 kg/m<sup>3</sup> (De Castrillo et al., 2021), 1357.70 kg/m<sup>3</sup> to 1575.60 kg/m<sup>3</sup> (wheat straw), and 1139.90 kg/m<sup>3</sup> to 1542.50 kg/m<sup>3</sup> (barley straw) (Parisi et al., 2015).

Giroudon et al. (2019) compared the effects on the utilisation of barley and lavender straw (3%, 6% by mass, and 10 mm) in unfired earth brick production. The test results showed that barley straw improved thermal performance but lowered engineering strength; however, better durability and fungus growth resistance were achieved with lavender straw. For both types of straw, the maximum compressive strengths of 3.90 MPa (lavender straw) and 3.80 MPa (barley straw) were achieved at 6% fibre addition. Thermal conductivity decreased as the percentage of both types of fibre increased, and

the lowest values were 0.28 W/mK (6% lavender straw) and 0.15 W/mK (6% barley straw). Moreover, the results indicated that the incorporation of lavender straw improved the dry abrasion resistance, while it was reduced by the addition of barley straw.

Ouedraogo et al. (2019) investigated the physical, thermal, and engineering properties of adobe blocks incorporating fonio straw (0.2, 0.4, 0.6, 0.8, 1.0wt% and a maximum length of 10 mm). It was observed that the association of fonio straw with the clay matrix increased water absorption and reduced thermal conductivity. However, the inclusion of small quantities of straw improved the engineering properties of the samples and made them less fragile. Compressive (2.90 MPa) and flexural (1.30 MPa) strengths were optimum at 0.4% and 0.2% fibre content, respectively. However, the lowest thermal conductivity (0.35 W/mK) was shown by 1% of the fibre sample. The capillarity water absorption coefficients were maximum around  $1.82 \text{ g/m}^2/\text{s}^{1/2}$  (0.2% fibre) and minimum around  $0.139 \text{ g/m}^2/\text{s}^{1/2}$  (1% fibre). The research concluded that 0.2 to 0.4% of fonio straw could contribute to improving the properties of the adobe blocks.

Babe et al. (2021) added neem straw and leaf (2-4%) to reinforce adobe brick and found that the sample with 2% neem fibre had the highest strength. However, the lowest thermal conductivity (0.43 W/mK) was achieved for 4% neem leaf fibre. Also, the fibre-reinforced samples performed better in the durability test compared to the fibre-free samples.

Laborel-Préneron et al. (2017 ; 2018 ; 2021) utilised 3wt% and 6wt% of hemp shiv and barley straw to produce unfired earth blocks and investigated the mechanical and hygrothermal properties. The average length of 15 mm straw fibre was used for bending strength testing. The test results showed that bulk density decreased from  $1603 \text{ kg/m}^3$  to  $1221 \text{ kg/m}^3$  and from  $1519 \text{ kg/m}^3$  to  $1315 \text{ kg/m}^3$ , and thermal conductivity reduced from 0.20 W/mK to 0.30 W/mK and from 0.14 W/mK to 0.28 W/mK with the addition of hemp shiv and straw fibre, respectively (Laborel-Préneron et al., 2018). Moreover, compressive and flexural strengths reduced with a higher amount of hemp shiv addition but increased for the straw fibre blended samples, where maximum compressive strength (3.80 MPa) was found at 6% fibre addition. The optimum compressive strength (2.40 MPa) of the hemp sample was recorded at 3% fibre content. Furthermore, peak flexural strength (1.80 MPa) was achieved by straw mixed samples, followed by hemp (1.34

MPa) (Laborel-Préneron et al., 2017). Based on the test results, it can be concluded that the straw mixed sample displayed the best thermal performance, which reduced the thermal conductivity by 75% compared to the waste-free sample.

Serrano et al. (2016) studied the feasibility of using corn plant, fescue, and straw (1-3wt%) as additives in the manufacture of adobe blocks. The mechanical test results indicated that the highest flexural strength was achieved by fescue admixed samples (0.33 MPa-0.60 MPa), followed by corn plant (0.25 MPa-0.39 MPa) and straw (0.15 MPa-0.29 MPa), while the highest compressive strength was obtained by corn plant (1.98 MPa-3.25 MPa), followed by straw (2.04 MPa-2.90 MPa) and fescue (1.93 MPa-2.88 MPa).

Kumar and Barbato (2022) studied the mechanical and durability characteristics of compressed earth blocks using sugarcane bagasse fibres (0.5, 1%, 55 mm length) and cement (6 and 12%). The test results revealed that fibre integration increased the mechanical strength of the samples as compared to the unstabilised sample. When the fibre content was raised but the cement content remained the same, compressive strength declined, and flexural strength improved. However, fibre reinforced samples with 12% cement showed better mechanical and durability performance. Besides, water absorption increased with increasing both fibre and cement content. Density decreased from 1575 kg/m<sup>3</sup> to 1485 kg/m<sup>3</sup> and from 1628 kg/m<sup>3</sup> to 1588 kg/m<sup>3</sup>, while water absorption increased from 4.12% to 5.29% and from 8.07% to 12.55%, respectively, for fibre addition from 0.5% to 1% at 6% and 12% cement content, respectively.

Khedari et al. (2005) analysed the thermal properties of unfired soil blocks incorporating coconut coir fibre (10%, 15%, and 20% of reference cement volume). The findings showed that coconut coir addition reduced the density (1754.94 kg/m<sup>3</sup> to 1344.60 kg/m<sup>3</sup>), thermal conductivity (1 W/mK to 0.6 W/mK) and compressive strength (5.79 MPa to 1.50 MPa) of the samples. Purnomo and Arini (2019) conducted experimental studies to investigate the influence of humidity on the physical and mechanical properties of unfired bricks made with treated coconut coir. It was found that in wet conditions, the sample with 4% treated and 25 mm coir fibre showed the highest mechanical strength. At 90 days, the average maximum compressive and bending strengths were 3.50 MPa and 0.70 MPa, respectively. Moreover, there was a variation in water absorption rate in

different humid conditions, though the tendency to have a higher absorption rate (30-50%) was in more humid conditions. Thanushan et al. (2021) incorporated 0.2, 0.4, and 0.6% of mass portions of coconut fibre with unfired soil blocks and presented that fibre addition increased water absorption (215.20 kg/m<sup>3</sup> to 293.30 kg/m<sup>3</sup>). On the other hand, there was a progressive decrease in compressive (2.72 MPa to 3.44 MPa) and flexural (0.87 MPa to 0.99 MPa) strengths. The dry and wet density of all samples were more similar, with a slight increase from 1765 kg/m<sup>3</sup> to 1785 kg/m<sup>3</sup> and from 2025 kg/m<sup>3</sup> to 2060 kg/m<sup>3</sup>, respectively. Besides, the freeze and thaw test revealed that the compressive strength of the samples decreased up to 19% after 12 freezing cycles, while for the unreinforced sample the decrease was 33%. In another study, Thanushan and Sathiparan (2022) produced cement-stabilised soil blocks reinforced with coconut coir and banana fibre. The results revealed that banana fibre reinforced blocks performed better in post-peak compression behaviour, while coconut coir blocks performed better in post-peak flexural behaviour. Also, both fibre reinforcements improved durability compared to the control blocks; however, coconut coir reinforced blocks were found to be more durable than the banana fibre reinforced blocks. Sangma et al. (2019) examined the effects of coir fibre (5wt% and 20 to 80 mm) addition on the physical and mechanical properties of unfired earth blocks. The study concluded that the peak compressive and tensile strengths of reinforced blocks were 1.67 MPa and 0.56 MPa, respectively, which were 1.45 and 4 times higher than the unreinforced block. In the case of fibre length, samples reinforced with 40 mm of coconut fibre displayed the best performance.

Mostafa and Uddin (2015; 2016) studied the mechanical properties of compressed earth blocks by mixing various proportions (1-5wt%) and lengths (25-100 mm) of banana fibre. The blocks reinforced with fibre lengths of 60 mm and 70 mm had the highest compressive (6.58 MPa) and bending (1.02 MPa) strengths. The compressive strength improved up to 68% (70 mm) and 71% (60 mm), while the flexural strength increased up to 82% (70 mm) and 77% (60 mm) over the sample (Mostafa and Uddin, 2016). The water absorption rate of the banana fibre-reinforced compressed earth blocks was an average of 10.60% (Mostafa and Uddin, 2015).

Chan (2011) studied the performance of clay bricks using oil palm fruit bunch and pineapple leaf fibre (0.25, 0.5, 0.75wt%, and 10 mm). The results presented that the

sample density ranged from 1300 kg/m<sup>3</sup> to 1500 kg/m<sup>3</sup> (oil palm), 1250 to 1430 kg/m<sup>3</sup> (pineapple leaf), and the water absorption rate varied from 1.10% to 2% (oil palm) and 1.10% to 1.25% (pineapple leaf). The maximum compressive strength was similar and achieved at 0.75% fibre content for both samples, being 19.50 MPa (oil palm fibre) and 18 MPa (pineapple leaf fibre), which satisfied the minimum strength requirement for conventional brick. Eslami et al. (2022) used pam fibre (0.25, 0.5, 0.75, 1%, 10-60 mm) to make adobe bricks that were evaluated for compressive strength, tensile strength, ductility, and durability. The experimental results indicated that the compressive strength decreased from 5.03 MPa to 3.36 MPa while the tensile strength improved from 0.55 MPa to 1.12 MPa with increasing the fibre amount. Furthermore, the erosion test findings revealed that the erosion depth decreased as the fibre content increased. Vodounon et al. (2018) investigated the influence of treated (sodium hydroxide solution) and untreated pineapple leaf fibres (1-5wt%) on the mechanical strength of earth bricks stabilised with cement (3% and 5%). The results showed that the treated leaves performed better than the untreated fibres and 3% of treated fibres with 5% cement samples had the highest compressive (4.81 MPa) and flexural (0.92 MPa) strengths.

Taallah et al. (2014), Taallah and Guettala (2016) and Atiki et al. (2021) studied the utilisation of date palm fibre on compressed earth block production. Various percentages of fibres (0.05, 0.10, 0.15, 0.2wt%, and 20 mm, 35 mm (Taallah et al., 2014; Taallah and Guettala, 2016); 0.1, 0.2, 0.3, 0.4, 0.5 wt%, and 1-4 mm (Atiki et al., 2021) were incorporated to conduct the tests. Taallah et al. (2014) produced the samples using cement (5, 6.5, and 8%), whereas Taallah and Guettala (2016) and Atiki et al. (2021) used lime (10-12%). The results of the experiments exhibited that strength decreased as the amount of fibre was increased in the mixture. Taallah et al. (2014) showed that samples with 0.05% of fibre and 8% cement had the highest dry compressive (12.50 MPa) and tensile (1.50 MPa) strengths. Atiki et al. (2021) reported the maximum compressive (13.50 MPa) and flexural (5.26 MPa) strengths were found at 0.1% fibre content. Besides, higher fibre content reduced the thermal conductivity from 0.80 W/mK to 0.76 W/mK (Taallah and Guettala, 2016) and from 0.945 W/mK to 0.846 W/mK (Atiki et al., 2021), while bulk density decreased from 1910 kg/m<sup>3</sup> to 1892 kg/m<sup>3</sup> (Taallah and Guettala, 2016) and from 2032 kg/m<sup>3</sup> to 2066 kg/m<sup>3</sup> (Atiki et al., 2021). Mellaikhafi et al. (2021) employed 3% and 6% of fibres from five different parts of date

palm trees (pinnate leaves, palm fibre mesh, palm trunk, petiole, and palm cluster) to reinforce adobe blocks and investigated the thermal properties. The results indicated that the thermal properties of the adobe blocks improved with the addition of fibres, but they differed based on the type of fibres used. Among all the fibre types, the samples with pinnate leaf fibres performed the best, with the lowest thermal conductivity of 0.265 W/mK. Also, according to the numerical simulation results, pinnate leaf fibre addition contributed to decreasing a maximum heat flux of about 46% through the walls.

Danso et al. (2015b) and Danso (2017) assessed the suitability of sugarcane bagasse (SB), coconut husk (CH), and oil palm fruit (OP) incorporation in two different types of soil to produce unfired building blocks. Various proportions (0.25, 0.5, 0.75, and 1wt%) and lengths (50 mm, 80 mm, and 38 mm) were used to strengthen the earth blocks. The test results exhibited that water absorption increased, and dry density decreased with increasing fibre content. The dry density varied from 1772 kg/m<sup>3</sup> to 1857 kg/m<sup>3</sup>, 1790 kg/m<sup>3</sup> to 1867 kg/m<sup>3</sup>, and 1802 kg/m<sup>3</sup> to 1889 kg/m<sup>3</sup>, and water absorption ranged from 9.80% to 15.30%, 10.40% to 16.50%, and 9.40% to 14.30% for CH, SB, and OP reinforced samples, respectively. Moreover, the results showed that there was a significant improvement in compressive (3 MPa for CH and 2.80 MPa for SB) and tensile (0.32 MPa for CH and 0.30 MPa for SB) strengths by incorporating fibre up to 0.5%. The values continued to drop with the addition of fibre from 0.5% to 1%. On the other hand, OP fibre samples reached the highest compressive (3 MPa) and tensile (0.36 MPa) values at 0.25% of fibre content. Therefore, the study indicated that 0.5% of the fibres would be ideal for enhancing the strength of unfired earth blocks.

Lamrani et al. (2019) assessed the thermal efficiency of unfired clay masonry bricks combining 10, 20, and 30vol% of olive waste fibre (OW), date palm fibre (DPF), and straw (S). The study reported that the addition of S and DPF improved the thermal performance of the samples, while OW began to degrade the performance. The density of the samples ranged from 1398.30 kg/m<sup>3</sup> to 1642.59 kg/m<sup>3</sup> (OW), 1218.74 kg/m<sup>3</sup> to 1572.19 kg/m<sup>3</sup> (DPF), and 1221.43 kg/m<sup>3</sup> to 1554.35 kg/m<sup>3</sup> (S). In the case of thermal conductivity, straw fibre reinforced samples performed the best (0.26 W/mK), followed by DPF (0.28 W/mK) and OW (0.40 W/mK) samples.

Tran et al. (2018) experimented on the mechanical properties of soil blocks incorporating

waste corn silk fibre (0.25, 0.5, 1wt%, and 10 mm). The results showed that the compressive (9 MPa) and tensile (1.30 MPa) strengths reached a peak at 0.5% and 0.25% of fibre content, respectively. Further increasing fibre content from this range resulted in a decline or slight increase in strength. Also, the dry unit weight decreased with the addition of fibre and ranged from 13.10 kN/m<sup>3</sup> to 12.20 kN/m<sup>3</sup>. Therefore, the optimum fibre content was proposed as 0.25%-0.5% as it showed around 177% and 88% improvement in compressive and tensile strengths, respectively, compared to the fibre-free sample.

Demir (2008) conducted experiments to develop unfired clay bricks using grass and tobacco residues (2.5, 5, and 10wt%). Based on the test results, it can be concluded that the compressive strength of the unfired brick samples improved from 3.10 MPa to 4.75 MPa and from 3.40 MPa to 5.15 MPa for tobacco residues and grass addition, respectively.

Heath et al. (2009) and Piani et al. (2020) investigated the utilisation of wood fibre in the development of unfired earth blocks. Heath et al. (2009) noticed that wood fibre incorporation resulted in a dry density reduction of about 12% compared to the control sample. The study found a compressive strength of 10.50 MPa. On the other hand, Piani et al. (2020) utilised wood and straw fibre together (<2%, 17-18%, and a maximum length of 20 mm) in adobe blocks to examine the compressive strength. The results showed that the density of the samples varied between 1180 kg/m<sup>3</sup> and 1790 kg/m<sup>3</sup>, and the maximum compressive strength (6 MPa) was attained at <2% fibre addition.

Islam and Iwashita (2010) utilised waste jute fibre (0.5, 1, 2, 3, 4wt%, and 5, 10, 20, 30 mm) and straw fibre (0.5, 1.5, 3wt%, and 10, 20, 30 mm) to produce low-cost earthquake-resistant adobe blocks. The results presented that a higher amount of fibre in the samples caused the dry density to decrease slightly from 1110 kg/m<sup>3</sup> to 820 kg/m<sup>3</sup>. The results also showed that ductility significantly improved with the addition of 1.5% of straw fibre, although it caused a drop in compressive strength. In the case of samples containing 20 mm straw fibre, the toughness seemed to show an increasing rate, and for 30 mm straw samples, the toughness displayed a slightly declining rate after the addition of 1.5% fibre. Therefore, to improve the ductility of the adobe, 1.5% straw and 20 mm long fibre were recommended as optimum values. The study also found that samples

made of crushed straw had higher compressive strength than samples that contained whole straw. On the other hand, compressive strength decreased, and ductility improved by increasing the quantity of jute fibre in the samples. The sample with jute fibre reached the highest toughness with 2% and 20 mm fibre. The optimum compressive strengths for straw and jute fibre samples were 0.55 MPa and 1.30 MPa, respectively. Araya-Letelier et al. (2021) utilised jute fibre (0.5, 2% and 7, 15, 30 mm) to produce adobe blocks and found the highest compressive (2.25 MPa) and flexural (0.63 MPa) strengths at 0.5% fibre content and 15 mm fibre length. The results also revealed that thermal conductivity decreased with increasing fibre percentage but increased with increasing fibre length. The sample with 2% fibre and 7 mm length had the lowest thermal conductivity (0.409 W/mK).

Zak et al. (2016) investigated the mechanical properties of unfired earth bricks incorporating flax and hemp fibre (1 and 3 mass%). The test findings presented that the addition of flax fibre did not considerably change the compressive strength of the samples compared to the control sample, but the brittle breaking behaviour of the sample decreased. However, hemp fibre inclusion induced a slight reduction in the compressive strength of the unfired bricks. The highest compressive strengths were 3.75 MPa and 4.50 MPa for hemp and flax fibre samples, respectively, at 3% fibre addition. Sample density ranged from 1060 kg/m<sup>3</sup> to 1700 kg/m<sup>3</sup> for hemp fibre and from 1080 kg/m<sup>3</sup> to 1700 kg/m<sup>3</sup> for flax fibre. Bruno et al. (2020) examined the thermal performance of unfired earth brick walls utilising hemp fibre (1.5wt% and 1-5 mm). The hemp brick samples were developed in the laboratory by hyper-compacting to 100 MPa, resulting in a high dry density and bulk density value of 2244 kg/m<sup>3</sup> and 2316 kg/m<sup>3</sup>, respectively. The thermal conductivity of the individual sample was 1.28 W/mK, whereas the result from the tested hemp brick wall presented a conductivity of 1.27 W/mK. Fernea et al. (2019) conducted experimental research on the properties of clay building material using hemp and clay binder in a ratio of 1: 1, 2: 1, and 3: 1. From the tests, it was observed that the sample with a 1:2 ratio reached the highest density above 1000 kg/m<sup>3</sup>. At the same time, this composition had an optimum flexural strength value of 0.47 MPa. Conversely, a 1:3 ratio sample showed the lowest density, close to 966.73 kg/m<sup>3</sup>, and the highest compressive strength of 0.94 MPa. Furthermore, thermal conductivity increased from 0.09 W/mK to 0.18 W/mK when the density increased.

Ojo et al. (2019) investigated the properties of extruded alkali-activated earth building blocks incorporated with sisal (0.5-2vol% and 10 mm) and eucalyptus pulp (wood kraft pulp) microfibre (0.5-2vol% and 0.7 mm). According to the study, sisal fibre admixed samples showed a higher improvement in tensile strength (74%) than eucalyptus pulp blended samples (29%). Waste addition increased density from 1700 kg/m<sup>3</sup> to 1740 kg/m<sup>3</sup> (sisal) and 1680 kg/m<sup>3</sup> to 1700 kg/m<sup>3</sup> (eucalyptus pulp), and water absorption ranged from 19% to 20% (sisal) and 20% to 21.25% (eucalyptus pulp). Sisal fibre reinforced sample had the highest flexural strength (5.50 MPa) at 0.5% of fibre content and the eucalyptus pulp sample reached its peak strength (4.5 MPa) at 1% of fibre content. Namango (2006) investigated the different properties of sisal fibre (0.25, 0.5, 0.75, 1.0, 1.25wt%, and 10 mm) stabilised compressed earth blocks. The test results revealed that the optimum flexural (1.63 MPa) and compressive (9.14 MPa) strengths were achieved for 0.75% sisal, which corresponded to a 64.30% and 90.50% improvement in strength compared to the fibre-free block. The density of the sisal reinforced blocks increased with 0.75% fibre addition (1895 kg/m<sup>3</sup>) and subsequently dropped with 1.25% fibre addition (1738 kg/m<sup>3</sup>).

Millogo et al. (2014) examined the prospect of utilising kenaf fibre in the production of pressed adobe blocks, and Laibi et al. (2018) conducted experiments to investigate the influences of different kenaf fibre lengths on the thermal and engineering properties of compressed earth blocks. The adobe sample blocks were reinforced with 0.2 to 0.8 wt.% and two different lengths (30 and 60 mm) of fibres (Millogo et al., 2014), while compressed earth blocks were produced using 1.2wt% and three different lengths (10, 20, and 30 mm) of fibres (Laibi et al., 2018). The results showed that for short (30 mm) and long (60 mm) fibres, compression strength improved by around 16% and 8%, respectively. Moreover, the addition of 0.2 to 0.6% of 30 mm fibres reduced the pore size of the samples. Furthermore, the amount of 0.8wt% of 60 mm fibres negatively influenced the compressive strength of the adobe samples (Millogo et al., 2014). The study of Laibi et al. (2018) showed the maximum compressive and flexural strengths were 6.40 MPa (20 mm) and 2.75 MPa (30 mm), respectively. The results also indicated that the thermal conductivity decreased when both the fibre length and percentage were raised. Thermal conductivity values were 1.30 W/mK (0.8% and 60 mm) (Millogo et al., 2014) and 1 W/mK (1.2% and 20 mm) (Laibi et al., 2018). Hence, the studies

recommended the 30 mm fibre length of kenaf as suitable for stabilisation of unfired clay blocks.

Murillo et al. (2005) evaluated the effects of the addition of henequen fibre (0.25, 0.5, 0.75, and 1.0mass%) on the engineering properties of unfired earth blocks. The findings indicated that 1% fibre addition led to a decrease in compressive strength of up to 33% and linear shrinkage of up to 36% in comparison to the fibre-free sample. The compressive strength and the linear shrinkage of the samples decreased from 5.22 MPa to 4.21 MPa and 3% to 4.1%, respectively. However, the lowest density was measured at 0.75% fibre (1884 kg/m<sup>3</sup>) and the highest was reported at 0.5% fibre (1906 kg/m<sup>3</sup>) addition.

Demir (2006) examined the durability and mechanical properties of unfired clay bricks utilising processed waste tea (2.5 and 5% by mass). The results showed that the unit weight of unfired samples decreased with an increasing waste ratio in mixtures and ranged from 1.52 to 1.70 kg/dm<sup>3</sup>. The compressive strength of unfired samples was above 5 MPa, which met the Turkish standard (1 MPa) (TS 2514, 1977). In another study, Chung et al. (2021) used an alkali-activation technique at low temperature to produce unfired clay bricks containing 1-10wt% tea waste additives. The findings showed that as the amount of waste additives in the mixture increased, the density and linear shrinking decreased, while porosity and water absorption increased. Besides, the samples with 1wt% tea waste had the highest compressive strength (22.51 MPa) and any further increase in tea waste content resulted in a lower compressive strength. However, according to ASTM C62 (ASTM C62, 2005), all samples with tea additives met the minimum compressive strength requirement of 8.60 MPa for structural applications with appropriate moisture absorption values under negligible weathering.

Sharma et al. (2015a; 2015b; 2016) investigated the compressive strength and durability of rural adobe blocks incorporating pinus roxburghii fibre (PR), grewia optiva fibre (GO) in the Indian state of Himachal Pradesh. Different proportions of fibres (0.5, 1, 1.5, 2wt%, and 30 mm) were used in the sample, along with 2.5% cement. The results revealed that GO fibre-mixed samples showed better improvement in durability than PR fibre-mixed samples. GO and PR samples reported a 72% and 56% decrease in water absorption, respectively, resulting in a proportionate durability increase compared to the

control sample. Furthermore, the compressive strength of the sample blocks increased from around 94% to 200% for GO and 73% to 137% for PR fibre. The compressive strength value reached its peak at 1% fibre (2.25 MPa) and 2% fibre (3 MPa) addition for PR and GO, respectively. The water absorption test presented that it ranged from 2.33% to 3.62% for PR samples and 2.07% to 2.67% for GO samples (Sharma et al., 2016). The study recommended using 2% GO and 1% PR fibres for earth block construction in seismic-prone areas.

Achenza and Fenu (2006) and Dove (2014) incorporated seaweed fibre additives for unfired clay brick production. Achenza and Fenu (2006) used 10 mm long and 10wt% seaweed fibre and natural polymers (beetroot and tomato residues) with soil. Dove (2014) utilised 0.1% Scottish seaweeds (*Laminaria hyperborean*) with silt loam to prepare the blocks. According to the test results, the density of the samples varied from 1690 kg/m<sup>3</sup> to 2250 kg/m<sup>3</sup> (Dove, 2014) and 1720 kg/m<sup>3</sup> to 1810 kg/m<sup>3</sup> (Achenza and Fenu, 2006). It was observed that the compressive strength improved (up to 75%) with the addition of natural polymers, and the highest compressive strength was 4.40 MPa. The test results also presented a water absorption value of around 2.10 g/cm<sup>2</sup> (Achenza and Fenu, 2006). On the other hand, Dove (2014) presented maximum compressive and flexural strengths of 1.64 MPa and 0.95 MPa, respectively.

Villamizar et al. (2012) studied the effects of coal ash (5, 7.5, and 10wt%) and cassava peel (2.5 and 5wt%) on the strength of compressed earth block. The test results demonstrated that the stabilised earth blocks exhibited the highest compressive (3.37 MPa) and flexural (0.75 MPa) strengths for 5% coal ash addition, while for the 5% cassava peel incorporated sample the values were 2.21 MPa and 0.50 MPa, respectively. At 2.5% cassava peel and 7.5% coal ash combination, the sample presented a compressive strength of 2.60 MPa and a flexural strength of 0.58 MPa. Besides, 10% of coal ash sample showed the lowest compressive (1.09 MPa) and flexural (0.40 MPa) strengths. Water absorption, however, appeared to decline as the percentages of cassava peel increased. The average water absorption rate was 30.65% (10% coal ash), 28.64% (5% coal ash), 27.77% (2.5% cassava peel and 7.5% coal ash), and 27.01% (5% cassava peel). The study suggested that the optimum percentages should be 2.5% cassava peel and 7.5% coal ash.

Araya-Letelier et al. (2018) measured the efficacy of using pig hair as reinforcement in adobe (0.5, 2wt%, and 7, 15, 30 mm). The test results presented a reduction in strength with the incorporation of a higher amount (2%) and longer length (15 mm and 30 mm) of pig hair. After 28 days of curing, the average flexural and compressive strengths ranged from 0.34 MPa to 0.49 MPa and 1.20 MPa to 2.02 MPa, respectively. Moreover, the incorporation of a larger quantity (2%) and a higher length (30 mm) of fibre minimised the drying shrinkage of the samples. The research recommended 0.5% and 7 mm of pig hair for adobe manufacturing since it exhibited the best performances in flexural toughness and drying shrinkage cracking compared to waste-free adobe.

Galán-Marín et al. (2010; 2013), Statuto et al. (2018), and Benkhadda and Khaldoun (2019) examined the utilisation of sheep wool to reinforce unfired earth blocks. Statuto et al. (2018) used 3wt%, whereas Galán-Marín et al. (2010; 2013) and Benkhadda and Khaldoun (2019) incorporated 0.25-1wt% of 10-50 mm sheep wool and alginate as a natural polymer to produce the blocks. The studies reported that density increased with the increasing amount of wool fibre and ranged from 1790 kg/m<sup>3</sup> (19.5% alginate and 0.25% wool) to 1800 kg/m<sup>3</sup> (19.5% alginate and 0.50% wool) (Galán-Marín et al., 2010). The optimum compressive strengths were 4.44 MPa (Galán-Marín et al., 2010) and 3.04 MPa (Benkhadda and Khaldoun, 2019), and the maximum flexural strength were 1.45 MPa (Galán-Marín et al., 2010) and 1.83 MPa (Benkhadda and Khaldoun, 2019) at 0.25% sheep wool and 19% alginate content.

### **2.3.1.2 Agro-waste Powder**

Demir (2008) examined the compressive strength of unfired clay bricks containing 2.5-10% sawdust and reported that sawdust addition enhanced the compressive strength of the bricks. Similarly, Ouattara et al. (2016) observed an improvement in the compressive strength of clay bricks with 15-20% sawdust content. However, the study of Ganga et al. (2014) showed no improvement in the compressive strength of the samples with the addition of sawdust or mahogany shavings. Vilane (2010) produced adobe bricks using sawdust (0-20%) and obtained the optimum percentage to be 15%, as it gave the highest compressive strength. Besides, Jokhio et al. (2018) found higher compressive strength values by replacing sand with 20% sawdust. According to Charai et al. (2020; 2022), the

density and thermal conductivity of the sawdust clay composites decreased with increasing sawdust percentages (2-10%). The lowest conductivity (0.501 W/mK) was recorded at 8% sawdust content, representing a 39% decrease compared to the control sample. De Castrillo et al. (2021) and Tatane et al. (2018a) also noticed that the bulk density, thermal conductivity, and compressive strength of the samples reduced, while capillary water absorption increased as the proportion of sawdust increased.

Ayodele et al. (2019) employed sawdust ash and eggshell ash (0, 2, 4, 8, and 16wt%) to manufacture lateralised unfired bricks. The results exhibited that the sample with 4% ash had the lowest density (1749 kg/m<sup>3</sup>), while the 16% ash blended sample had the maximum density (1489 kg/m<sup>3</sup>). Moreover, compressive strength decreased as the amount of ash percentage increased, and maximum compressive strength (1.25 MPa) was achieved at 2% and 4% ash content. Adogla et al. (2016) utilised eggshell powder (10, 20, 30, and 40wt%) to examine its potential to partially substitute soil in the production of lateralised unfired compressed bricks. From the density tests, it was noticed that the dry density of the samples gradually increased (2101 kg/m<sup>3</sup> to 2044 kg/m<sup>3</sup>) as the amount of waste increased. On the other hand, the findings of the compressive strength test revealed that there was an upward trend in the compressive strength values as the amount of ash percentage increased to a maximum of 30%, and after that, the compressive strength showed a decrease in value.

Lima et al. (2012) incorporated sugarcane bagasse ash (2, 4, and 8wt%) to produce compressed earth blocks aiming at the application in non-structural masonry elements. According to the test results, block blended with 8% sugarcane bagasse ash and 12% Portland cement had higher compressive (2.89 MPa) and tensile (0.39 MPa) strengths at 28 days than the minimum value specified in the Brazilian Standard: ABNT-NBR 8492 (2 MPa) (ABNT-NBR 8492, 1984). Therefore, this mixer proportion was proposed for the manufacture of non-structural masonry components.

Huynh et al. (2017) investigated the effects of rice husk ash (10-50wt%) on the various properties of unfired bricks. A solution of sodium hydroxide (NaOH) was used as an activator when producing the samples. The study concluded that the strength of the samples improved with the curing period, and the compressive and flexural strengths of all samples at 28 days ranged from 16.20 MPa to 30.30 MPa and 4.04 MPa to 6.17 MPa,

respectively. The highest strength was obtained at 10% rice husk addition, and the strength steadily declined at a higher percentage of ash content. The maximum compressive and flexural strengths were respectively 3.50% and 2.70% higher than the values of the control brick sample. Moreover, water absorption rate for all samples was between 7.50% and 10.40%, substantially lower than the 12% maximum limit for the M15 and M20 brick grades. Furthermore, oven-dried samples had remarkably lower thermal conductivity (0.68 W/mK-1.25 W/mK) than the sun-dried samples (1.24 W/mK-1.68 W/mK). The discrepancy was mainly due to the sample temperature variation because, generally, the thermal conductivity decreases with an increase in sample temperature. Muntohar (2011) studied the application of rice husk ash and lime (5, 10, and 15wt%) for the manufacture of compressed earth blocks. The results showed that the ratio of 1:1 rice husk and lime had the highest compressive (20.70 MPa) and flexural (0.05 MPa) strengths. As the lime and rice husk ratio increased, the water absorption rate decreased significantly from 9.60% to 0.80%. In another study, Nshimiyimana et al. (2018) investigated the compressive strength of compressed earth blocks utilising calcium carbide residue (CCR) and rice husk ash (RHA). In the first phase of the experiments, different fractions of CCR (0-15wt%) were used to determine the effect of CCR on the samples and its optimum compressive strength. The results revealed that due to the pozzolanic interaction between earth particles and the CCR, the compressive strength nearly doubled (3.40 MPa) for 8% CCR content in comparison to the control sample (1.90 MPa). However, more than 8% CCR addition decreased compressive strength. Therefore, in the second phase, the compressive strength of the samples with more than 8% CCR was further enhanced by the partial replacement of CCR by RHA (10-40%). It was observed that in the case of 10% and 15% CCR, the optimum RHA replacement was 20% and 30%, respectively. The compressive strengths for 20% and 30% RHA substitution were 5.30 MPa and 6.60 MPa, respectively, which were twice and three times higher than the only 10% CCR (2.50 MPa) and 15% CCR (2.20 MPa) samples.

Amina et al. (2018) assessed the potential use of corn husk ash (10 and 20wt%) as a stabiliser for rammed earth to improve the thermophysical properties. The results showed a considerable reduction in thermal conductivity from 0.63 W/mK to 0.48 W/mK and a slight increase in density from 942.50 kg/m<sup>3</sup> to 959.50 kg/m<sup>3</sup> with an increasing

percentage of corn husk ash. Hence, the study recommended 20% of corn husk ash as the optimum percentage to improve the thermal properties of rammed earth blocks.

Namango (2006) reported on the various characteristics of compressed earth blocks stabilised with cassava powder (1.5, 2.5, 4, 5, 7, 10, 15, and 20 wt%). The results exhibited that the samples had compressive strengths between 7.36 MPa (1.5% cassava) and 4.29 MPa (7% cassava). The trend of flexural strengths was similar to that of compressive strengths and ranged between 0.94 MPa and 1.71 MPa. The optimum value of compressive and flexural strengths of cassava powder blended samples provided up to 53.50% and 72.50% strength increase, respectively, compared to the non-reinforced block.

The effects of argan nut shell powder (ANSP) (2, 4, and 6%) and cement (5%) on the mechanical and thermal performances of the compressed earth block were examined by Tatane et al. (2018a; 2018b) and Akhzouz et al. (2020). The test results indicated that the thermal conductivity of the samples decreased with increasing ANSP content, and conductivity values for cement-free samples (0.87 W/mK to 0.75 W/mK) were higher than cement-stabilised samples (0.64 W/mK to 0.48 W/mK). This decrease is attributed to the low thermal conductivity of ANSP (0.16 W/mK) compared to clay matrix (0.30 W/mK). Besides, the addition of cement further limited the manoeuvrability of the mixture, which ultimately reduced the good compaction. This resulted in additional air inside the samples, which increased the porosity and decreased the thermal conductivity. Also, tensile strength slightly reduced for both cement-free (0.75 MPa to 0.65 MPa) and cement-stabilised samples (0.90 MPa to 0.68 MPa) with the increase of ANSP content from 0-6%. Moreover, dry compressive strength decreased from 2.21 MPa to 1.89 MPa for the same amount of ANSP because of the poor adhesion between the clay matrix and ANSP. However, cement developed some rigid connections between the soil particles, which induced a little improvement in strength. But for the cement-stabilised samples, the optimum compressive strength (3.12 MPa) was achieved at 2% waste content since it adhered well to the clay matrix, and above this amount, cement content became inadequate to bind ANSP. Furthermore, due to the non-absorbing characteristics of ANSP (absorption=26.3%), the water absorption coefficient declined from 16.92% to 10.10% as ANSP was added (0-6%), which was below the limit stated in the XP 13-901

standard (NF XP P13-901, 2001) (20%).

### **2.3.1.3 Others (Neither Fibre nor Powder)**

Masuka et al. (2018) investigated the utilisation of wood aggregate in the development of unfired earth blocks. The study initially prepared four samples of the various ratios of lime (L), coal fly ash (F), and wood aggregate (W) (L: 4-8%, F: 10-16%, W: 1.5-3%). The results revealed that the compressive strength of the L-10%, F-10%, and W1.5% sample was significantly higher (8.30 MPa) than the other samples. Later, cement (4% and 10%) was used with this mixture for further investigation. The study also evaluated the water resistance of the samples using a qualitative scoring system by observing their damage evidence after a shorter immersion period (2 hours and 4 hours), where the findings showed that the L-10%, F-10%, and W-1.5% samples had the maximum water resistance. Moreover, according to the study, the sample prepared with 10% lime, 10% fly ash, and 4% cement was the most cost-effective composition (based on the cost of raw materials lime and cement). Oskouei et al. (2017) utilised rice husk and wood chips carpentry (0.3%, 0.6%, and 0.9wt%) to produce unfired mud bricks. The results demonstrated that the addition of rice husk and wood chips increased tensile strengths by around 57% to 70% and 69% to 85%, respectively, over the control sample. In another study, Ige and Danso (2022) reported on the properties of adobe bricks stabilised with rice husk (0.25-1%) and lime (10%). The study suggested that 0.75% rice husk is the optimal content since it enhanced compressive and tensile strengths by nearly 62% and 95%, respectively, when compared to the unstabilised sample. Also, rice husk and lime additions considerably enhanced the durability properties. Furthermore, the cost analysis data revealed that the manufacture of adobe bricks was around 71% less expensive than the production of sandcrete bricks.

Fadele and Ata (2018) assessed the water absorption properties of compressed earth blocks incorporating sawdust lignin additives and cement. Samples were prepared separately using 4%, 8%, and 12% by mass of cement and sawdust additives. The findings showed that, in contrast to the cement-stabilised samples, the sawdust additive mixed samples exhibited an improvement in the water absorption properties. The water absorption rate ranged from 6% to 15% for cement-stabilised samples, while it varied

between 2% and 6% for sawdust additives.

Laborel-Préneron et al. (2017; 2018) reported on the mechanical and hygrothermal properties of unfired earth blocks incorporating corn cob (3 and 6wt%). The test results demonstrated that with increasing waste content, bulk density (1878 kg/m<sup>3</sup> to 1754 kg/m<sup>3</sup>) and compressive strength (3.20 MPa to 1.80 MPa) declined. Also, a decrease in thermal conductivity was observed when corn cob percentage increased. The lowest thermal conductivity obtained was 0.26 W/mK for 6% corn cob, indicating a nearly 55% reduction over the reference sample. In a different investigation, Laborel-Préneron et al. (2021) showed that earth blocks produced with 3wt% rice husk outperformed the reference sample in terms of durability (resistance to impact and resistance to water erosion).

Serrano et al. (2016) investigated the potential of using olive stones (5-15wt%) to produce adobe bricks. According to the test findings, olive stones mixed adobe samples had compressive and flexural strengths ranging from 0.98 MPa to 1.61 MPa and 0.07 MPa to 0.16 MPa, respectively. Besides, the results revealed that samples exhibited maximum strength when the percentage of olive stone and sand was minimised.

Mirón et al. (2017) developed compressed earth brick incorporating various percentages of walnut nut shell (5-20%). It was observed that the introduction of walnut nut shell negatively affected the properties of the samples. Only the control sample met the compressive strength requirement (6 MPa) of the Mexican Standard: NMX-C-404-ONNCCE-2005 (NMX-C-404-ONNCCE, 2005) (6 MPa). The walnut nut shell mixed samples showed a drop of up to 94% in strength. In order to improve the properties of the walnut nut shell blended samples, later lime (7%) and gypsum (3%) were incorporated into the mixture, resulting in a strength loss of up to 65%. Moreover, the control sample exceeded the water absorption (30%) allowed by the standard (21%). Also, samples with 5% walnut nut shell and 10% cement exhibited water absorption of 23.8%. However, lime and gypsum stabilised samples containing 20% walnut nut shell (18.55%) and 10% walnut nut shell (19.39%) had comparatively lower water absorption values.

Udawattha et al. (2018) evaluated the performance of natural polymer addition (5-20wt%) to earth blocks as a stabiliser. Seven natural polymers, such as pines resin (PR),

Dawul Kurudu (DK), bael resin (BS), sugarcane bagasse (SB), agarwood resin (AWR), wood apple resin (WAR), and jack resin (JR) were collected from vernacular polymer technologies of Sri Lanka. According to the results, DK (0.85MPa-1.17 MPa), PR (0.98MPa-1.70 MPa), and SB (0.54MPa-0.87 MPa) additions presented the proper compressive strengths, while BR, WAR, AWR, and JR functioned against the block strength. The optimum compressive strengths found were 0.13 MPa (20% BR), 0.25 MPa (10% WAR), 0.20 MPa (5% AWR), and 0.24 MPa (15% JR). Moreover, the results showed a decline in sample density from 1925 kg/m<sup>3</sup> to 2052 kg/m<sup>3</sup>, 1800 kg/m<sup>3</sup> to 1850 kg/m<sup>3</sup>, and 1800 kg/m<sup>3</sup> to 1825 kg/m<sup>3</sup>, and a rise in water absorption rates from 9.30 to 15%, 9.50 to 13.30%, and 10 to 11.30% with the increasing amounts of PR, DK, and SB, respectively. From the tensile splitting test, it was observed that for PR (2.58 MPa at 15%) and DK (0.25 MPa at 15%), the tensile strength increased with an increased percentage of polymer, whereas for SB the maximum value was recorded as 1.75 MPa at 5% polymer content.

### **2.3.1.4 Summary**

Table 2.2 presents that density and water absorption are two physical properties extensively examined by the authors. The density of the composite material is an important measurement because many other properties, including mechanical and thermal properties can be associated with it. The types of earthen materials and agro-wastes employed affected the samples' density. According to Danso et al. (2015b), the density of the samples decreased when coconut husk, sugarcane bagasse, and oil palm fruit fibres were added. Huynh et al. (2017) and Namango (2006) also reported comparable findings with the addition of powdered materials, such as rice husk ash and cassava powder, which was attributed to the lower density of the agro-waste materials than the soil. When lightweight agro-waste materials were increased in the soil mixture, they replaced the heavier soil particles, resulting in a decrease in density. On the other hand, Ayodele et al. (2019) noticed that the density of the samples increased with the increase of eggshell ash by a certain percentage as the very fine ash particles filled the voids in the lateritic soil. However, the sample density dropped by further increasing the amount of ash since the ash had a lower specific gravity compared to the laterite. Moreover, the results of several studies showed that porosity and water absorption were

inversely related to bulk density. Therefore, more pores in the low-density samples permitted increased water flow due to the capillary effect, leading to a higher water absorption coefficient (Demir, 2006; Danso et al., 2015b; Muntohar, 2011; Taallah and Guettala, 2016; Ayodele et al., 2019; Ojo et al., 2019). Also, from the different research studies reviewed, it could be generalised that the addition of agro-wastes increased the water absorption rate because of the hydrophilic nature of lignocellulosic fibres (Ojo et al., 2019).

Furthermore, the findings of the previous studies showed that almost all the researchers examined the compressive strength of the samples. The results demonstrated that the majority of the waste materials contributed to improving the strength of the samples. The strength increased because of the isotropic matrix formation between the structure of the earthen mixture and the all-directional fibre network, which resisted the movement of particles and provided stability (Mostafa and Uddin, 2016). The impacts of fibre length on the mechanical properties of earth blocks were also investigated by some of the authors (Danso et al., 2015b; Mostafa and Uddin, 2016; Araya-Letelier et al., 2018; Laibi et al., 2018; Sangma et al., 2019). Mostafa and Uddin (2016), Araya-Letelier et al. (2018), and Sangma et al. (2019) found that strength decreased as the length of the fibre increased. It is due to the cluster generation caused by the higher fibre length in the mixture, which induced poor adhesion between the fibres in the clusters and the earth matrix. In addition, fibre clusters in the matrix functioned as porosity, impacting its average strength. On the other hand, Oskouei et al. (2017) observed that the non-fibrous rice husk particles (almost a powder) decreased the adhesion of clay with other constituents, which also reduced the friction of components by separating the soil particles. As a result, the compressive strength decreased as the amount of rice husk increased in the samples. Muntohar (2011) showed that the addition of lime and rice husk ash increased the compressive strength and reached a maximum value at a 1:1 ratio, but strength continued to decrease as the ratio increased. The author noticed that in moist conditions, lime and rice husk ash consumed water for exothermic reactions and generated cementitious materials (calcium silicate hydrate), which bound the clay particles together, imparting strength to the soil mixture. Moreover, when the amount of rice husk ash was higher than the amount of lime in the mixtures, there was an insignificant increase in strength due to the insufficient presence of calcium in the lime-

rice husk ash system for the reaction. Furthermore, for higher lime ratios, unreacted lime caused the formation of portlandite, which increased the porosity and reduced the mechanical resistance. Nevertheless, the majority of the research in the literature revealed that compressive strength generally enhanced with the addition of cement or other binders. According to the findings, flexural strength also improved when agro-wastes were added; however, strength decreased at higher percentages of cassava powder, sisal fibre, pig hair, banana fibre, rice husk, and hemp shiv (Namango, 2006; Muntohar, 2011; Mostafa and Uddin, 2016; Huynh et al., 2017; Laborel-Préneron et al., 2017; Araya-Letelier et al., 2018; Ojo et al., 2019).

The studies also presented that density, void volume, and thermal conductivity were correlated (Huynh et al., 2017), where thermal conductivity decreased with the reduction in density but had an inverse relationship with the void volume of the samples. Overall, the results of the review papers indicated that the thermal efficiency of the unfired earth samples enhanced with the inclusion of agro-wastes. The effects of waste incorporation into the samples differed among the studies depending on the types of waste materials and testing procedures employed. For example, with the same soil and the same testing procedure, the addition of different waste materials can accomplish the opposite results. Therefore, there can be no generalisation of the results.

**Table 2.1:** Different agro-waste additives for the production of unfired earth blocks.

Agro-waste fibre			
Agro-wastes	Source(s)	Countries	References
Straw (Wheat, Barley)	Agricultural by-product (Stalk)	Burkina Faso, China, Egypt, France, Germany, Iran, Italy, Japan, Morocco, Peru, Spain, Turkey, Cyprus	Binici et al. (2005), Islam and Iwashita (2010), Vega et al. (2011), Mohamed (2013), Ashour et al. (2015), Parisi et al. (2015), Serrano et al. (2016), Abanto et al. (2017), El Azhary et al. (2017), Laborel-Préneron et al. (2017; 2018), Oskouei et al. (2017), Türkmen et al. (2017), Statuto et al. (2018), Giroudon et al. (2019), Lamrani et al. (2019), Wang et al. (2019), Piani et al. (2020), De Castrillo et al. (2021), Koutous and Hilali (2021)
Lavender straw	By-product of lavender oil production (Stalk)	France	Giroudon et al. (2019)
Fonio straw	Agricultural by-product (Stalk)	Burkina Faso	Ouedraogo et al. (2019)
Coconut coir	Agricultural by-product (Fruit)	Ghana, India, Indonesia, Sri Lanka, Thailand	Khedari et al. (2005), Danso et al. (2015b), Danso (2017), Purnomo and Arini (2019), Sangma et al. (2019), Thanushan et al. (2019), Thanushan and Sathiparan (2022)
Banana fibre	Agricultural by-product (Pseudo stem)	Egypt, India, Sri Lanka	Mostafa and Uddin (2015; 2016), Thanushan and Sathiparan (2022)
Hemp fibre	Agricultural by-product (Bast)	Egypt, France, Japan, Romania	Islam and Iwashita (2010), Zak et al. (2016), Laborel-Préneron et al. (2017; 2018; 2021), Fernea et al. (2019), Bruno et al. (2020)
Wood fibre	Waste of carpentry product (Trunk, Branch)	UK, Italy	Heath et al. (2009), Piani et al. (2020)
Corn plant fibre	Agricultural by-product (Stem)	Spain	Serrano et al. (2016)
Corn silk fibre	Agricultural by-product (Grain)	Japan	Tran et al. (2018)
Cassava peel	Agricultural by-product (Root)	Colombia	Villamizar et al. (2012)

*Table 2.1: Different agro-waste additives for the production of unfired earth blocks (continued).*

<b>Agro-wastes</b>	<b>Source(s)</b>	<b>Countries</b>	<b>References</b>
Olive waste fibre	Agricultural by-product (Leaf)	Morocco	Lamrani et al. (2019)
Pineapple leaf fibre	Agricultural by-product (Leaf)	Malaysia	Chan (2011)
Flax fibre	Agricultural by-product (Bast)	Egypt	Zak et al. (2016)
Sisal fibre	Agricultural by-product (Leaf)	Brazil, Kenya	Namango (2006), Ojo et al. (2019)
Fescue	Agricultural by-product (Stalk)	Spain	Serrano et al. (2016)
Kenaf fibre	Wild plant (Bast)	France, Benin	Millogo et al. (2014), Laibi et al. (2018)
Henequen fibre	Agricultural by-product (Leaf)	UK	Murillo et al. (2005)
Jute fibre	Agricultural by-product (Bast)	Japan, Chile	Islam and Iwashita (2010), Araya-Letelier et al. (2021)
Date palm fibre	Agricultural by-product (Leaf, Sheath)	Algeria, Morocco	Taallah et al. (2014), Taallah and Guettala (2016), Lamrani et al. (2019), Atiki et al. (2021), Koutous and Hilali (2021), Mellaikhafi et al. (2021)
Palm bark fibre	Agricultural by-product (Bark)	Iran	Oskouei et al. (2017), Eslami et al. (2022)
Oil palm fruit/bunch fibre	Agricultural by-product (Fruit)	Malaysia, Ghana	Chan (2011), Danso et al. (2015b), Danso (2017)
Eucalyptus pulp microfibre	By-product of paper manufacturing (Trunk)	Brazil	Ojo et al. (2019)
Pinus roxburghii fibre, Grewia optiva fibre	Forest waste, Fodder waste	India	Sharma et al. (2015a; 2015b; 2016)
Seaweeds fibre	Alginate extraction by-product (Stem, Frond)	UK, Italy	Achenza and Fenu (2006), Dove (2014)
Tea waste	Food industry waste (Leaf)	Turkey, Australia	Demir (2006), Chung et al. (2021)
Sheep wool	Textile industry waste	Italy, Morocco, Scotland	Galán-Marín et al. (2010; 2013), Statuto et al. (2018), Benkhadda and Khaldoun (2019)
Tobacco residue	Tobacco industry by-product	Turkey	Demir (2008)

Table 2.1: Different agro-waste additives for the production of unfired earth blocks (continued).

<b>Agro-wastes</b>	<b>Source(s)</b>	<b>Countries</b>	<b>References</b>
Pig hair	Food industry waste	Chile	Araya-Letelier et al. (2018)
Neem fibre	Agricultural by-product (Straw, Leaf)	Cameroon	Babé et al. (2021)
Sugarcane bagasse	Food industry waste (Stalk)	Ghana, Louisiana	Danso et al. (2015b), Danso (2017), Kumar and Barbato (2022)
<b>Agro-waste powder</b>			
<b>Agro-wastes</b>	<b>Source(s)</b>	<b>Countries</b>	<b>References</b>
Sugarcane bagasse ash	Food industry waste (Stalk)	Brazil	Lima et al. (2012)
Rice husk ash	Agricultural by-product (Grain)	Indonesia, Vietnam, Burkina Faso	Muntohar (2011), Huynh et al. (2017), Nshimiyimana et al. (2018)
Eggshell	Food industry waste	Ghana, Nigeria	Adogla et al. (2016), Ayodele et al. (2019)
Cassava powder	Agricultural by-product (Root)	Kenya	Namango (2006)
Corn husk ash	Agricultural by-product (Stem)	Nigeria	Amina et al. (2018)
Rice husk powder	Agricultural by-product (Grain)	Iran	Oskouei et al. (2017)
Sawdust	Sawmill waste (Trunk, Branch)	Nigeria, Turkey, Cyprus, Congo, Malaysia, Morocco, Eswatini, Ivory Coast	Demir (2008), Vilane (2010), Ganga et al. (2014), Ouattara et al. (2016), Jokhio et al. (2018), Tatane et al. (2018a), Ayodele et al. (2019), Charai et al. (2020; 2022), De Castrillo et al. (2021)
Argan nut shell powder	Agricultural by-product	Morocco	Tatane et al. (2018a; 2018b), Akhzouz et al. (2021)
<b>Others (neither fibre nor powder)</b>			
<b>Agro-wastes</b>	<b>Source(s)</b>	<b>Countries</b>	<b>References</b>
Walnut shell	Agricultural by-product	Mexico	Mirón et al. (2017)

*Table 2.1: Different agro-waste additives for the production of unfired earth blocks (continued).*

<b>Agro-wastes</b>	<b>Source(s)</b>	<b>Countries</b>	<b>References</b>
Dawul Kurudu, Pines gum, Bael resin, Jack resin, Agarwood resin, Wood apple resin, Sugarcane bagasse polymer	Agricultural by-product (Leaf, Fruit, Stem)	Sri Lanka	Udawattha et al. (2018)
Grounded olive stone	Agricultural co-product (Pellets)	Spain	Serrano et al. (2016)
Rice husk	Agricultural by-product (Grain)	Iran, Portugal, Ghana	Oskouei et al. (2017), Laborel-Préneron et al. (2021), Ige and Danso (2022)
Corn cob	Agricultural by-product (Grain)	France	Laborel-Préneron et al. (2017; 2018)
Wood aggregate/ Wood chips	Waste of carpentry product (Trunk, Branch)	Congo, Iran, Zimbabwe	Ganga et al. (2014), Oskouei et al. (2017), Masuka et al. (2018)
Sawdust lignin	Sawmill waste (Trunk, Branch)	Nigeria	Fadele and Ata (2018)

**Table 2.2:** Tests carried out in previous research.

References	Tests				
	Physical	Mechanical	Durability	Thermal	Others (SEM, Numerical simulation, Cost analysis)
Binici et al. (2005)	Total water absorption	Compressive strength	×	×	×
Vega et al. (2011)	Density, Drying shrinkage	Compressive strength, Flexural strength	×	×	×
Ashour et al. (2015)	Density	×	×	Thermal conductivity	×
Parisi et al. (2015)	×	Compressive strength, Flexural strength	×	×	×
Abanto et al. (2017)	Density	×	×	Thermal conductivity, Thermal diffusivity, Specific heat capacity	×
Türkmen et al. (2017)	Density, Drying shrinkage, Capillary water absorption coefficient	Compressive strength	Ultrasonic pulse velocity	×	×
El Azhary et al. (2017)	Density	×	×	Thermal conductivity, Thermal diffusivity, Specific heat capacity	Dynamic thermal simulation using EnergyPlus for Moroccan climate
Statuto et al. (2018)	Shrinkage	Compressive strength	×	×	×
Wang et al. (2019)	×	Compressive strength	×	×	×
Giroudon et al. (2019)	Density	Compressive strength	Dry abrasion resistance, Geelong drip, Sphere impact resistance, Mould growth kinetics	Thermal conductivity	×

Table 2.2: Tests carried out in previous research (continued).

References	Physical	Mechanical	Durability	Thermal	Others (SEM, Numerical simulation, Cost analysis)
Ouedraogo et al. (2019)	Density, Porosity, Capillary water absorption coefficient	Compressive strength, Flexural strength	Water spray test	Thermal conductivity	×
Khedari et al. (2005)	Density	Compressive strength	×	Thermal conductivity	×
Danso et al. (2015b), Danso (2017)	Density, Linear shrinkage, Capillary water absorption coefficient	Compressive strength, Splitting tensile strength, Pull-out test	Wetting and drying (Wearing), Water spray test	×	×
Thanushan et al. (2019)	Density, Capillary water absorption coefficient	Compressive strength, Flexural strength	Alkaline and acid resistance test, Freeze and thaw resistance, Wet and dry resistance	×	×
Laborel-Préneron et al. (2017; 2018; 2021)	Density	Compressive strength, Flexural strength	Ultrasonic pulse velocity, dry abrasion resistance, Low-pressure water absorption, Geelong drip, Sphere impact resistance	Thermal conductivity, Specific heat capacity, Water vapour permeability, Sorption and desorption isotherms, Moisture buffer value	×
Sangma et al. (2019)	×	Compressive strength, Splitting tensile strength	×	×	×
Purnomo and Arini (2019)	Density, Volume shrinkage, Total water absorption, Crack patterns	Compressive strength, Flexural strength	×	×	×
Mostafa and Uddin (2015; 2016)	Density, Total water absorption	Compressive strength, Flexural strength	×	×	×

*Table 2.2: Tests carried out in previous research (continued).*

References	Physical	Mechanical	Durability	Thermal	Others (SEM, Numerical simulation, Cost analysis)
Islam and Iwashita (2010)	Density	Compressive strength, Ductility, Toughness	×	×	×
Zak et al. (2016)	Density	Compressive strength, Flexural strength	×	×	×
Bruno et al. (2020)	Density, Porosity	×	×	Thermal conductivity	×
Fernea et al. (2019)	Density, Acoustical properties	Compressive strength, Flexural strength	×	Thermal conductivity	×
Muntohar (2011)	Total water absorption	Compressive strength, Flexural strength	×	×	×
Oskouei et al. (2017)	×	Compressive strength, Tensile strength	Durability against water	×	×
Huynh et al. (2017)	Density, Total water absorption, Void volume	Compressive strength, Flexural strength	×	Thermal conductivity	SEM observation
Nshimiyimana et al. (2018)		Compressive strength	×	×	×
Heath et al. (2009)	Density, Linear shrinkage	Compressive strength	×	×	×
Masuka et al. (2018)	Density, Drying shrinkage, Initial rate of water absorption, Total water absorption	Compressive strength	×	×	Estimation of cost of unfired earth bricks
Piani et al. (2020)	Density	Compressive strength	×	×	×
Demir (2008)	×	Compressive strength	×	×	×

*Table 2.2: Tests carried out in previous research (continued).*

References	Physical	Mechanical	Durability	Thermal	Others (SEM, Numerical simulation, Cost analysis)
Fadele and Ata (2018)	Total water absorption	×	×	×	×
Lima et al. (2012)	Total water absorption, Dry specific gravity	Compressive strength, Flexural strength, Diagonal tensile strength	×	×	×
Udawattha et al. (2018)	Density, Linear shrinkage, Total water absorption	Compressive strength, Splitting tensile strength	×	×	SEM observation
Serrano et al. (2016)	×	Compressive strength, Flexural strength	×	×	×
Tran et al. (2018)	×	Compressive strength, Splitting tensile strength	×	×	×
Amina et al. (2018)	Density	×	×	Thermal conductivity, Specific heat capacity	×
Villamizar et al. (2012)	Total water absorption, Linear Shrinkage	Compressive strength, Flexural strength	×	×	×
Namango (2006)	Density, Porosity	Compressive strength, Flexural strength	×	×	×
Ojo et al. (2019)	Density, Total water absorption	Flexural strength	×	×	SEM observation
Chan (2011)	Density, Total water absorption	Compressive strength	Efflorescence	×	×
Mohamed (2013)	Maximum dry density, Shrinkage limit	Compressive strength, Shear strength, Tensile strength	Swelling test	×	×

*Table 2.2: Tests carried out in previous research (continued).*

References	Physical	Mechanical	Durability	Thermal	Others (SEM, Numerical simulation, Cost analysis)
Millogo et al. (2014)	×	Compressive strength, Flexural strength	Water spray test, Abrasion strength	Thermal conductivity	SEM observation
Laibi et al. (2018)	Porosity	Compressive strength, Flexural strength	×	Thermal conductivity	×
Murillo et al. (2005)	Density, Linear shrinkage	Compressive strength	×	×	×
Taallah et al. (2014), Taallah and Guettala (2016)	Density, Capillary water absorption coefficient, Total water absorption	Compressive strength, Tensile strength	Swelling test	Thermal conductivity	×
Lamrani et al. (2019)	Density	×	×	Thermal conductivity, Specific heat capacity, Thermal diffusivity, Thermal effusivity	Dynamic thermal simulation using Design builder software based on EnergyPlus calculation for Moroccan climate
Sharma et al. (2015a; 2015b; 2016)	Density	Compressive strength	Wetting and drying cycling, Water absorption and expansion, Sponge water absorption, Total absorption test, Water spray test, Water strength coefficient	×	×
Galán-Marín et al. (2010; 2013)	Density	Compressive strength, Flexural strength	Ultrasonic pulse velocity	×	×
Adogla et al. (2016)	Density, Capillary water absorption coefficient	Compressive strength	Abrasion resistance	×	×

*Table 2.2: Tests carried out in previous research (continued).*

<b>References</b>	<b>Physical</b>	<b>Mechanical</b>	<b>Durability</b>	<b>Thermal</b>	<b>Others (SEM, Numerical simulation, Cost analysis)</b>
Ayodele et al. (2019)	Density	Compressive strength	×	×	×
Achenza and Fenu (2006)	Density, Porosity, Density, Capillary water absorption coefficient, Total water absorption	Compressive strength	Geelong drip	×	×
Dove (2014)	Density, Linear drying shrinkage	Compressive strength, Flexural strength	×	×	×
Demir (2006)	Density	Compressive strength	×	×	×
Benkhadda and Khaldoun (2019)	×	Compressive strength, Flexural strength	×	Thermal conductivity, Specific heat capacity	×
Vilane (2010)	×	Compressive strength	×	×	×
Ganga et al. (2014)	×	Compressive strength, Young's modulus	Ultrasonic pulse velocity	×	×
Ouattara et al. (2016)	Density	Compressive strength, Flexural strength	×	×	×
De Castrillo et al. (2021)	Density, Capillary water absorption coefficient	Compressive strength, Flexural strength	Weight-loss from immersion	Thermal conductivity	×
Jokhio et al. (2018)	×	Compressive strength, Flexural strength	×	×	×
Charai et al. (2020)	Density	×	×	Thermal conductivity, Thermal diffusivity, Volumetric specific heat	Dynamic thermal simulation using EnergyPlus for Moroccan climate

Table 2.2: Tests carried out in previous research (continued).

References	Physical	Mechanical	Durability	Thermal	Others (SEM, Numerical simulation, Cost analysis)
Chung et al. (2021)	Density, Porosity, Linear drying shrinkage, Moisture absorption	Compressive strength	Moisture absorption	×	SEM observation
Araya-Letelier et al. (2018)	Restrained drying shrinkage distributed cracking	Compressive strength, Flexural strength	Ultrasonic pulse velocity	×	×
Mirón et al. (2017)	Total water absorption	Compressive strength	×	×	×
Tatane et al., (2018a; 2018b), Akhzouz et al. (2021)	Density, Capillary water absorption coefficient	Compressive strength, Splitting tensile strength	×	Thermal conductivity, Thermal resistance, Thermal diffusivity	×
Atiki et al. (2021)	Density	Compressive strength, Flexural strength	Ultrasonic pulse velocity	Thermal conductivity, Volumetric specific heat	×
Charai et al. (2022)	Density, Porosity, Sorption isotherms, Moisture buffering	Compressive strength	×	Thermal conductivity, Thermal diffusivity, Specific heat capacity	Simulation study (Occupant satisfaction)
Thanushan and Sathiparan (2022)	Density, Porosity	Compressive strength, Flexural strength	Resistance against water, salt water and acid, Alkaline resistance, Sorptivity, Wetting and drying resistance, Freezing and thawing resistance	×	×
Araya-Letelier et al. (2021)	Capillary water absorption coefficient, Concentrated restrained drying shrinkage cracking	Compressive strength, Flexural strength	Geelong drip	Thermal conductivity	×

*Table 2.2: Tests carried out in previous research (continued).*

<b>References</b>	<b>Physical</b>	<b>Mechanical</b>	<b>Durability</b>	<b>Thermal</b>	<b>Others (SEM, Numerical simulation, Cost analysis)</b>
Eslami et al. (2022)	Restrained drying shrinkage distributed cracking	Compressive strength, Flexural strength	Water spray test	×	SEM observation
Koutous and Hilali (2021)	Density	Compressive strength, Splitting tensile strength	×	×	×
Kumar and Barbato (2022)	Density, Total water absorption	Compressive strength, Flexural strength	Wetting and drying	×	SEM observation
Mellaikhafi et al. (2021)	Density	×	×	Thermal conductivity, Thermal diffusivity, Thermal effusivity, Volumetric specific heat	Numerical simulation of heat flux, time lag, decremental factor
Ige and Danso (2022)	Capillary water absorption coefficient	Compressive strength, Splitting tensile strength	Geelong drip	×	Cost Analysis, SEM observation
Babé et al. (2021)	Capillary water absorption coefficient	Compressive strength, Flexural strength	Water spray test	Thermal conductivity	×

**Table 2.3:** Types of binders/chemical solutions used in previous research.

<b>References</b>	<b>Binders/Activators</b>
Binici et al. (2005)	Cement, Basaltic Pumice, Lime, Gypsum
Ashour et al. (2015)	Cement, Gypsum
Türkmen et al. (2017)	Gypsum, Elazığ Ferrochrome slag
Wang et al. (2019)	Cement, Gypsum, Gelling agent
Khedari et al. (2005)	Cement
Thanushan et al. (2019), Thanushan and Sathiparan (2022)	Cement
Purnomo and Arini (2019)	Lime
Mostafa and Uddin (2015; 2016)	Cement
Islam and Iwashita (2010)	Cement, Gypsum
Zak et al. (2016)	Cement, Gypsum
Fernea et al. (2019)	Lime
Muntohar (2011)	Lime
Huynh et al. (2017)	Fly ash, NaOH solution
Nshimiyimana et al. (2018)	Calcium carbide residue
Masuka et al. (2018)	Lime, Coal fly ash
Lima et al. (2012)	Cement
Tran et al. (2018)	Cement
Villamizar et al. (2012)	Coal ash
Namango (2006)	Cement
Ojo et al. (2019)	Sodium Hydroxide (NaOH) and Sodium Silicate (Na <sub>2</sub> SiO <sub>3</sub> ) solution
Chan (2011)	Cement

*Table 2.3: Types of binders/chemical solutions used in previous research (continued).*

<b>References</b>	<b>Binders/Activators</b>
Taallah et al. (2014), Taallah and Guettala (2016)	Cement, Lime
Sharma et al. (2015a; 2015b; 2016)	Cement
Chung et al. (2021)	Sodium Hydroxide (NaOH) and Sodium Silicate (Na <sub>2</sub> SiO <sub>3</sub> ) solution
Galán-Marín et al. (2010; 2013)	Alginate, Lignum
Ganga et al. (2014)	Cement
Mirón et al. (2017)	Cement, Lime, Gypsum
Tatane et al. (2018a; 2018b), Akhzouz et al. (2021)	Cement
Koutous and Hilali (2021)	Cement, Lime
Atiki et al. (2021)	Lime
Kumar and Barbato (2022)	Cement
Ige and Danso (2022)	Lime

**Table 2.4:** Overview of research on agro-waste additives for the production of unfired earth blocks.

Agro-waste fibre								
Agro-wastes	References	Content (wt%, vol%) and fibre length (mm)	Unit size (mm)	Soil, sand, and clay type	Density (kg/m <sup>3</sup> )	Max. compressive strength (CS), flexural strength (FS), and splitting tensile strength (STS) (MPa)	Min. Thermal conductivity (W/mK)	Total water absorption (wt%)
Straw (Wheat, Barley)	Binici et al. (2005)	2.5%	150×150×150	Clay	×	CS-5.80	×	36.80
	Islam and Iwashita (2010)	0.5, 1.5, 3% 10, 20, 30 mm	∅ 50×100 ∅ 100×200	Acadama, Bentonite clay, Toyoura sand	820-1110	CS-0.55	×	×
	Vega et al. (2011)	25, 33.3 vol% 50-100 mm	250×120×100	Local soil	1650-1820	CS-3.99 FS-0.82	×	×
	Ashour et al. (2015)	1, 3% 40 mm	240×120×60	Cohesive soil	1357.70-1575.60	×	0.30	×
	Parisi et al. (2015)	0.64% <10 mm	100×200×400 40×40×160	Clayey/silty sand	×	CS-0.46	×	×
	Serrano et al. (2016)	1, 2, 3%	160×40×40	Commercial clay sand	×	CS-2.90 FS-0.29	×	×
	Abanto et al. (2017)	1.5, 1.8, 2.1, 2.5, 3.7%	45×45×12	Soil, sand	1628.70-1766.20	×	0.25	×
	Türkmen et al. (2017)	1 mass% 20 mm	160×40×40	Cohesive soil	1400-1470	CS-4.58	×	×

Table 2.4: Overview of research on agro-waste additives for the production of unfired earth blocks (continued).

Agro-wastes	References	Content (wt%, vol%) and fibre length (mm)	Unit size (mm)	Soil, sand, and clay type	Density (kg/m <sup>3</sup> )	Max. compressive strength (CS), flexural strength (FS), and splitting tensile strength (STS) (MPa)	Min. Thermal conductivity (W/mK)	Total water absorption (wt%)
Straw (Wheat, Barley)	El Azhary et al. (2017)	2, 3, 4, 5% 20 mm	100×100×22	Local Clay	1544.98-1827.58	×	0.26	×
	Oskouei et al. (2017)	0.3, 0.6, 0.9% 10-40 mm	220×220×70 ø150×300	Clay, sand, and gravel	×	CS-8.70	×	×
	Statuto et al. (2018)	3%	×	Clay	×	CS-1.86	×	×
	Giroudon et al. (2019)	3, 6 mass% 10 mm	ø50×50 150×150×50	Quarry fines	1195-1520	CS-3.80	0.15	×
	Lamrani et al. (2019)	10, 20, 30 vol%	×	Clay	1221.43-1554.35	×	0.26	×
	Wang et al. (2019)	5, 10, 15% 2-3 mm	50×100×200	River dredging sludge	×	CS-11.70	×	×
	Koutous and Hilali (2021)	0.75% 10-30 mm	ø100 × 200	Marly earth of a whitish colour	1930	CS-2.74 STS-0.50	×	×
	Mohamed (2013)	0.5, 1, 1.5% 15-25 mm	ø25.4×63.5 ø25×50	Clayey soil	1550-1730	CS-0.50	×	×
De Castrillo et al. (2021)	30, 40, 50, 60, 70 vol%	450×300×50 450×150×50 100×100×50 50×50×50	Local soil	922-1479	CS-2.69 FS-2.03	0.20	×	

Table 2.4: Overview of research on agro-waste additives for the production of unfired earth blocks (continued).

Agro-wastes	References	Content (wt%, vol%) and fibre length (mm)	Unit size (mm)	Soil, sand, and clay type	Density (kg/m <sup>3</sup> )	Max. compressive strength (CS), flexural strength (FS), and splitting tensile strength (STS) (MPa)	Min. Thermal conductivity (W/mK)	Total water absorption (wt%)
Straw (Wheat, Barley)	Piani et al. (2020)	<2%, 17-18%	ø40×40	Clayey sandy silt	1180-1790	CS-6	×	×
	Laborel-Préneron et al. (2018)	3, 6%	ø50×20 180×70×35	Quarry fines	1100-1537	×	0.14	×
	Laborel-Préneron et al. (2017)	3, 6% 15 mm	ø50×20 180×70×35	Quarry fines	1315-1519	CS-3.80 FS-1.80	×	×
Lavender straw	Giroudon et al. (2019)	3, 6 mass% 10 mm	ø50×50 150×150×50	Quarry fines	1585-1772	CS-3.90	0.28	×
Fonio straw	Ouedraogo et al. (2019)	0.2, 0.4, 0.6, 0.8, 1.0% 10 mm	160×40×40	Reddish brown clayey local soil	×	CS-2.90 FS-1.30	0.35	×
Coconut coir	Danso et al. (2015b)	0.25, 0.5, 0.75, 1% 50 mm	290×140×100	Local red, brown soil	1772-1857	CS-3	×	9.80-15.30
	Thanushan and Sathiparan (2022)	0.4% 25 mm	150×150×150 100×100×400 100×100×60	Local soil	1778	CS-3.11 FS-0.92	×	×
	Sangma et al. (2019)	5% 20, 40, 60, 80 mm	150×150×150	Local soil	1450-1510	CS-1.67	×	×

Table 2.4: Overview of research on agro-waste additives for the production of unfired earth blocks (continued).

Agro-wastes	References	Content (wt%, vol%) and fibre length (mm)	Unit size (mm)	Soil, sand, and clay type	Density (kg/m <sup>3</sup> )	Max. compressive strength (CS), flexural strength (FS), and splitting tensile strength (STS) (MPa)	Min. Thermal conductivity (W/mK)	Total water absorption (wt%)
Coconut coir	Khedari et al. (2005)	10, 15, 20 vol%	125×250×100	Lateritic soil, river sand	1344.60-1754.94	CS-5.79	0.65	×
	Thanushan et al. (2019)	0.2, 0.4, 0.6 mass%	150×150×150 400×100×100	Local soil	Dry: 1765-1785 Wet: 2025-2060	CS-3.44 FS-0.99	×	×
	Purnomo and Arini (2019)	4% 250 mm	230×110×55 50×50×50	Soil from hill	×	CS-3.50 FS-0.70	×	30-50
Banana fibre	Mostafa and Uddin (2015)	0.35, 0.175% 25 50 mm	120×120×90 240×120×90	River soil	2050.36	CS-5.92 FS-0.95	×	10-20
	Mostafa and Uddin (2016)	1-5% 50,60,70,80,90,100 mm	120×120×90 240×120×90	River soil	1947	CS-6.19 FS-1.02	×	×
	Thanushan and Sathiparan (2022)	0.4% 25 mm	50×50×50	Local soil	1776	CS-3.16 FS-1.01	×	×
Hemp fibre	Islam and Iwashita (2010)	0.5, 1, 2, 3, 4% 10, 30 mm	∅ 50×100 ∅ 100×200	Acadama, Bentonite clay, Toyoura sand	820-1110	×	×	×
	Laborel-Préneron et al. (2018)	3, 6%	∅50×20 180×70×35	Quarry fines	1271-1591	×	0.20	×

Table 2.4: Overview of research on agro-waste additives for the production of unfired earth blocks (continued).

Agro-wastes	References	Content (wt%, vol%) and fibre length (mm)	Unit size (mm)	Soil, sand, and clay type	Density (kg/m <sup>3</sup> )	Max. compressive strength (CS), flexural strength (FS), and splitting tensile strength (STS) (MPa)	Min. Thermal conductivity (W/mK)	Total water absorption (wt%)
Hemp fibre	Laborel-Préneron et al. (2017)	3, 6% 15 mm	ø50×20 180×70×35	Quarry fines	1221-1603	CS-2.40 FS-1.34	×	×
	Zak et al. (2016)	1%, 3%	160×40×40	Cohesive soil	1060-1700	CS-3.75	×	×
	Bruno et al. (2020)	1.5% 1-5 mm	200×100×50	Illitic soil	2244-2316	×	1.27	×
	Fernea et al. (2019)	50, 66, 75 vol%	150×150×30 40×40×160	Earth clay	966-1060	CS-0.94 FS-0.47	0.09	×
Wood fibre	Heath et al. (2009)	×	222.8×105.6× 66.9	Conventional Clay	1597	CS-10.50	×	×
	Piani et al. (2020)	<2%, 17-18% 20 mm	ø 40×40	Clayey sandy silt	1180-1790	CS-6	×	×
Sugarcane bagasse	Danso et al. (2015b)	0.25, 0.5, 0.75, 1% 80 mm	290×140×100	Local red, brown soil	1790-1867	CS-2.80	×	10.40- 16.50
	Kumar and Barbato (2022)	0.5, 1% 55 mm	290×145×75 100×100×75	Local soil	1628-1485	CS-4.50 FS-0.89	×	12.55-4.12
Corn plant fibre	Serrano et al. (2016)	1, 2, 3%	160×40×40	Commercial clay Sand	×	CS-3.25 FS-0.39	×	×

Table 2.4: Overview of research on agro-waste additives for the production of unfired earth blocks (continued).

Agro-wastes	References	Content (wt%, vol%) and fibre length (mm)	Unit size (mm)	Soil, sand, and clay type	Density (kg/m <sup>3</sup> )	Max. compressive strength (CS), flexural strength (FS), and splitting tensile strength (STS) (MPa)	Min. Thermal conductivity (W/mK)	Total water absorption (wt%)
Corn silk fibre	Tran et al. (2018)	0.25, 0.5, 1% 10 mm	ø50×100	Silty sand	×	CS-9	×	×
Cassava peel	Villamizar et al. (2012)	2.5, 5%	320×80×150	Raw clay from local brick plant	×	CS-2.60 FS-0.58	×	26.38- 29.36
Olive waste fibre	Lamrani et al. (2019)	10, 20, 30 vol%	×	Clay	1398.30-1642.59	×	0.40	×
Pineapple leaf fibre	Chan (2011)	0.25, 0.5, 0.75% 10 mm	100×50×30	Clay soil	1250-1430	CS-18	×	1.10-1.25
	Vodounon et al. (2018)	1, 2, 3, 4, 5%	×	Laterite soil	×	CS- 4.81 FS-0.92	×	×
Flax fibre	Zak et al. (2016)	1, 3%	160×40×40	Cohesive soil	1080-1700	CS-4.50	×	×
Wheat hay fibre	Mohamed (2013)	0.5, 1, 1.5% 15-25 mm	ø25.4×63.5 ø25×50	Clayey soil	1550-1730	CS-0.50	×	×
Sisal fibre	Namango (2006)	0.25, 0.5, 0.75, 1.0, 1.25% 3-10 mm	160×40×40	Bautzen clay	1738-1895	CS-9.14 FS-1.63	×	×
	Ojo et al. (2019)	0.5, 1.0, 2.0% 10 mm	200×50×15	Ceramic company soil	1700-1740	FS-5.50	×	19-20

Table 2.4: Overview of research on agro-waste additives for the production of unfired earth blocks (continued).

Agro-wastes	References	Content (wt%, vol%) and fibre length (mm)	Unit size (mm)	Soil, sand, and clay type	Density (kg/m <sup>3</sup> )	Max. compressive strength (CS), flexural strength (FS), and splitting tensile strength (STS) (MPa)	Min. Thermal conductivity (W/mK)	Total water absorption (wt%)
Fescue	Serrano et al. (2016)	1, 2, 3%	160×40×40	Commercial clay sand	×	CS-2.88 FS-0.60	×	×
Kenaf or Hibiscus cannabinus fibre	Millogo et al. (2014)	0.2, 0.4, 0.8% 30, 60 mm	295×140×100	Lateritic soil	×	CS-2.85 FS-1.15	1.30	×
	Laibi et al. (2018)	1.2% 10, 20, 30 mm	40×40×160	Local soil	×	CS-6.40 FS-2.75	1	×
Henequen fibre	Murillo et al. (2005)	0.25, 0.5, 0.75, 1.0%	ø50×100	Brick manufacturer clay	1884-1906	CS-5.22	×	×
	Islam and Iwashita (2010)	0.5, 1, 2, 3, 4% 5, 10, 20, 30 mm	ø50×100 ø100×200	Acadama, Bentonite clay, Toyoura sand	820-1110	CS-1.30	×	×
Jute fibre	Araya-Letelier et al. (2021)	0.5, 2% 7, 15 30 mm	155×105×70 ø70×140 100×100×100 310×105×70 300×150×80 300×300×60	Clayey soil	×	CS-2.25 FS-0.63	0.409	×
Grass	Demir (2008)	2.5, 5, 10%	100×75×40	Raw brick clay	×	CS-5.15	×	×

Table 2.4: Overview of research on agro-waste additives for the production of unfired earth blocks (continued).

Agro-wastes	References	Content (wt%, vol%) and fibre length (mm)	Unit size (mm)	Soil, sand, and clay type	Density (kg/m <sup>3</sup> )	Max. compressive strength (CS), flexural strength (FS), and splitting tensile strength (STS) (MPa)	Min. Thermal conductivity (W/mK)	Total water absorption (wt%)
Oil palm fruit fibre	Danso et al. (2015b)	0.25, 0.5, 0.75, 1% 38 mm	290×140×100	Local red and brown soil	1802-1889	CS-3	×	9.40-14.30
	Lamrani et al. (2019)	10, 20, 30 vol%	×	Clay	1218.74-1572.19	×	0.28	×
Date palm fibre	Taallah et al. (2014), Taallah and Guettala (2016)	0.05, 0.10, 0.15, 0.2% 35 120 mm	100×100×200	Local soil, crushed sand	1892-1930	CS-12.50	0.76	9.50-11.30
	Koutous and Hilali (2021)	0.75% 30 mm	ø100 × 200	Marly earth of a whitish colour	1960	CS-3.25 STS-0.46	×	×
	Atiki et al. (2021)	0.1, 0.2, 0.3, 0.4, 0.5% 1-4 mm	100×100×200	Local soil, crushed sand	2032-2066	CS-13.50 FS-5.26	0.846	×
	Mellaikhafi et al. (2021)	3, 6% 5-10 mm	ø110×22.5	Local soil	1122.3-1197.8	×	0.265	×
Oil palm fruit bunch fibre	Chan (2011)	0.25, 0.5, 0.75 % 10 mm	100×50×30	Clay soil	1300-1500	CS-19.50	×	1.10-2

Table 2.4: Overview of research on agro-waste additives for the production of unfired earth blocks (continued).

Agro-wastes	References	Content (wt%, vol%) and fibre length (mm)	Unit size (mm)	Soil, sand, and clay type	Density (kg/m <sup>3</sup> )	Max. compressive strength (CS), flexural strength (FS), and splitting tensile strength (STS) (MPa)	Min. Thermal conductivity (W/mK)	Total water absorption (wt%)
Eucalyptus pulp microfibre	Ojo et al. (2019)	0.5, 1.0, 2.0% 0.7 mm	200×50×15	Ceramic company soil	1680-1700	FS-4.50	×	20-21.25
Palm bark fibre	Oskouei et al. (2017)	0.3, 0.6, 0.9%	220×220×70 ø150×300	Clay, sand, gravel	×	CS-16.53	×	×
	Eslami et al. (2022)	0.25, 0.5, 0.75, 1% 10-60 mm	220×220×50 220×50×50 50×50×50 ø5×180	Local soil	×	CS-5.03 FS-1.12	×	×
Pinus roxburghii fibre (PR), Grewia optiva (GO) fibre	Sharma et al. (2015a; 2015b; 2016)	PR-0.5, 1, 1.5, 2% 30 mm GO-0.5, 1, 2% 30 mm	ø38×76 190×90×90	Local sand, clay	PR: 1700-1950 GO: 1650-1890	PR: CS-2.25 GO: CS-3	×	PR: 2.33-3.62 GO: 2.07-2.67
Seaweed fibre	Achenza and Fenu (2006)	10% 10 mm	100×100×100	Quaternary sediment	1720-1810	CS-4.44	×	×
	Dove (2014)	0.1%	160×40×40	Silt loam	1690-2250	CS-1.64 FS-0.95	×	×

Table 2.4: Overview of research on agro-waste additives for the production of unfired earth blocks (continued).

Agro-wastes	References	Content (wt%, vol%) and fibre length (mm)	Unit size (mm)	Soil, sand, and clay type	Density (kg/m <sup>3</sup> )	Max. compressive Strength (CS), flexural Strength (FS), and splitting tensile strength (STS) (MPa)	Min. Thermal conductivity (W/mK)	Total water absorption (wt%)
Tea waste	Demir (2006)	2.5, 5 mass%	40×70×100	Clay	×	CS-7.60	×	×
	Chung et al. (2021)	1, 2.5, 5, 10, 15%	115×110×76	Mill clay residues	1400-2160	CS-22.51	×	×
Tobacco residue	Demir (2008)	2.5, 5, 10%	100×75×40	Raw brick clay	×	CS-4.75	×	×
Pig hair	Araya-Letelier et al. (2018)	0.5, 2% 7, 15, 30 mm	310×105×70	Clayey soil	×	CS-1.92 FS-0.49	×	×
	Galán-Marín et al. (2010; 2013)	0.25, 0.5% 10 mm	160×40×40 40×40×40	Soil from brick manufacturer	1790-1800	CS-4.44 FS-1.45	×	×
Sheep wool	Statuto et al. (2018)	3%	×	Local clay	×	CS- 4.32	×	×
	Benkhadda and Khaldoun (2019)	0.25, 0.5, 1% 30-50 mm	160×40×40 100×50×50	Local red clay Illite	×	CS-3.04 FS-1.83	0.19	×
Neem fibre	Babé et al. (2021)	1, 2, 3, 4% 2-6 mm (Straw) 2-4 (Leaf)	160×40×40 100×100×30	Local soil	1740-1801(Straw) 1559-1736 (Leaf)	CS-6.35 (Straw) 5.59 (Leaf) FS- 0.22 (Straw) 0.11 (Leaf)	0.74 (Straw) 0.43 (Leaf)	×

Table 2.4: Overview of research on agro-waste additives for the production of unfired earth blocks (continued).

Agro-waste powder								
Agro-wastes	References	Content (wt%, vol%) and fibre length (mm)	Unit size (mm)	Soil, sand, and clay type	Density (kg/m <sup>3</sup> )	Max. compressive strength (CS), flexural strength (FS), and splitting tensile strength (STS) (MPa)	Min. Thermal conductivity (W/mK)	Total water absorption (wt%)
Eggshell powder	Adogla et al. (2016)	10, 20, 30, 40%	200×100×75	Laterite soil	2001-2044	CS-3.05	×	×
Eggshell and sawdust ash	Ayodele et al. (2019)	2, 4, 8, 16%	291×138×115	Laterite soil	1489-1749	CS-1.25	×	×
Corn husk ash	Amina et al. (2018)	10, 20%	×	Local rammed earth	942.50-959.50	×	0.48	×
Argan nut	Tatane et al. (2018b), Akhzouz et al. (2021)	2, 4, 6 mass%	14×29.50	Local soil	1825-2062.50	CS-3.12 FS-0.80	0.48	10.10-11
Sugarcane bagasse ash	Lima et al. (2012)	2, 4, 8%	340×340×110	Sandy earth	×	CS-2.89	×	11.57-13.79
	Huynh et al., (2017)	10, 20, 30, 40, 50%	220×105×60	Natural sand	1930-2075	CS-30.30 FS-6.17	0.68	7.50-10.40
Rice huk ash	Nshimiyimana et al. (2018)	10-40%	140×140×95	Clayey soil	×	CS-6.60	×	×
	Muntohar (2011)	5, 10, 15%	230×110×55 600×150×150	Clay soil	×	CS-20.70 FS-0.05	×	0.80-9.60

Table 2.4: Overview of research on agro-waste additives for the production of unfired earth blocks (continued).

Agro-wastes	References	Content (wt%, vol%) and fibre length (mm)	Unit size (mm)	Soil, sand, and clay type	Density (kg/m <sup>3</sup> )	Max. compressive strength (CS), flexural strength (FS), and splitting tensile strength (STS) (MPa)	Min. Thermal conductivity (W/mK)	Total water absorption (wt%)
Rice husk powder	Oskouei et al. (2017)	0.3, 0.6, 0.9%	220×220×70 ø150×300	Clay, sand, gravel	×	CS-4.14	×	×
Cassava powder	Namango (2006)	1.5, 2.5, 4, 5, 7, 10, 15, 20%	×	Bautzen clay	1635.31-1781.25	CS-7.36 FS-1.71	×	×
	Demir (2008)	2.5, 5, 10%	100×75×40	Raw brick clay	×	CS-5.10	×	×
	Vilane (2010)	5, 10, 15, 20	152.4×228.6	Local soil	×	CS-3.30	×	×
	Ganga et al. (2014)	2, 4, 6, 8%	160×40×40	Local clayey soil	×	CS-13.45	×	×
	Jokhio et al. (2018)	10, 20, 30, 40%	150×150×150 150×150×500	Clay	×	CS-2.43 FS- 0.45	×	×
	Charai et al. (2020)	2, 4, 6, 8, 10%	×	Local clayey soil	1648.51- 1985.45	×	0.63	×
Sawdust	Ouattara et al. (2016)	5, 10, 15, 20%	220×110×80	Clay	1220.20-2000	CS-4.50 FS-1.40	×	×
	De Castrillo et al. (2021)	30, 40, 50, 60, 70 vol%	450×300×50 450×150×50 100×100×50 50×50×50	Local soil	935-1505	CS-4.25 FS-2.99	0.23	×
	Tatane et al. (2018a)	2, 4, 6 mass%	14×29.50	Local soil	×	CS-2.56	0.46	11.28-13
	Charai et al. (2022)	8%	150×150×40	Local soil	2380	CS-1.24	0.50	×

Table 2.4: Overview of research on agro-waste additives for the production of unfired earth blocks (continued).

Others (neither fibre nor powder)								
Agro-wastes	References	Content (wt%, vol%) and fibre length (mm)	Unit size (mm)	Soil, sand, and clay type	Density (kg/m <sup>3</sup> )	Max. compressive strength (CS), flexural strength (FS), and splitting tensile strength (STS) (MPa)	Min. Thermal conductivity (W/mK)	Total water absorption (wt%)
Rice husk	Ige and Danso (2022)	0.25, 0.5, 0.75, 1%	100×100×140	Local soil	×	CS- 5.17 STS-0.95	×	×
Dawul Kurudu	Udawattha et al. (2018)	5, 10, 15, 20%	×	Podzolic soil	1800-1850	CS-0.50	×	9.50-13.30
Pines gum	Udawattha et al. (2018)	5, 10, 15, 20%	×	Podzolic soil	1925-2052	CS-2.65	×	9.30-15
Bael resin	Udawattha et al. (2018)	5, 10, 15, 20%	×	Podzolic soil	×	CS-0.13	×	×
Jack Resin	Udawattha et al. (2018)	5, 10, 15, 20%	×	Podzolic soil	×	CS-0.24	×	×
Agarwood	Udawattha et al. (2018)	5, 10, 15, 20%	×	Podzolic soil	×	CS-0.20	×	×
Sugarcane bagasse polymer	Udawattha et al. (2018)	5, 10, 15, 20%	×	Podzolic soil	1800-1825	CS- 0.50	×	10-11.30
Wood apple	Udawattha et al. (2018)	5, 10, 15, 20%	×	Podzolic soil	×	CS-0.25	×	×

Table 2.4: Overview of research on agro-waste additives for the production of unfired earth blocks (continued).

Agro-wastes	References	Content (wt%, vol%) and fibre length (mm)	Unit size (mm)	Soil, sand, and clay type	Density (kg/m <sup>3</sup> )	Max. compressive strength (CS), flexural strength (FS), and splitting tensile strength (STS) (MPa)	Min. Thermal conductivity (W/mK)	Total water absorption (wt%)
Grounded olive stone	Serrano et al. (2016)	5, 10, 15%	160×40×40	Commercial clay sand	×	CS-1.61 FS-0.16	×	×
Walnut shell	Mirón et al. (2017)	5, 10, 15, 20%	100×200×50	Local soil	×	CS-6.00	×	18.50-30
Corn cob	Laborel-Préneron et al. (2017)	3, 6% 15 mm	ø50×20 180×70×35	Quarry fines	1754-1878	CS-3.20	×	×
	Laborel-Préneron et al. (2018)	3, 6%	ø50×20 180×70×35	Quarry fines	1565-1671	×	0.25	×
Wood aggregate/ Wood chips	Masuka et al. (2018)	1.5, 3%	225×105×65 ø 60×85	Clayey soil	1600	Dry CS-8.30 Wet CS-1.49	×	11-16
	Ganga et al. (2014)	2, 4, 6, 8%	160×40×40	Local clayey soil	×	CS-13.72	×	×
	Oskouei et al. (2017)	0.3, 0.6, 0.9% 10 mm	220×220×70 ø150×300	Clay, sand, gravel	×	CS-6.91	×	×
Sawdust lignin	Fadele and Ata (2018)	4, 8, 12 mass%	285×130×115	Laterite	×	×	×	2-6

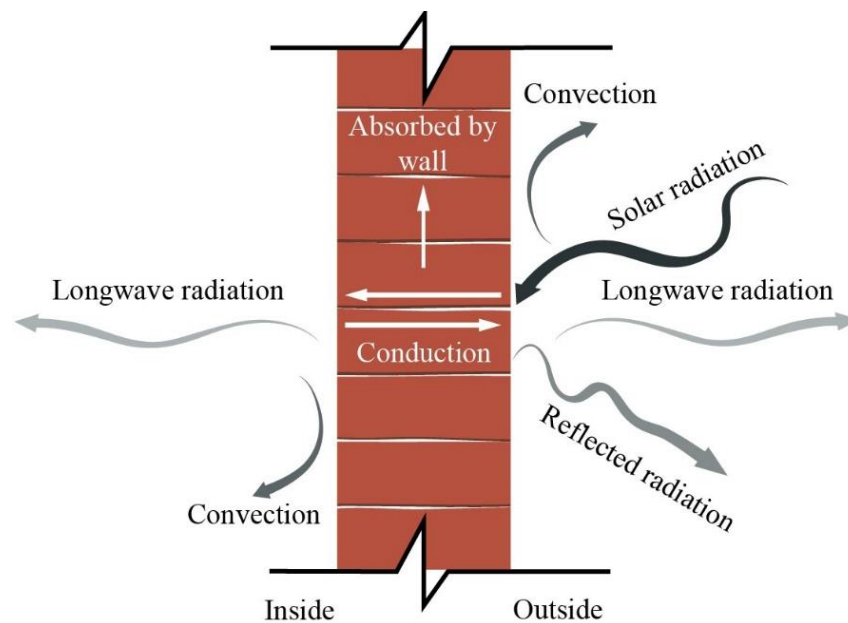
## **2.4 Thermal Performances of Building Materials**

The building envelope, consisting of various components such as the foundation, wall, fenestration, roof, shading device, etc., serves as a key interface between the indoor and outdoor environments (Sadineni et al., 2011). Building walls, which form the bulk of the envelope, provide thermal comfort inside the building by regulating variations in outdoor weather conditions and thereby determining the heating and cooling loads (Gorantla et al., 2016). Udawattha and Halwatura (2016) described the building envelope wall as the third skin of the human body that supports to keep the body temperature steady even though the outside temperature fluctuates. Watson (1983) stated that the building envelope is a system that controls heat exchange between indoor and outdoor environments. The basic control mechanism is the acceptance or rejection of heat gain from the external and internal heat sources, establishing a new microclimate for the interior. According to Givoni (1976), the thermal behaviour of materials has a very strong impact on occupants' comfort conditions both in the presence and absence of the mechanical control system since the thermophysical properties of the materials determine the indoor air temperature and heating or cooling demand.

### ***2.4.1 Heat Transfer Through the Walls***

Heat is a form of energy that can be transferred between objects or systems with different temperatures (transmitting from a warmer object to a cooler object or from a higher temperature system to a lower temperature system) (Day et al., 2010). Heat transfer through the building wall is a complex as well as dynamic process that happens via conduction, convection, and radiation (Givoni, 1976) (Figure 2.5). Conduction is the process by which heat is transported due to the molecular excitement within solid and stagnant fluid materials as a result of temperature differences. As the molecules vibrate more in the warmer part of the material than the cooler part, they transfer some of their energy to the molecules nearby, which are less vibrating, thus contributing to the heat transfer from the warmer side of the material to the cooler side. Convection is the characteristic of fluids (liquids and gases) that occurs due to the movement of the fluid's molecules. Radiation, on the other hand, refers to heat transmission by electromagnetic

waves (infrared radiation), rather than particles (Sidebotham, 2015; Stewart, 2021). All heat transfer modes through the building envelope depend on the size, shape, composition of the materials, and orientation of the construction (Radivojević and Đukanović, 2018). The primary mechanism for heat flow through building envelopes is the temperature-dependent heat transfer from a fluid to a solid body and vice versa. For example, in the daytime, solar radiation hits the external wall surface, a part of which is released to the outdoor environment and the other part is absorbed and conducted across the material. The interior surface of the wall then exchanges heat with the room air and other surfaces through convection and radiation. These heat transfer methods regulate the indoor air temperature and consequently influence the state of thermal comfort. The heat exchange rate and direction through the building envelope depend on several parameters, including solar gain, indoor temperature, outdoor temperature, material thermophysical properties, and exposed surface area. The material thermophysical properties that affect the heat transfer rate are density, thermal conductivity, heat capacity, thermal resistance, thermal transmittance, and surface characteristics (Givoni, 1976; Schiavoni et al., 2016).



(a)

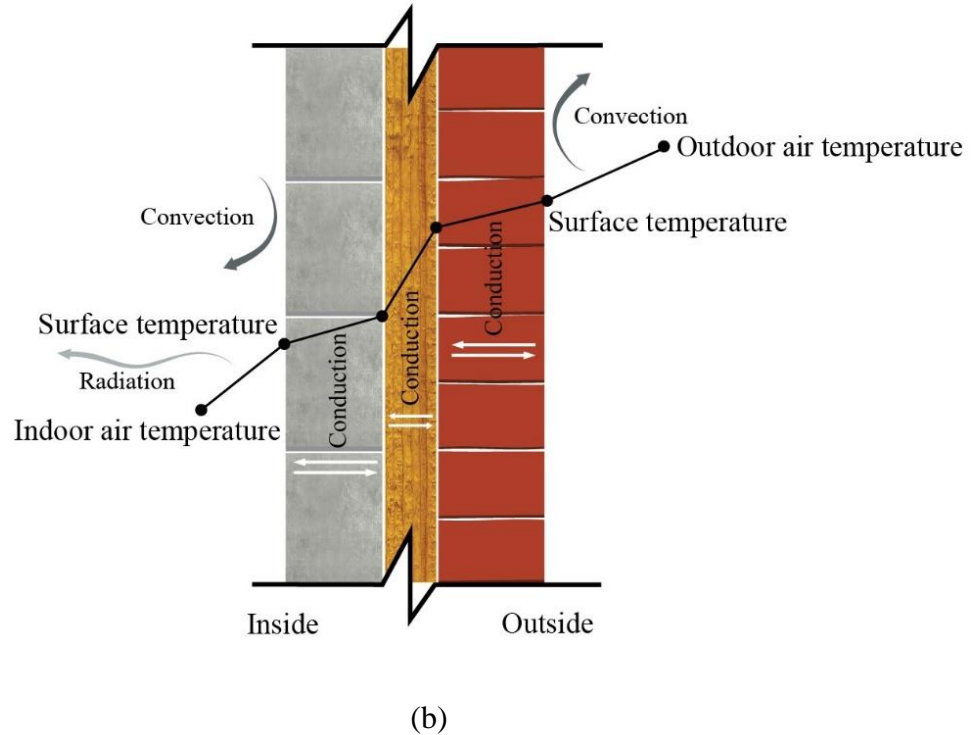


**Figure 2.5:** Heat transfer process across: (a) solid wall (Nayak and Prajapati, 2006) and (b) composite wall (Paraschiv et al., 2020).

### ***2.4.2 Thermophysical Properties of the Building Materials***

The responses of different building wall materials to the environment vary depending on their inherent characteristics, and the most significant energy-saving aspects of building materials are heat absorption and transmission capability. The density, thermal conductivity, and specific heat capacity are the three basic thermophysical properties required for the thermal behaviour analysis of the building materials (Vincelas et al., 2017; Wonorahardjo et al., 2020). Other properties such as thermal transmittance, thermal resistance, thermal diffusivity, thermal effusivity, and thermal mass can be determined from the basic properties.

**Density:** Density is defined as the mass of material per unit volume, and it increases with the decrease in pore space in the material. The thermal properties of the material significantly depend on the density since lightweight materials have more insulating

characteristics while heavyweight materials have more heat storage capacity (Hall and Hamilton, 2015).

**Thermal conductivity:** Thermal conductivity is the rate of heat transmission by the conduction process through a unit cross-section area of the material in the presence of a temperature gradient. Materials with lower thermal conductivity transmit less heat than materials with higher conductivity (Mahlia et al., 2007; Zhao et al., 2016).

**Specific heat capacity:** Specific heat capacity is the amount of heat required to raise the temperature per unit mass. Specific heat capacity is independent of the size of the material. However, heat absorption per volume of the material can be optimised with higher density and heat capacity (Pan et al., 2017).

**Thermal transmittance:** Thermal transmittance, or U-value, is the heat transfer rate through a structure (single or composite), divided by the temperature differences across the structure. The U-value of a structure depends on the thermal resistance, or R-value, of each layer in the construction (Evangelisti et al., 2015; Zheng et al., 2016). The U-value is inversely proportional to the R-value and can be calculated by summing the thermal resistances of the layers that make up the structure plus its internal and external surface resistances. The higher the resistance of a material, the less the heat it loses.

**Thermal diffusivity and effusivity:** Thermal diffusivity corresponds to the unsteady state of heat transfer. It shows how quickly the temperature of a material reaches thermal equilibrium with the surrounding temperature. A higher value of thermal diffusivity indicates faster heat propagation through the material (Corasaniti et al., 2020). On the other hand, thermal effusivity is the speed at which the material surface gets warm (Verbeke and Audenaert, 2018). In other terms, it is defined as the material's ability to exchange thermal energy with its surroundings (Demezhko, 2011). The formulas are:

$$\alpha = \lambda / \rho C_p \quad (2.1)$$

$$\tau = \sqrt{\lambda \rho C_p} \quad (2.2)$$

where  $\alpha$  ( $\text{m}^2/\text{s}$ ) is the thermal diffusivity,  $\tau$  ( $\text{Ws}^{1/2}/\text{m}^2\text{K}$ ) is the thermal effusivity,  $\lambda$  ( $\text{W}/\text{mK}$ ) is the thermal conductivity,  $\rho$  ( $\text{kg}/\text{m}^3$ ) is the density, and  $C_p$  ( $\text{J}/\text{kgK}$ ) is the specific heat capacity.

**Thermal mass:** Thermal mass is the amount of heat energy that an object can absorb and store. In the building, thermal mass can significantly minimise indoor temperature fluctuation, thereby reducing the heating and cooling demand. Ideal materials for thermal mass require a combination of properties such as a high specific heat capacity (optimising the heat stored), a high density (heavier materials can store more heat), and moderate thermal conductivity (sustaining heat flow rates with the variation of the heating and cooling cycle) (Gregory et al., 2008). Thermal mass absorbs heat during warm weather conditions and makes the interior comfortable, reducing the cooling demand substantially. Then, accumulated heat energy is released into the interior of the building during the night as it cools, eventually decreasing the heating demand. Thermal mass can also be used in areas with high night temperatures; however, in this situation, the building must be ventilated to release the stored heat energy to cooler outdoor night air (Shaviv et al., 2001; Memarian et al., 2020).

### ***2.4.3 Thermal Performance Assessment of the Building***

Thermal comfort is regarded as the most important parameter of IEQ and has an influence on the design of the building envelope (Frontczak and Wargocki, 2011; Yang et al., 2014). Thermal comfort is defined as “the state of mind that expresses satisfaction with the thermal environment in which it is located” (ASHRAE Standard 55, 2010). The human body tries to maintain a temperature of around 37 °C, which is achieved by heat exchange between the human body and the environment via convection, radiation, and evaporation (ASHRAE Standard 55, 2010). Occupants’ thermal comfort directly influences the energy consumption of a building since uncomfortable conditions lead to adjustments of inefficient systems (heating, cooling, lighting, etc.). Thermal discomfort can also be caused by a building itself if the appropriate envelope materials are not selected for its construction during the design phase. The building envelope serves as both a separation from the outside environment and a barrier against climate variables that directly affect the building. Therefore, the thermophysical properties of building

materials have an impact on indoor thermal comfort because heat and cold can enter the building through them. Studies revealed that materials with lower thermal conductivity and diffusivity values exhibit less indoor temperature fluctuation than materials with higher values, thereby contributing to thermal comfort and energy savings (Kumar and P Singh, 2013; Latha et al., 2015).

Thermal performance assessment of the building is the method of modelling the energy transfer between the building and its surrounding environment (Nayak and Prajapati, 2006). This method not only depends on the weather conditions but also on whether it is a conditioned or non-conditioned building. In the conditioned building, the heating and cooling loads are estimated to select or design the proper heating, ventilation and air conditioning (HVAC) system, whereas for the non-conditioned building, indoor temperature variations are analysed to estimate the comfortable periods by the thermal performance assessment (Badea, 2015). Therefore, it is essential to know how to measure the thermal efficiency of the building to achieve energy efficiency under comfortable indoor conditions. A range of factors determines the thermal performance of the building, including design variables (orientation, wall, roof, window types, shape, etc.), material properties (thermal conductivity, density, specific heat capacity, etc.), weather data (temperature, humidity, radiation, wind speed, etc.), and building operation data (internal gain, air exchange, etc.) (Pathirana et al., 2019). Hsieh and Wu (2012) stated that the building envelope is the most important element to evaluate the energy efficiency of the building, and improving the properties of the envelope can lead to a successful energy-saving design that can reduce energy loss during the operation.

The envelope material properties govern the time lag or thermal lag (TL) and decrement factor (DF) which determine the heat transfer rate across a wall. The time taken by the maximum outside surface temperature waves for propagation into the internal surface is termed TL. On the other hand, DF indicates the decrease in the rate of indoor temperature variations (Figure 2.6) and is calculated by the following Equation (2.3) (Asan, 2006; Kontoleon and Bikas, 2007),

$$DF = \frac{T_{i,max} - T_{i,min}}{T_{e,max} - T_{e,min}} \quad (2.3)$$

where  $DF$  is the decrement factor,  $T_{i,max}$ ,  $T_{i,min}$  denote the maximum and minimum inside surface temperatures and  $T_{e,max}$ ,  $T_{e,min}$  represent the maximum and minimum outside surface temperatures of the wall, respectively. TL and DF vary according to the thermophysical properties, wall configuration, and thickness of the materials (El Fgaier et al., 2015; El Fgaier et al., 2016). The heat waves need a longer time to pass through the materials with increased thickness, density, and resistivity (Udawattha and Halwatura, 2016). When TL is longer, the internal temperature variations relative to the outside temperature will be delayed, and a lower DF is advantageous to keep the indoor temperature stable regardless of unstable outdoor temperature.

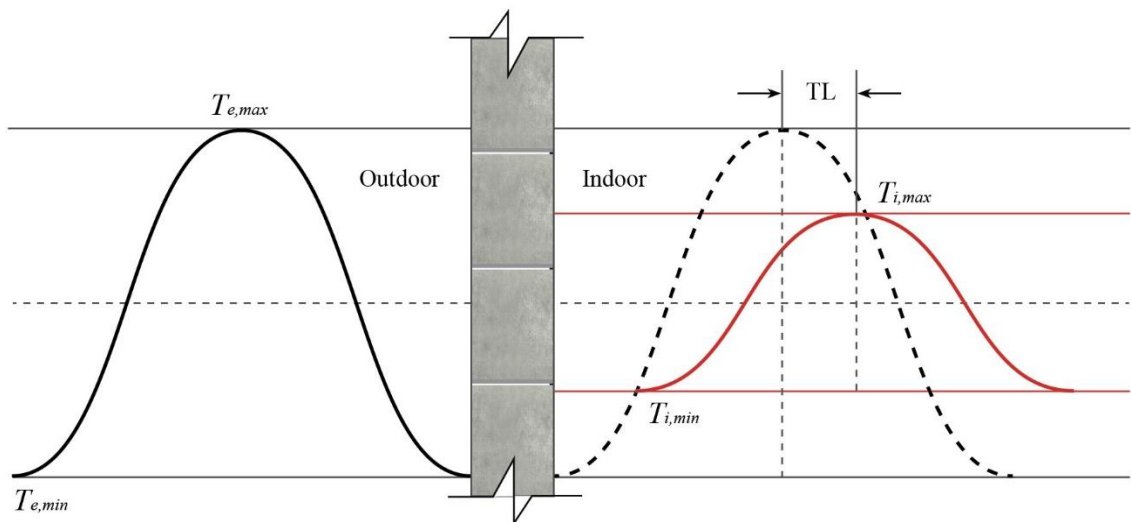


**Figure 2.6:** Heatwave propagation through an opaque wall and representation of TL and DF.

#### ***2.4.4 Previous Numerical Simulation Investigations on Building Wall Materials***

Several simulation studies have been conducted on the thermal efficiency assessment of the building envelope in different climatic conditions. Chowdhury et al. (2015) experimentally and numerically investigated the indoor thermal condition of the

production spaces of the ready-made garment factory building in Dhaka, Bangladesh. The study considered two variables (material categories and exterior wall thickness) for the simulation studies, where nineteen different exterior wall constructions were examined. They developed a correlation matrix between the air temperature, operative temperature, and mean radiant temperature of different zones of the production spaces for different building material construction types. Udawattha and Halwatura (2016) analysed field measurements and computer-based simulation studies to understand the thermal efficiency and structural cooling of three common wall materials (brick, cement block, and concrete mud block) in Sri Lanka. The field study was carried out on three selected buildings constructed with three different wall materials of dissimilar thicknesses. To create a comparable situation, the study then simulated one building, keeping wall thickness similar for three materials. The research further assessed the various thicknesses of wall materials to determine the most appropriate one for the Sri Lankan climate. Mohammad and Shea (2013) investigated the steady-state and dynamic thermal properties of five modern wall constructions with different materials in Tehran. The study stated that steady-state analysis overlooks the dynamic behaviour of the building under realistic conditions. Hence, the thermal transmittance calculated from the steady-state study is not a reliable measure for the building materials' thermal performance since materials with an equal thermal transmittance value can absorb and emit heat at different rates under dynamic weather conditions. The study highlighted the evaluation of the dynamic behaviour of the entire building to optimise the choice of envelope materials for maximum thermal comfort and energy efficiency. Ascione et al. (2015) proposed the residential building envelope optimisation for the Mediterranean climates by performing simulation analysis in EnergyPlus and MATLAB. The study included different variables such as the density and thickness of the masonry layers, insulation layer thickness, and window quality. Zhu et al. (2009) compared the energy impacts of mass walls and traditional wood-framed walls in Las Vegas, Nevada, using the Energy10 simulation tool. The research considered two equal-sized houses where only the external walls were contrasted with the mass walls and traditional walls. Rattanongphisat and Rordprapat (2014) assessed the impact of the air conditioning unit on a traditional building's cooling energy demand using energy simulation. The research revealed that building energy demand can be reduced up to 28% by only using low thermal conductivity building wall

materials. As a case study, Sadeghifam et al. (2016) evaluated the energy efficiency of the University Technology Malaysia library building with 8 different wall construction styles in the Ecotect programme. The simulation inputs included temperature, operation type, user number, working period, cooling system, and running time. The authors also compared the simulation results with the field measurements to determine the most appropriate construction for the Malaysian climate. Kisilewicz (2019) simulated a small office space (4 m × 5 m), including a south-facing glazing and a high thermal load from the equipment to investigate the role of external walls on indoor thermal comfort in Poland. The simulation was performed in EnergyPlus by only modifying the two-layer wall structure consisting of ceramic blocks and an insulation layer. In the same climate, Strzałkowski and Garbalińska (2018) investigated the thermal performance of a typical flat (50 m<sup>2</sup>) constructed of different load-bearing wall materials using WUFI Plus software. In order to accurately evaluate the parameters associated with the thermal accumulation, the transmittance value of the walls was kept equal by making the insulation width variable.

The numerical simulation studies in the literature aimed at minimising building energy consumption, taking into account a range of parameters and underlined that these parameters should be carefully considered when assessing the actual performance of the wall materials.

## **2.5 Tropical Climate Context**

The tropical climate zone occupies around 40% of the earth's surface and refers to the regions around the equator between the Tropic of Cancer in the Northern Hemisphere (23°26'12.6"N) and the Tropic of Capricorn in the Southern Hemisphere (23°26'12.6"S) (Figure 2.7). The tropical climate is classified into three types: tropical wet and dry (savannah), tropical rainforest (equatorial), and tropical monsoon (Kiprop, 2017). Typical features of tropical weather include high temperatures exceeding 30 °C, high humidity exceeding 80%, and intense solar insolation. The Köppen climate classification system describes the tropical climate as a non-arid one in which the mean annual temperature is approximately 18 °C (Kottek et al., 2006). As rainfall dominates variations in different seasons in tropical areas, temperatures in this zone are fairly stable throughout the year,

in contrast with the subtropical areas, which are characterised by temperature fluctuations of varying degrees and lengths of the day. In the tropical zone, sun rays hit nearly overhead at midday, and the cool day quickly gets warm until the early afternoon when temperatures reach the warmest. Afterwards, space starts to cool off somewhat by the late afternoon when less heat energy hits the surface of the Earth. Nevertheless, it remains warm until the early evening after the sunset but begins to cool quickly before the sunrise of the next morning.



**Figure 2.7:** Tropical climate zone (Feeley and Stroud, 2018).

## 2.6 Research Gap and Contribution to the Novelty

- In recent years, agro-wastes incorporated unfired earthen materials have been earning an increasing interest due to their environment-friendly nature with high energy efficiency potential. The findings of previous studies reveal that eggshell, sawdust, and coconut husk have the potential to enhance the characteristics of earthen materials. However, it has been observed that most of the studies concentrated on assessing physico-mechanical properties, and limited research is available on durability and thermal properties tests. Also, the majority of the studies in the literature have employed chemical binders with these agro-wastes to

produce the samples. These materials are responsible for environmental degradation with a high carbon footprint and embodied energy (Udawattha and Halwatura, 2016). Consequently, the production of agro-wastes incorporated unfired earth blocks without chemical binders provides the greatest advantages in terms of sustainability. This study, therefore, investigated the physico-mechanical, durability, as well as thermal properties of the eggshell, sawdust, and coconut husk blended unfired earth blocks without any chemical binders.

- Moreover, this study employed the agro-wastes in the mixture not only separately but also in combination, which is another novel aspect of this study. There has been no published study on the effects of mixing eggshell with sawdust, coconut husk, and walnut shell. Since eggshell is one of the most efficient natural sources of calcium that can be used as a substitute for lime as a stabiliser, it was mixed with the other three agro-wastes to produce the samples.
- The influence of different fibre lengths on the properties of unfired clay blocks is also gaining particular attention in the literature. Hence, this research also examined how different sawdust particle sizes affect the properties of unfired clay blocks, which has not been previously reported in the literature.
- Furthermore, there is a lack of research on the durability of unfired clay blocks incorporating eggshell and sawdust. However, very few studies have reported certain durability tests for the coconut fibre-reinforced soil blocks. This study examined the durability of the produced sample blocks by simulating two different types of rainfall conditions (Geelong drip test and water spray test) in the laboratory. Additionally, ultrasound pulse velocity was measured to assess the porosity of the sample blocks, which has received little attention in the literature.
- The literature also shows that studies which measured the thermal properties of the eggshell, sawdust, and coconut husk-incorporated brick were conducted at the individual sample scale. There is no reported case available on the thermal performance of these agro-wastes incorporated clay blocks at wall scale. The examination of heat transfer rates through building wall materials is important for determining building energy efficiency. Therefore, this study not only measured

the thermal properties of individual samples but also evaluated the thermal performance of the constructed walls in the laboratory using an adapted hot box method (Asdrubali and Baldinelli, 2011; Lu and Memari, 2018; Zhao et al., 2019b; Lu and Memari, 2022).

- Besides, the numerical simulation analyses of the thermal behaviour of these agro-wastes incorporated samples under dynamic weather conditions is also very rare in the literature. Charai et al. (2020) conducted a simulation analyses with sawdust-clay composite materials as the building envelope using Moroccan climatic data. The simulation study aimed at establishing the ability of the material to provide good thermal comfort in summer by reducing overheating and in winter by maintaining heat without heating and cooling systems. This present study performed computer-based numerical simulation analyses using the climate data of the tropical country Bangladesh. The simulation analyses focused on determining the yearly energy consumption for heating and cooling as well as the indoor temperature profile for the space modelled with the developed agro-wastes incorporated unfired earth blocks. It also analysed the time lag and decrement factor for the materials during summer days. The simulation analyses were further extended by altering the material thickness.

The findings of this study are likely to contribute to the knowledge of unfired earthen materials development as well as to the solution of the costly and energy-intensive process issues in manufacturing conventional building materials such as fired clay brick. The production of unfired earth blocks is an energy-efficient and cost-effective approach with a high potential to meet the present and future demands of the construction sector. Moreover, this research investigates the application of agro-wastes/by-products to develop unfired earth blocks, which addresses a potential solution to the waste management problem.

## *Chapter 3*     **RESEARCH METHODOLOGY AND MATERIALS**

### **3.1 Introduction**

This chapter provides an overview of the overall methodology and analytical techniques employed in this present work. This chapter also describes the materials used in this work. In order to optimise the use of agro-wastes as construction materials, it is necessary to improve the understanding of their properties. Therefore, the basic characterisation (physical properties, chemical composition, mineralogical phases, and surface morphology) of the agro-wastes used in the present work was performed and presented in this chapter.

### **3.2 Research Methodology Outline**

Research methodology is considered the most important part of any research work, and it must be established prior to the commencement of data collection. The systematic way to solve a research problem is known as the research methodology, which guides the researchers to employ appropriate procedures to perform their research. Research methodologies can be classified as qualitative (described by words) or quantitative (numerical) (Ghani, 2014). On the other hand, research methods consist of different techniques, schemes, and instruments used by a researcher to collect data and solve the research problem. Particular scientific research methods require experimentation to validate the explanation. Besides, the research approach is another important aspect of scientific research, which can be inductive, deductive, or a combination of both. In engineering and the built environment, most researchers choose the deductive approach, which involves identifying a research problem and then confirming its cause and effects using experimental data (Ghani, 2014). According to the definitions, the main methodology for the current study is quantitative, and the methodological approach is deductive.

Firstly, this study identified the problem through a literature survey. The purpose of the literature survey was to develop a research approach that would provide a comprehensive understanding of how to carry out the work properly in order to achieve its aim. This research followed “the state-of-the-art review” with an emphasis on recent studies in the relevant field. A “systematic review” of experiments on agro-wastes incorporated unfired brick was conducted to identify potential local agro-wastes. The literature review, therefore, contributes to achieving research objective 1, outlined in Section 1.4 of Chapter 1. Moreover, this study used experimental and numerical research methods to collect data to reach research objectives 2-6. The laboratory experiments were designed to determine the properties of the produced sample in accordance with the standards and obtain the required data, which were later used as input in numerical simulation analyses. In situ experiments of the materials’ thermal performance were not possible in this study due to time and resource constraints. Therefore, numerical simulation analyses were performed under dynamic weather conditions to strengthen the experimental results and provide reasons for the choice of stabilised unfired clay blocks in construction. The findings of laboratory tests and numerical simulations complement each other to provide a thorough understanding of the thermal performance of the developed materials.

This study was affected by several lockdowns during the COVID-19 pandemic. The restrictions on lab access and scarcity of materials influenced the formulation of the research method. Although samples were prepared following the standards, their number and size varied based on the test methods. This study examined three samples (160 mm × 40 mm × 40 mm) for physico-mechanical properties and two samples (40 mm × 40 mm × 160 mm and 215 mm × 65 mm × 102 mm) for thermal properties. For durability properties, only one sample (215 mm × 65 mm × 102 mm) was assessed since the samples were larger, requiring more materials to manufacture them, and the test procedures were also time consuming. In this study, mean, standard deviation (SD), and coefficient of variation (CV) were used for statistical analysis to assess the variability of the data obtained from different tests results.

### ***3.2.1 Laboratory Tests***

#### ***Characterisation of the Raw Materials: Assessment of Surface Morphology, Mineralogical, and Chemical Composition***

At the beginning of the laboratory experiments, the characterisation of the raw materials (clay and potential agro-wastes) was conducted. The suitability of agro-wastes for use as construction materials depends on their physical properties. The two fundamental characteristics of their physical properties are high porosity and microstructure. Naturally, agro-wastes have a low density and a complex pore structure. The low density is related to low strength as well as low thermal conductivity. For this reason, some of the agro-wastes are suitable for structural materials, and others are only for filler in composite materials. As a result, a deeper understanding of the microstructure of agro-wastes is required to optimise their utilisation as construction materials. Several techniques are available to study the microstructure of the materials (Suryanarayana, 2017). This study used Scanning Electron Microscope (SEM) to characterise the raw materials because of their easy operation with very smooth analysis and imaging quality (Mohammed and Abdullah, 2018). SEM is a type of electron microscope that images the sample surface by scanning it with a high-energy beam of electrons in a raster scan pattern. The electrons interact with the atoms that make up the sample, producing signals that contain information about the sample's surface topography, composition, and other properties such as electrical conductivity (Akhtar et al., 2018). Besides, X-ray diffraction analysis (XRD) was used to identify the crystallographic structure of the materials. XRD is a rapid, non-destructive method that is done with an X-ray source of Cu K $\alpha$  radiation (wavelength=1.5406 Å) for determining the crystalline or amorphous nature of materials (Vishwakarma and Uthaman, 2020; Fleck et al., 2021). Moreover, since XRD does not provide elemental composition, X-ray fluorescence (XRF) analysis was conducted to identify the chemical composition of the raw materials, including what elements are present and their concentration. Consequently, the above-stated analysis concerns research objectives 2.

#### ***Preparation of Clay Samples***

Following the selection of agro-wastes, clay samples were prepared in the laboratory

using the hand compaction method for further detailed laboratory experiments. Based on the literature, different percentages of agro-wastes were mixed with clay and water to produce the samples. Before testing, all samples were dried in a laboratory environment for 28 days. The details of sample preparation are presented in Section 4.1 of Chapter 4. The experimental work was carried out in three sequential parts.

### **Part 01: Physico-mechanical Properties Tests**

The following physico-mechanical properties tests were carried out to assess the suitability of the agro-wastes for unfired clay block production:

- Density
- Linear shrinkage
- Capillary water absorption coefficient
- Compressive strength
- Flexural strength

The methods for the aforementioned experimental tests are described in Chapter 4. At this stage, the results were analysed, and a preliminary screening was done based on the standard requirements.

### **Part 02: Durability Properties Tests**

After the first preliminary screening from the physio-mechanical properties tests, selected mix ratios proceeded to the second detailed evaluation stage, which includes the following durability properties tests:

- Ultrasonic pulse velocity (UPV)
- Geelong drip
- Water spray

Chapter 5 provides a description of the durability tests. After obtaining the results of the

durability tests, a second screening was performed, and the selected mix ratios were investigated for the thermal properties tests.

### **Part 03: Thermal Properties Tests**

At first, selected samples were examined individually to determine their thermal properties. The data obtained from the thermal properties tests were utilised in two ways. Primarily, the data were analysed and compared to rank the performances of the materials. Then, the required data were used as input data in numerical simulation software to determine their thermal performance under dynamic weather conditions. At the individual sample level, the following thermal properties were determined:

- Thermal conductivity
- Volumetric heat capacity
- Specific heat capacity
- Thermal diffusivity
- Thermal effusivity

After analysing the properties of individual samples, small walls with the best-performing mix ratio from each agro-waste type were built to measure the thermal transmittance and thermal resistance using an adapted hot box method. The methods for the individual sample test and wall test are elaborated on in Chapter 6.

#### ***3.2.2 Numerical Simulation***

In order to promote the newly developed materials, their performances have to be compared with the those of the conventional materials. For this reason, results acquired from the laboratory tests were used for indoor climate simulation of a space using the recognised simulation engine IES-VE (Azhar et al., 2011). In this part, a space was simulated separately with conventional materials as well as newly developed agro-wastes incorporated unfired earth blocks, which performed better in the laboratory tests. The simulation was carried out under dynamic outdoor weather conditions using real climate

data. The dynamic thermal performance of the building materials depends on three basic properties, i.e., specific heat capacity, density, and thermal conductivity, which were obtained from the laboratory tests. In the IES-VE software, the space was modelled without any openings. While running the simulation, ventilation in the form of infiltration was included, and occupants, heating/cooling system, lighting or appliance profiles for internal heat gains were excluded. This approach is considered to make a clear evaluation of the performance of the materials when exposed to dynamic weather conditions. The results obtained from the simulations were compared to find the best-performing material as well as make conclusions and recommendations. The numerical simulation method is described in detail in Chapter 7.

Figure 3.1 illustrates the full research plan.

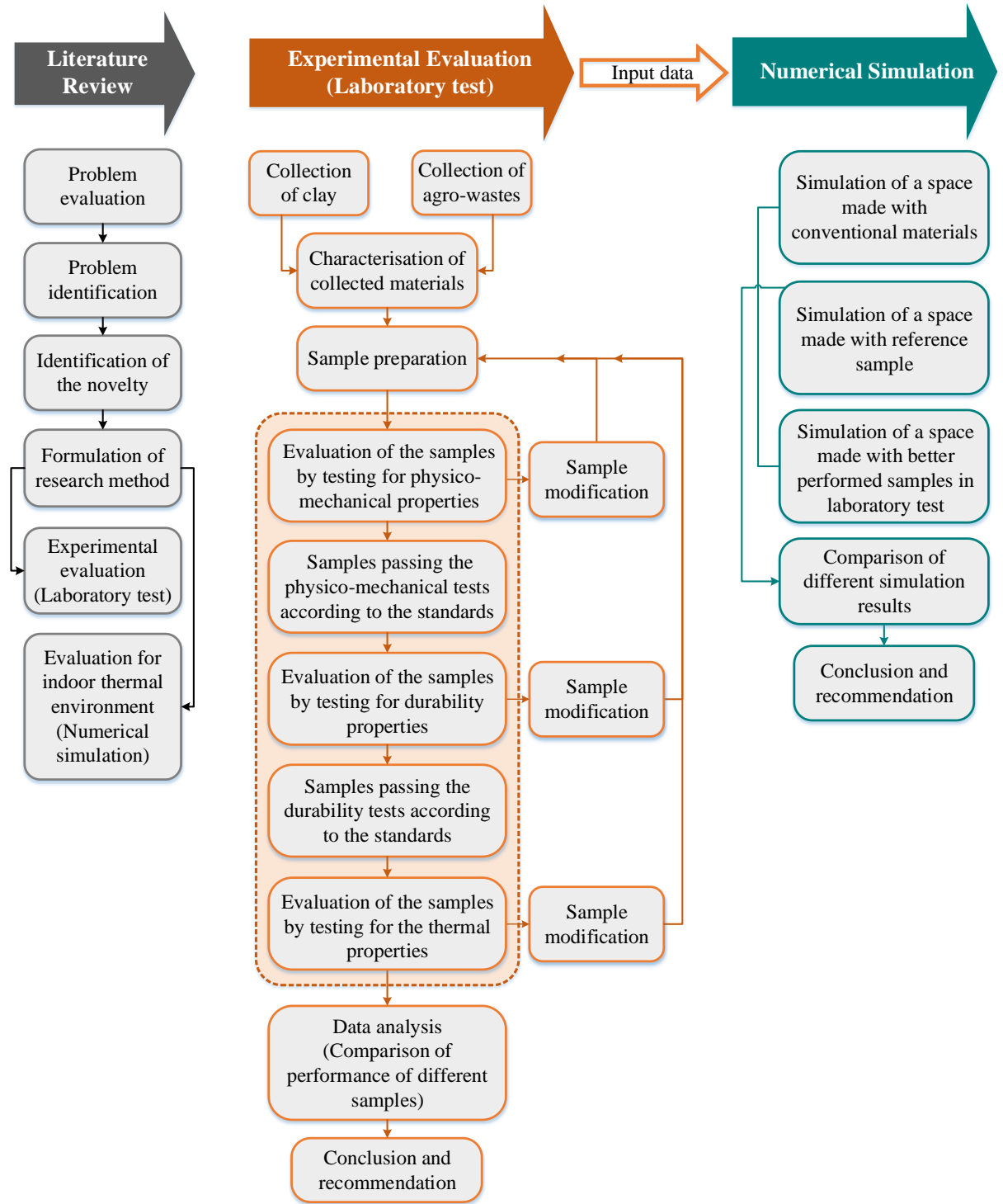


**Figure 3.1:** Research plan flow chart.

### 3.3 Materials

The materials utilised in this study to produce the unfired clay samples are red clay powder (RCP), eggshell powder (ESP), sawdust powder (SDP), coconut husk powder (CHP), and walnut shell grit (WSG). These materials were selected based on their availability since the material supply was highly affected by the COVID-19 pandemic lockdowns during the time of the study. Also, the selected agro-wastes are widely available in tropical areas as low-cost materials. The clay was provided by Bath Potters' Supplies, which is a UK-based company. Eggshell powder, sawdust, coconut husk, and walnut shell grit were also obtained from local retailers in the UK.

The standard proctor compaction test (ASTM D698, 2012) was used to experimentally determine the optimum moisture content and maximum dry density of the clay, while its Atterberg limit was established by following the BS 1377-2 standard (BS 1377-2, 1990). Besides, the chemical compositions of RCP, ESP, SDP, CHP, and WSG were examined employing non-destructive XRF analysis (EDX-720 Shimadzu, Japan) (Figure 3.2). Additionally, the mineralogical phase evolution was performed by XRD (Rigaku MiniFlex) (Figure 3.3) analysis using Cu K $\alpha$  radiation generated at 30 kV and 15 mA. In XRD analysis, finely ground samples were scanned in continuous scan mode at an angular speed of 2°/min, and the measurements were taken at the 2 $\theta$  angle from 5° to 60°. The calibrations of the XRF and XRD machines were done by a third party using certified reference materials. To ensure stability, repeatability tests (10 runs) on the samples were performed. Moreover, the surface morphology of raw materials was characterised by means of SEM using an FEI Inspect S SEM model at 20 kV accelerating voltage after gold-coating the materials (Figure 3.4). Furthermore, the density and specific gravity of the materials were determined according to the cylinder method and the BS EN 1097-6 standard (BS EN 1097-6, 2013), respectively. Also, porosity was assessed following the method of Horisawa et al. (1999). The thermal conductivity and volumetric heat capacity values were measured using a portable heat transfer analyser ISOMET 2114, equipped with a needle probe (thermal conductivity range: 0.035 to 0.20 W/m.K, accuracy: 5% of reading + 0.001 W/m.K; volume heat capacity range: 4.0 $\times 10^4$  to 3.0 $\times 10^6$  J/m<sup>3</sup>.K, accuracy: 15% of reading + 1.10<sup>3</sup> J/m<sup>3</sup>.K; temperature range: -20 °C to +70 °C, accuracy: 1°C) (Figure 3.5). The instrument was calibrated in accordance

with the ASTM D5334-08 standard (ASTM D5334, 2008). Thermal measurements were carried out at the laboratory room temperature of 23-26 °C and relative humidity of 30-34%. Following the above-mentioned procedures, three samples were analysed to assess the characteristics of the raw materials and the results are presented in Tables 3.1, 3.2, 3.3, 3.4, and 3.5.



**Figure 3.2:** XRF analyser machine, EDX-720 Shimadzu.



**Figure 3.3:** XRD instrument, Rigaku MiniFlex.

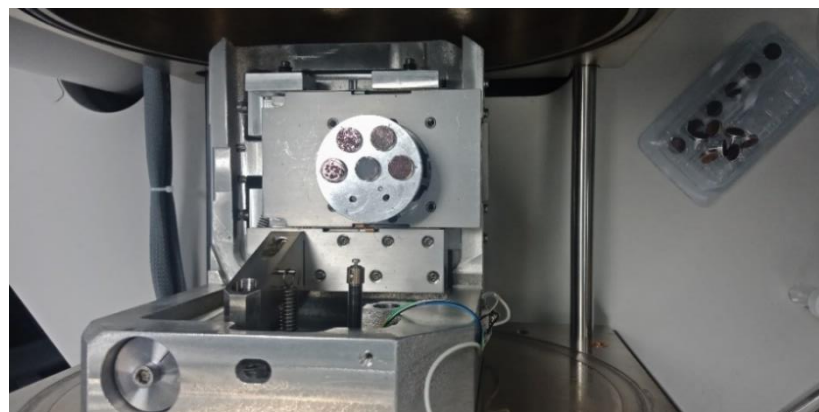


**Figure 3.4:** FEI Inspect S SEM.



**Figure 3.5:** Measurement of the thermal properties of the raw materials.

### 3.3.3 Clay

The clay used in this study is raw, reddish powdered clay (Figure 3.6) that is dug directly from the ground and contains some pebbles since it is in its natural state. It is dried and pulverised Etruria Marl with high clay content. It has a pH ranging between 5 and 9. It's a popular red brick clay for the areas in Stoke-on-Trent and North Staffordshire, UK. This clay is extremely inert, being resistant to decomposition by weathering, biological activity, and further oxidation.

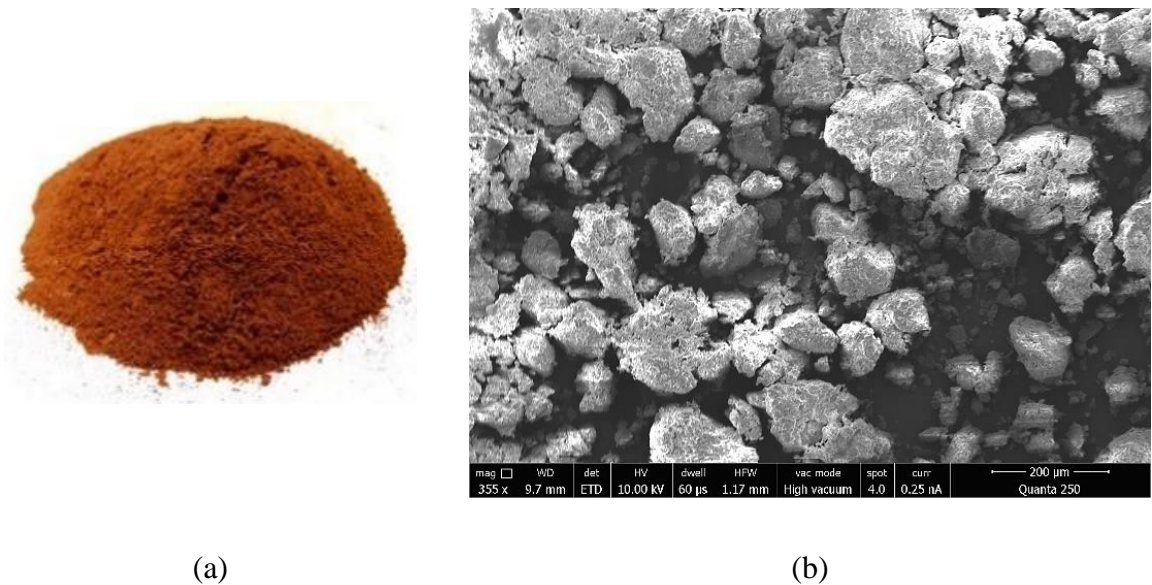


**Figure 3.6:** (a) Photograph and (b) SEM micrograph of RCP.

The proctor compaction test on RCP revealed a maximum dry density of  $2320 \text{ kg/m}^3$  at an optimum moisture content of 15.50% (Figure 3.7). Besides, RCP had a plastic limit of 19.25% water content and a liquid limit of 31.61%, indicating that it was a medium-

plastic clay with a plasticity index of 12.36%. Figure 3.8 shows the grain size distribution curve of the RCP determined by the sieve analysis (ASTM D422-63, 2002). The XRD analysis (Figure 3.9) displays the presence of quartz ( $\text{SiO}_2$ ), kaolinite ( $\text{Al}_2(\text{Si}_2\text{O}_5)(\text{OH})_4$ ) and haematite ( $\text{Fe}_2\text{O}_3$ ) in RCP. This is also supported by the XRF test findings shown in Table 3.1. Moreover, silica and aluminium were found in RCP, making it a pozzolan. Also, the presence of ferric oxide ( $\text{Fe}_2\text{O}_3$ ) highlights the redness of RCP. Furthermore, the bulk density and specific gravity of RCP were recorded as  $1430 \text{ kg/m}^3$  and 2.32, respectively (Table 3.1).

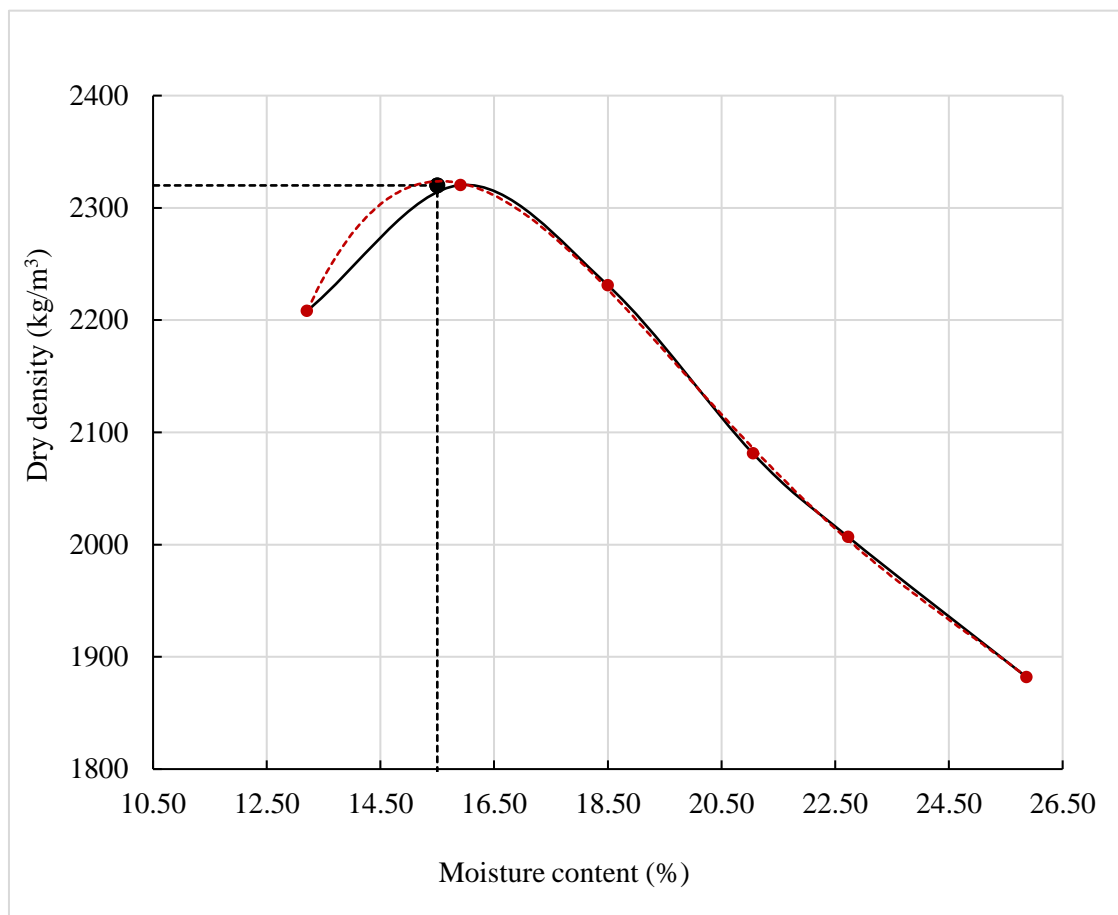


**Figure 3.7:** Compaction curve to determine the maximum dry density and optimum moisture content of RCP.

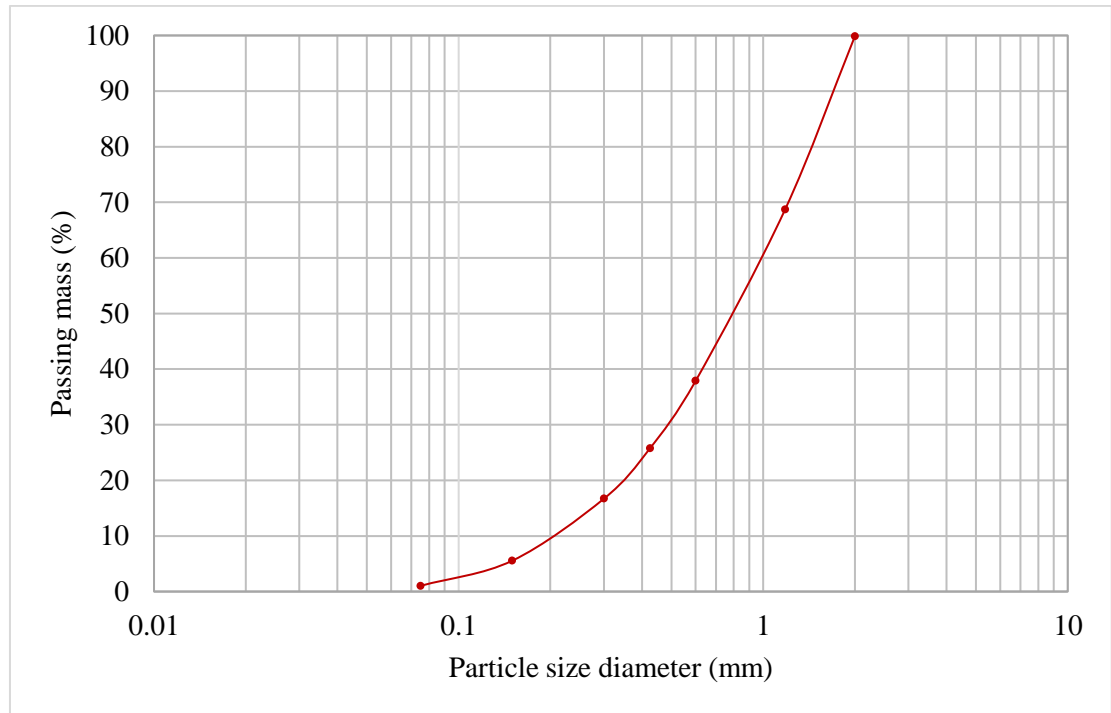


**Figure 3.8:** Particle size distribution curve of RCP.

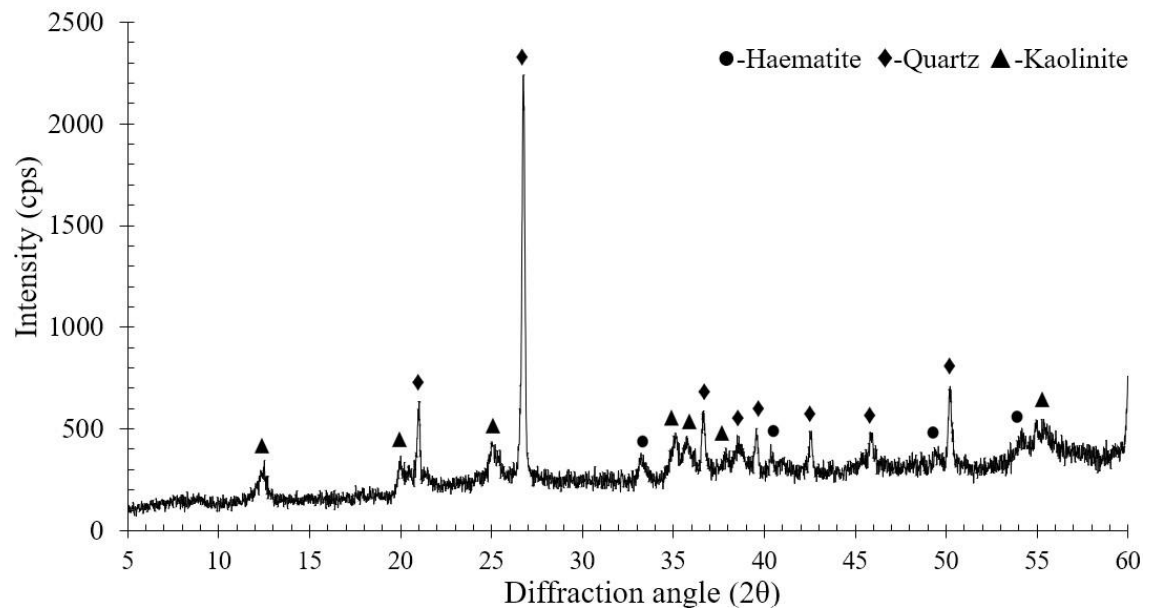


**Figure 3.9:** XRD spectrum of RCP.

**Table 3.1:** Properties of RCP.

<b>Physical properties</b>			
Optimum moisture content		15.50% ± 0.71	
Maximum dry density (kg/m <sup>3</sup> )		2320 ± 2.83	
Liquid limit (%)		31.61 ± 2.55	
Plastic limit (%)		19.25 ± 1.06	
Plasticity index (%)		12.36 ± 2.58	
Bulk density (kg/m <sup>3</sup> )		1430 ± 4.95	
Specific gravity		2.32 ± 0.24	
Natural moisture content (%)		6.47 ± 0.48	
Thermal conductivity (W/mK)		0.302 ± 0.031	
Volumetric heat capacity (×10 <sup>6</sup> J/m <sup>3</sup> K)		1.291 ± 0.042	
Specific heat capacity (J/m <sup>3</sup> K)		902.80 ± 3.79	
Colour		Red	
<b>Chemical compounds (%)</b>			
SiO <sub>2</sub>	41.454 ± 6.647	SrO	0.011 ± 0.008
Al <sub>2</sub> O <sub>3</sub>	15.214 ± 4.384	CuO	0.006 ± 0.006
K <sub>2</sub> O	1.636 ± 0.424	ZnO	0.007 ± 0.004
MgO	5.114 ± 1.394	Y <sub>2</sub> O <sub>3</sub>	0.006 ± 0.001
Fe <sub>2</sub> O <sub>3</sub>	8.104 ± 2.828	F	0.050 ± 0.000
Na <sub>2</sub> O	1.027 ± 0.389	Cl	0.040 ± 0.000
TiO <sub>2</sub>	1.411 ± 0.255	Co <sub>2</sub> O <sub>3</sub>	0.007 ± 0.001
CaO	0.633 ± 0.154	Rb <sub>2</sub> O	0.004 ± 0.001
SO <sub>3</sub>	0.047 ± 0.020	NiO	0.003 ± 0.001
BaO	0.216 ± 0.092	BaO	0.097 ± 0.021
MnO	0.040 ± 0.014	Cr <sub>2</sub> O <sub>3</sub>	0.016 ± 0.004
ZrO <sub>2</sub>	0.035 ± 0.010	CHO	24.572 ± 1.414
P <sub>2</sub> O <sub>5</sub>	0.250 ± 0.007		

### ***3.3.4 Eggshell***

Eggshells are considered waste, which is mainly generated by the poultry and food industries. Such waste has a negative impact on the environment because it raises waste management costs and produces a bad smell at the site. The total global production of eggshells is around 110 billion, which eventually ends up going to landfill sites (Waheed et al., 2019). Figure 3.10 specifies the leading egg-producing countries in the world (FAO, 2020). In general, eggshells are known to have no economic value, even though they are rich in various minerals and amino acids. The poultry eggshells are grainy in texture and constitute about 9-12% of the overall egg weight (Chambers et al., 2017; Waheed et al., 2019). It is observed that eggshells are high in calcium levels, ranging from 94% to 98% (Ajala et al., 2018; Shwetha et al., 2018; Philippe et al., 2020). However, eggshells contain other microelements such as magnesium carbonate (1%), calcium phosphate (1%), and organic matter (4%) (Ketta and Tůmová, 2016; Ajala et al., 2018; Chen et al., 2019; Philippe et al., 2020). Usually, eggshell has a structure of three layers, i.e., a thin external bloom or cuticle layer that protects against dust and bacteria, a second spongy calcareous layer, and an inner lamellosis or mammalian layer (Ajala et al., 2018; Arzate-Vázquez et al., 2019). Eggshell also contains a thick outer membrane attached to the shell and a thin internal membrane. Both of the membranes are semipermeable and composed of protein fibres (Arzate-Vázquez et al., 2019). The layers of calcareous and lamellosis are formed in such a way that many pores are present there, allowing the passage of air and humidity through the pores (La Scala Jr et al., 2000). Also, the cuticle layer enables the exchange of humidity and air. The calcium quantity present in eggshells has been reported to be more absorbable than the calcium contained in limestone or coral sources (King'Ori, 2011), and it contributes to reinforcing material bonding (Adogla et al., 2016). These characteristics of the poultry eggshell have made it an attractive choice for natural reinforcement. Hence, scientists have started investigating the use of eggshells for developing different types of valuable and usable products (King'Ori, 2011; Mittal et al., 2016; Faridi and Arabhosseini, 2018; Souza et al., 2019; Waheed et al., 2019; Rahmani-Sani et al., 2020; Waheed et al., 2020). Several studies have shown that eggshell powder and eggshell ash can be used for soil stabilisation (Amu et al., 2005; Olarewaju et al., 2011; Walia et al., 2015; Prasad et al., 2016; Alzaidy, 2019)

as well as in the production of building materials such as unfired laterite brick (Adogla et al., 2016; Ayodele et al., 2019), fired brick (Tangboriboon et al., 2016; Ashiq and Kumar, 2019), sandcrete block (Afolayan et al., 2017), concrete block (Aarcha et al., 2019; Hamada et al., 2020), and soil cement brick (Amaral et al., 2013).

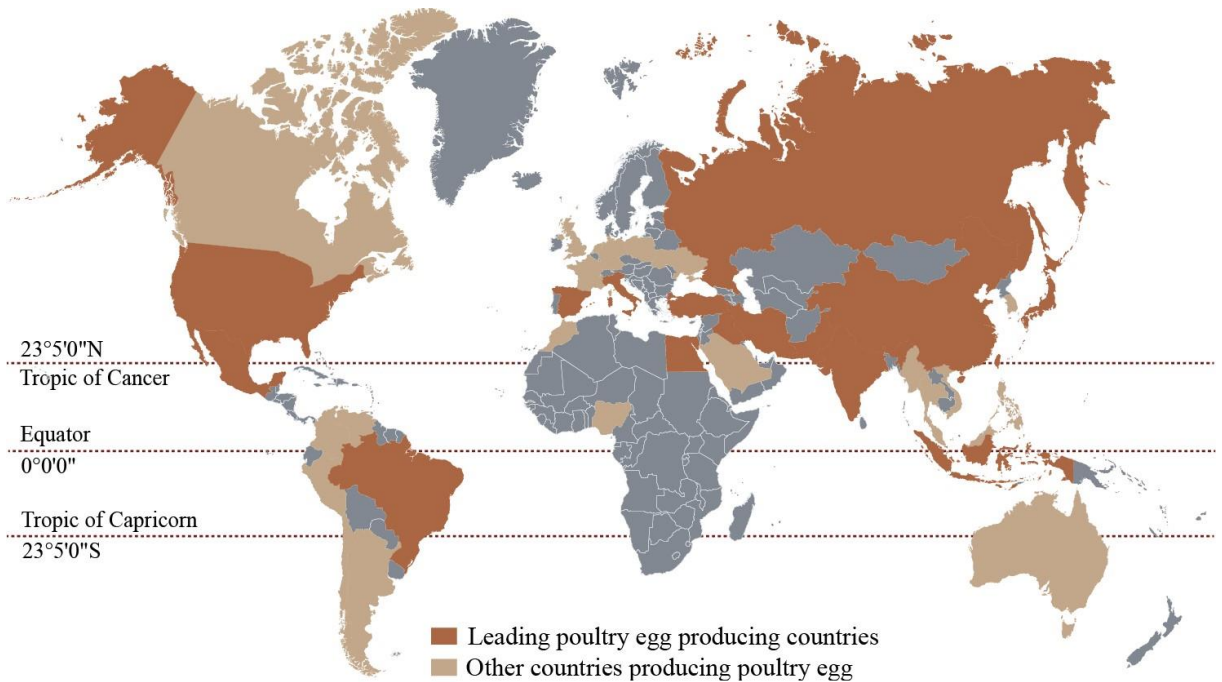


**Figure 3.10:** Global poultry egg-producing countries (FAO, 2020).

The XRD pattern of ESP is shown in Figure 3.11. All the calcite ( $\text{CaCO}_3$ ) specific diffraction peaks were found in ESP, where a major phase was present at  $29.50^\circ$ . The XRF analysis showed that ESP was a non-pozzolanic material since it lacked siliceous and aluminous elements. However, ESP had a significant quantity of calcium oxide ( $\text{CaO}$ ) obtained from the calcination of calcite ( $\text{CaCO}_3$ ), which is necessary for a pozzolanic reaction to affect the cementitious characteristics of clay bricks (Table 3.2). Besides, ESP had a bulk density of  $1170 \text{ kg/m}^3$ , a specific gravity of 1.74, and a thermal conductivity of  $0.146 \text{ W/mK}$ . Also, the water absorption test indicated that ESP had a lower absorption value (39.42%). Moreover, from the SEM image, it can be observed that eggshells had agglomerated irregular stone-like particles (Figure 3.12(b)).

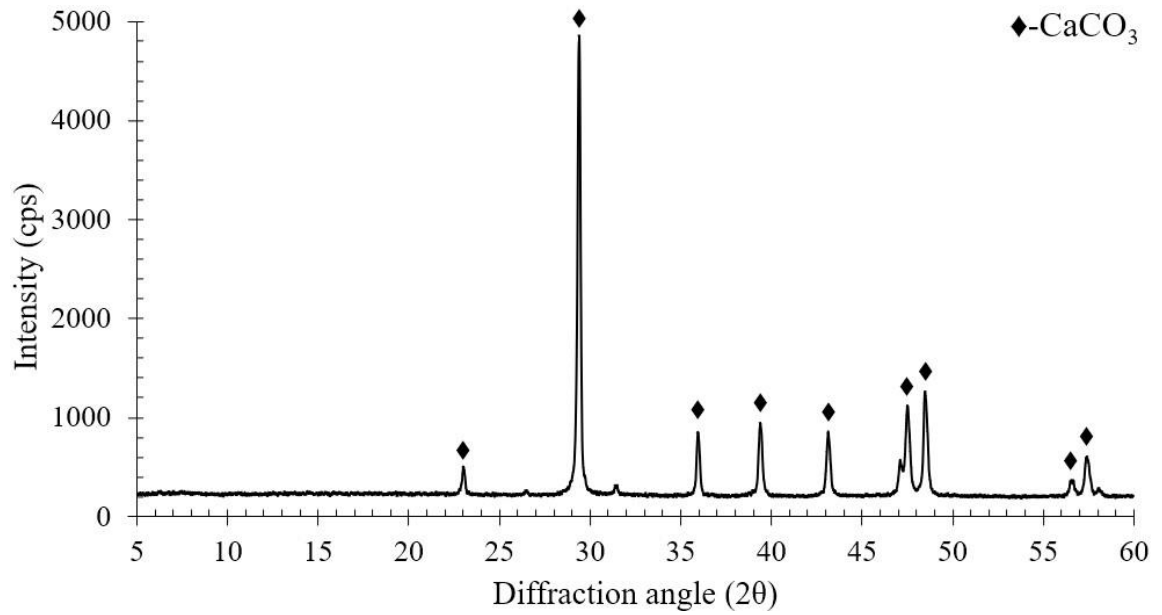


**Figure 3.11:** XRD spectrum of ESP.

**Table 3.2:** Properties of ESP.

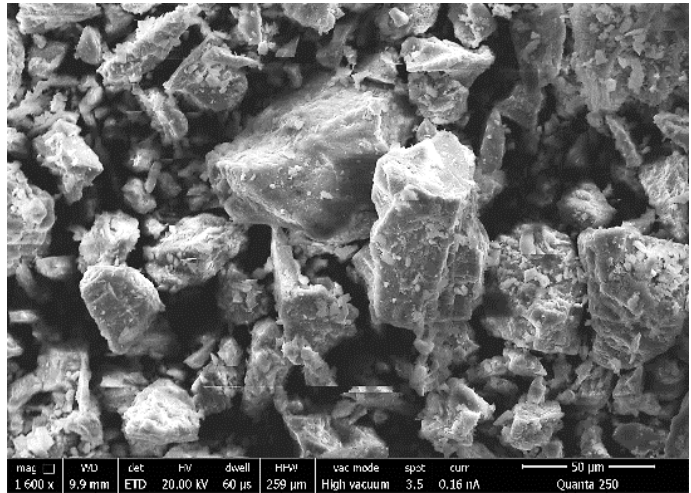
<b>Physical properties</b>			
Bulk density (kg/m <sup>3</sup> )		1170 ± 3.54	
Specific gravity		1.74 ± 0.13	
Porosity		0.56 ± 0.10	
Water absorption after 24 hrs under water (%)		39.42 ± 4.36	
Thermal conductivity (W/mK)		0.146 ± 0.020	
Volumetric heat capacity (×10 <sup>6</sup> J/m <sup>3</sup> K)		0.877 ± 0.028	
Specific heat capacity (J/m <sup>3</sup> K)		749.91 ± 6.51	
Natural moisture content (%)		0.31 ± 0.14	
Colour		White	
<b>Chemical compounds (%)</b>			
SiO <sub>2</sub>	0.097 ± 0.011	P <sub>2</sub> O <sub>5</sub>	0.250 ± 0.042
K <sub>2</sub> O	0.155 ± 0.028	SrO	0.042 ± 0.017
MgO	0.522 ± 0.017	CuO	0.004 ± 0.001
Na <sub>2</sub> O	1.423 ± 0.173	ZnO	0.002 ± 0.001
TiO <sub>2</sub>	0.096 ± 0.020	Y <sub>2</sub> O <sub>3</sub>	0.003 ± 0.001

Table 3.2: Properties of ESP (continued).

Chemical compounds (%)			
CaO	$78.111 \pm 4.711$	F	$0.050 \pm 0.000$
SO <sub>3</sub>	$0.345 \pm 0.086$	Cl	$0.040 \pm 0.000$
BaO	$0.189 \pm 0.074$	GeO <sub>3</sub>	$0.002 \pm 0.001$
ZrO <sub>2</sub>	$0.008 \pm 0.001$	CHO	$18.661 \pm 3.118$



(a)



(b)

**Figure 3.12:** (a) Photograph and (b) SEM micrograph of ESP.

### 3.3.5 Sawdust

Sawdust or wood dust are the fine wood particles produced as a by-product of the wood or timber industry. Every year, sawmills produce huge volumes of sawdust (Kirilenko and Sedjo, 2007; FAO, 2020) (Figure 3.13). According to one report, the average annual growth rate of the global wood harvest was 0.20% between 1990 and 2015 (Zhang et al., 2020) and the FAO estimates a 55% increase in the potential industrial roundwood supply by 2030 (Penna, 2010). As a result, the timber industry is becoming more concerned about the cost-effective disposal of sawdust as the bulk of it is burned off, polluting the environment (Rominiyi et al., 2017; Charis et al., 2019; Lopez et al., 2020). On the other hand, sawdust can be used as a valuable raw material in a variety of

industries due to its abundance and low cost. Generally, sawdust has wood-like characteristics, although certain structural properties have been modified due to its particle nature. The chemical composition of dry wood varies by species of tree. The main chemical components in sawdust are lignin (18-35%) and carbohydrate (65-75%), while small quantities of extraneous materials (4-10%) are also found (Pettersen, 1984; Horisawa et al., 1999; Lachowicz et al., 2019). The bulk density of sawdust is found to be very low (150-200 kg/m<sup>3</sup>) (Thiffault et al., 2019) and it has very low thermal conductivity, making it suitable for insulation material (Okunade, 2008; Tiuc et al., 2019). It is most commonly used in the energy, agriculture, and manufacturing industries (Rominiyi et al., 2017). However, little research has been performed on the application of sawdust in the production of building materials (Mwango and Kambole, 2019). Sawdust-based insulation material (Zou et al., 2020), particleboard (Akinyemi et al., 2016; Savov et al., 2019; Mirski et al., 2020a; Mirski et al., 2020b; Atoyebi et al., 2021; Orelma et al., 2021; Tawasil et al., 2021), cement concrete brick (Mageswari and Vidivelli, 2009; Ghimire and Maharjan, 2019), fired clay brick (Okunade, 2008; Aramide, 2012; Chemani and Chemani, 2012; Chemani and Chemani, 2013; Hassan et al., 2014; Cultrone et al., 2020), and unfired brick (Demir, 2008; Vilane, 2010; Ganga et al., 2014; Ouattara et al., 2016; Fadele and Ata, 2018; Jokhio et al., 2018; Ayodele et al., 2019; Charai et al., 2020; De Castrillo et al., 2021) are some of the developed building materials.

Table 3.3 presents that the bulk density and specific gravity of different particle sizes of SDP ranged from 200 kg/m<sup>3</sup> to 260 kg/m<sup>3</sup> and from 1.02 to 1.23, respectively. According to the water absorption test, SDP showed a higher absorption value (127.66%). Also, SDP was found to have higher porosity (5.09). On the other hand, thermal conductivity measurements indicate that SDP had a lower conductivity (0.064 W/mK). Besides, sawdust contained amorphous phases such as hemicelluloses and lignin, as evidenced by the disordered nature of the XRD pattern (Figure 3.14). The only crystalline phase found was cellulose, which exhibited a sharp peak at 22.6° and a broad peak between 15° and 18° as well as a wideband peak at 35°. Furthermore, the SEM micrograph revealed that sawdust particles came in a variety of sizes and forms with rough surfaces, including heterogeneous fibres with multiple protrusions and folds (Figure 3.15(b)).

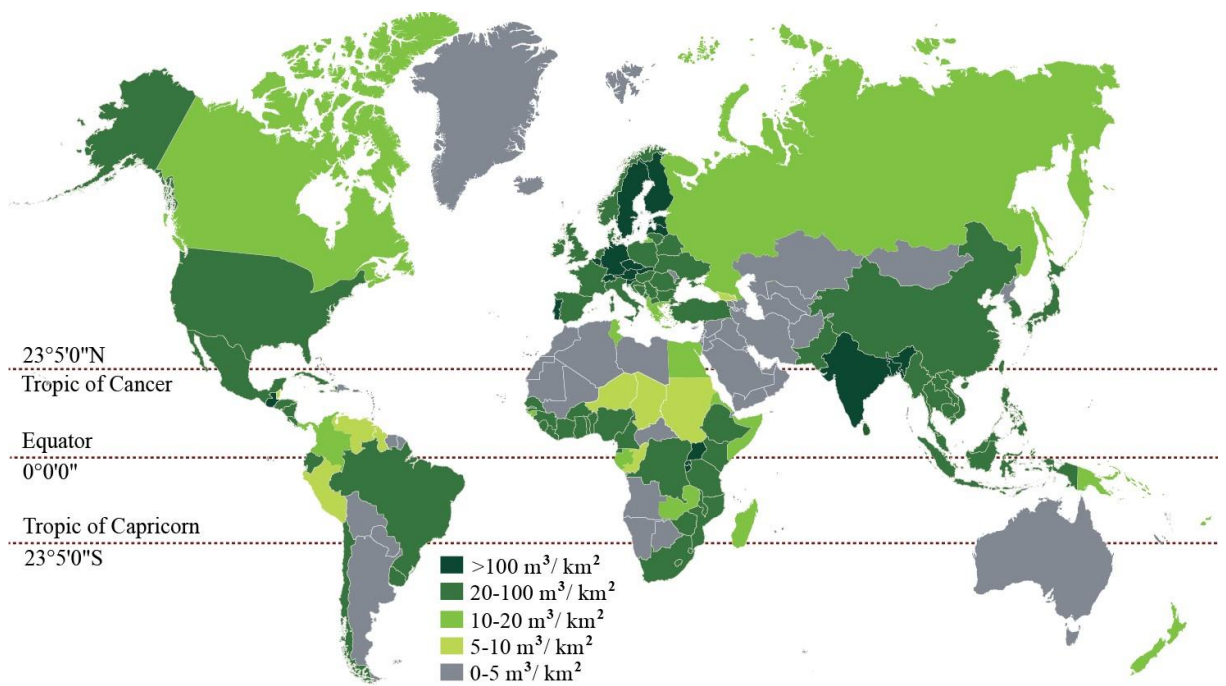


**Figure 3.13:** Global wood harvest (FAO, 2020).

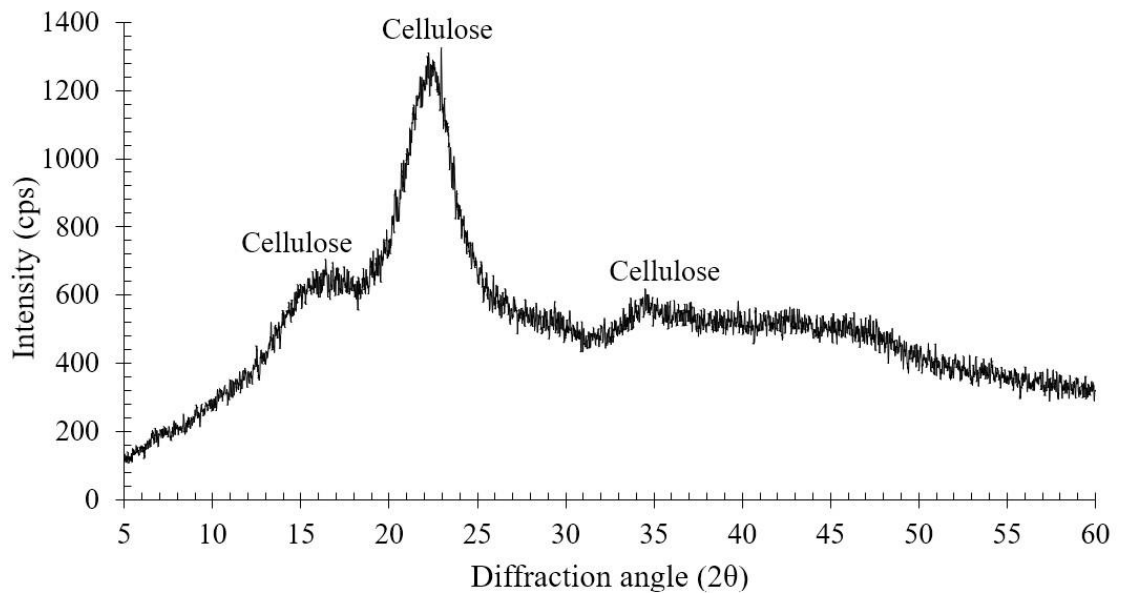


**Figure 3.14:** XRD spectrum of SDP.

**Table 3.3:** Properties of SDP.

<b>Physical properties</b>			
			a - $260 \pm 5.24$ b - $230 \pm 6.36$ c - $200 \pm 5.02$
Bulk density ( $\text{kg/m}^3$ )			
			a - $1.23 \pm 0.08$ b - $1.14 \pm 0.11$ c - $1.02 \pm 0.14$
Specific gravity			
Porosity			$5.09 \pm 0.64$
Water absorption after 24 hrs under water (%)			$127.66 \pm 5.46$
Thermal conductivity (W/mK)			$0.064 \pm 0.014$
Volumetric heat capacity ( $\times 10^6 \text{ J/m}^3\text{K}$ )			$0.239 \pm 0.017$
Specific heat capacity ( $\text{J/m}^3\text{K}$ )			$1040.43 \pm 4.53$
Natural moisture content (%)			$5.02 \pm 0.85$
Colour			Light brown
<b>Chemical compounds (%)</b>			
SiO <sub>2</sub>	$0.348 \pm 0.069$	ZrO <sub>2</sub>	$0.002 \pm 0.001$
Al <sub>2</sub> O <sub>3</sub>	$0.390 \pm 0.095$	P <sub>2</sub> O <sub>5</sub>	$0.021 \pm 0.007$
K <sub>2</sub> O	$0.340 \pm 0.057$	CuO	$0.003 \pm 0.001$
MgO	$0.408 \pm 0.079$	ZnO	$0.004 \pm 0.002$
Fe <sub>2</sub> O <sub>3</sub>	$0.186 \pm 0.040$	Y <sub>2</sub> O <sub>3</sub>	$0.001 \pm 0.001$
Na <sub>2</sub> O	$0.926 \pm 0.072$	F	$0.050 \pm 0.000$
TiO <sub>2</sub>	$0.171 \pm 0.055$	Cl	$0.040 \pm 0.000$
CaO	$1.681 \pm 0.327$	Co <sub>2</sub> O <sub>3</sub>	$0.002 \pm 0.001$
SO <sub>3</sub>	$0.049 \pm 0.021$	CHO	$95.278 \pm 4.243$
BaO	$0.074 \pm 0.013$		
MnO	$0.026 \pm 0.008$		
<i>Note: a (<math>212 \mu\text{m} &lt; x &lt; 300 \mu\text{m}</math>), b (<math>425 \mu\text{m} &lt; x &lt; 600 \mu\text{m}</math>), and c (<math>1.18 \text{ mm} &lt; x &lt; 2.00 \text{ mm}</math>) represent the three different particle sizes of SDP.</i>			

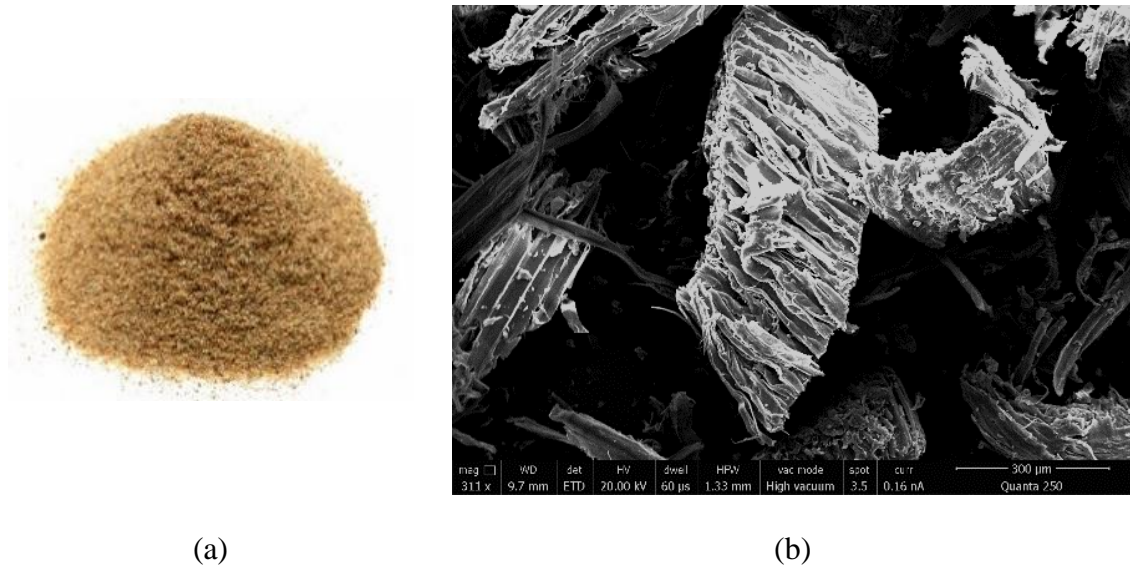


**Figure 3.15:** (a) Photograph and (b) SEM micrograph of SDP.

### 3.3.6 Coconut Husk

Coconut husk is another agricultural waste that is a by-product of coconut cultivation and is mainly obtained from the outer shell. Coconut is a tropical plant that grows largely at latitudes between 20 °N and 20 °S (Nagaraj, 2009) (Figure 3.16). Although billions of coconuts are produced each year, only 15% of the residual fibres from the harvesting process are used as materials for manufacturing purposes (Wang and Huang, 2009). Coconut husk contains approximately 75% of coconut coir fibres and 25% of the pith (Harish et al., 2009; Carlile et al., 2019). Coconut coir is reddish-brown in colour and composed of cellulose, hemicellulose, lignin, and pectin (Kosseva, 2016). According to the studies, coconut coir is four to six times stronger than other natural fibres with a strength of 21.51 MPa (Syed et al., 2020; Ahmad et al., 2022). Studies also show that the addition of coconut coir can reduce the thermal conductivity of the composite and result in a lightweight product due to its low bulk density (Khedari et al., 2001; Asasutjarit et al., 2007). Because of its excellent physico-mechanical properties, coconut coir has been examined by many researchers in manufacturing different construction materials such as insulation board (Panyakaew and Fotios, 2011), fibreboard (Freire et al., 2017), particleboard (Khedari et al., 2003; Tawasil et al., 2021), concrete block (Ali et al., 2012; Ramli et al., 2013; Mydin et al., 2015; Syed et al., 2020), fired brick (Kadir et al.,

2016; Hamzah et al., 2017; Kanna and Dhanalakshmi, 2018), and unfired earth block (Khedari et al., 2005; Danso et al., 2015b; Purnomo and Arini, 2019; Sangma et al., 2019; Thanushan et al., 2019). Besides, it has been used for soft soil stabilisation (Sivakumar Babu and Vasudevan, 2008; Singh and Mittal, 2014; Lakshmi et al., 2018).

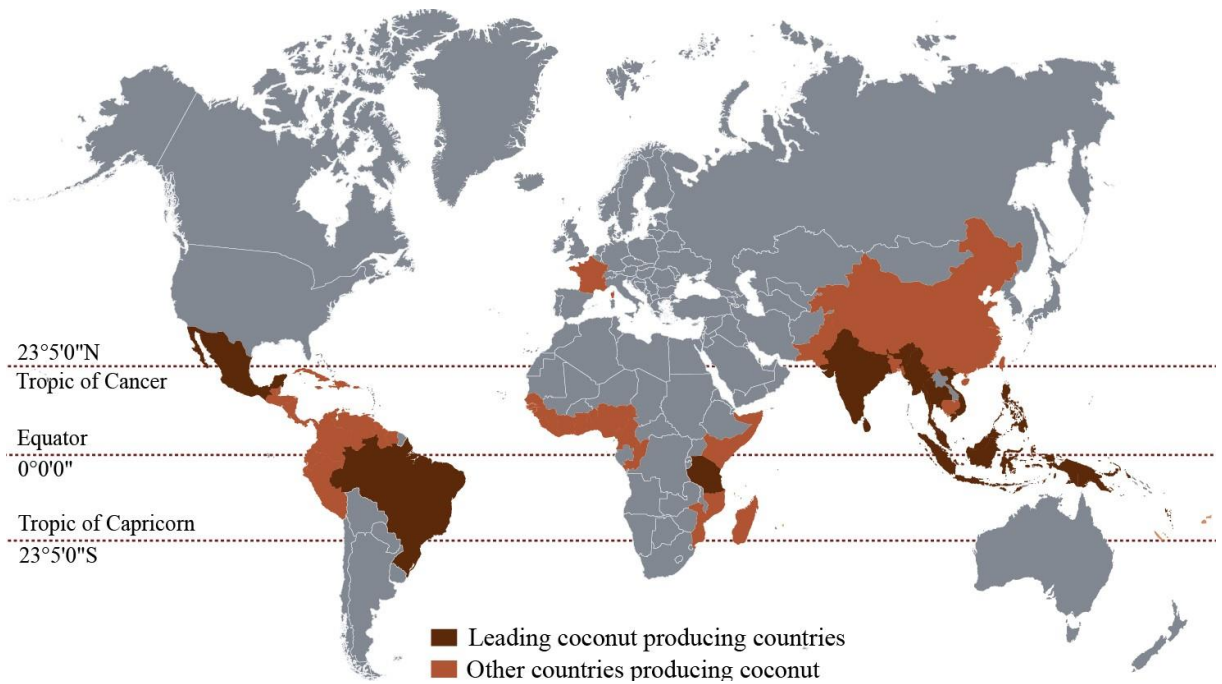


**Figure 3.16:** Global coconut producing countries (FAO, 2020).

Table 3.4 summarises the properties of CHP. It can be observed that CHP had a low bulk density of  $130 \text{ kg/m}^3$ , a low specific gravity of 0.61, and a low conductivity of  $0.050 \text{ W/mK}$ . On the other hand, CHP had a higher porosity (7.65) and water absorption value (195.16%). Besides, the disordered XRD pattern indicates the presence of amorphous phases (hemicelluloses and lignin) in CHP (Figure 3.17). Moreover, Figure 3.18(b) shows that coconut husk particles have an irregular honeycomb-like spongy structure consisting of many pores.

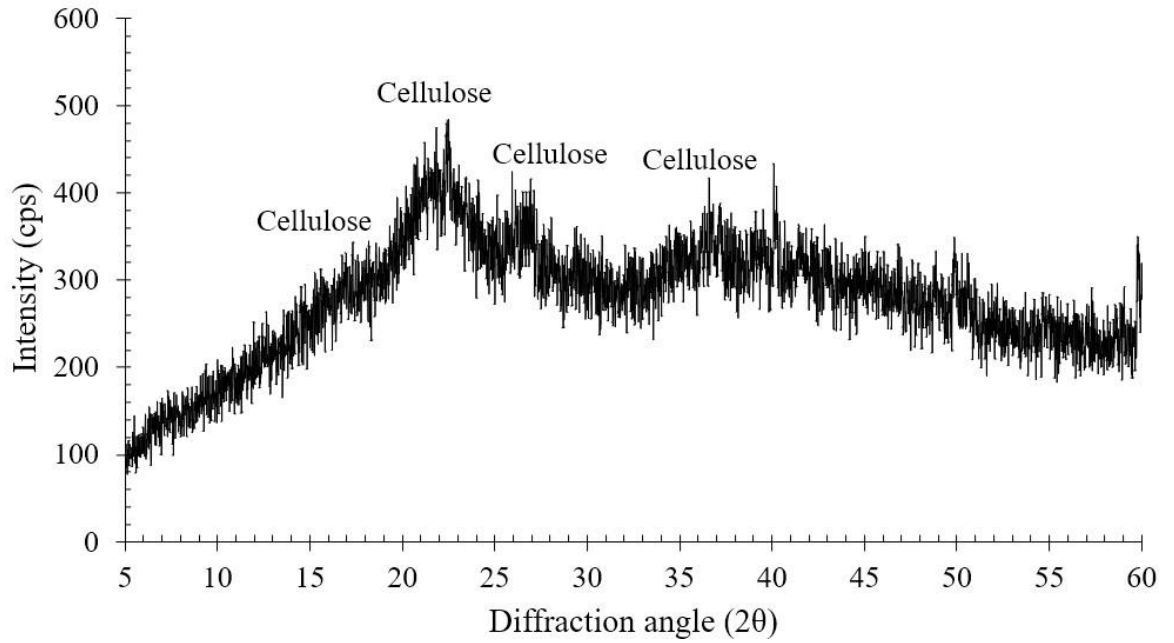


**Figure 3.17:** XRD spectrum of CHP.

**Table 3.4:** Properties of CHP.

<b>Physical properties</b>			
Bulk density (kg/m <sup>3</sup> )		130 ± 4.24	
Specific gravity		0.61 ± 0.17	
Porosity		7.65 ± 1.13	
Water absorption after 24 hrs under water (%)		195.16 ± 6.94	
Thermal conductivity (W/mK)		0.050 ± 0.008	
Volumetric heat capacity (×10 <sup>6</sup> J/m <sup>3</sup> K)		0.206 ± 0.021	
Specific heat capacity (J/m <sup>3</sup> K)		1583.08 ± 5.66	
Natural moisture content (%)		5.62 ± 1.10	
Colour		Brown	
<b>Chemical compounds (%)</b>			
SiO <sub>2</sub>	4.059 ± 0.692	ZrO <sub>2</sub>	0.011 ± 0.004
Al <sub>2</sub> O <sub>3</sub>	1.206 ± 0.283	P <sub>2</sub> O <sub>5</sub>	0.094 ± 0.018
K <sub>2</sub> O	3.942 ± 0.923	SrO	0.005 ± 0.002

Table 3.4: Properties of CHP (continued).

Chemical compounds (%)			
MgO	0.767 ± 0.117	CuO	0.002 ± 0.001
Fe <sub>2</sub> O <sub>3</sub>	1.184 ± 0.246	ZnO	0.006 ± 0.003
Na <sub>2</sub> O	1.183 ± 0.231	Y <sub>2</sub> O <sub>3</sub>	0.001 ± 0.001
TiO <sub>2</sub>	0.596 ± 0.119	F	0.050 ± 0.000
CaO	2.782 ± 0.467	Cl	0.040 ± 0.000
SO <sub>3</sub>	0.275 ± 0.028	CO <sub>2</sub> O <sub>3</sub>	0.001 ± 0.001
BaO	0.089 ± 0.021	Br	0.001 ± 0.001
MnO	0.013 ± 0.006	CHO	83.693 ± 3.616



Figure 3.18: (a) Photograph and (b) SEM micrograph of CHP.

### 3.3.7 Walnut Shell

Walnut trees grow widely in the Asian belt extending from the Balkans to China (Fernandez-Lopez et al., 2002; Potter et al., 2002) (Figure 3.19). In Europe, it was grown as far back as 1000 BC. and later, it spread to the Mediterranean regions (Martínez et al.,

2010). Global walnut production was recorded around 965,402 tonnes in 2019, where China, the USA, and Iran were the top producers (FAO, 2020; The International Nut and Dried Fruit Council Foundation (INC), 2020). Walnut shell comprises up to 67% of the total weight of the fruit (Uzun and Yaman, 2017; Członka et al., 2020). The principal feature of walnut shell microstructure is the high lignification stone cells, which are relatively short-sized and isodiametric sclereids. The cell walls, which possess high strength and stiffness, account for almost 90% of cell volume (Antreich et al., 2019; Zhao et al., 2019a). Walnut shells contain higher amounts of hydrophobic materials (lignin, 50.3%) than hygroscopic materials (cellulose (23.9%) and hemicellulose (22.4%)) (Sarsari et al., 2016; Xiao et al., 2020). Walnut shell can be crushed or ground into different grits that range from coarse grits to fine powders. Because of its high hardness, walnut shell is used as an abrasive to blast clean (Srinivasan and Viraraghavan, 2008) and render cementitious surfaces (Fleming and Temyer, 2009). Besides, walnut shell finds its place in the building construction industry as it has sound technical features such as lower water absorption, better strength, and bio-resistance (Shafigh et al., 2014). Studies have been conducted using walnut shell in the production of bio-composite (Ayrilmis et al., 2013; Nitin and Singh, 2013; Zahedi et al., 2013; Gope et al., 2015; Salasinska et al., 2018; Orue et al., 2020; Hekimoğlu et al., 2021), particleboard (Gürü et al., 2008; Pirayesh et al., 2013), MDF panels (Khanjanzadeh et al., 2014; Da Silva et al., 2017) as well as a replacement for aggregates in concrete (Cheng et al., 2017; Husain et al., 2017; Kamal et al., 2017; Hilal et al., 2020; Venkatesan et al., 2021) and alternative material for the load-bearing wall (Mirón et al., 2017).

The physical and chemical properties of WSG are summarised in Table 3.5. WSG was found to have a bulk density of  $630 \text{ kg/m}^3$  and a specific gravity of 1.28. Besides, the lower porosity (0.92) and lower water absorption (29.90%) of WSG revealed its non-absorbent nature. Moreover, the XRD pattern of WSG exhibits a significant amount of amorphosity (Figure 3.20), and the SEM image shows that, due to the high lignin concentration, WSG has a very rigid and thick structure in the cell wall (Figure 3.21(b)) (Han et al., 2018).

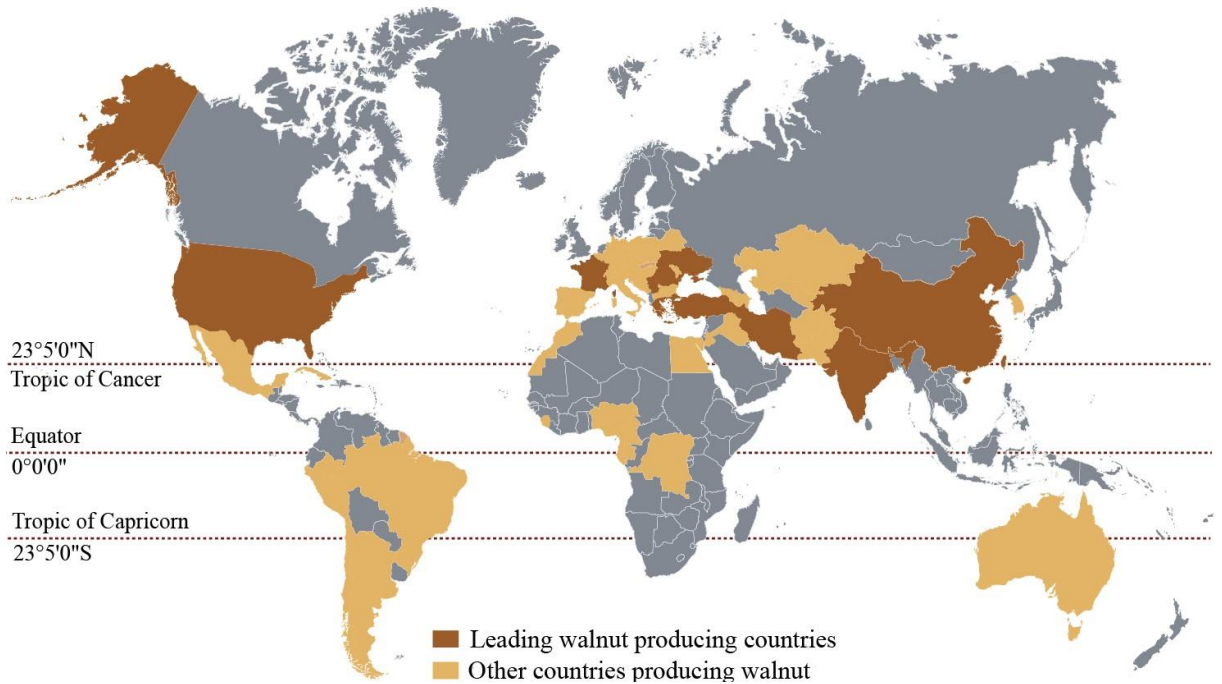


**Figure 3.19:** Global walnut producing countries (FAO, 2020).

**Table 3.5:** Properties of WSG.

<b>Physical properties</b>			
Bulk density (kg/m <sup>3</sup> )		630 ± 2.12	
Specific gravity		1.28 ± 0.10	
Porosity		0.92 ± 0.08	
Water absorption after 24 hrs under water (%)		29.90 ± 3.93	
Thermal conductivity (W/mK)		0.109 ± 0.011	
Volumetric heat capacity (×10 <sup>6</sup> J/m <sup>3</sup> K)		0.577 ± 0.030	
Specific heat capacity (J/m <sup>3</sup> K)		915.08 ± 2.97	
Natural moisture content (%)		6.75 ± 0.33	
Colour		Sandy brown	
<b>Chemical compounds (%)</b>			
SiO <sub>2</sub>	1.103 ± 0.132	MnO	0.002 ± 0.001
Al <sub>2</sub> O <sub>3</sub>	0.536 ± 0.034	ZrO <sub>2</sub>	0.002 ± 0.001
K <sub>2</sub> O	1.871 ± 0.178	P <sub>2</sub> O <sub>5</sub>	0.073 ± 0.013
MgO	0.512 ± 0.021	SrO	0.001 ± 0.001
Fe <sub>2</sub> O <sub>3</sub>	0.062 ± 0.017	CuO	0.005 ± 0.002
Na <sub>2</sub> O	0.930 ± 0.167	ZnO	0.003 ± 0.001

Table 3.5: Properties of WSG (continued).

Chemical compounds (%)			
TiO <sub>2</sub>	0.098 ± 0.014	Y <sub>2</sub> O <sub>3</sub>	0.001 ± 0.001
CaO	1.722 ± 0.139	F	0.050 ± 0.000
SO <sub>3</sub>	0.057 ± 0.020	Cl	0.040 ± 0.000
BaO	0.075 ± 0.011	CHO	92.857 ± 3.396

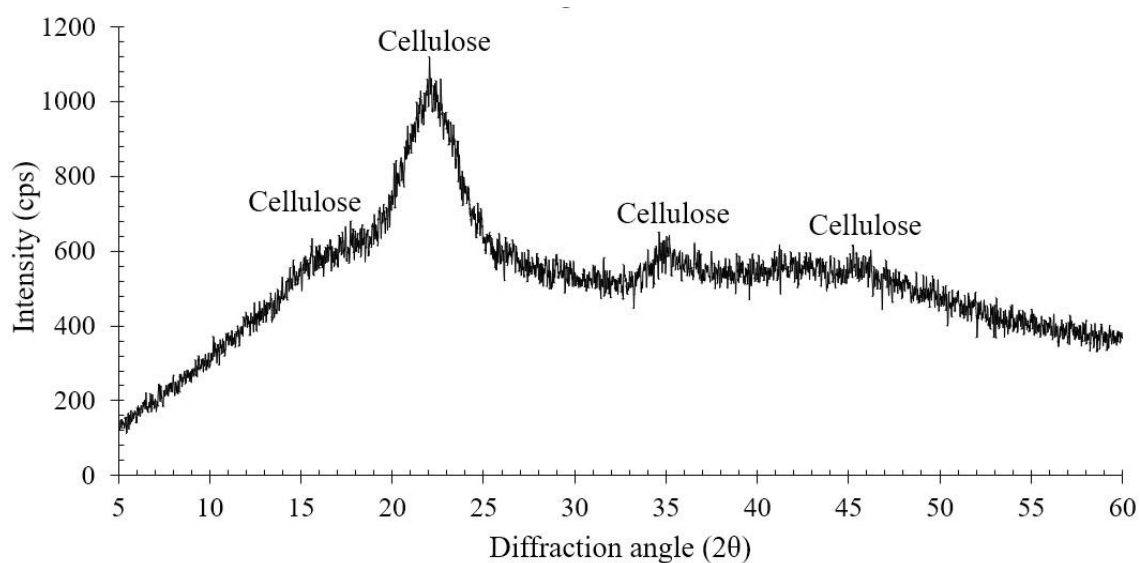
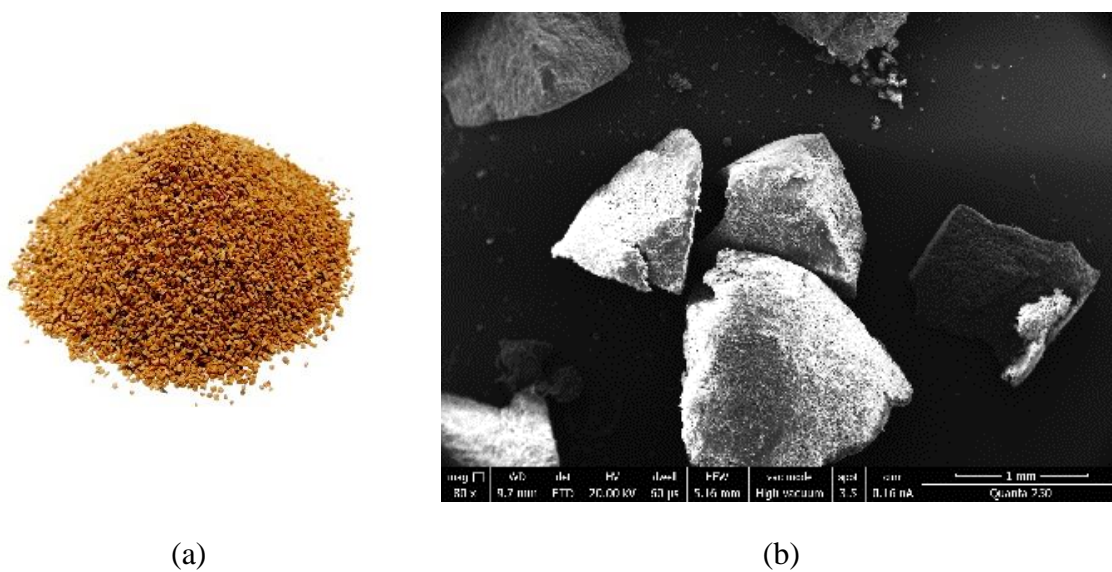


Figure 3.20: XRD spectrum of WSG.



(a)

(b)

Figure 3.21: (a) Photograph and (b) SEM micrograph of WSG.

### 3.4 Summary of the Chapter

This chapter outlined the research methodology and methods. Moreover, the properties of selected agro-wastes used as an enhancement in clay blocks were investigated and presented in this chapter. The findings can be summarised as follows:

- This study followed a quantitative research methodology that consists of experimental and numerical research methods to obtain the data and solve the research problem.
- The maximum dry density of clay was  $2320 \text{ kg/m}^3$  at an optimum moisture content of 15.50%, and it was medium plastic clay with a plasticity index of 12.36%. Besides, quartz ( $\text{SiO}_2$ ) was identified as the main mineralogical phase in clay by the XRD analysis. Other mineralogical phases found were kaolinite ( $\text{Al}_2(\text{Si}_2\text{O}_5)(\text{OH})_4$ ) and haematite ( $\text{Fe}_2\text{O}_3$ ). Moreover, clay had a bulk density of  $1430 \text{ kg/m}^3$  and a specific gravity of 2.32.
- The bulk density and specific gravity varied depending on the type of agro-wastes. The highest density and specific gravity were found in eggshell ( $1170 \text{ kg/m}^3$ , 1.74) followed by walnut shell ( $630 \text{ kg/m}^3$ , 1.28) and sawdust ( $230 \text{ kg/m}^3$ , 1.13), and the lowest in coconut husk ( $130 \text{ kg/m}^3$ , 0.61). Specific gravity affects the natural moisture content of the agro-wastes since a high specific weight may result in a low dry moisture content.
- The water absorption test revealed that coconut husk had a higher absorption rate (195.16%) than sawdust (127.66%), eggshell (39.42%), and walnut shell (29.90%).
- Furthermore, coconut husk (7.65) was more porous in nature compared to sawdust (5.09), eggshell (0.56), and walnut shell (0.92).
- According to the thermal conductivity measurements, sawdust (0.064 W/mK) and coconut husk (0.050 W/mK) had lower conductivity values than eggshell (0.146 W/mK) and walnut shell (0.109 W/mK).
- XRD spectra revealed that all diffraction peaks in ESP indicated the existence of

calcite ( $\text{CaCO}_3$ ) as the major component and other additives were amorphous in nature.

- SEM images showed that ESP had irregular and stone-like particles. On the other hand, CHP had more porous and rough surfaces than SDP, whereas WSG displayed a very rigid and thick structure.

## *Chapter 4*    **EXPERIMENTAL EVALUATION (PART A-PHYSICO-MECHANICAL PROPERTIES TESTS)**

### **4.1 Introduction**

This chapter describes the experimental programme for determining the physico-mechanical properties of the produced clay samples. The experiment programme of Part A was conducted in two phases. In phase 1, various percentages of eggshell, sawdust, coconut husk, and walnut shell grit were individually added to the mixture to produce the samples, and their properties were examined. Based on the results from phase 1, phase 2 was performed to assess their combined effect. The results from both experimental test phases were analysed and discussed in this chapter.

### **4.2 Sample Preparation**

The raw materials were sieved with the square mesh sieve to have a controlled particle size range between  $150 \mu\text{m} < x < 212 \mu\text{m}$  for ESP,  $300 \mu\text{m} < x < 1.18 \text{ mm}$  for CHP, and  $1.18 \text{ mm} < x < 2 \text{ mm}$  for WSG. In this study, SDP was categorised into three particle size ranges: SDP-a ( $212 \mu\text{m} < x < 300 \mu\text{m}$ ), SDP-b ( $425 \mu\text{m} < x < 600 \mu\text{m}$ ), and SDP-c ( $1.18 \text{ mm} < x < 2.00 \text{ mm}$ ) as it came into wide particle size range. Clay block with no additives was made as the reference sample (REF), and for the composite samples, the waste materials were mixed in relation to the dry weight of the clay. Table 4.1 and Table 4.2 give the mixing proportions for the composite samples. The water used was normal tap water at a temperature of  $20 \pm 2 \text{ }^\circ\text{C}$ . Samples for the physical and mechanical properties tests were prepared in prismatic moulds of  $40 \text{ mm} \times 40 \text{ mm} \times 160 \text{ mm}$  (Figure 4.1) following the British standard BS EN 1015-11 (BS EN 1015-11, 2019) for cement mortars. This standard is frequently used for unfired brick studies due to the lack of consistent and internationally established laboratory test procedures for assessing material properties and design parameters for earthen building construction (Schroeder,

2012). Three prism samples were produced for each mix composition, and the physio-mechanical tests results represent the average of the three tested samples. First, clay was passed through a sieve with a 2.00 mm<sup>2</sup> mesh size to remove any lumps. Then dry clay and waste materials were thoroughly mixed in a mechanical mixer machine (Figure 4.2(a)). Afterwards, based on the proctor test, 15.50% of water by dry weight of clay was gradually added to the dry mixture to obtain the optimum moisture content and homogeneity for moulding the samples (Figure 4.2(b)). The amount of water in each series was adjusted to maintain the same consistency for moulding. The mixture was put into the moulds in two layers, and each layer was manually compacted with 25 blows. This investigation may not have accomplished uniform compaction due to hand compaction. However, hand compaction was applied to interpret the production of unfired clay brick in rural areas where advanced apparatus is unavailable. The samples were covered with plastic bags for 24 hours after being moulded to ensure uniform water absorption and no sudden loss of moisture. Before demoulding, the samples were dried at the laboratory room temperature of around 23-26 °C, and relative humidity of 30-34% for 7 days. Clay samples were dried naturally to slowly dissipate the moisture and reduce internal cracks due to shrinkage. After demoulding, the samples were dried for another 21 days in the same laboratory conditions before being examined. Although the absence of cement in the blends implies that the standards need no curing period, this drying period was chosen because most traditional unfired clay brick manufacturers use it.

**Table 4.1:** Mix details (Phase 1).

Sample ID	Clay (g)	Agro-wastes (g)				Agro-wastes (wt%)			
		ESP	SDP	CHP	WSG	ESP	SDP	CHP	WSG
REF	550	-	-	-	-	-	-	-	-
E-10	550	55	-	-	-	10	-	-	-
E-20	550	110	-	-	-	20	-	-	-
E-30	550	165	-	-	-	30	-	-	-
E-40	550	220	-	-	-	40	-	-	-
E-50	550	275	-	-	-	50	-	-	-
S-a-2.5	550	-	13.75	-	-	-	2.5	-	-
S-a-5	550	-	27.50	-	-	-	5	-	-

Table 4.1: Mix details (Phase 1) (continued).

Sample ID	Clay (g)	Agro-wastes (g)				Agro-wastes (wt%)			
		ESP	SDP	CHP	WSG	ESP	SDP	CHP	WSG
S-a-7.5	550	-	41.25	-	-	-	7.5	-	-
S-a-10	550	-	55	-	-	-	10	-	-
S-b-2.5	550	-	13.75	-	-	-	2.5	-	-
S-b-5	550	-	27.50	-	-	-	5	-	-
S-b-7.5	550	-	41.25	-	-	-	7.5	-	-
S-b-10	550	-	55	-	-	-	10	-	-
S-c-2.5	550	-	13.75	-	-	-	2.5	-	-
S-c-5	550	-	27.50	-	-	-	5	-	-
S-c-7.5	550	-	41.25	-	-	-	7.5	-	-
S-c-10	550	-	55	-	-	-	10	-	-
C-2.5	550	-	0	13.75	-	-	-	2.5	-
C-5	550	-	-	27.5	-	-	-	5	-
C-7.5	550	-	-	41.25	-	-	-	7.5	-
C-10	550	-	-	55	-	-	-	10	-
W-5	550	-	-	-	27.50	-	-	-	5
W-10	550	-	-	-	55	-	-	-	10
W-15	550	-	-	-	82.50	-	-	-	15
W-20	550	-	-	-	110	-	-	-	20



(a)



(b)

**Figure 4.1:** Reference samples: (a) Prism samples in 40 mm × 40 mm × 160 mm mould and (b) Full prism samples after demoulding.



(a)

(b)

**Figure 4.2:** Sample preparation: (a) dry mixing and (b) wet mixing.

### 4.3 Tests

The samples were subjected to five different tests, including density, linear shrinkage, capillary water absorption, compressive strength, and flexural strength tests. The tests were selected based on a review of previous research (Riza et al., 2010; Jannat et al., 2020), where most of the authors considered them highly important tests for assessing the key physical and mechanical properties of unfired clay blocks. Moreover, XRD analysis was conducted to study the crystal structure of the clay composites. For the analysis, samples were prepared by grinding them into a fine powder with an agate mortar and pestle. Prior to the preparation of each sample, mortars and pestles were properly washed with tap water, followed by distilled water, and then dried in order to prevent cross-contamination between samples. Furthermore, sample holders were cleaned after every run and then filled with a portion of the next sample that was discarded before preparing the sample for analysis.

#### 4.3.1 Density

The density of materials influences their properties like strength, heat, and conductivity. In this study, the BS EN 771-1 (BS EN 771-1, 2003) standard was followed to determine the density of the samples. The test procedure can be described as follows: the 28-day dry samples (an average of three samples per mix composition) were carefully cleaned

with a cloth to eliminate any loose substances attached. Then all dimensions of the sample along each axis (length, width, and thickness) were measured using a digital calliper (precision 0.01 mm), and the average value for each dimension was calculated. Due to the limitations in using digital callipers to record precise measurements and slight deformations in the shape of the prism samples after the drying period, ten measurements were taken for each axis at various locations in order to get representative values. The volume ( $V$ , m<sup>3</sup>) and mass ( $M$ , kg) of the samples were measured, and the density ( $\rho$ , kg/m<sup>3</sup>) was determined using the following Equation (4.1):

$$\rho = \frac{M}{V} \quad (4.1)$$

### ***4.3.2 Linear Shrinkage***

Shrinkage control is crucial for preventing the deformation and cracking of the samples. It is a physical phenomenon that is caused by the evaporation of moisture content in the samples during the drying process. The linear shrinkage test was performed following the BS EN 772-14 (BS EN 772-14, 2002) standard on three samples per mix composition. For the test procedure, four dimensions of the prism mould length ( $L_i$ , mm) were measured, and at the end of the 28-day drying period, the four dimensions of the prism sample length ( $L_d$ , mm) were recorded using a digital calliper. The average length was then taken, and Equation (4.2) was used to calculate the linear shrinkage ( $S_d$ , %):

$$S_d = \frac{L_i - L_d}{L_i} \times 100 \quad (4.2)$$

### ***4.3.3 Flexural Strength***

A 25 kN frame capacity Tinius Olsen H25KS was used to test the flexural strength under three-point loading in accordance with BS EN 1015-11 (BS EN 1015-11, 2019). The test was performed on the full prism samples (40 mm × 40 mm × 160 mm) after 28 days of the drying period. The clear span between the two supports was 100 mm, as shown in

Figure 4.3, and the load was applied at a rate of 10 N/s at the middle of the samples until it failed. Three samples from each mix design were tested, resulting in the formation of half samples at the end of the test, which were then used for compressive strength and capillary water absorption tests. The following Equation (4.3) from EN 1015-11 was used to determine the flexural strength:

$$f = \frac{1.5FL}{bd^2} \quad (4.3)$$

where  $f$  (MPa) is the flexural strength,  $F$  (N) is the obtained load,  $L$  (mm) is the distance between the supports,  $b$  (mm) is the height of the sample, and  $d$  (mm) is the width of the sample.

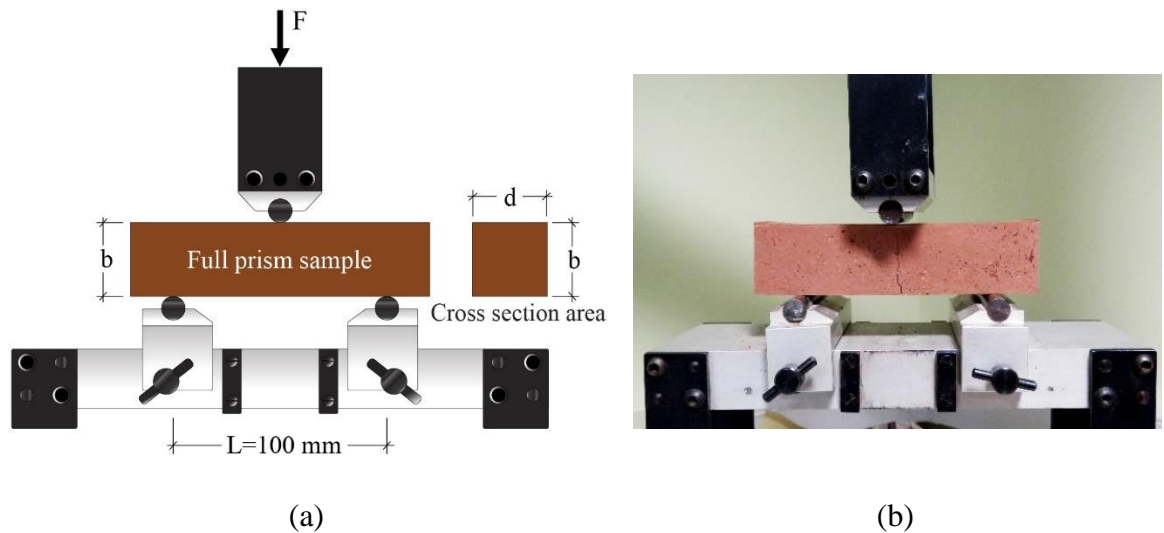


**Figure 4.3:** Flexural strength test: (a) schematic and (b) experimental.

#### 4.3.4 Compressive Strength

Half prism samples with an average dimension of  $40 \text{ mm} \times 40 \text{ mm} \times 80 \text{ mm}$  were tested for compressive strength according to the BS EN 1015-11 (BS EN 1015-11, 2019) standard. Three samples were examined, and mean values were calculated for each mix design. A computerised and motorised triaxial machine was used for the test (Figure 4.4). According to the standard, the samples were aligned centrally between two bearing steel

plates of 40 mm × 40 mm and the charge velocity used was 0.40 MPa/s until the compression caused visible damage. The compressive strength was determined using Equation (4.4):

$$C = \frac{F}{A} \quad (4.4)$$

where  $C$  (MPa) is the compressive strength,  $F$  (kN) is the ultimate load and  $A$  (mm<sup>2</sup>) is the area of the bed face. In this study, compressive strength test was performed for both air-dried and oven-dried samples.

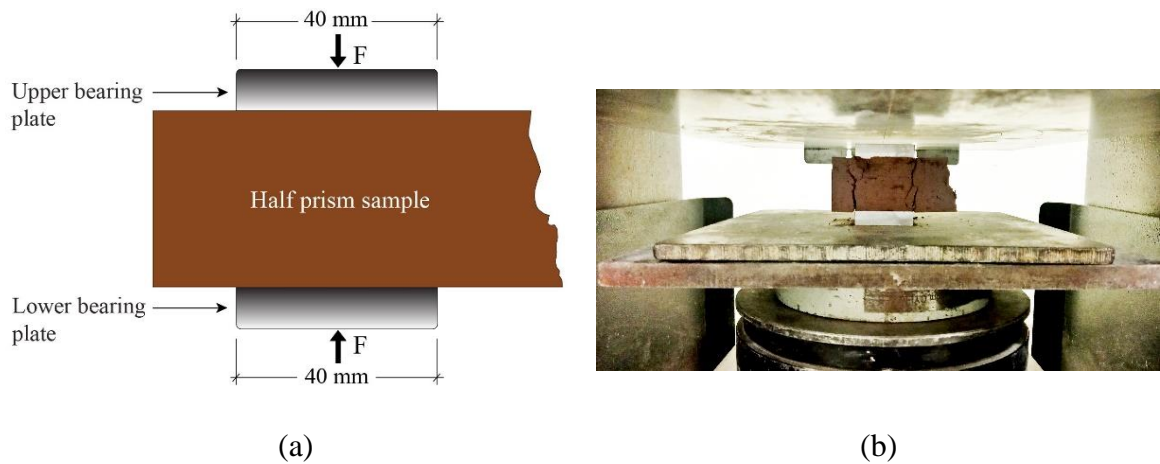


**Figure 4.4:** Compressive strength test: (a) schematic and (b) experimental.

#### 4.3.5 Capillary Water Absorption

The capillary water absorption test was performed to determine the ability of the waste-incorporated clay samples to resist the absorption and retention of water. BS EN 1015-18 (BS EN 1015-18, 2002) specifies the test method on one half prism sample (40 mm × 40 mm × 80 mm) obtained from the flexural strength test. Following the standard, to attain a constant mass, the half prisms were first dried for 24 hours at  $60 \pm 5$  °C in a ventilated oven and the mass of the oven-dried samples were recorded. As the samples had dissimilar sizes after the breakage in the flexural strength test, the flat faces of the samples were immersed in a constant head-water bath to a depth of 5 mm for 10 min to

ensure consistency (Figure 4.5). Then, after 10 minutes, the samples were removed from the water and their mass were noted. The capillary water absorption was calculated (average of three samples per mix composition) by the following Equation (4.5) (BS EN 1015-18, 2002):

$$C_w = 0.1 \times (M_t - M_i) \quad (4.5)$$

where  $C_w$  ( $\text{kg}/(\text{m}^2 \times \text{min}^{0.5})$ ) is the capillary water absorption coefficient,  $M_i$  (g) is the initial mass of the sample, and  $M_t$  (g) is the mass of the sample after 10 min.

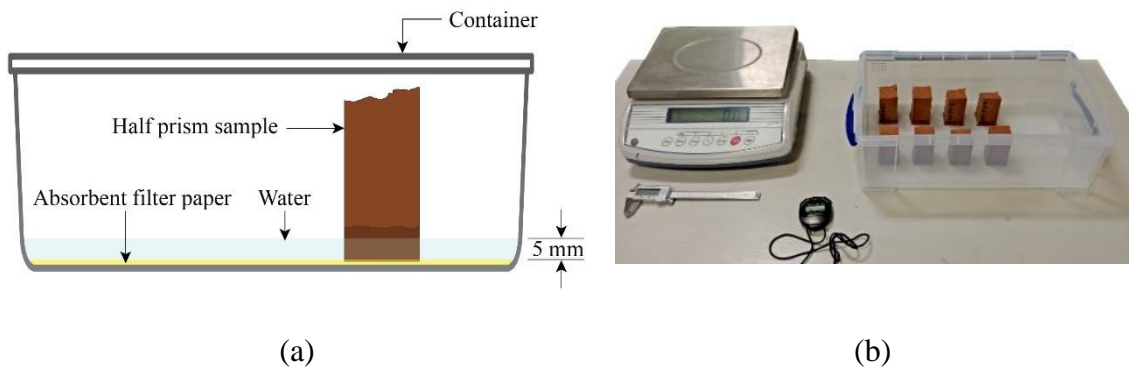


**Figure 4.5:** Capillary water absorption test: (a) schematic and (b) experimental.

## 4.4 Results and Discussions (Phase 1)

This section presents and discusses the test results of the physico-mechanical properties of samples produced by incorporating agro-wastes individually. The data are plotted with error bars showing the standard deviation of the obtained results from three tested samples for each mixture.

### 4.4.1 Density

The effect of various ESP, SDP, CHP, and WSG ratios on the density of the samples is shown in Figure 4.6. The results are average values of three samples per mix composition (see Appendix A). It can be observed that the density of the samples decreased with higher ESP, SDP, CHP, and WSG contents, which were lower than the reference sample.

This decrease in density is mainly attributed to the lower specific gravity of ESP, SDP, CHP, and WSG particles as compared to the RCP used in this study. The increased lighter waste content displaced the heavier clay content, resulting in a drop in sample density. The decrease in density for increasing ESP content from 10% to 50% in the mixture corresponds to a decrease of about 6% to 14%, while for 2.5% to 10% CHP and 5% to 20% WSG additions, the decreases were about 17% to 34% and 9% to 21%, respectively, in comparison to the reference clay sample. Furthermore, with the same percentages of SDP content, SDP-a-blended samples had slightly higher density compared to the other two groups. This is in line with the fact that SDP-a had a higher specific gravity (1.23) than SDP-b (1.14) and SDP-c (1.02). This can also be explained by the particle size difference between each group. SDP-c had a larger particle size, resulting in more gaps between SDP and clay matrix, but SDP-a had considerably smaller particle dimensions, resulting in a more homogenous end product, with fewer pores and a higher density.

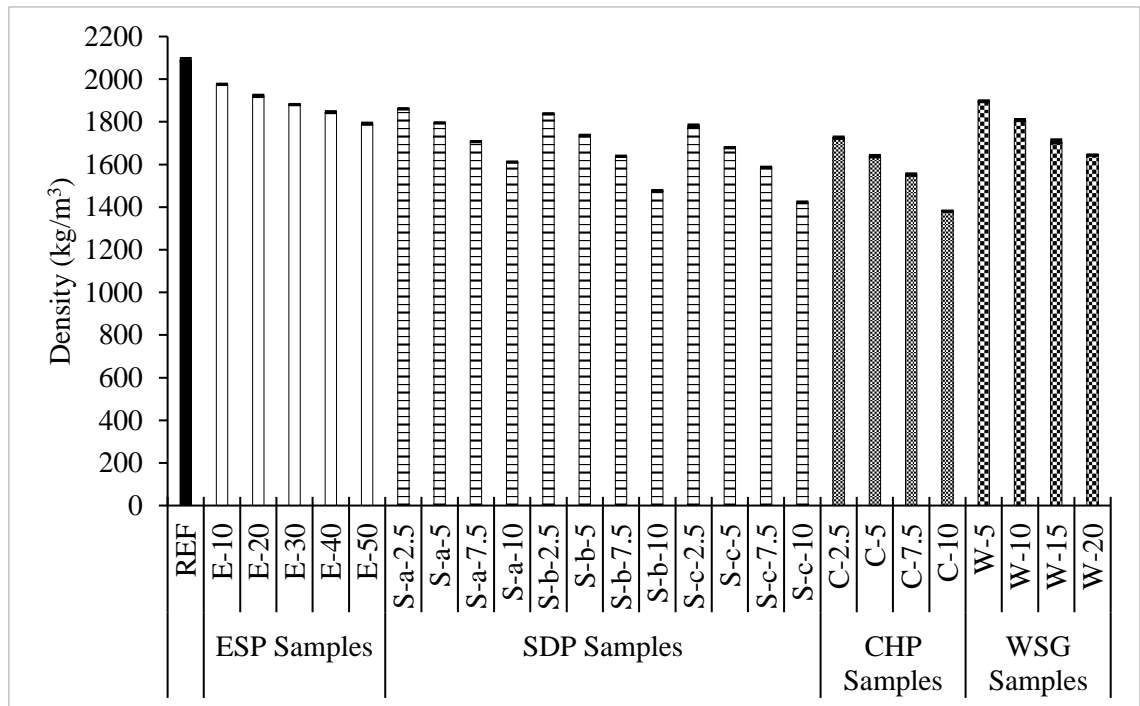


**Figure 4.6:** Density test results (Phase 1).

*Error bar represents the standard deviation of data.*

The density of the samples decreased from 1861 kg/m<sup>3</sup> to 1611 kg/m<sup>3</sup> (SDP-a), 1837

kg/m<sup>3</sup> to 1476 kg/m<sup>3</sup> (SDP-b) and 1781 kg/m<sup>3</sup> to 1422 kg/m<sup>3</sup> (SDP-c) with 2.5% to 10% sawdust addition, corresponding to around 23%, 29%, and 32% decreases, respectively, compared to the reference sample (2091 kg/m<sup>3</sup>). From Figure 4.6, it can be observed that both the reference and all ESP achieved density that exceeded the minimum value of 1750 kg/m<sup>3</sup> stipulated in the Indian Standard: IS 1725 (IS: 1725, 1982) and Sri Lankan Standard: SLS 1382 (SLS 1382, 2009). However, in the case of WSG addition, samples with 5%-10% content met the standard requirement. Besides, for all three groups of SDP samples, 2.5% sawdust had density  $\geq 1750$  kg/m<sup>3</sup>. Additionally, the sample with 5% SDP-a met the standard criteria, with a density of 1776 kg/m<sup>3</sup>. Therefore, they can be used as load-bearing units according to the standards. Other manufactured samples can be categorised as lightweight clay brick as a construction material by the standards (Limami et al., 2021). Several authors noticed similar results with natural fibre addition in unfired clay blocks, where density dropped with increasing the amount of fibres (Khedari et al., 2005; Demir, 2008; Ashour et al., 2015; Danso et al., 2015b; Zak et al., 2016; Laborel-Préneron et al., 2017; Giroudon et al., 2019; Ojo et al., 2019; Thanushan et al., 2019; Wang et al., 2019; Charai et al., 2020; Limami et al., 2021). However, the results from this study were contrary to the findings of Amaral et al. (2013) and Adogla et al. (2016), which established that the density of the compressed laterite brick and soil-cement brick increased steadily with increasing ESP content. This might be due to the mechanical compaction technique used to manufacture the samples (Baiden and Asante, 2004; Danso, 2016).

#### ***4.4.2 Linear Shrinkage***

Shrinkage is highly affected by the nature and quantity of additives as well as their surface characteristics. Furthermore, the moisture absorption behaviour, water loss, and porosity of the samples all have an impact on shrinkage (Parveen et al., 2017; Türkmen et al., 2017). The linear shrinkage of each combination was calculated by taking the average of the three measurements (see Appendix A). Figure 4.7 shows that by increasing SDP-b and SDP-c in the mixture, the shrinkage of the samples gradually decreased from 6.05% to 5.53% and 5.99% to 4.47%, respectively. The SDP-c samples with a larger particle size had a greater linear shrinkage reduction of around 45% (10%

SDP-c), whereas the SDP-b (10%) had a shrinkage reduction of 31% compared to the reference sample. This is consistent with previous studies (Bouhicha et al., 2005; Murillo et al., 2005; Vilane, 2010; Danso et al., 2015b), which indicated that adding natural fibres to the mixture improved shrinkage. Bouhicha et al. (2005) and Araya-Letelier et al. (2018) observed that increasing the percentage and length of barley straw and pig hair, respectively, reduced the drying shrinkage of the samples. This could be due to the fibres being long enough for the development of bond stresses at the fibre-soil interface, therefore opposing soil deformation and contraction. In the case of SDP-a, the 2.5% content had lower linear shrinkage than the reference sample, but linear shrinkage increased with increasing SDP-a content. This result might be explained by the fact that the fibre length is insufficient for the bond stresses to build; however, additional research is required to confirm this.

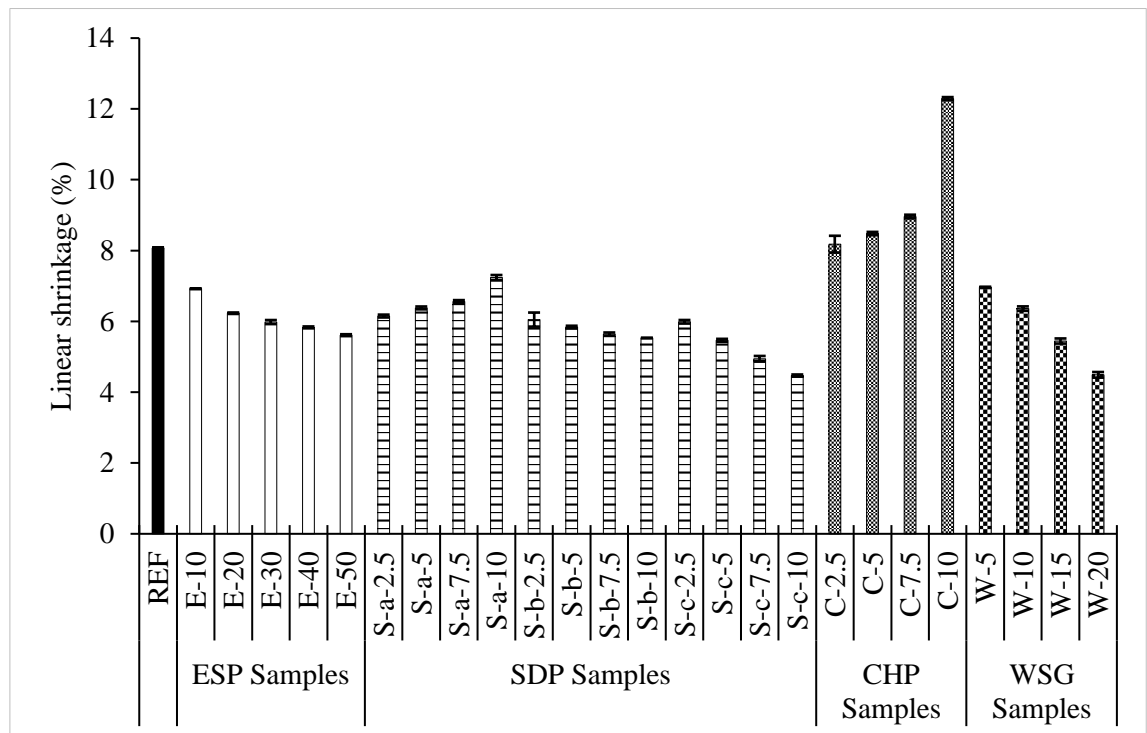


**Figure 4.7:** Linear shrinkage test results (Phase 1).

*Error bar represents the standard deviation of data.*

On the other hand, the samples with CHP tended to shrink gradually from 8.18% to 12.29% (around a 52% increase relative to the reference sample) when the CHP content increased from 2.5% to 10%. It may be due to the higher water absorption potential of

CHP relative to SDP, which weakened the waste particle-clay bonding, resulting in increased shrinkage during the drying period due to evaporation. Besides, CHP's ability to absorb water from capillary pores may cause volume reduction (contraction) and an increase in sample shrinkage (deformation). For ESP samples, shrinkage gradually decreased from 6.92% to 5.61%, with waste content varying from 10% to 50%. It might be related to the adsorption of calcium ions from ESP, which caused a rise in pore fluid viscosity (Bhuvaneswari et al., 2010; Sivapullaiah and Jha, 2014; Jha and Sivapullaiah, 2015). Also, the addition of WSG from 5% to 20% induced a reduction in linear shrinkage from 13.74% to 44.36%. It is stated that if the material shrinks more than 8%, the drying process can produce internal fractures and cracking (Türkmen et al., 2017). Concerning this, the present study found shrinkage values within allowable ranges except for the reference and CHP samples.

#### ***4.4.3 Compressive and Flexural Strength***

The results of the mechanical strength tests are presented in Figure 4.8. At each mixture, both compressive and flexural strengths were determined by taking the average of the three results (see Appendix B). The strength enhancement in the waste-incorporated clay mixture largely depends on the development of waste particle-clay matrix adhesion, clay matrix-clay matrix bonding, and waste particle-waste particle cohesion. These bonds can be influenced by particle size, surface conditions, and the amount of waste present (Salih et al., 2020). In this study, compressive strength was determined for both air-dried and oven-dried samples. After 28 days, both the reference and waste-incorporated samples fulfilled the minimum compressive strength requirement of the standards (1 MPa-2.80 MPa) (TS 2514, 1977; CID-GCBNMBC-91-1, 1991; NZS 4298, 1998; SLS 1382, 2009).

The results show that the compressive strength for the samples with ESP increased gradually with an increase in waste content up to 40%, and then the strength decreased for samples with 50% ESP. Amaral et al. (2013) and Adogla et al. (2016) reported comparable results, where the highest compressive strength was recorded at 30% ESP for soil-cement bricks and compressed earth blocks. The increase in strength can be explained by the pozzolanic reaction of the clay minerals with the high amount of calcium available in ESP, which formed a cementitious compound that dispersed among

the clay particles and improved the adhesion of the clay matrix and ESP particles. As a pozzolan, the clay contains siliceous and aluminium elements, while ESP is a non-pozzolan material (Papadakis and Tsimas, 2002; ASTM C618-9, 2005).

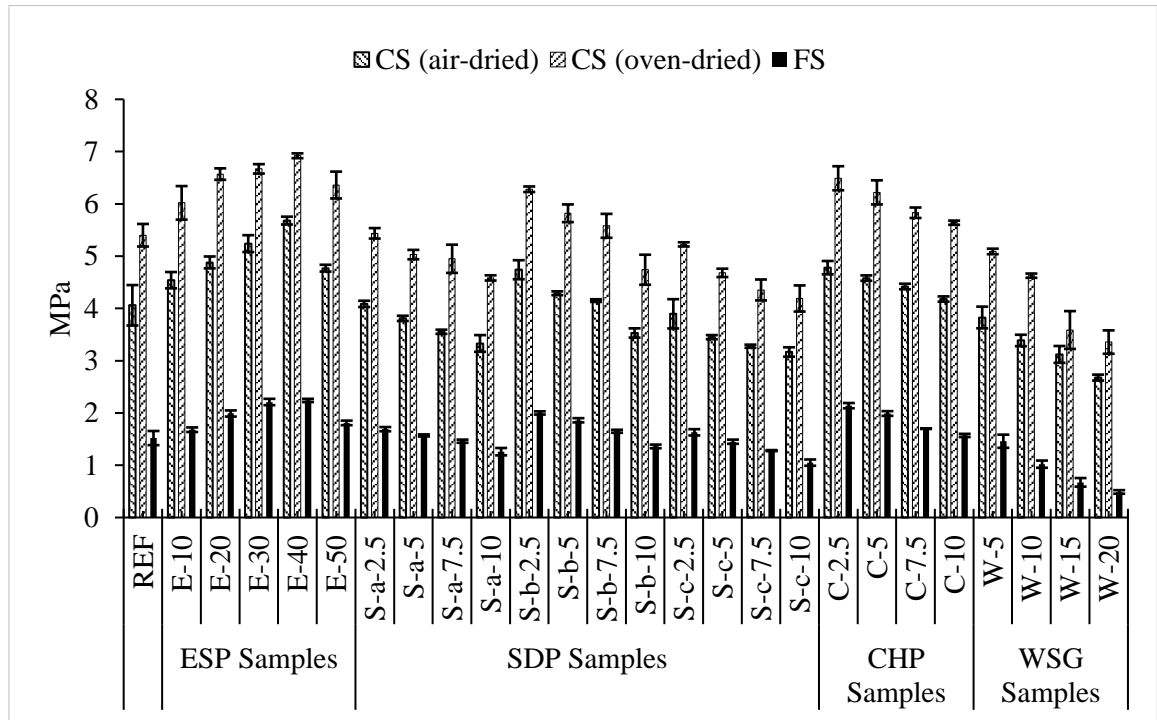
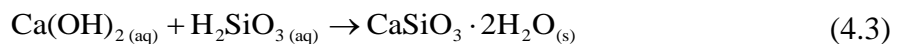
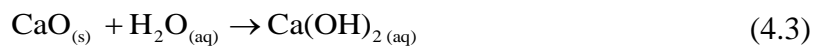
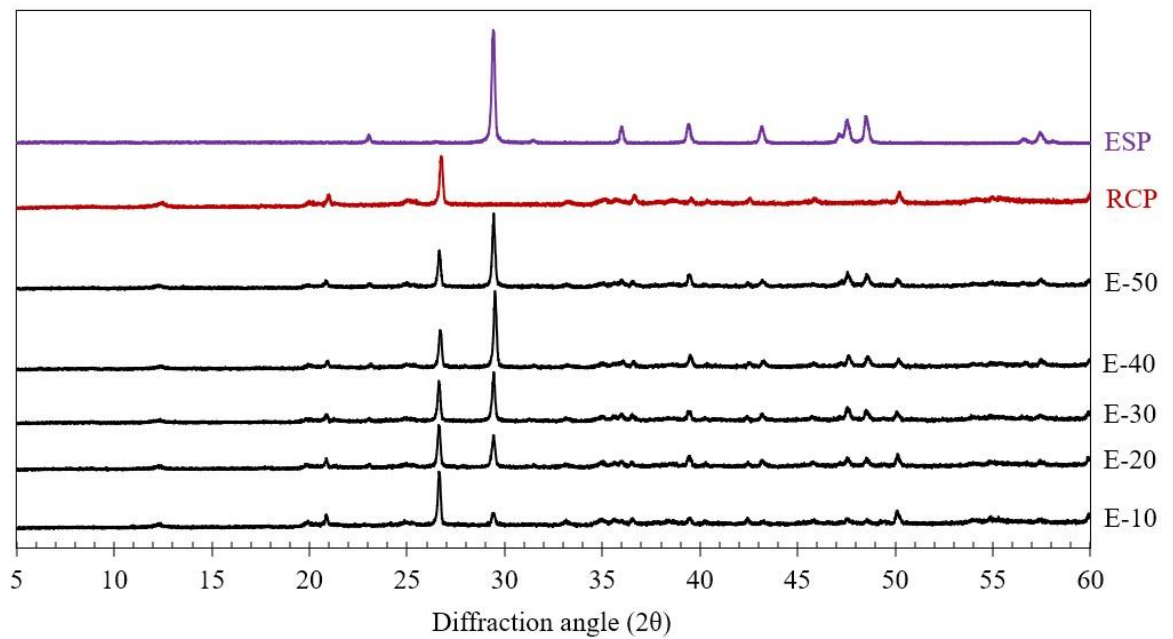


**Figure 4.8:** Compressive strength (CS) and flexural strength (FS) test results (Phase 1).  
Error bar represents the standard deviation of data.

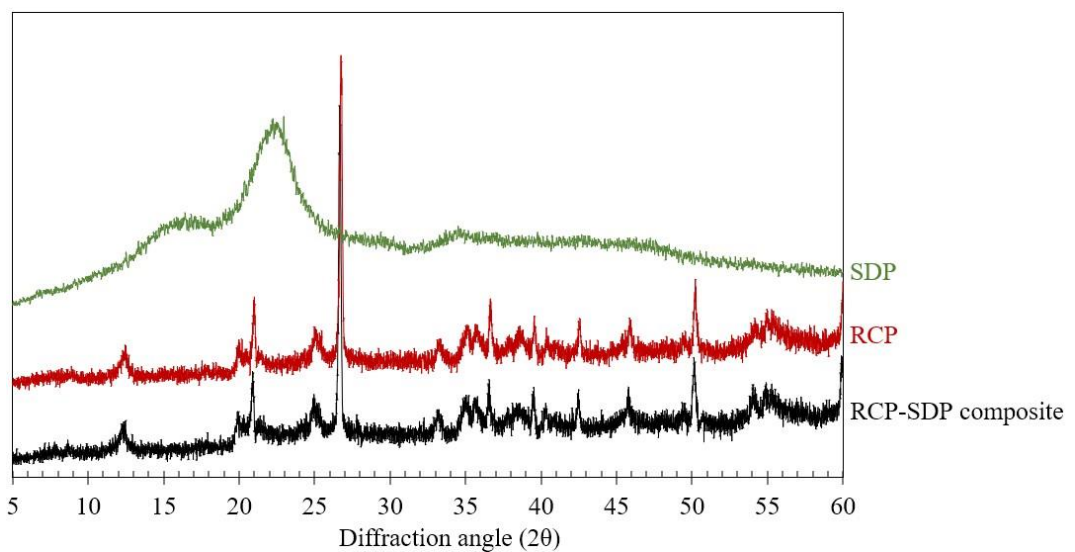
When clay, ESP, and water are mixed, a pozzolanic reaction occurs, which produces samples with cementitious properties. The ESP's calcium oxide ( $\text{CaO}$ ) reacts with water at first, leading to the production of calcium hydroxide ( $\text{Ca(OH)}_2$ ), also known as portlandite. Subsequently, portlandite ( $\text{Ca(OH)}_2$ ) and silica ( $\text{SiO}_2$ ) or silicic acid ( $\text{Si(OH)}_4$ ) are converted to form calcium silicate hydrate ( $\text{CaSiO}_3 \cdot 2\text{H}_2\text{O}$ ) which has strong cementing properties responsible for the strength of the materials (Ngayakamo et al., 2020).



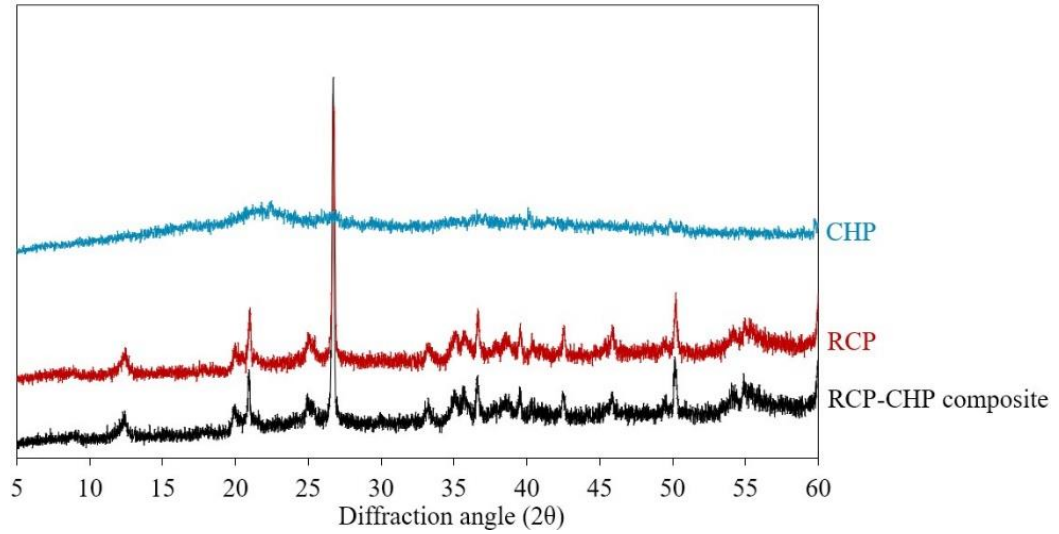
The lower compressive strength associated with higher ESP content may be due to the insufficient presence of silica content in the clay matrix as a result of a higher additive amount. Therefore, fewer pozzolanic reactions occurred, and unreacted portlandite was prevalent in the mixture, resulting in a decrease in mechanical strength and an increase in porosity (Millogo et al., 2008; Muntohar, 2011). This result is also accompanied by the XRD analysis of ESP incorporated samples (Figure 4.9(a)).



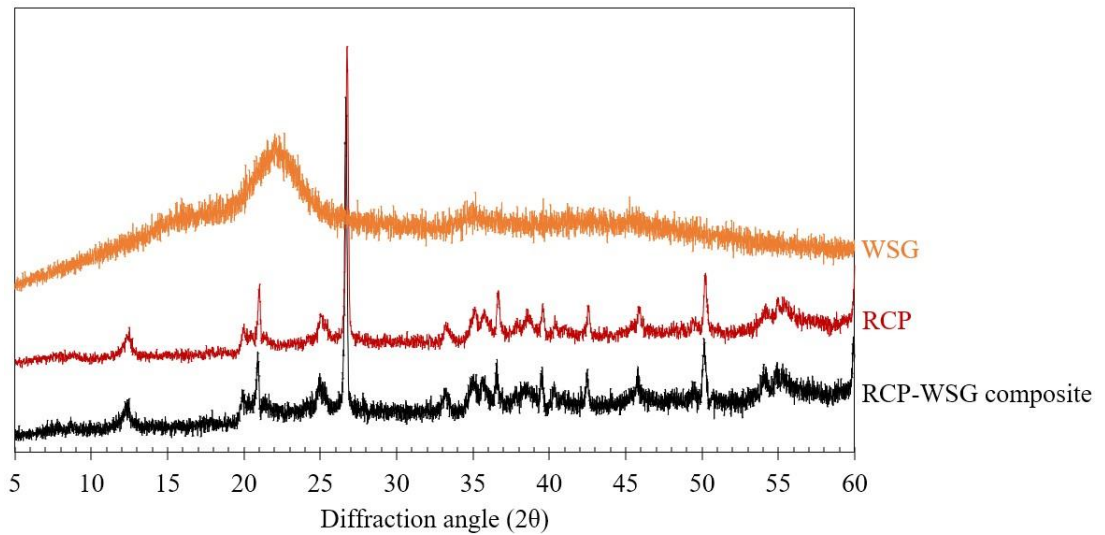
(a)



(b)



(c)



(d)

**Figure 4.9:** XRD analysis: (a) ESP samples, (b) SDP samples, (c) CHP samples and (d) WSG samples.

The XRD spectra revealed that when SDP, CHP, and WSG were mixed with clay, no reaction occurred ((Figure 4.9(b), (c), and (d)). It was observed that the addition of CHP enhanced the compressive strength of the samples in comparison to the reference sample; nevertheless, the highest compressive strength was obtained with the least amount of waste percentage (2.5%). This increase in strength for 2.5% dosage is attributed to the improved molecular cohesion since higher cohesion leads to better compressive strength, and for more than 2.5% content, strength decreased because of the poor adhesion of the

clay to the waste particles. These results are in line with the findings of Khedari et al. (2005), Murillo et al. (2005), Wang et al. (2019), and Thanushan et al. (2019), where the authors reported that the compressive strength of the samples decreased with increasing fibre percentages. This loss in strength is also associated with the increase in porosity caused by the inclusion of lightweight CHP in the blend. The hydrophilic characteristic of natural fibres might cause them to absorb water and expand, efficiently pushing out on the clay matrix throughout the mixing and drying stages of sample production. Then, at the end of the drying period, the fibres lose their absorbed water and shrink back nearly to their original dimensions, forming very fine voids around their periphery, which weaken the interfacial bond (Figure 4.10) (Ghavami et al., 1999; Hejazi et al., 2012). Furthermore, CHP was added to the mixture at the expense of clay, resulting in a reduction in silica content, which led to the production of more porous structures with lower compressive strength than silica composites without additives (Limami et al., 2021).

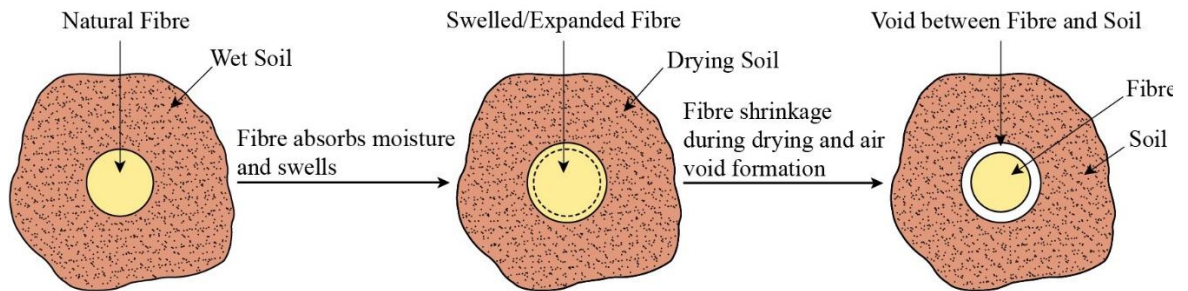


**Figure 4.10:** Interaction between natural fibre and soil (Ghavami et al., 1999; Hejazi et al., 2012).

A similar result was observed for the SDP samples (Figure 4.8), where an increase in the content of sawdust led to a decrease in the compressive strength, irrespective of the particle size dimension. Moreover, the highest mechanical strength was obtained for SDP-b. The study by Mostafa and Uddin (2016) demonstrated that the strength of compressed earth blocks gradually increased for 50-70 mm banana fibres and then decreased for the higher lengths of fibres (80-100 mm). As already highlighted by the authors, the decrease in strength depends on the decline in bulk density, non-homogenous fibre distribution, larger gaps produced by longer fibre lengths, and decreased cohesion

and bonding between the fibres and the soil matrix of the final products. The results showed that at a 2.5% content, SDP-b significantly improved the compressive strength compared to the reference sample, while SDP-a marginally enhanced it, and SDP-c did not improve it. The relatively lower compressive strength values of the SDP samples compared to the CHP samples could be due to the roughness of the CHP particle surface, which contributed to the good adhesion of the fibres to the clay matrix. Furthermore, the inclusion of WSG had a negative impact on the samples' compressive strength. The compressive strength of WSG samples dropped from 3.83 MPa to 2.68 MPa when the waste content increased from 5% to 20% (Figure 4.8), which can be explained by the weak bond between the clay particles and WSG. For the air-dried samples, the maximum compressive strengths were measured as 5.68 MPa at 40% ESP, 4.74 MPa at 2.5% SDP-b, and 4.78 MPa at 2.5% CHP. It can be observed that the compressive strength trend for oven-dried samples was similar to that of air-dried samples, although oven-dried samples exhibited a higher compressive strength level. This could be attributed to the presence of extra water in air-dried samples that may reduce their compressive strength, while oven drying removes more water and results in hardened samples, thus improving the strength. According to Walker (1995) and Kasinikota and Tripura (2022), the inherent strength of clay upon drying is related to the enhanced mechanical strength of oven-dried samples. In comparison to the reference sample, ESP, SDP-b, and CHP addition improved the compressive strength of the air-dried clay samples up to about 40%, 17%, and 18%, and oven-dried samples up to 28%, 16%, and 20%, respectively (Figure 4.11).

The results (Figure 4.8) also demonstrated that the flexural strength test results had similar trends to the compressive strength test results with increasing ESP, SDP, CHP, and WSG content. All the samples met the requirements of the standards (0.25 MPa-0.50 MPa) (IS: 1725, 1982; CID-GCBNMBC-91-1, 1991; NZS 4298, 1998) for unfired earth blocks. The optimum values of flexural strength were recorded as 2.24 MPa at 40% ESP, 2.00 MPa at 2.5% SDP-b, and 2.14 MPa at 2.5% CHP, representing around 47%, 32%, and 41% increases over the reference sample (1.52 MPa) (Figure 4.11). On the other hand, the maximum flexural strength was found in the 5% WSG sample (1.46 MPa), which was lower than the reference sample.

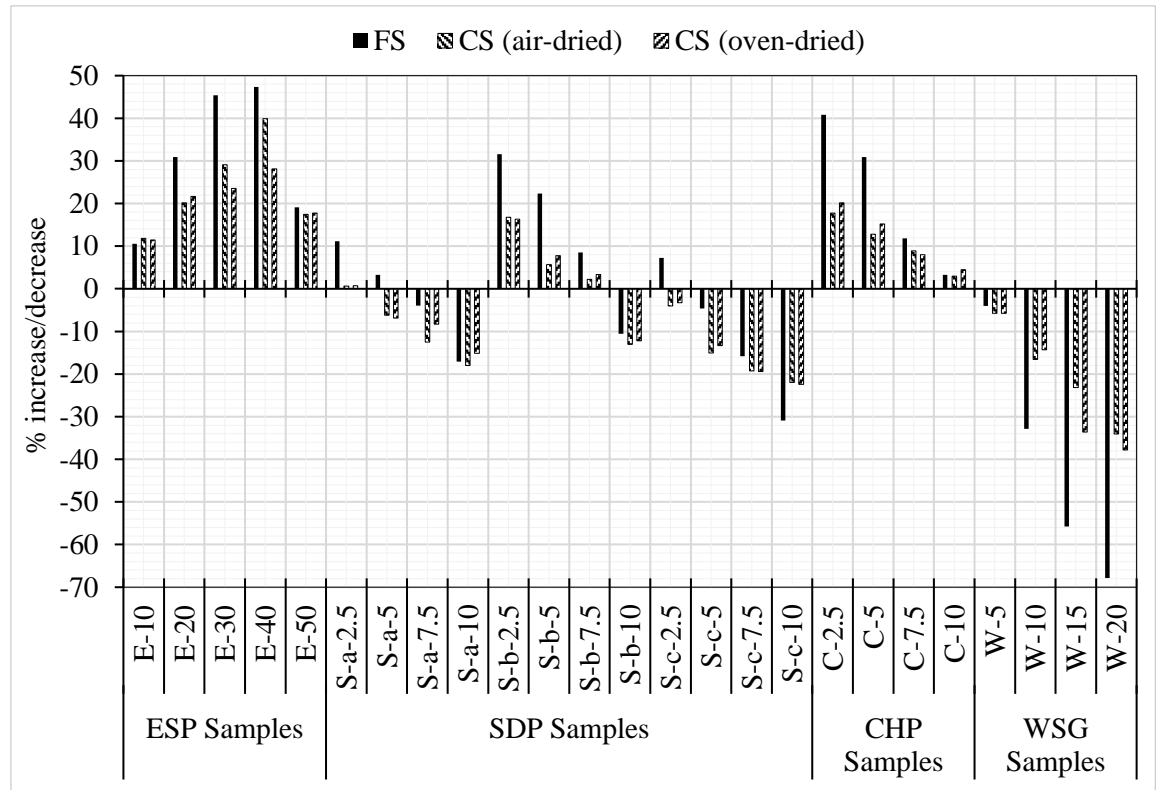


**Figure 4.11:** Percentage increase/decrease in Compressive strength (CS) and flexural strength (FS) compared to the reference sample (Phase 1).

#### 4.4.4 Capillary Water Absorption

The capillary water absorption test is usually used to determine the immersion resistance and durability in wet environments of clay bricks. The incorporation of additives into clay bricks results in the formation of porosity, which increases capillary water absorption. The structure of pores and how they are interconnected determine the rate of capillary water absorption (Harries and Sharma, 2019; Lu et al., 2020; Salih et al., 2020). Samples with higher coefficients absorb more water, showing higher porosity, whereas samples with lower coefficients absorb less water, indicating lower porosity. In this study, capillary water absorption was determined by testing three samples for each mix composition and taking the average value (see Appendix A). Figure 4.12 presents a decreasing trend in capillary water absorption coefficient values with increasing ESP content from 10% to 40% before rising slightly at 50% ESP. This is consistent with the results of Amaral et al. (2013) and Adogla et al. (2016). This decrease can be attributed

to the pozzolanic reaction induced by the calcium ions in ESP, which increased bonding within the clay matrix while reducing open porosity, similar to traditional lime (Adogla et al., 2016). The addition of ESP resulted in a 15% decrease in capillary water absorption compared to the reference sample, while CHP boosted it by 45%. Besides, the non-absorbent nature of WSG particles caused a reduction in the capillary water absorption of the samples. The capillary water absorption coefficient steadily amplified when CHP content increased from 2.5% to 10%, since beyond 2.5% additives the bonding between the particles and the clay matrix became weak, resulting in the formation of interconnecting voids, which led to the increase in water absorption kinetics. Moreover, the absorbent nature of CHP may potentially play a role in the increase in capillary water absorption (Danso, 2017). Also, it was observed that the capillary water absorption coefficient increased as the amount of SDP increased in all three groups of samples. The capillary water absorption was higher for SDP-a samples than for the other two groups. The increase was up to around 34%, 27%, and 25% for SDP-a, SDP-b, and SDP-c, respectively, compared to the reference sample. This might be related to the pore structure of the samples, which is caused by the particle size of the sawdust. Capillary water absorption is inversely proportional to the diameter of the pores, where the smaller the diameter, the greater the capillary absorption (Borrelli, 1999; Harries and Sharma, 2019; Kim et al., 2019). When sawdust with larger particle dimensions was used to make clay blocks, it typically resulted in a more porous microstructure with pores of larger diameters. On the other hand, sawdust with smaller particle dimensions resulted in better compaction and therefore the formation of finer pores, and finer pores absorb water faster because of the increased capillary pressures produced by them (De Castrillo et al., 2021; Hall and Hoff, 2021). In addition, the results indicate that capillary water absorption is inversely related to the sample density, with a lower density indicating more porosity and greater capillary water absorption. This finding is in accordance with previous research on lignocellulosic fibre-earth composites, which found that increasing percentages of fibre resulted in higher absorption levels (Taallah et al., 2014; Danso et al., 2015b; Ouedraogo et al., 2019; Thanushan et al., 2019). On the other hand, Villamizar et al. (2012) and Sharma et al. (2016) found that increasing the amount of natural fibres in compressed and adobe blocks reduced water absorption. In general, the discrepancies in the impacts of all the additives studied on

capillary water absorption may be linked to their stabilisation mechanism, type of bonding, and rearrangement pattern of particles, which were influenced by the nature of the additives, their particle size, and the compaction method (Villamizar et al., 2012; Fadele and Ata, 2018; De Castrillo et al., 2021).

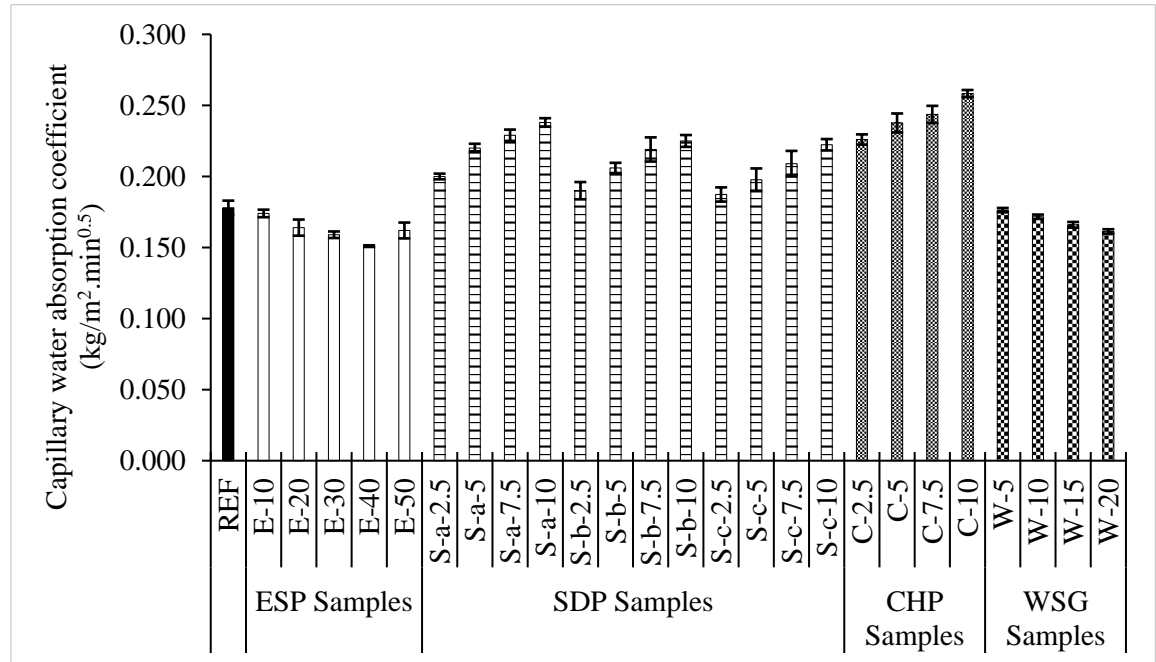


**Figure 4.12:** Capillary water absorption results (Phase 1).

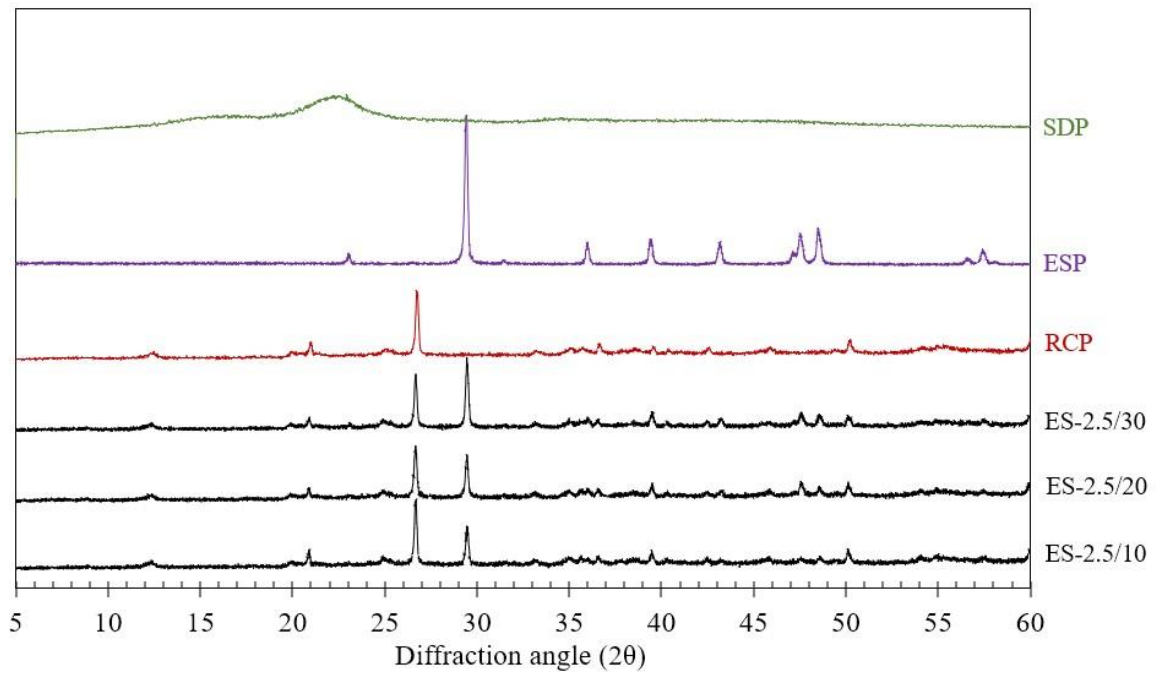
*Error bar represents the standard deviation of data.*

## 4.5 Results and Discussions (Phase 2)

The results of the first phase indicated that the strength of eggshell samples gradually increased with the addition of ESP up to 40%, while for sawdust, coconut husk, and walnut shell, the highest strength was obtained using 2.5% SDP-b, 2.5% CHP, and 5% WSG, respectively. Therefore, in phase 2, 2.5% SDP-b, 2.5% CHP, and 5% WSG were blended with 10% to 30% ESP to further examine the properties of the clay samples (Table 4.2). Figure 4.13, Figure 4.14, and Figure 4.15 present the XRD analyses of the eggshell-sawdust (ES), eggshell-coconut husk (EC), and eggshell-walnut shell (EW) samples, respectively.

**Table 4.2:** Mix details (Phase 2).

Sample ID	Clay (g)	Agro-wastes (g)				Agro-wastes (wt%)			
		ESP	SDP	CHP	WSG	ESP	SDP	CHP	WSG
ES-b-2.5/10	550	55	13.75	-	-	10	2.5	-	-
ES-b-2.5/20	550	110	13.75	-	-	20	2.5	-	-
ES-b-2.5/30	550	165	13.75	-	-	30	2.5	-	-
EC-2.5/10	550	55	-	13.75	-	10	-	2.5	-
EC-2.5/20	550	110	-	13.75	-	20	-	2.5	-
EC-2.5/30	550	165	-	13.75	-	30	-	2.5	-
EW-5/10	550	55	-	-	27.50	10	-	-	5
EW-5/20	550	110	-	-	27.50	20	-	-	5
EW-5/30	550	165	-	-	27.50	30	-	-	5

**Figure 4.13:** XRD analysis of ES samples.

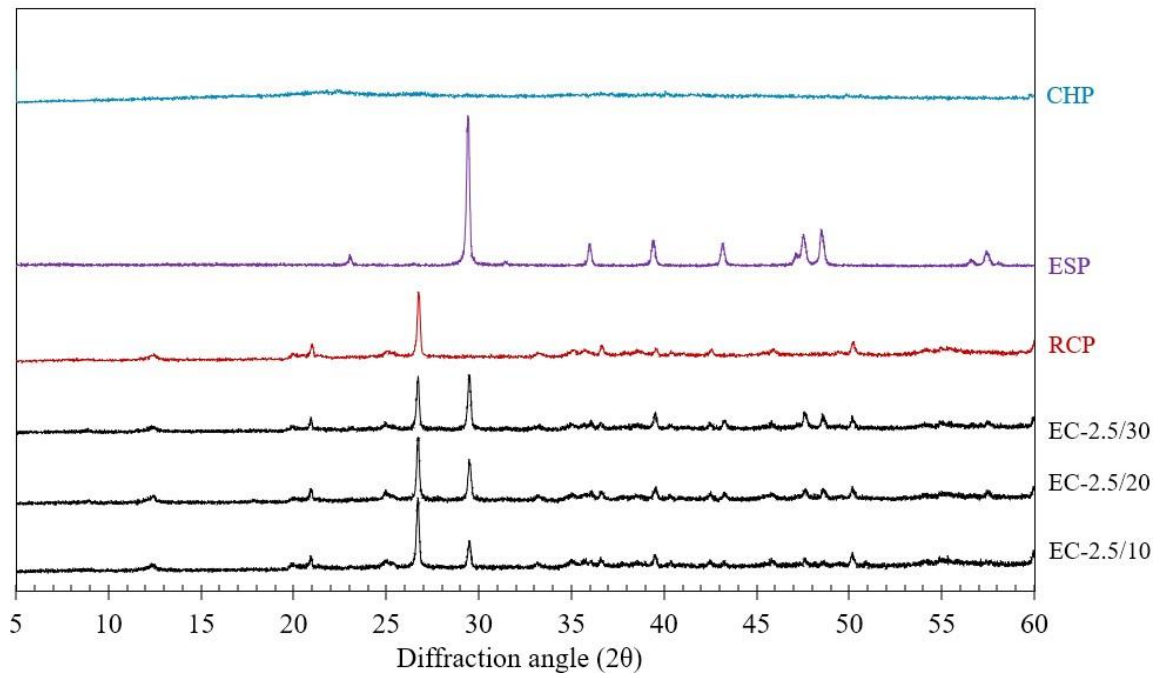


**Figure 4.14:** XRD analysis of EC samples.

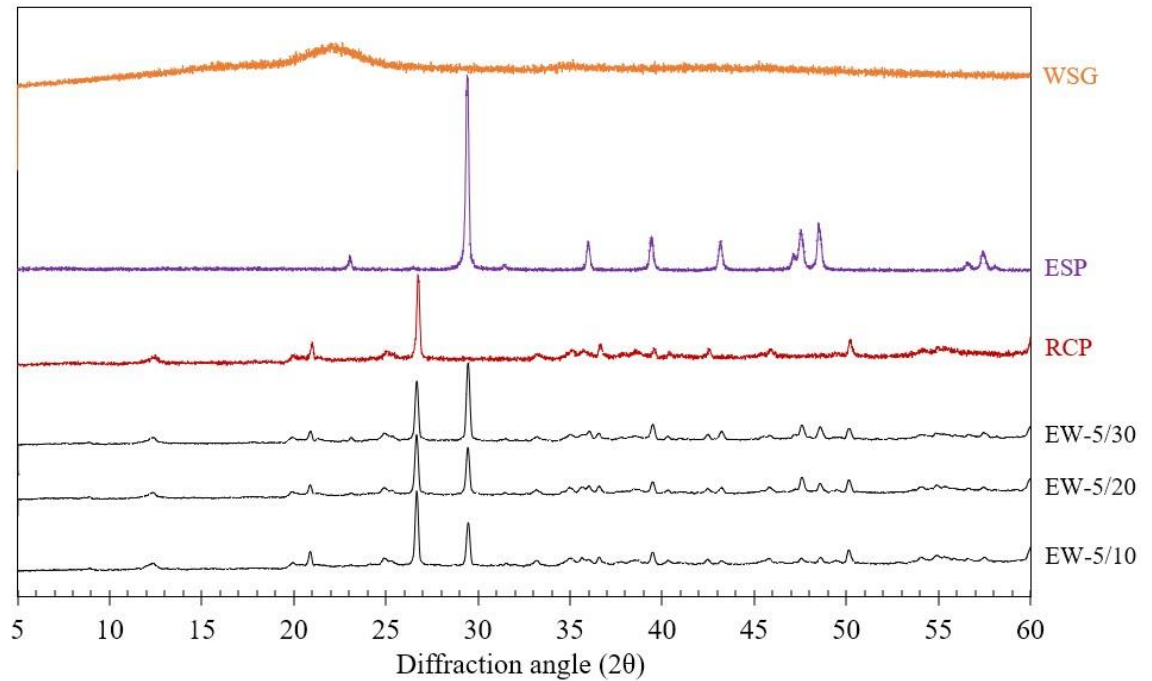


**Figure 4.15:** XRD analysis of EW samples.

When ESP was combined with SDP-b, CHP, and WSG, the density decreased from 1792.37 kg/m<sup>3</sup> to 1649.57 kg/m<sup>3</sup>, 1675.35 kg/m<sup>3</sup> to 1535.55 kg/m<sup>3</sup>, and 1810.88 kg/m<sup>3</sup> to 1682.90 kg/m<sup>3</sup> (Figure 4.16), and linear shrinkage reduced from 5.90% to 5.13%, 8.08% to 7.40% and 6.60% to 5.11% (Figure 4.17), respectively. Concerning capillary water absorption, eggshell-sawdust and eggshell-coconut husk samples showed a slightly increasing trend from 0.160 kg/m<sup>2</sup>.min<sup>0.5</sup> to 0.188 kg/m<sup>2</sup>.min<sup>0.5</sup> and 0.185 kg/m<sup>2</sup>.min<sup>0.5</sup> to 0.214 kg/m<sup>2</sup>.min<sup>0.5</sup>, respectively, though these values were lower than the values for 2.5% SDP (0.190 kg/m<sup>2</sup>.min<sup>0.5</sup>) and 2.5% CHP (0.226 kg/m<sup>2</sup>.min<sup>0.5</sup>) samples (Figure 4.18). On the other hand, capillary water absorption further reduced for eggshell-walnut shell samples from 0.169 kg/m<sup>2</sup>.min<sup>0.5</sup> to 0.158 kg/m<sup>2</sup>.min<sup>0.5</sup>. Furthermore, combining ESP with SDP-b, CHP, and WSG resulted in a loss of strength (Figure 4.19 and Figure 4.20), although, they met the standard criteria. However, strength was found to be higher than the reference sample when 10% to 20% ESP was added to SDP-b and CHP, but it was lower when 30% ESP was added. When 10% ESP was mixed with SDP-b and CHP, compressive strength of the samples (air-dried) enhanced around 7% and 11%, respectively, compared to the reference sample. For the same percentages, flexural strength improved about 12% and 17%, respectively. A small increase in strength was also observed when 20% ESP was added. This is again due to the fact that the calcium oxide (CaO) in ESP interacts with water to produce portlandite (Ca(OH)<sub>2</sub>), which then reacts with silica (SiO<sub>2</sub>) in the clay to form calcium silicate hydrate (CaSiO<sub>3</sub>·2H<sub>2</sub>O) which gives the materials their strength. Nevertheless, when clay was substituted by SDP, CHP or WSG in a mixture, the amount of silica (SiO<sub>2</sub>) available to react with portlandite Ca(OH)<sub>2</sub> decreased, and unreacted portlandite had a detrimental influence on strength (Ngayakamo et al., 2020).

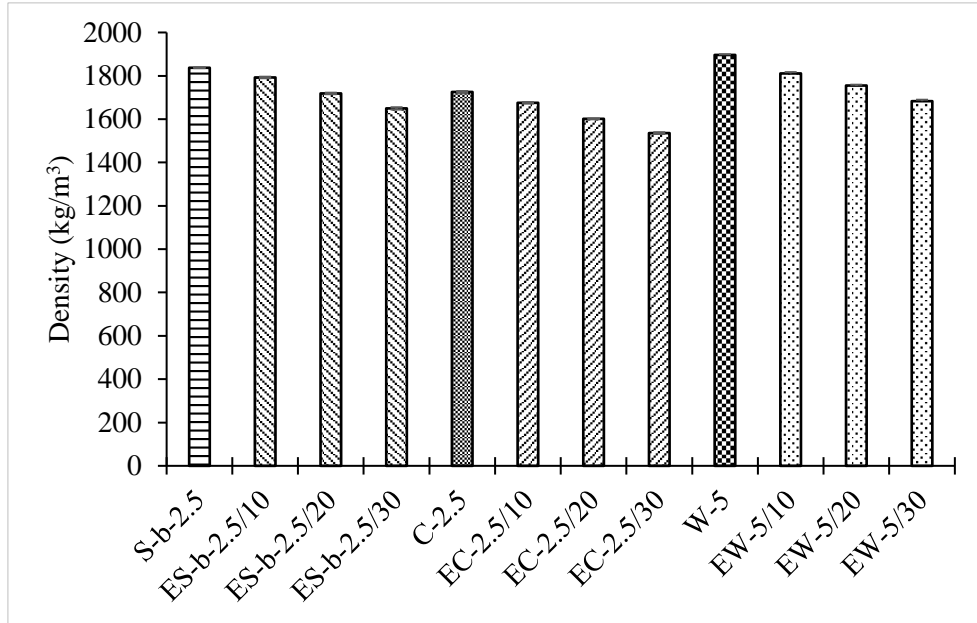


**Figure 4.16:** Density results (Phase 2).

*Error bar represents the standard deviation of data.*

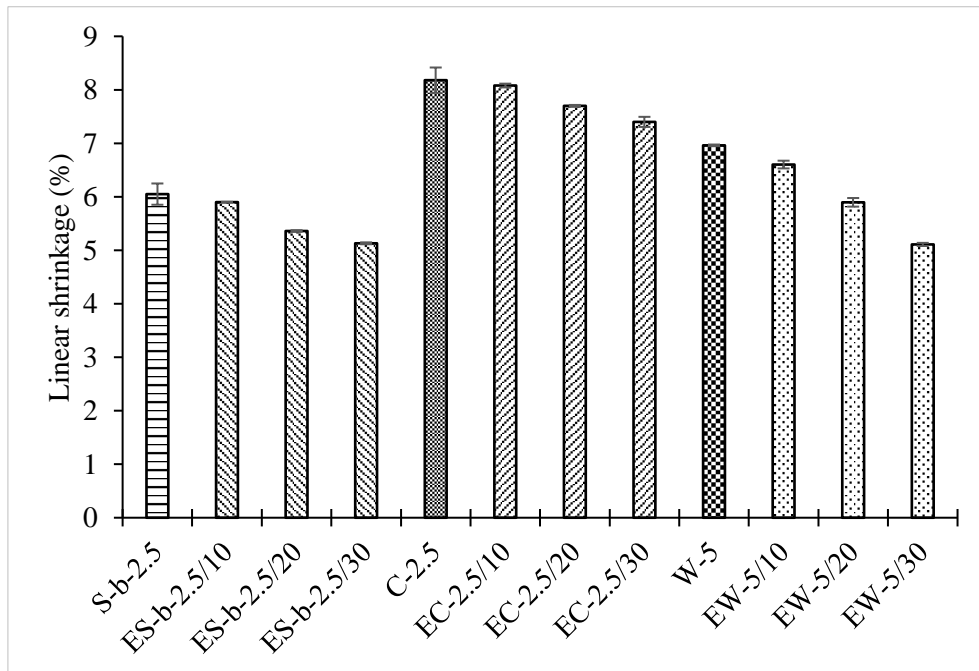


**Figure 4.17:** Linear shrinkage results (Phase 2).

*Error bar represents the standard deviation of data.*

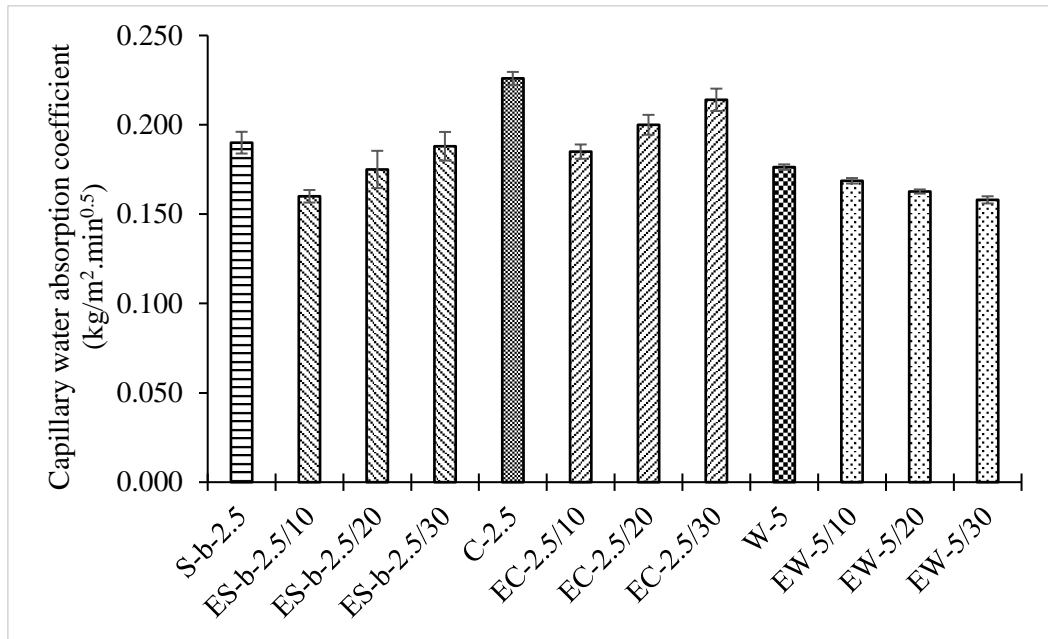


**Figure 4.18:** Capillary water absorption results (Phase 2).

*Error bar represents the standard deviation of data.*

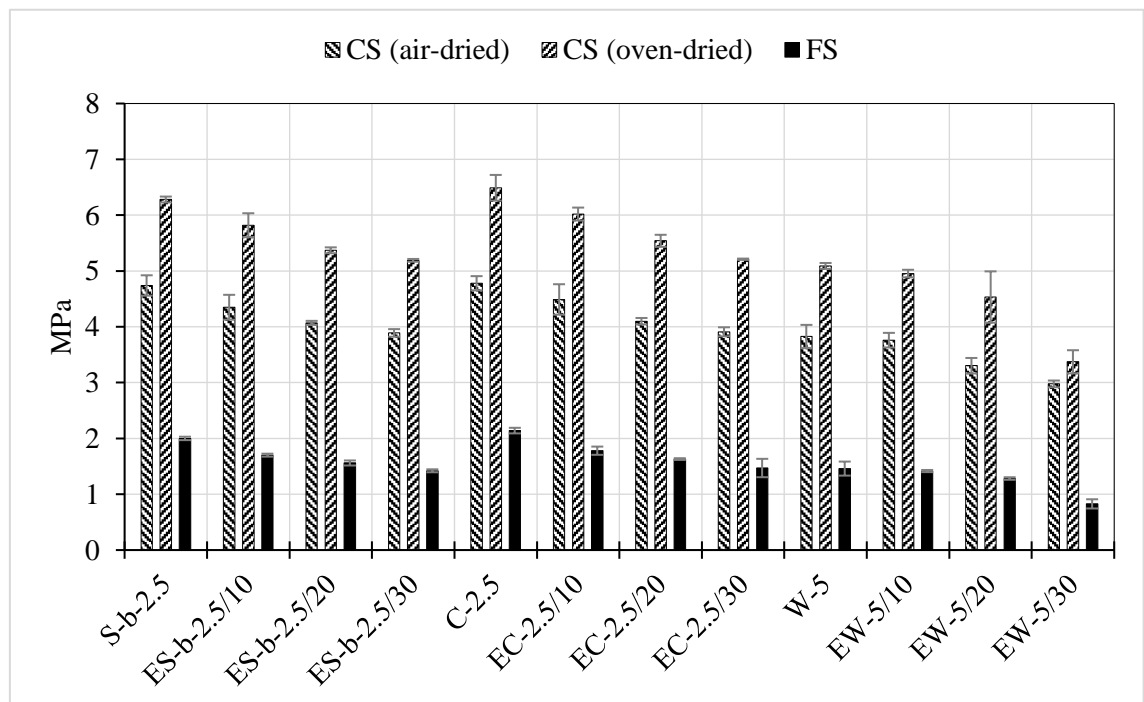


**Figure 4.19:** Compressive strength (CS) and flexural strength (FS) test results (Phase 2).

*Error bar represents the standard deviation of data.*

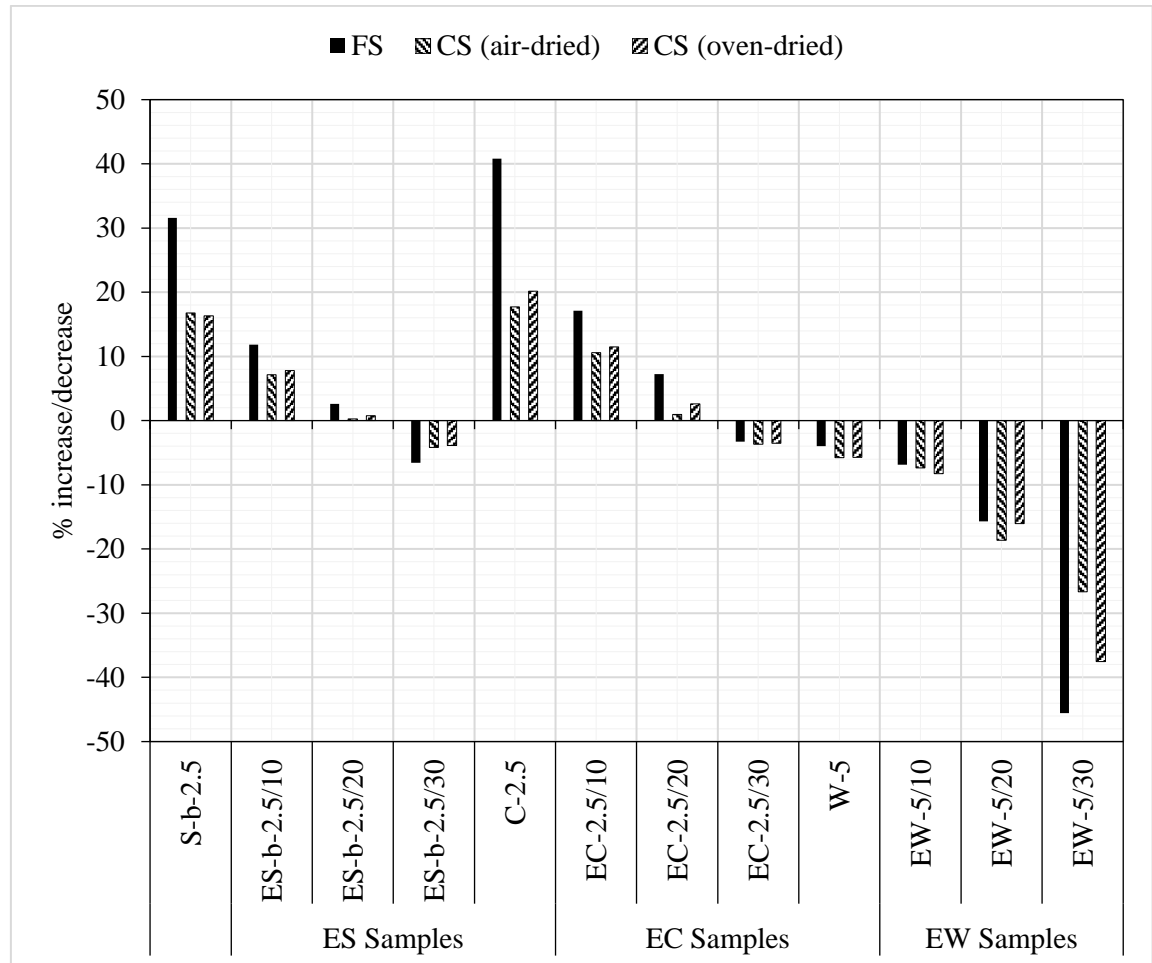


**Figure 4.20:** Percentage increase/decrease in Compressive strength (CS) and flexural strength (FS) compared to the reference sample (Phase 2).

## 4.6 Summary of the Chapter

Experimental tests on the physico-mechanical properties of the agro-wastes blended unfired clay blocks revealed the following conclusions:

### *Phase 1*

- The density of the samples gradually decreased as the percentages of waste materials increased in the mixture. Despite a decrease in the density of ESP incorporated samples from  $1975.78 \text{ kg/m}^3$  to  $1791.04 \text{ kg/m}^3$ , they reached the minimum value of  $1750 \text{ kg/m}^3$  required by the Indian Standard: IS 1725 and Sri Lankan Standard: SLS 1382 for the load-bearing blocks. Besides, 2.5% CHP ( $1725.44 \text{ kg/m}^3$ ), 5% WSG

(1896.33 kg/m<sup>3</sup>), and 10% WSG (1808.05 kg/m<sup>3</sup>) samples satisfied the standard criteria. For sawdust samples, all three groups with 2.5% content (SDP-a: 1860.64 kg/m<sup>3</sup>, SDP-b: 1837.05 kg/m<sup>3</sup>, SDP-c: 1781.39 kg/m<sup>3</sup>) and sample with 5% SDP-a (1794.61 kg/m<sup>3</sup>) achieved the standard requirement. Other percentages can be used to produce lightweight masonry blocks.

- The XRD analyses indicated that there was no reaction when SDP, CHP, and WSG were mixed with clay. In the presence of water, however, ESP reacted with clay to create cementitious material, significantly improving the properties of the samples.
- The addition of ESP and WSG resulted in a decrease in linear shrinkage from 6.92% to 5.61% and 6.96% to 4.49%, respectively. On the other hand, an increase from 8.18% to 12.29% was observed with CHP addition, representing around a 52% increase over the reference sample. Moreover, SDP-b and SDP-c with larger particle sizes reduced the linear shrinkage from 6.05% to 5.53% and 5.99% to 4.77%, respectively, while SDP-a with the smaller particle size increased it from 6.15% to 7.24%.
- A decrease in the capillary water absorption coefficient over the reference sample of around 15% and 9% was achieved with the incorporation of ESP and WSG, respectively. On the other hand, capillary water absorption gradually increased with increasing CHP and SDP percentages. The increase was up to around 45% for CHP samples, whereas it was around 34%, 27%, and 25% for SDP-a, SDP-b, and SDP-c samples, respectively, compared to the reference sample.
- In terms of mechanical properties, after 28 days, all the agro-waste incorporated samples fulfilled the minimum compressive strength (1 MPa-2.80 MPa) and flexural strength (0.25 MPa-0.50 MPa) requirements of the standards. For the sawdust, SDP-a and SDP-b improved the compressive strength of the samples over the reference sample. However, SDP-c did not improve the compressive strength. Besides, SDP-b had higher strength than the other groups at the same waste percentage. Moreover, ESP samples showed higher compressive and flexural strength values (FS: 2.24 MPa, CS: 5.68 MPa) than SDP-b (FS: 2 MPa, CS: 4.74 MPa) and CHP (FS: 2.14 MPa, CS: 4.78 MPa) samples. On the other hand, the addition of WSG adversely affected the

strength of the samples. The compressive strength (3.83 MPa) and flexural strength (1.46 MPa) of WSG samples were the highest for 5% content, which were lower than the strength values of the reference sample. Furthermore, all the oven-dried samples showed higher compressive strength values than the air-dried samples.

### *Phase 2*

- The density of the samples further decreased when 10% to 30% ESP was combined with 2.5% SDP-b (1792.37 kg/m<sup>3</sup> to 1649.57 kg/m<sup>3</sup>), 2.5% CHP (1675.35 kg/m<sup>3</sup> to 1535.55 kg/m<sup>3</sup>), and 5% WSG (1810.88 kg/m<sup>3</sup> to 1682.90 kg/m<sup>3</sup>). Also, linear shrinkage reduced for eggshell-sawdust (5.90% to 5.13%), eggshell-coconut husk (8.08% to 7.40%), and eggshell-walnut (6.60% to 5.11%) samples with increasing ESP content.
- Capillary water absorption slightly increased for eggshell-sawdust (0.160 kg/m<sup>2</sup>.min<sup>0.5</sup> to 0.188 kg/m<sup>2</sup>.min<sup>0.5</sup>) and eggshell-coconut husk (0.185 kg/m<sup>2</sup>.min<sup>0.5</sup> to 0.214 kg/m<sup>2</sup>.min<sup>0.5</sup>) samples but decreased for eggshell-walnut shell (0.169 kg/m<sup>2</sup>.min<sup>0.5</sup> to 0.158 kg/m<sup>2</sup>.min<sup>0.5</sup>) samples with the addition of 10% to 30% ESP.
- Moreover, the strength of all the samples further decreased when ESP was combined with other agro-wastes. Nevertheless, 10% ESP addition to SDP-b and CHP enhanced compressive strength of the samples (air-dried) over the reference sample up to nearly 7% and 11%, respectively, while flexural strength increased up to around 12% and 17%, respectively. Besides, there was a small improvement in strength when 20% ESP was combined. On the other hand, strength decreased in comparison to the reference sample at 30% ESP addition. Also, the oven-dried samples had higher compressive strength than the air-dried samples.

## *Chapter 5*    **EXPERIMENTAL EVALUATION (PART B-DURABILITY PROPERTIES TESTS)**

### **5.1 Introduction**

Earthen materials are less durable and more vulnerable to extreme weather conditions than conventional construction materials. The durability of earthen construction mainly indicates its resistance against water-induced erosion (Medvey and Dobszay, 2020), which is a major problem in tropical countries due to heavy rainfall (Goodman-Elgar, 2008; Morton, 2008; Gunawardana et al., 2021). According to the articles reviewed on the durability tests of unfired earth blocks, a wide range of test procedures were found. In this study, the Geelong drip test and water spray test were selected, which are frequently used in the laboratory by simulating different rainfall conditions. In addition, measurements of UPV, a popular non-destructive approach for assessing the durability of materials were taken. The test procedures and results are discussed in this chapter.

### **5.2 Sample Preparation**

The results of the physico-mechanical properties tests revealed that, except for WSG, other additives improved the properties of the samples in comparison to the reference sample. As a result, the samples for the durability tests were produced using ESP, SDP-b, and CHP. The mix proportions were the same as in Table 4.1 and Table 4.2. The samples were cast in 100 mm × 100 mm × 100 mm and 215 mm × 102 mm × 65 mm moulds (Figure 5.1(a) and Figure 5.1(b)), following the same procedure as described in Section 4.2 Sample Preparation in Chapter 4.



**Figure 5.1:** Samples: (a) 100 mm × 100 mm × 100 mm and (b) 215 mm × 102 mm × 65 mm.

### 5.3 Tests

#### 5.3.1 Ultrasonic Pulse Velocity (UPV)

Ultrasonic pulse velocity (UPV) is a popular non-destructive test that is widely used in assessing several characteristics of building materials, including homogeneity, elastic modulus, mechanical resistance, and the presence of cracks (Latif and Rasoul, 2009; Laborel-Préneron et al., 2021). This test is intriguing since it reveals some degradation inside the material that may affect durability. The test method involves measuring the travel time of a sound pulse through a known area of a material. This is based on elastic wave propagation theory, which states that a sound pulse travels faster in dense materials than in porous ones (Saint-Pierre et al., 2016; Sabbağ and Uyanık, 2017). In this study, the UPV test was conducted on the 215 mm × 102 mm × 65 mm samples after 28 days of casting using a Proceq Pundit PL-200 ultrasonic pulse equipment. This equipment measures the delay time required for a transmitted ultrasonic wave to travel from the transducer and return to the transducer through the interposed sample. A coupling gel was applied between the samples and transducers to avoid the existence of voids in the contact area. Before the test, samples were measured for length (L), width (W), and height (H) to determine the UPV for each direction (Figure 5.2(a)). Direct transmission (Figure 5.2(b)) was used to measure the UPV, as it is considered the most reliable configuration (Ndagi et al., 2019). The test findings can be used in determining the durability of the samples by assessing the decrease of voids inside the samples as

velocity increases with the decrease of voids, suggesting a compact and denser composition.

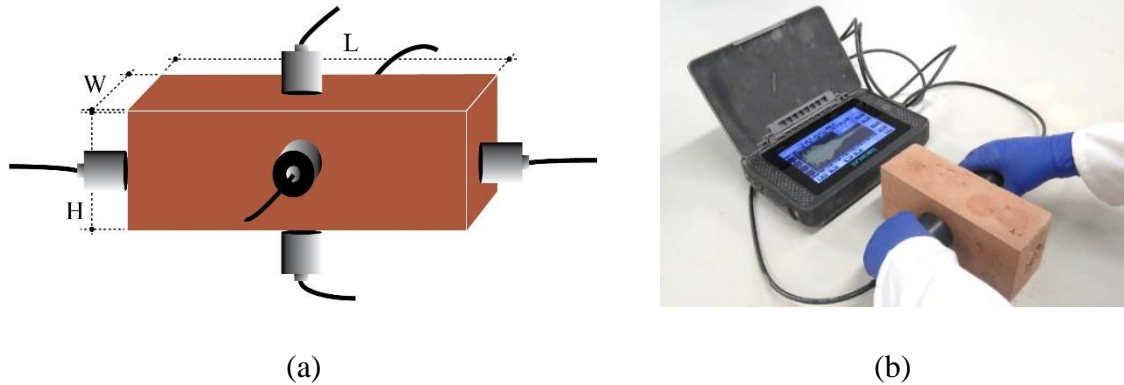


**Figure 5.2:** UPV test: (a) schematic and (b) experimental.

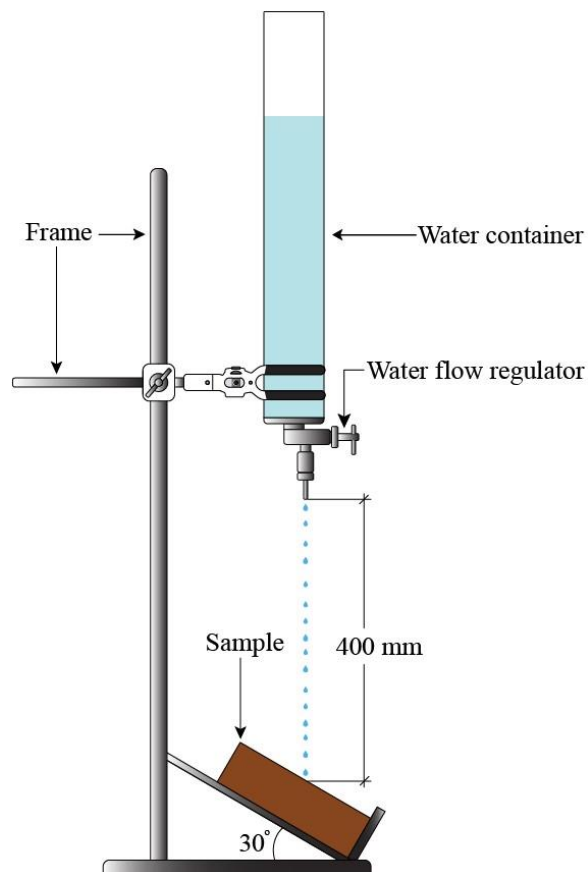
### 5.3.2 Geelong Drip

The Geelong drip test was performed in accordance with the New Zealand Standard NZS 4298 (NZS 4298, 1998) to evaluate the capacity of earthen materials to withstand erosion caused by light and indirect rainfall. The first drip test was developed by Yttrup et al. (1981) at Deakin University in Australia, aiming to provide a simple test helpful for adobe owner-builders to assess the suitability of their soil. During the test, an inclined brick sample is exposed to water droplets from a certain height at a specific rate. The “depth of pitting” is then assessed by averaging the pitting depths on both sides of the sample. The test was further developed by Frencham (1982), who related the depth of pitting to an erodibility index. He performed drip test on brick samples taken from 20 existing buildings and correlated the test results with the performance of the source buildings. Based on the correlation, he defined four classifications of “erodibility indexes” (Table 5.1) (Heathcote, 1995). The test was carried out on the 100 mm × 100 mm × 100 mm samples by simulating rain droplets. According to the procedure, the samples were positioned at a 30° angle at the base and 400 mm vertically away from a water container, from which water was allowed to drop on the surface of the samples at a controlled flow for 60 min (Figure 5.3). After testing, the erodibility index was calculated by measuring the pit depth created by the water drops on the samples with a digital

calliper of 0.01 mm resolution. This simple test can be acceptable in areas where annual precipitation is around 500 mm, but its applicability in areas with higher rainfall levels has yet to be determined (Heathcote, 1995).

**Table 5.1:** Scale of assessment for drip test.

Depth of erosion, $d$ (mm)	Frencham (Frencham, 1982) recommendation	Erodibility index as per NZS 4298 (NZS 4298, 1998)
0	Non-erosive	1
$0 \leq d < 5$	Slightly erosive	2
$5 \leq d < 10$	Erosive	3
$10 \leq d < 15$	Very erosive	4
$15 \leq d$	-	5 (Fail)



(a)



(b)

**Figure 5.3:** Drip test: (a) schematic and (b) experimental.

### 5.3.3 Water Spray (Pressure Spray Method)

The pressure spray test, also known as the ‘accelerated erosion test’, is frequently used in practice (Cid-Falceto et al., 2012). However, according to Heathcote (2002) and Walker et al. (2005), this test is more extreme than real climatic conditions. This empirical test was developed by the Commonwealth Scientific and Industrial Research Organisation (CSIRO) in Australia. The purpose of this test is to assess the resistance of the samples against continuous rainfall conditions. The principle of the test involves exposing the face of a sample to a horizontal water spray at a specific pressure for a period of an hour or until the sample is penetrated. In this study, the test was carried out following the New Zealand Standard NZS 4298 (NZS 4298, 1998). According to the standard, the samples must be cured for a minimum of 28 days before testing. The test simulates two real-life conditions that cause earthen materials to erode due to moderate to heavy rainfall: humidification and kinetic energy. Humidification reduces the internal cohesion between the material particles by increasing the moisture content, while kinetic energy is responsible for breaking the already weakened bonds between the material particles. The test was performed on 65 mm × 102 mm × 215 mm samples imitating real-life conditions of average to heavy rainfall (Figure 5.4).

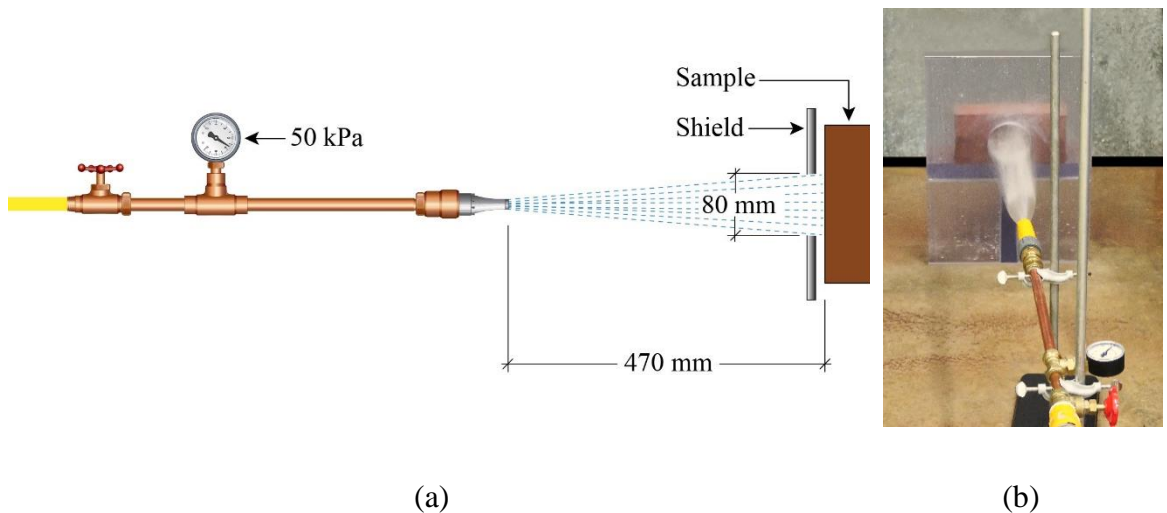


**Figure 5.4:** Water spray test: (a) schematic and (b) experimental.

The samples were placed behind a shield board, and the external surface was exposed to a pressure spray through an 80 mm diameter hole (adapted from the standard 100 mm diameter hole) on the shield board. The pressure spray was positioned at 470 mm from the shield, and tap water was sprayed through the nozzle at a pressure of 50 kPa onto the samples for an hour or until failure occurred. In addition, samples were inspected by eye to assess the degree of moisture penetration. The erodibility index for the water spray test is specified in Table 5.2.

**Table 5.2:** Erodibility indices for pressure spray erosion test.

Erosion rate, $d$ (mm/hr)	Erodibility index
0	-
$0 \leq d < 20$	1 (Pass)
$20 \leq d < 50$	2 (Pass)
$50 \leq d < 90$	3 (Pass)
$90 \leq d < 120$	4 (Pass)
$120 \leq d$	5 (Fail)

## 5.4 Results and Discussions

### 5.4.1 UPV

The shape, size, and number of pores affect the wave propagation speed, making it a good indicator of porosity and compactness. The greater the increase in porosity, the lower the ultrasonic speed. This implies that porosity and UPV are inversely related. The test results (Figure 5.5) demonstrated that UPV increased from 1263 m/s to 1453.33 m/s with the addition of 10% to 40% ESP, then decreased to 1350.67 m/s for the 50% ESP sample. This rise in UPV might be explained by pozzolanic reactions in the ESP samples, which contributed to decreasing the porosity. On the other hand, in the case of SDP-b and CHP samples, UPV gradually decreased from 1560.33 m/s to 1318.33 m/s and 1384.67 m/s to 1123.00 m/s, respectively, for 2.5% to 10% addition. The porosity of the

SDP-b and CHP samples increased with increasing waste content due to the poor adhesion between the clay and waste particles, resulting in a decrease in UPV. Unfired earth blocks are rarely studied for UPV, and there is only a little research that shows a link between UPV and the compressive strength of earthen materials (Galán-Marín et al., 2013; Türkmen et al., 2017; Araya-Letelier et al., 2018; Martín-del-Río et al., 2020; Abid et al., 2021). In this study, UPV results followed a similar trend to compressive strengths (Figure 5.6), indicating that the samples with the highest compressive strength (40% ESP, 2.5% SDP-b, and 2.5% CHP) also had the maximum UPV value. This is again related to the fact that pozzolanic reactions in ESP samples caused a decrease in porosity, which improved the stiffness of the samples. Nevertheless, when SDP-b and CHP percentages increased, bonding in the clay matrix weakened, leading to a rise in porosity and a decrease in strength.

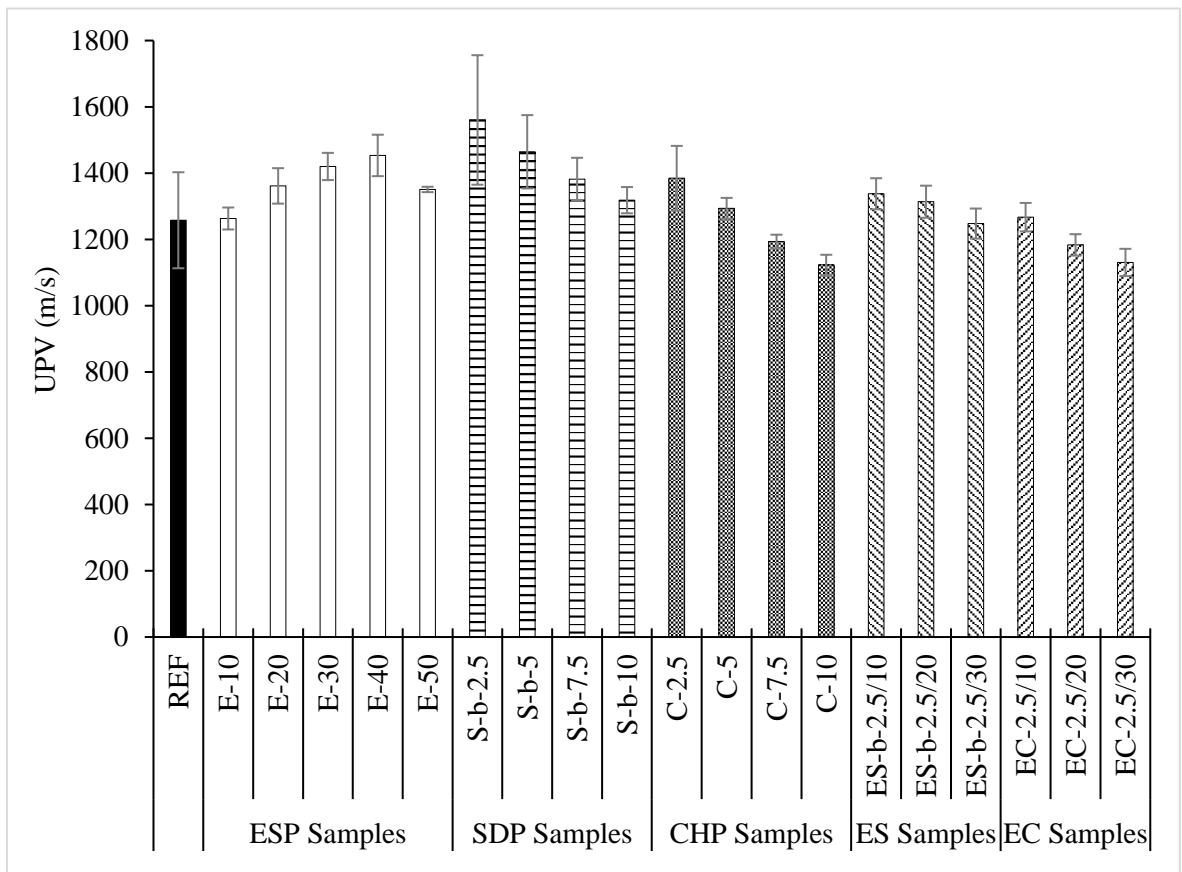
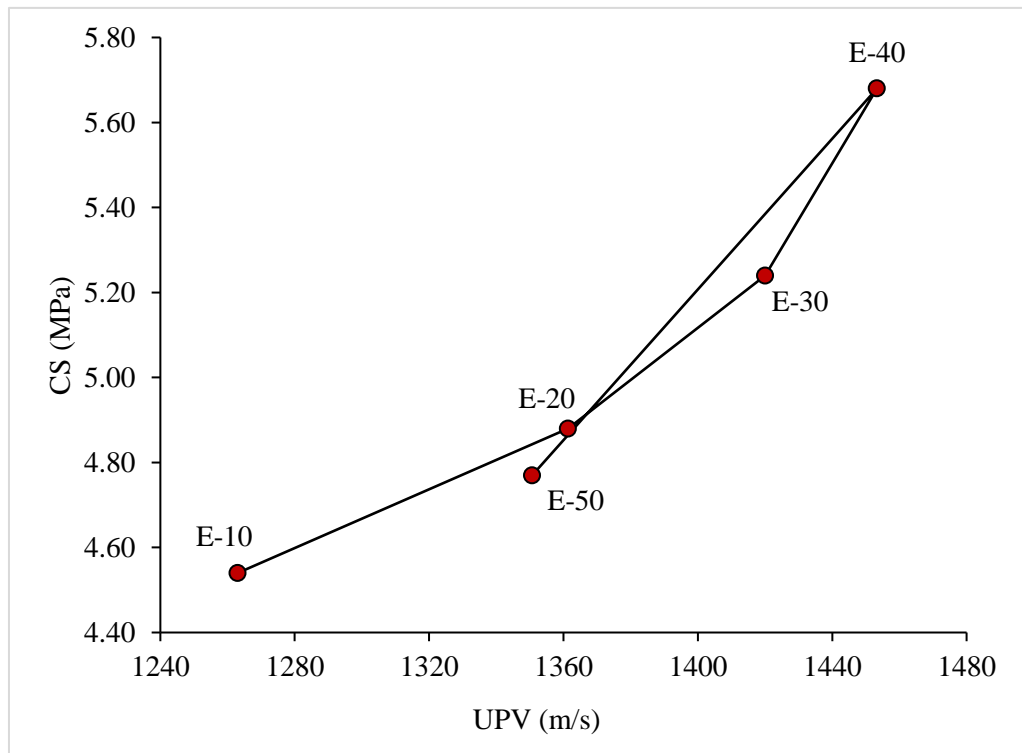
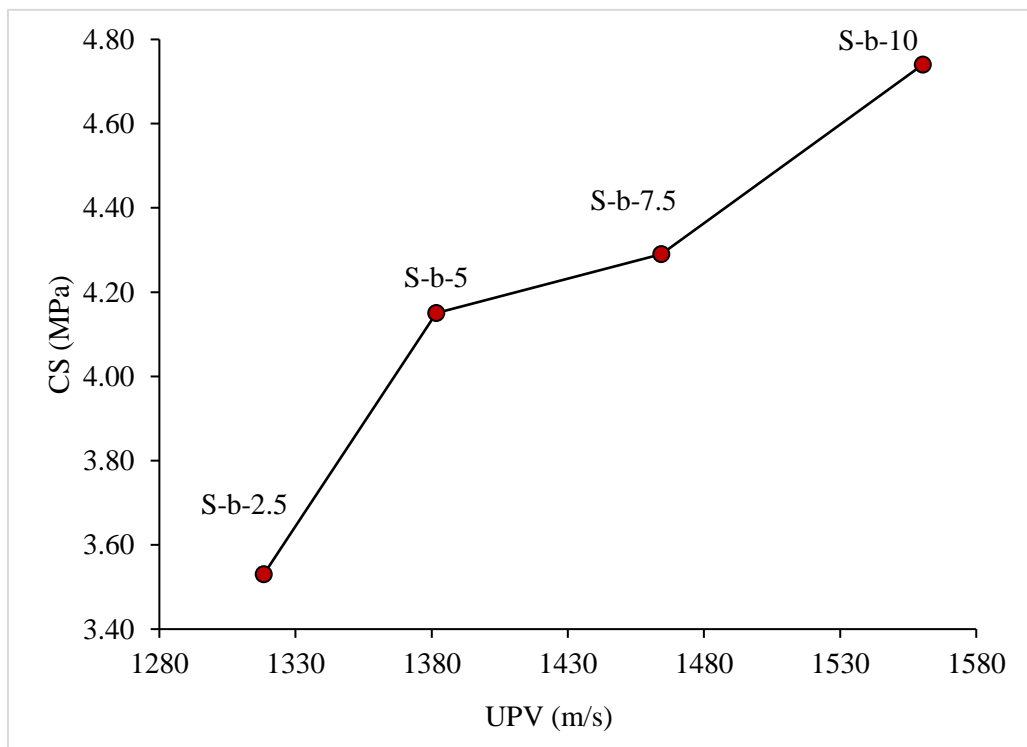


**Figure 5.5:** UPV test results of stabilised clay blocks.

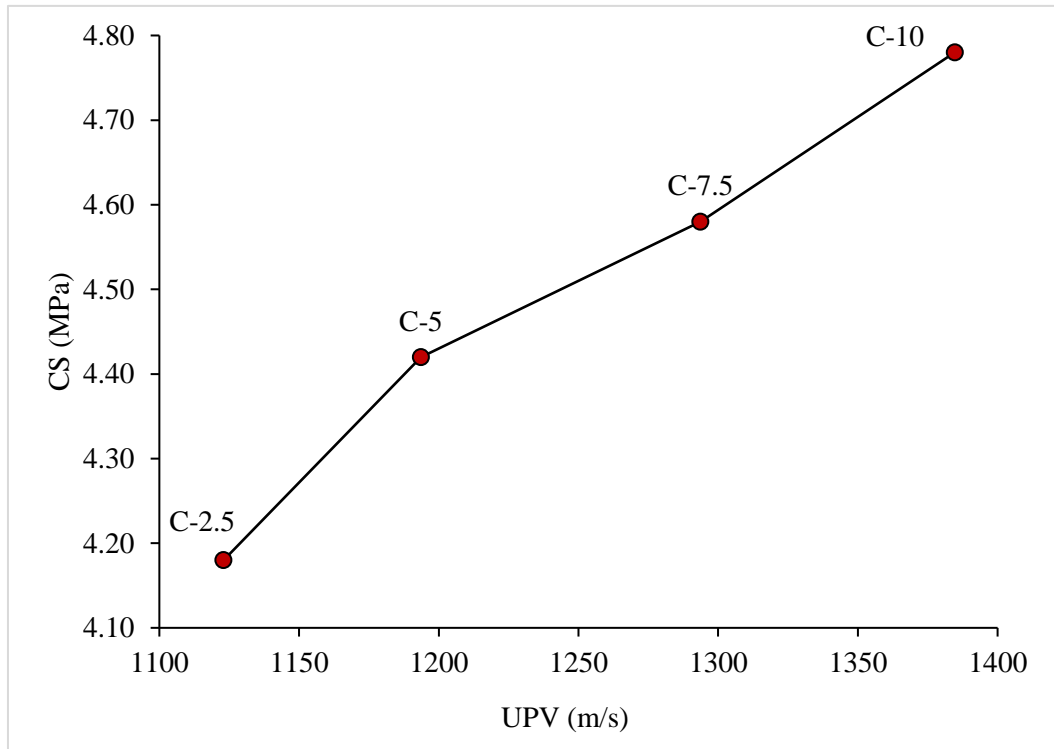
*Error bar represents the standard deviation of data.*



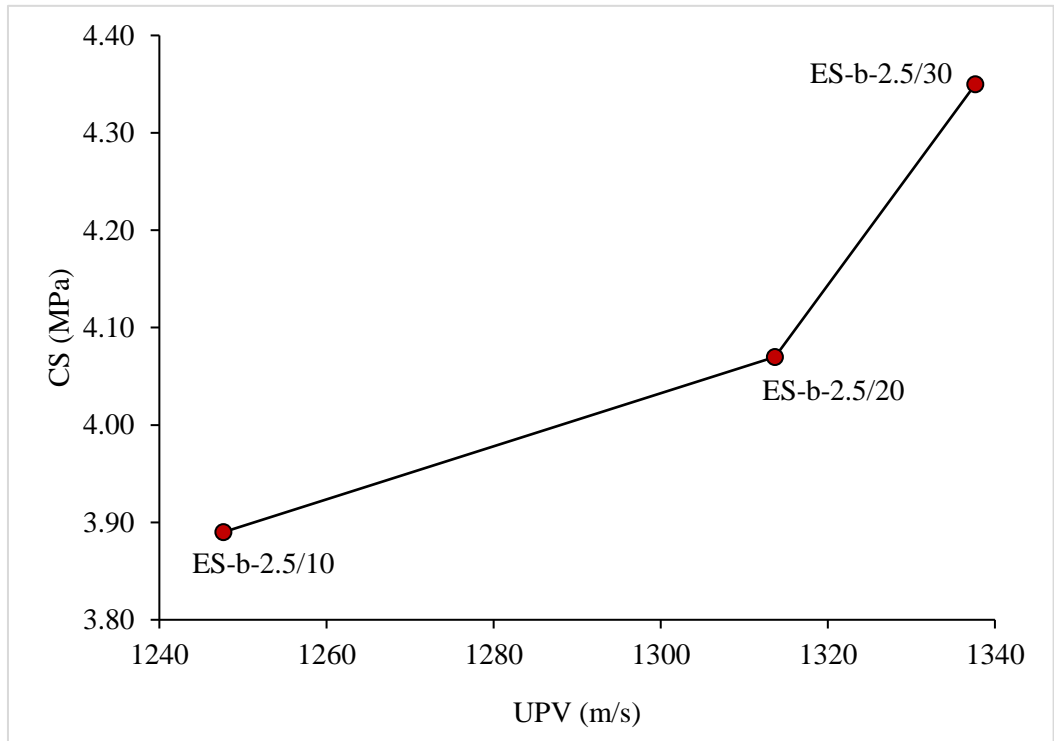
(a)



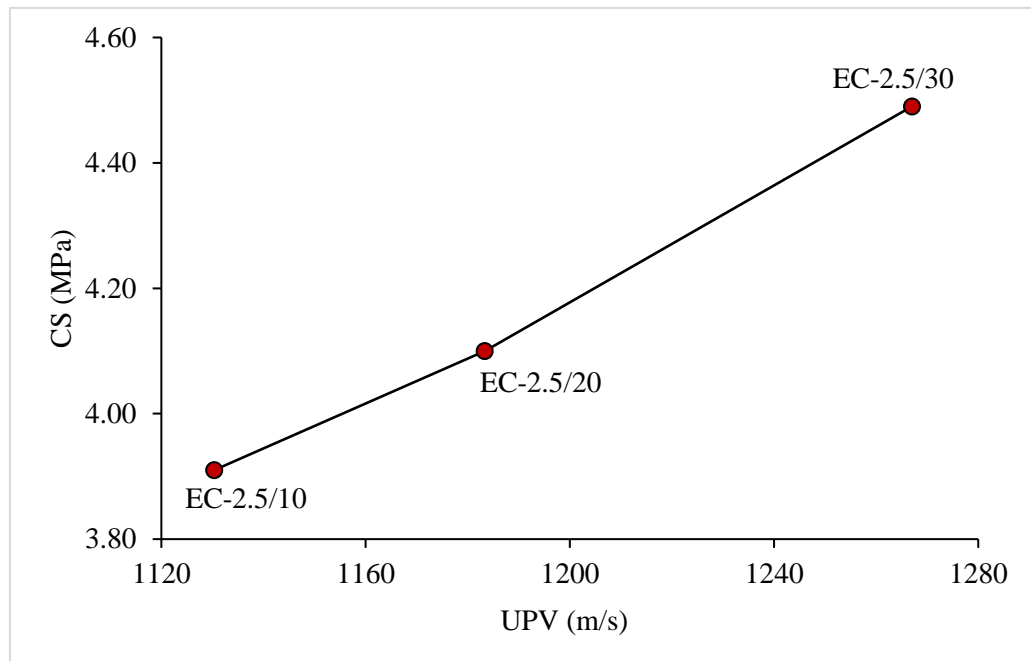
(b)



(c)



(d)



(e)

**Figure 5.6:** UPV vs Compressive strength (CS): (a) ESP samples, (b) SDP samples, (c) CHP samples, (d) ES samples, and (e) EC samples.

Furthermore, the results revealed that UPV declined when the amount of ESP increased with SDP-b/CHP, indicating the formation of more porous materials. In eggshell-sawdust and eggshell-coconut husk samples, UPV decreased from 1337.67 m/s to 1247.67 m/s and from 1267.00 m/s to 1130.33 m/s, respectively. The variations in sample performance for different orientations (see Appendix C) might be explained by a lack of homogenisation of the clay mixture. The UPV findings might provide an intriguing supplementary data set that is closely related to the mechanical strength results. Consequently, this non-destructive method may be used to qualitatively assess the quality of unfired earth blocks.

#### 5.4.2 Geelong Drip

The test was performed on cube samples of each mixture. The lower the depth, the better the sample's erosion resistance. Table 5.3 shows that all the samples passed the drip test, and the pitting depths were between 0 and 5 mm, which means an erodibility index of 2

(see Table 5.1), indicating that they are “slightly erodible”. The results demonstrate that the addition of ESP, SDP-b, and CHP to clay improves its erosion resistance compared to the reference sample. The least erosive mixture with SDP-b and CHP was 2.5%, whereas the best performance with ESP was obtained at 40%. The good cohesion between waste particles and clay prevents water from penetrating the sample and clay particles from being washed away by water, which appears to be the explanation for the sample’s good performance (Laborel-Préneron et al., 2021).

**Table 5.3:** Drip test results of stabilised clay blocks.

Sample ID	Dept of pitting (mm)	Erodibility Index	Rating
REF	4.87	2	Slightly erosive
E-10	3.58	2	Slightly erosive
E-20	3.75	2	Slightly erosive
E-30	2.60	2	Slightly erosive
E-40	2.16	2	Slightly erosive
E-50	2.37	2	Slightly erosive
S-b-2.5	2.18	2	Slightly erosive
S-b-5	2.38	2	Slightly erosive
S-b-7.5	2.46	2	Slightly erosive
S-b-10	3.23	2	Slightly erosive
C-2.5	2.73	2	Slightly erosive
C-5	3.10	2	Slightly erosive
C-7.5	3.64	2	Slightly erosive
C-10	3.82	2	Slightly erosive
ES-b-2.5/10	3.12	2	Slightly erosive
ES-b-2.5/20	3.20	2	Slightly erosive
ES-b-2.5/30	3.28	2	Slightly erosive
EC-2.5/10	3.47	2	Slightly erosive
EC-2.5/20	3.53	2	Slightly erosive
EC-2.5/30	3.80	2	Slightly erosive

### 5.4.3 Water Spray

The results of water spray test demonstrate the durability of the clay brick under severe rain. The erosion rates of clay samples containing different waste percentages are shown in Table 5.4. Every 15 minutes, the depth of pitting was measured using a calliper (see Appendix D), and the rate of erosion in mm per hour was determined by dividing the total depth of erosion by 60. The results revealed that all the samples exhibited erosion rates of less than 1 mm/hr, indicating that they could resist exposure to harsh weather conditions. Since little investigation on the impact of agro-waste additives on the erosion resistance of earth bricks has been undertaken, it's difficult to generalise the findings, however, in this study, incorporating the ESP, SDP-b, and CHP in the clay mixture considerably increased its resistance to water erosion when compared to the reference sample. Furthermore, when the results were compared, it could be concluded that SDP-b provided better resistance than the other additives. It was also observed that the rate of erosion increased as the percentage of SDP-b and CHP increased in the sample. The poor interface between the waste particles and the clay was related to the reduced durability. But for ESP, the erosion rate decreased gradually up to 40% of waste content and then increased for 50% ESP. This is related to the high filling capacity of the ESP in the clay matrix, which resulted in firm bonding. Furthermore, when ESP was combined with SDP-b/CHP, the samples showed a slight increase in erosion rate compared to only 2.5% SDP-b and 2.5% CHP samples. The reference sample showed the highest erosion rate of 0.75 mm/hr, while the 2.5% sawdust sample had the lowest erosion rate of 0.37 mm/hr. Besides, according to visual inspection following the water spray test, the reference sample displayed multiple surface cracks, whereas the other samples had smoother surfaces (Figure 5.7). Danso et al. (2015b) and Sharma et al. (2016) showed that when the amount of natural fibre increased, the durability of the soil matrix improved. According to the authors, this might be due to the improved interaction between fibres and soil, which binds soil particles together more firmly. Obonyo et al. (2010), on the other hand, found that adding coir fibres to soil-cement blocks significantly reduced their durability against water. Also, Akinwumi et al. (2019) observed that the durability of compressed earth blocks decreased with the increasing percentage of shredded waste plastic due to the poor interaction of the shredded waste plastic with the soil.

**Table 5.4:** Water spray test results of stabilised clay blocks.

<b>Sample ID</b>	<b>Depth of erosion (mm)</b>	<b>Rate of erosion (mm/hr)</b>	<b>Erodibility index</b>
REF	44.94	0.75	2 (Pass)
E-10	39.45	0.66	2 (Pass)
E-20	36.52	0.61	2 (Pass)
E-30	35.92	0.60	2 (Pass)
E-40	30.88	0.51	2 (Pass)
E-50	38.47	0.64	2 (Pass)
S-b-2.5	22.46	0.37	2 (Pass)
S-b-5	25.95	0.43	2 (Pass)
S-b-7.5	27.71	0.46	2 (Pass)
S-b-10	28.68	0.48	2 (Pass)
C-2.5	32.56	0.54	2 (Pass)
C-5	33.49	0.56	2 (Pass)
C-7.5	38.78	0.65	2 (Pass)
C-10	40.63	0.68	2 (Pass)
ES-b-2.5/10	33.05	0.55	2 (Pass)
ES-b-2.5/20	35.91	0.60	2 (Pass)
ES-b-2.5/30	36.79	0.61	2 (Pass)
EC-2.5/10	38.84	0.65	2 (Pass)
EC-2.5/20	40.09	0.67	2 (Pass)
EC-2.5/30	40.38	0.67	2 (Pass)

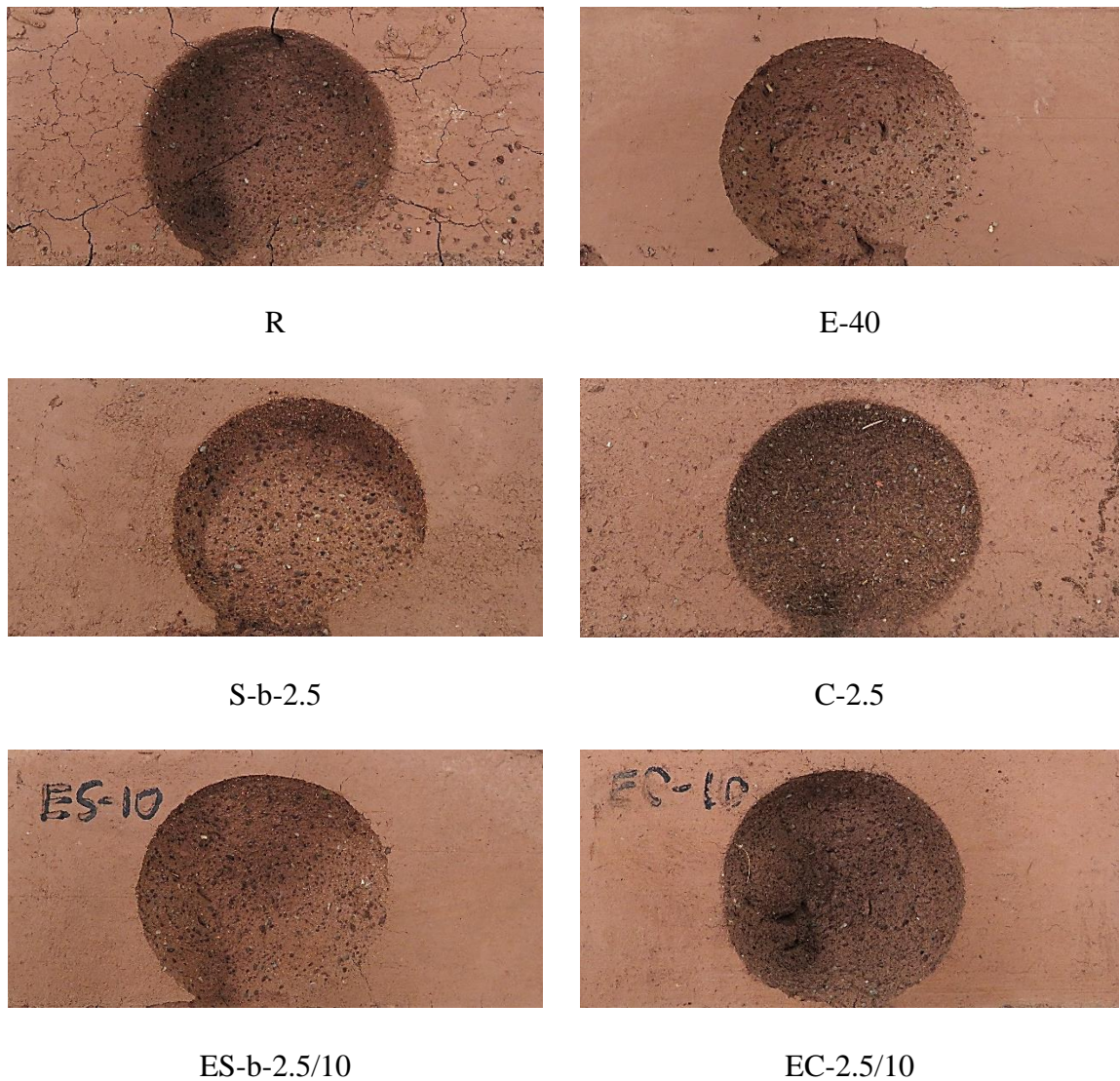


**Figure 5.7:** Samples after water spray test.

In this study, only one sample was assessed for durability tests due to time constraints and a limited supply of materials, which were caused by the COVID-19 pandemic situation during the time of the investigation. Nevertheless, based on the observations, it can be concluded that the incorporation of agro-wastes certainly enhanced the durability of the clay samples, while there is a scope for future research to evaluate durability performance through more comprehensive investigations.

## 5.5 Summary of the Chapter

The following conclusions can be drawn from the test results:

- It was noticed that UPV decreased with increasing additives in the mixture, and there was a direct correlation between UPV and compressive strength. The samples with the highest compressive strength of each group were found to have the highest UPV. For ESP, SDP-b, and CHP mixed samples, UPV ranged from 1263.00 m/s to 1453.33 m/s, 1560.33 m/s to 1318.33 m/s, and 1384.67 m/s to 1123.00 m/s, respectively. Moreover, UPV decreased from 1337.67 m/s to 1247.67 m/s for eggshell-sawdust samples and from 1267 m/s to 1130.33 m/s for eggshell-coconut husk samples when the amount of eggshell powder increased in the mixture.
- Moreover, according to New Zealand standard NZS 4298, all samples passed the drip test and water spray test, where an erodibility index of 2 was recorded, suggesting that they are “slightly erodible”. The results also revealed that when ESP, SDP-b, and CHP were added individually and in combination, erosion resistance improved compared to the reference sample. The highest erosion rate was 0.75 mm/hr for the reference sample, and the lowest was 0.37 mm/hr for the 2.5% sawdust sample.

## *Chapter 6*    **EXPERIMENTAL EVALUATION (PART C-THERMAL PROPERTIES TESTS)**

### **6.1 Introduction**

This chapter details the thermal experiments performed on the various clay samples. The thermal properties tests were carried out in two phases. Individual samples were tested for thermal properties in phase 1. Based on the results of the different properties of the samples, in phase 2, small walls were built with the best-performing mixture from each agro-waste type and evaluated for thermal performance using an adapted hot box method. The thermal efficiency of the walls was assessed by determining the amount of heat exchanged between the hot and cold environments and comparing the results to the reference wall and the literature.

### **6.2 Tests**

#### ***6.2.1 Phase 1 (Thermophysical Properties of Individual Samples)***

The thermal properties, such as thermal conductivity and volumetric heat capacity of each mixture were measured using a portable apparatus ISOMET 2114 model that directly does the measurement value via a surface probe (thermal conductivity range: 0.04 to 0.3 W/m.K, accuracy: 5% of reading + 0.001 W/m.K; volume heat capacity range:  $4.0 \times 10^4$  to  $3.0 \times 10^6$  J/m<sup>3</sup>.K, accuracy: 15% of reading +  $1.10^3$  J/m<sup>3</sup>.K; temperature range: -15 °C to +50 °C, accuracy: 1°C) attached to a temperature sensor (Figure 6.1). The experiment was conducted in a controlled room environment with a temperature of  $25 \pm 1$  °C and a relative humidity of  $32 \pm 2\%$ . Prior to the test, each sample was cleaned with a cloth to remove dust or any other interferents. During the experiment, the samples were positioned on a polyurethane block of 50 mm thickness to avoid any potential

interference from the adjacent apparatus. For each mix design, two measurements were taken (see Appendix E), and the mean was calculated. Knowing the volumetric heat capacity and density of the sample, specific heat capacity was calculated by dividing the volumetric heat capacity by the density value. Besides, thermal diffusivity and thermal effusivity were determined using Equation (2.1) and Equation (2.2).



**Figure 6.1:** Thermal test: (a) 100 mm × 100 mm × 100 mm sample and (b) 215 mm × 100 mm × 100 mm.

### 6.2.2 Phase 2 (Thermal Properties of Wall Samples)

Following the findings of the first phase of the experiment, the optimal percentage of each agro-waste was chosen for use in phase 2 of the experiment to construct small walls to evaluate thermal transmittance and resistance. The walls were constructed using two 215 mm × 100 mm × 100 mm blocks and two 100 mm × 100 mm × 100 mm blocks joined together with earth mortar similar to each sample composition. Each wall had a vertical surface area of around 310 × 215 mm<sup>2</sup> and a thickness of 100 mm.

Thermal transmittance, also known as the U-value (W/m<sup>2</sup>K), is one of the key parameters used to assess the thermal performance of a building envelope and can be determined theoretically or experimentally. The theoretical method for calculating the U-value is described in the BS EN ISO 6946 standard (BS EN ISO 6946, 2017). The results obtained from the theoretical method often differ from the in-situ U-values (Gaspar et al., 2016; Gaspar et al., 2018; Choi and Ko, 2019). The in-situ U-value is widely measured

following the heat flow meter method described in the BS ISO 9869-1 standard (BS ISO 9869-1, 2014). In this method, the U-value is calculated by measuring the heat flux through a wall and the temperature difference between the two surfaces (inside and outside) of the wall since heat is transferred from the warmer to the colder side when there is a temperature difference between the two surfaces of a wall. The standard recommends a minimum duration of three days for the test if the temperature around the heat flux meter is kept steady unless it should be at least seven days to get consistent results. Gaspar et al. (2018a) showed that a temperature difference of more than 19 °C requires a 72-hr test length for low U-value facades, whereas lower temperature differences necessitate a 144-hr test time. However, since the temperatures of the hot and cold boxes are controlled in the laboratory, the test duration can be adapted considering the temperature stability (Soares et al., 2019).

This study followed the adapted hot-box technique (BS ISO 9869-1, 2014) (Figure 6.2) which is a reliable and accurate method for measuring thermal transmittance in laboratory experiments (Asdrubali and Baldinelli, 2011; Lu and Memari, 2018; Zhao et al., 2019b; Lu and Memari, 2022). In this method, the heat flux between hot and cold chambers was estimated using heat flux sensors. The hot chamber (800 mm × 600 mm × 650 mm) was made of commercially available 50 mm thick polyisocyanurate insulation board (PIR,  $\lambda=0.022$  W/mK,  $R=2.25$  m<sup>2</sup>K/W), which has a thin aluminium foil covering on both sides to keep it isolated from the outside environment. The  $\lambda$  value of this insulation material is comparable to polystyrene foam (0.035 W/m K) (Zhao et al., 2019b), expanded polystyrene (0.034 W/mK) (Asdrubali and Baldinelli, 2011), and foam polyurethane (0.0245 W/mK) (Buratti et al., 2016), which were used in the previous studies to build the hot chamber. Two thermostatic tubular heaters (DIMPLEX ECOT1FT 40 W, 230-240 V) were placed inside the hot chamber for an internal heat source. On the other hand, the cold chamber (450 mm × 600 mm × 750 mm) was a refrigerator used to cool the inside air. The temperatures of the hot and cold chambers were controlled by the EMKO ESM-3711-H temperature controller. The sample wall was positioned between the hot and cold chambers in a sample holder made of double insulation boards (100 mm). Besides, any gaps between the wall and the sample holder were filled with insulation material (polyisocyanurate insulation,  $\lambda=0.022$  W/mK,  $R=2.25$  m<sup>2</sup>K/W), and then sealed with aluminium foil tape to ensure heat propagation could only

occur through the exposed wall surfaces. Furthermore, inside both chambers, a small fan was placed to prevent any thermal stratification and ensure uniform heating and cooling (Asdrubali and Baldinelli, 2011).

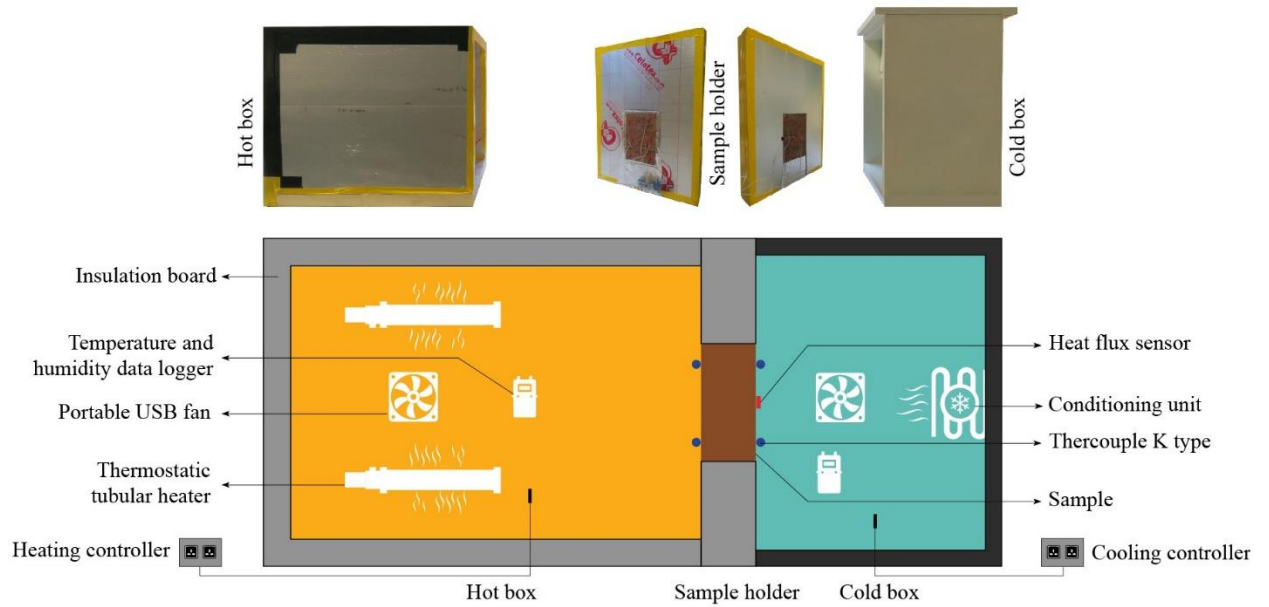


**Figure 6.2:** Test setup for thermal transmittance measurement.

The surface temperature of the sample wall was measured using thermocouple K-type sensors attached to the sample wall. On either side of each block of the sample wall, two thermocouple K sensors were installed. In addition, two heat-flux sensors (gSKIN-XP 26 9C) were installed on the sample wall facing the cold room (Figure 6.3). In order to prevent any influence of air gaps, sandpaper was used to smooth the wall surfaces where the sensors were installed, and adhesive tape was used to fix the sensors to the wall, ensuring that all sensors had good thermal contact with the wall surface. All the sensors were connected to a data logger (Pico USB TC-08) to record the continuous readings for 3 days (72 hours) with a sampling period of 5 minutes. Besides, a temperature and relative humidity data logger was also installed inside both chambers to monitor the temperature and relative humidity of the chambers. Table 6.1 lists the equipment used in this experiment.

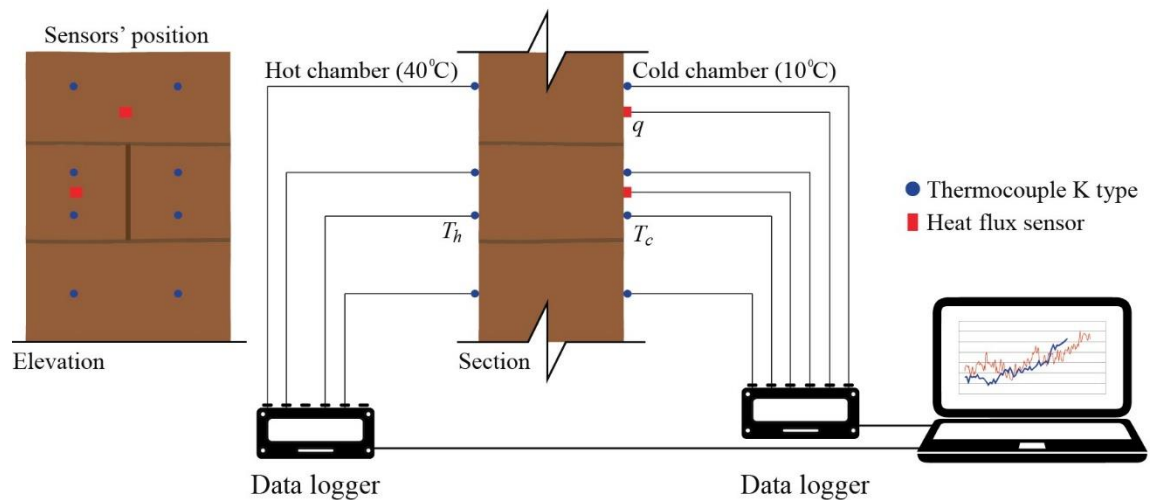


**Figure 6.3:** Configuration of the sample wall and position of the sensors.

**Table 6.1:** Equipment used for thermal transmittance test setup and measurement.

Equipment	Model	Parameters	Values
Temperature sensor	K-type thermocouple	Accuracy (°C)	±1.5
		Range (kW/m <sup>2</sup> )	-150 to +150
Heat flux sensor	gSKIN-XP 26 9C	Sensitivity [ $\mu\text{V}/(\text{W}/\text{m}^2)$ ]	1.5
		Calibration accuracy (%)	±3
		Resolution (W/m <sup>2</sup> )	0.41

*Table 6.1: Equipment used for thermal transmittance test setup and measurement (continued).*

<b>Equipment</b>	<b>Model</b>	<b>Parameters</b>	<b>Values</b>
Temperature controller	EMKO ESM-3711-H	Accuracy (%)	$\pm 1$
		Voltage input range (mV)	$\pm 70$
		Temperature range ( $^{\circ}\text{C}$ )	-270 to +1820
Data logger	Pico USB TC-08	Temperature accuracy ( $^{\circ}\text{C}$ )	Sum of $\pm 0.2\%$ of reading and $\pm 0.5$
		Voltage accuracy ( $\mu\text{V}$ )	Sum of $\pm 0.2\%$ of reading and $\pm 10$
Temperature and relative humidity data logger	EL-USB-2 RH/TEMP	Temperature range ( $^{\circ}\text{C}$ )	-35 to +80
		Relative humidity range (%)	0 to 100
		Temperature accuracy ( $^{\circ}\text{C}$ )	$\pm 0.5$
		Relative humidity accuracy (%)	$\pm 2.25$
Heating source	DIMPLEX ECOT1FT thermostatic tubular heater	Heat output (W)	40
		Capacity (V)	230–240
Fan	4" portable USB fan	Capacity (V)	5

BS ISO 9869-1-2014 specifies the average progressive method to determine the U-value in steady-state conditions. This method is popular since it simplifies the calculating procedure despite the longer test period. The reliability of this method depends on the difference in temperatures between the two chambers. The higher the temperature difference, the more reliable the results are. Meng et al. (2017) revealed that raising the temperature difference on both sides of walls reduces the maximum system error (measurement error) and recommended maintaining a temperature difference of over 20  $^{\circ}\text{C}$  on both sides of the wall to decrease the maximum system error. Hence, in this study, throughout the test period, the average air temperatures of the hot and cold chambers were maintained at 40  $^{\circ}\text{C}$  and 10  $^{\circ}\text{C}$ , respectively. The heat flux was measured at two locations on the sample wall over a period of at least 3 days (72 hours), fulfilling the minimum duration requirement stipulated by the standard. Using Equation (6.1) from the BS ISO 9869-1 standard (BS ISO 9869-1, 2014) the U-value of the sample wall was derived by dividing the average values of the heat flux through the wall by the average temperature difference between the two surfaces (hot and cold) of the wall.

$$U\text{-value} = \frac{\sum q}{\sum (T_h - T_c)} \quad (6.1)$$

where  $q$  is the density of heat flow rate ( $\text{W}/\text{m}^2$ ),  $T_h$  is the hot side temperature ( $^{\circ}\text{C}$ ), and  $T_c$  is the cold side temperature ( $^{\circ}\text{C}$ ) of the sample.

The thermal resistance, or R-value ( $\text{m}^2\text{K}/\text{W}$ ) of the wall can be obtained by inverting the total thermal transmittance determined ( $R=1/U$ ).

## 6.3 Results and Discussions

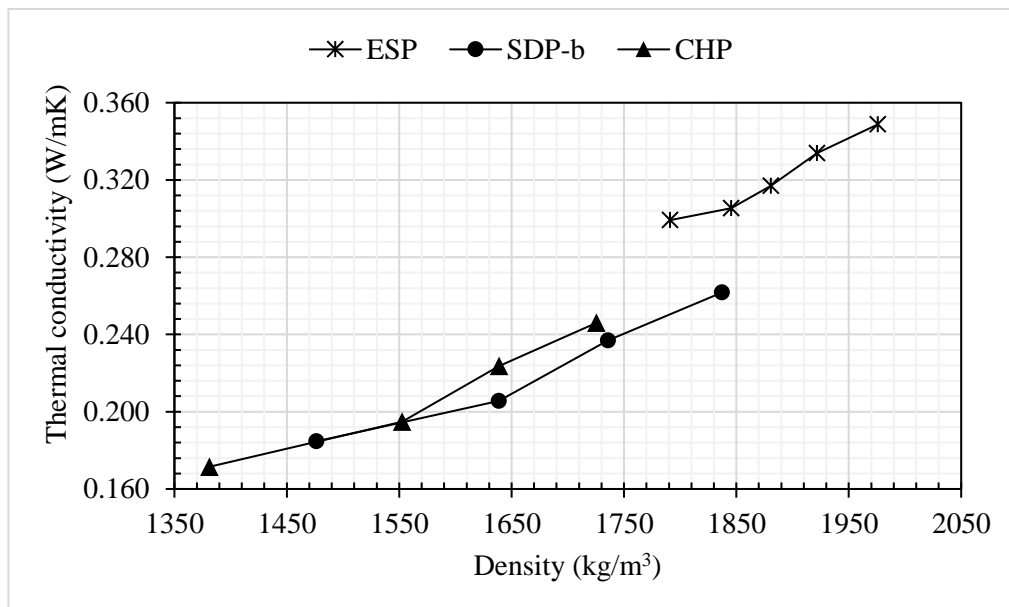
### 6.3.1 Phase 1 (*Thermophysical Properties of Individual Samples*)

Table 6.2 presents the results of the thermal properties of different agro-wastes blended samples. The thermal conductivity of building materials is an important factor for evaluating thermal performance since it has a direct influence on heat losses and energy consumption in the building (Tornay et al., 2017; Kazmi et al., 2018; Babé et al., 2021). The thermal conductivity of a material is affected by various variables, including its morphology, density, and homogeneity (Stapulionienė et al., 2016; Pásztor, 2021). The results indicate a gradual decrease in thermal conductivity with an increase in waste percentages. This drop can be attributed to both the lower thermal conductivity of the agro-waste materials employed and an increase in the amount of air in the sample combination. The thermal conductivity of a material is inversely proportional to its porosity (Ouedraogo et al., 2019). The addition of agro-wastes reduced the density of the samples, resulting in a higher void volume, which is usually filled with air. Due to the low conductivity of air ( $0.024\text{-}0.026 \text{ W}/\text{mK}$ ), the thermal conductivity of the samples decreases as the volume of air in the void increases (Raut and Gomez, 2017; Zhang et al., 2018a; Kandula et al., 2022).

**Table 6.2:** Average values and coefficient of variation (% in parenthesis) of thermophysical properties of sample blocks.

Sample ID	Density, $\rho$ (kg/m <sup>3</sup> )	Thermal conductivity, $\lambda$ (W/mK)	Volumetric heat capacity, $\rho C_p$ ( $\times 10^6$ J/m <sup>3</sup> K)	Specific heat capacity, $C_p$ (J/kgK)	Thermal diffusivity, $\alpha$ ( $\times 10^{-6}$ m <sup>2</sup> /s)	Thermal effusivity, $\tau$ (Ws <sup>1/2</sup> /m <sup>2</sup> K)
REF	2090.96 (0.32)	0.361 (0.14)	1.662 (0.33)	794.75 (0.12)	0.217 (0.14)	774.70 (0.27)
E-10	1975.78 (0.08)	0.349 (0.10)	1.591 (0.37)	805.28 (0.24)	0.219 (0.36)	744.90 (0.18)
E-20	1921.58 (0.21)	0.334 (0.19)	1.574 (0.22)	819.22 (0.06)	0.212 (0.22)	725.05 (0.11)
E-30	1880.72 (0.08)	0.317 (0.25)	1.565 (0.20)	831.94 (0.11)	0.203 (0.22)	704.21 (0.34)
E-40	1845.32 (0.18)	0.305 (0.14)	1.554 (0.30)	842.13 (0.04)	0.196 (0.04)	688.79 (0.25)
E-50	1791.04 (0.20)	0.299 (0.28)	1.535 (0.27)	856.82 (0.02)	0.195 (0.04)	677.61 (0.26)
S-b-2.5	1837.05 (0.08)	0.262 (0.22)	1.514 (0.31)	824.12 (0.16)	0.173 (0.01)	629.44 (0.28)
S-b-5	1735.85 (0.13)	0.237 (0.30)	1.475 (0.33)	849.41 (0.17)	0.161 (0.04)	591.14 (0.32)
S-b-7.5	1638.64 (0.09)	0.206 (0.41)	1.418 (0.43)	865.39 (0.28)	0.145 (0.05)	539.96 (0.37)
S-b-10	1476.38 (0.03)	0.185 (0.27)	1.355 (0.51)	917.48 (0.43)	0.136 (0.09)	500.12 (0.43)
C-2.5	1725.44 (0.24)	0.246 (0.23)	1.464 (0.41)	848.68 (0.11)	0.168 (0.43)	600.19 (0.22)
C-5	1638.79 (0.25)	0.224 (0.32)	1.409 (0.39)	859.45 (0.02)	0.159 (0.04)	561.19 (0.33)
C-7.5	1552.52 (0.27)	0.195 (0.47)	1.376 (0.47)	886.20 (0.08)	0.142 (0.26)	517.77 (0.59)
C-10	1381.24 (0.03)	0.172 (0.41)	1.304 (0.44)	944.37 (0.45)	0.131 (0.08)	472.97 (0.45)

In Figure 6.4, the thermal conductivity of the samples tested are plotted against their density. There is a linear connection between sample density and thermal conductivity, with lower-density samples having lower thermal conductivity than higher-density samples. The findings are consistent with the conclusions reached in previous investigations (Millogo et al., 2014; Laborel-Préneron et al., 2018; Babé et al., 2020; Babé et al., 2021). Moreover, the microscopic examination of the raw materials revealed that SDP-b and CHP particles exhibited cellular porous structures that may contain air, explaining their low thermal conductivity values. Furthermore, it appeared that the use of CHP led to marginally better insulation (i.e., lower thermal conductivity) than SDP-b. This may be due to the lower bulk density and spongy structure of CHP particles, containing more air voids than SDP-b. The lowest thermal conductivity for CHP and SDP-b samples was achieved at 10% content, which was about a 53% and 49% decrease compared to the reference sample. On the other hand, ESP addition reduced the conductivity up to around 17% at 50% content.



**Figure 6.4:** Correlation between thermal conductivity and density.

The volumetric heat capacity of the agro-wastes incorporated samples dropped because of the considerable decrease in the samples' density. However, the specific heat capacity of the samples increased as the waste percentage increased since the agro-wastes, which had a lower mass content than clay, had greater specific heat capacity values (Laborel-

Préneron et al., 2018). The experimental results revealed that 10% CHP, 10% SDP-b, and 50% ESP addition increased the specific heat capacity from 848.68 J/kgK to 944.37 J/kgK, 824.12 J/kgK to 917.48 J/kgK, and 805.28 J/kgK to 856.82 J/kgK, respectively, increasing it around 19%, 15%, and 9% over the reference sample. Besides, CHP samples had a slightly higher specific heat capacity than SDP-b samples. The higher porosity in the CHP samples than in the SDP-b samples might be responsible for this, as the pores are primarily filled with air, which has a specific heat capacity of 1005 J/kgK (Khoudja et al., 2021).

The thermal inertia of buildings contributes to both thermal comfort and a reduction in energy consumption by keeping the indoor air temperature stable. There are two forms of inertia: transmission and absorption. Transmission inertia is defined by thermal diffusivity, whereas absorption inertia is described by thermal effusivity. Building materials with low diffusivity and high effusivity should be used to improve thermal inertia (Medjelekh et al., 2016; Zeghari et al., 2021). In areas where cooling is a major issue, using low thermal diffusivity materials can delay heat transfer from the outside of the building to the inside, decreasing the indoor temperature of the building and reducing the demand for air conditioning during the summer. Also, materials with high thermal effusivity can help keep the indoor temperature of a building stable in the summer by storing and releasing heat. When the internal temperature of a building rises above its comfort level, the walls absorb heat until a steady temperature is attained. This heat is released when the building's internal temperature falls below a comfortable level. Similarly, in the winter, these highly effusive materials can also aid in the reduction of heating demand (Jeanjean et al., 2013; Lizana et al., 2017). As a result, it is recommended that two distinct materials be used to improve indoor thermal comfort: one with low diffusivity on the exterior side as an insulating material, and the other with high effusivity on the interior side of the building wall as a structural material (Zeghari et al., 2021). Table 6.2 also shows that both the thermal diffusivity and thermal effusivity of the samples decreased as the percentage of agro-wastes increased in the mixture. Laborel-Préneron et al. (2018) also observed a similar trend in results using barley straw, hemp shiv and corn cob in unfired earth bricks. The thermal diffusivity of CHP, SDP-b, and ESP samples decreased from  $0.168 \times 10^{-6} \text{ m}^2/\text{s}$  to  $0.131 \times 10^{-6} \text{ m}^2/\text{s}$ ,  $0.173 \times 10^{-6} \text{ m}^2/\text{s}$  to  $0.136 \times 10^{-6} \text{ m}^2/\text{s}$ , and  $0.219 \text{ m}^2/\text{s}$  to  $0.195 \text{ m}^2/\text{s}$  when waste content increased from 2.5%

to 10%, 2.5% to 10%, and 10% to 50%, respectively, indicating a positive influence of agro-wastes on dampening the thermal diffusion in the produced clay blocks (Atiki et al., 2021). For increasing the same percentages of CHP, SDP-b, and ESP, the thermal effusivity values reduced from 600.19  $Ws^{1/2}/m^2K$  to 472.97  $Ws^{1/2}/m^2K$ , 629.44  $Ws^{1/2}/m^2K$  to 500.12  $Ws^{1/2}/m^2K$ , and 744.90  $Ws^{1/2}/m^2K$  to 677.61  $Ws^{1/2}/m^2K$ , respectively. According to the results, the addition of agro-wastes to the unfired clay block increased the transmission inertia and decreased the absorption inertia. These types of materials would be better suited to the construction of exterior walls that delay the transmission of heat from the outside to the inside (Laborel-Préneron et al., 2018).

### ***6.3.2 Phase 2 (Thermal Properties of Wall Samples)***

Following the test results of the physico-mechanical, durability, and thermal properties of different mix designs, in this phase, one mixture was selected for each agro-waste type to make small walls to evaluate their thermal transmittance and resistance. The results indicated that the optimum content for the eggshell sample was 40% since it performed the best in all tests. This higher percentage can be an issue during the manufacturing of large volumes of clay blocks since the supply of eggshell may not be sufficient. This issue must be considered prior to the practical implementation of the work. In the case of sawdust, the selected mix composition was S-b-7.5 because beyond this percentage, the strength of the samples decreased compared to the reference sample, and S-b-7.5 also showed improved thermal properties. Although the thermal conductivity of the samples declined as the amount of coconut husk in the mixture increased, C-7.5 was chosen as C-10 was found to have very high shrinkage and water absorption values.

Thermography analysis was performed on both sides of the walls to check for any irregularities present due to the heating and cooling sources. According to Figure 6.5, the wall surface areas were not affected by any probable source of error. The 72-hour temperature profiles of the two sides (hot and cold) of the wall surfaces are shown in Figure 6.6. The figure shows that all walls had almost similar temperatures on both surfaces, indicating that wall temperatures were unaffected by materials' properties, which was also confirmed by the experimental results of Bruno et al. (2020). The slight temperature difference was due to the position of the temperature sensors on the surface

of the sample block. Despite the sensors being attached as near to the surface as feasible, a gap between the sensor and the surface may be created, leading it to record the temperature of the surrounding air at some point. Figure 6.7 illustrates the monitored relative humidity inside the hot and cold boxes during the test period. The last 24 hours average relative humidity in the hot chamber varied between 14.62% and 15.35%, whereas it was between 36.84% and 41.29% in the cold chamber.

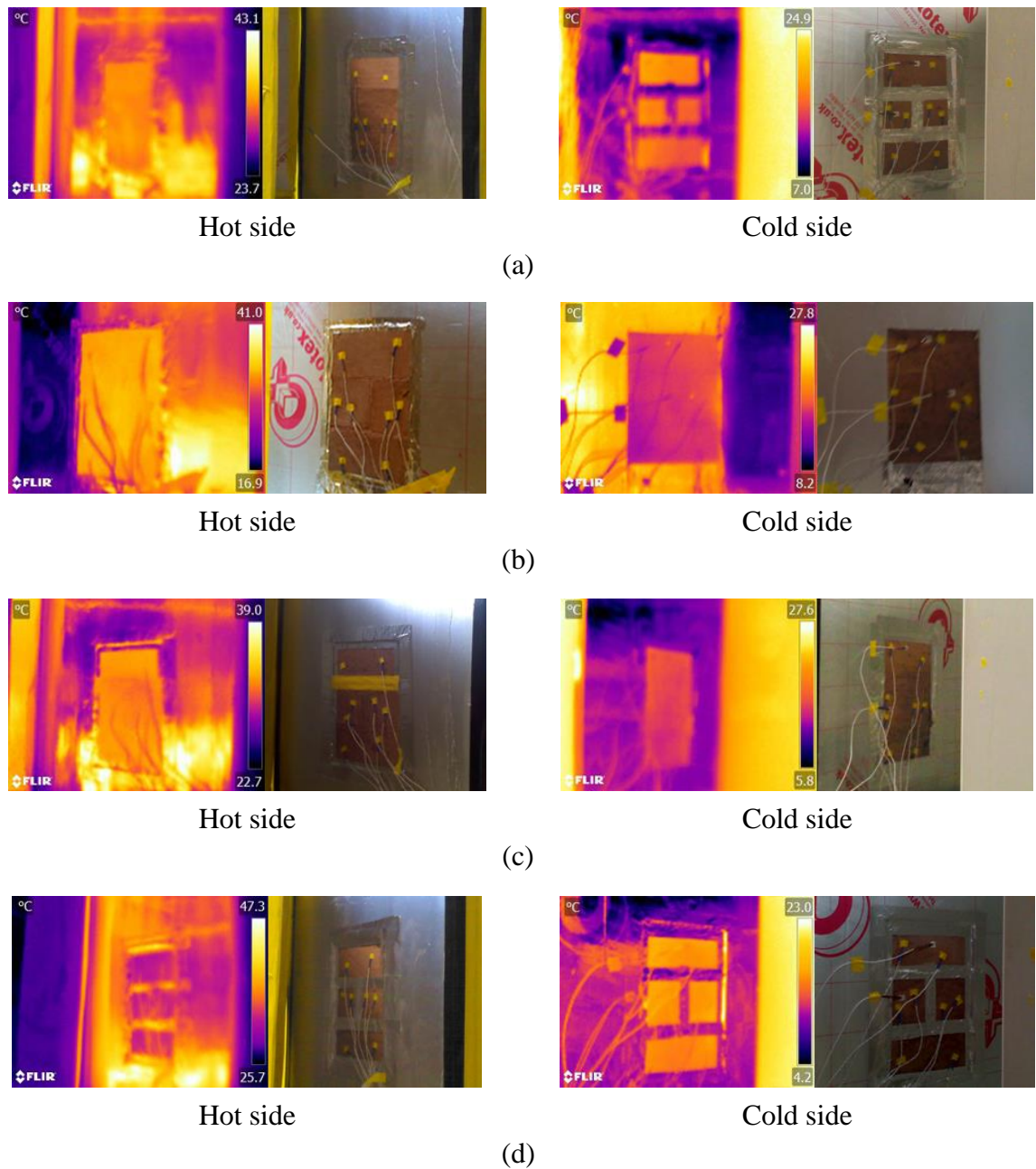
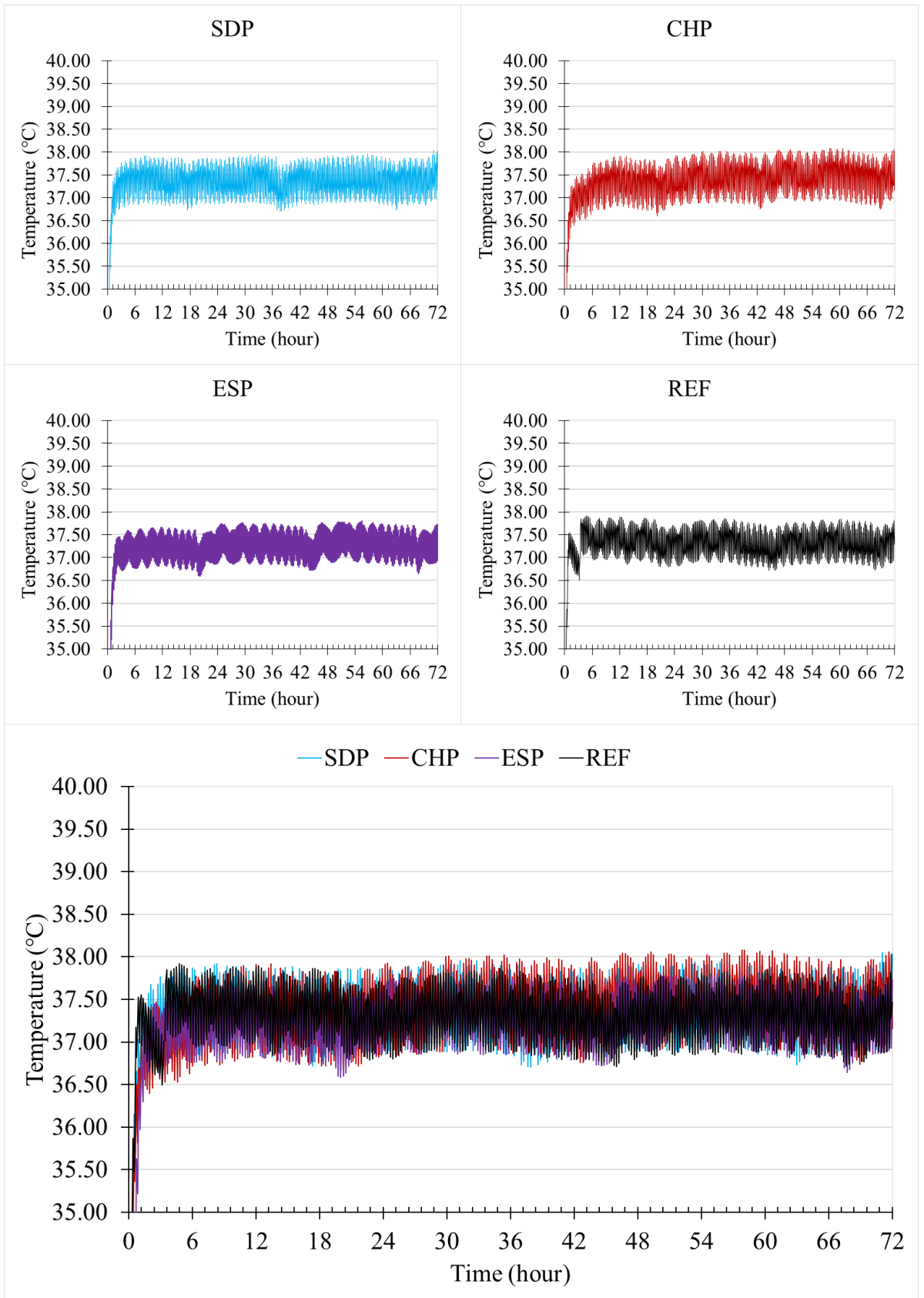
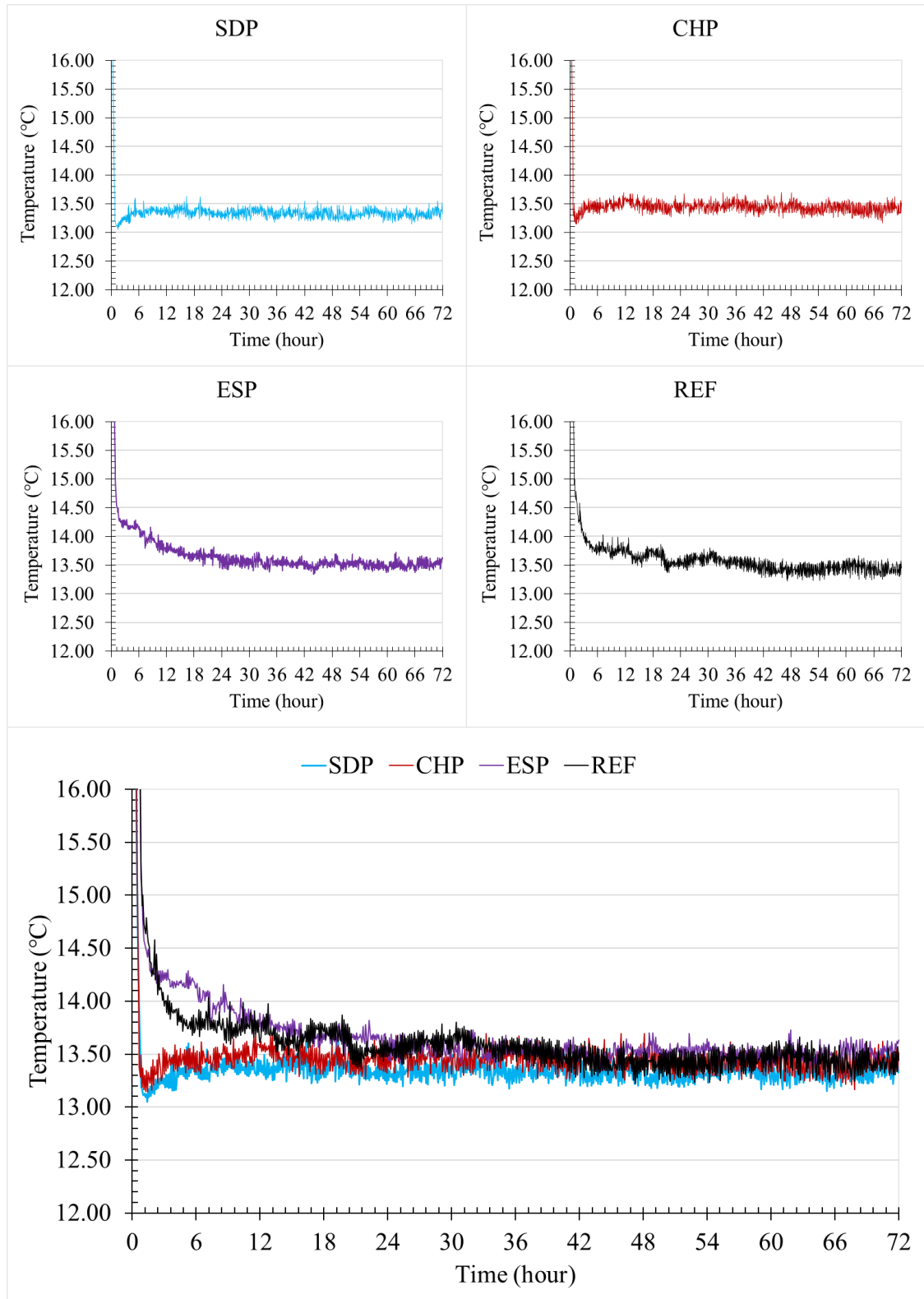


**Figure 6.5:** Thermographs of different wall surfaces: (a) Reference wall, (b) SDP wall, (c) CHP wall and (d) ESP wall.

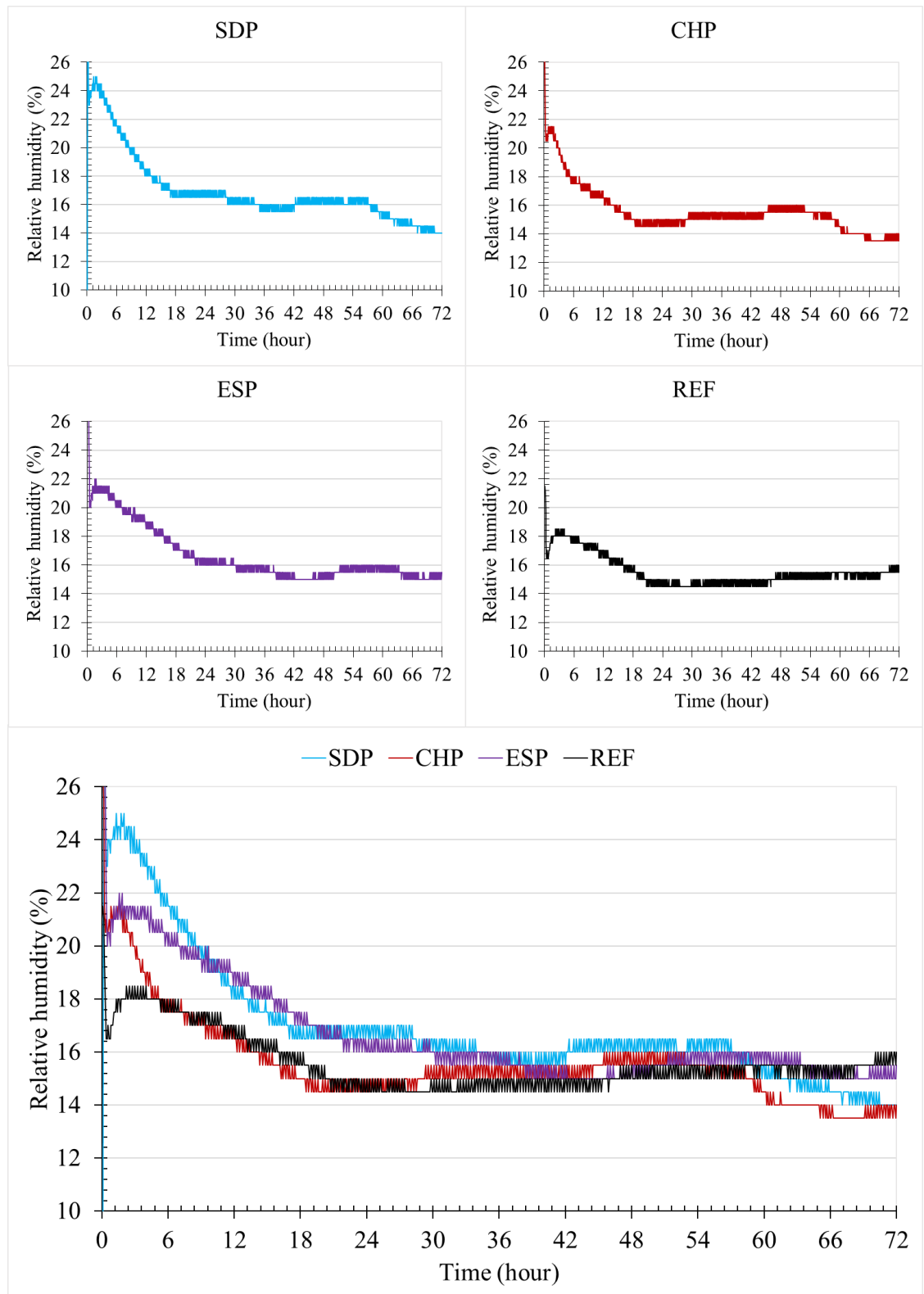


(a)

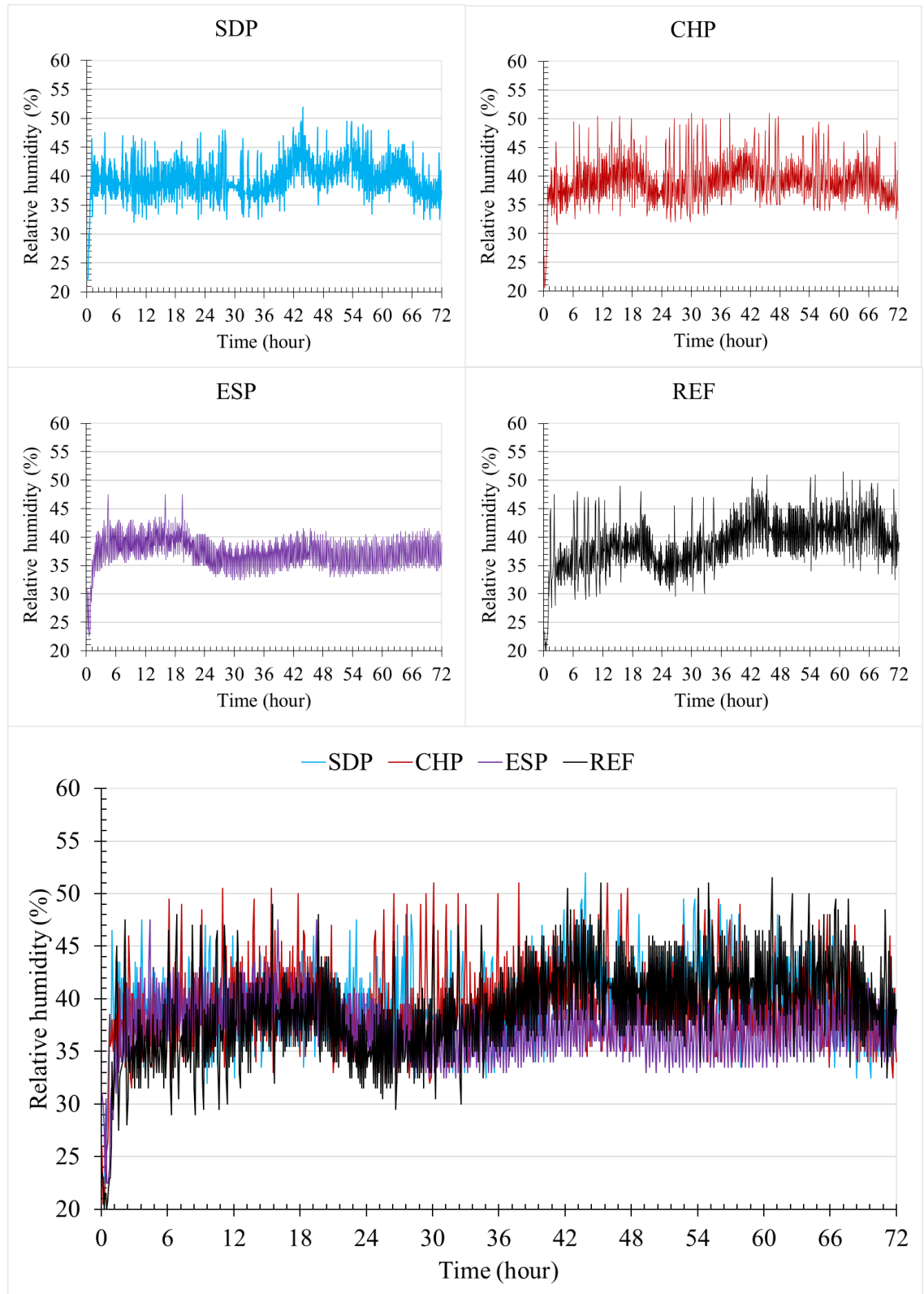


(b)

**Figure 6.6:** Wall surface temperature profiles (72 hours): (a) hot side and (b) cold side.



(a)



(b)

**Figure 6.7:** Measured relative humidity (72 hours): (a) hot chamber and (b) cold chamber.

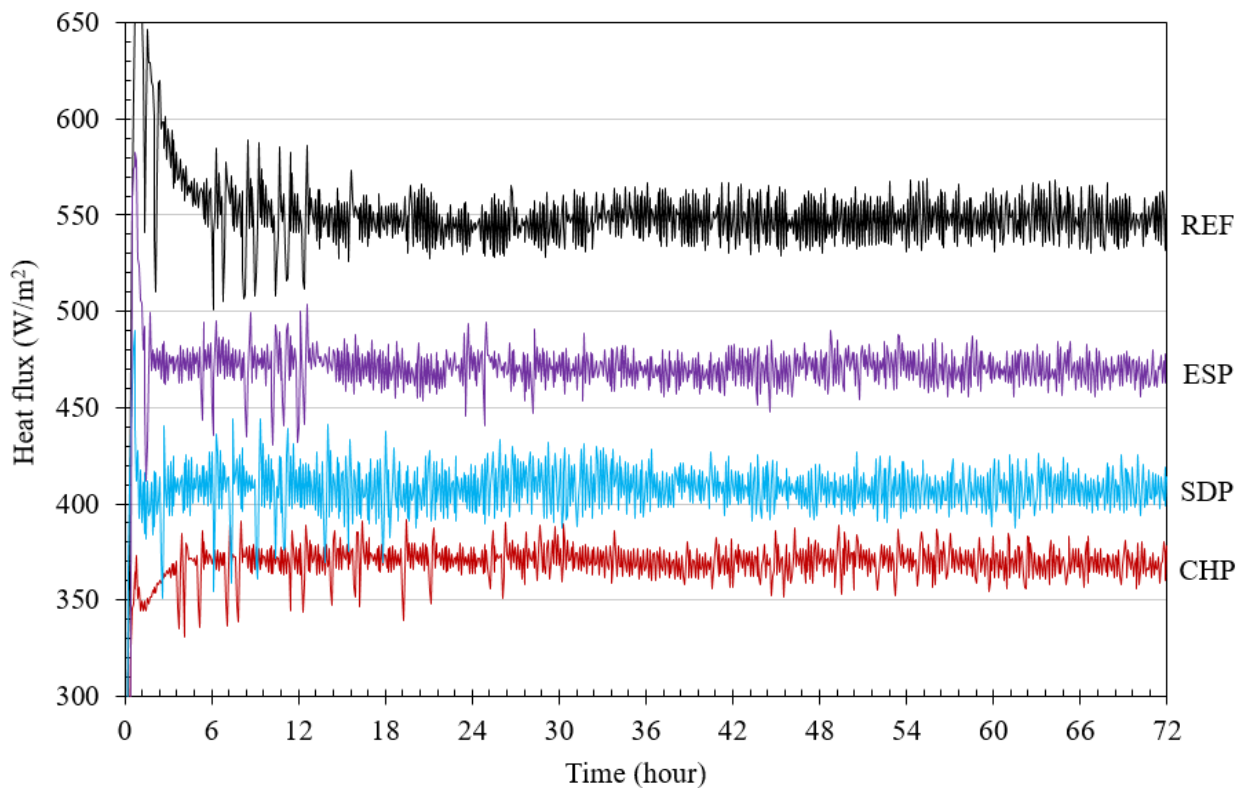
Instead of collecting data immediately, data was taken for at least 24 hours after the system attained thermal steady-state condition. Table 6.3 lists the test results of the last 24 hours of the various wall samples. The heat flux measured through the walls exhibited a similar pattern (Figure 6.8), however, with different magnitudes. The reference wall had the highest heat flux value of  $548.17 \text{ W/m}^2$ , followed by the heat flux in the ESP and SDP walls with a value of  $470.41 \text{ W/m}^2$  and  $407.53 \text{ W/m}^2$ , respectively, while the heat flux of the CHP wall showed the lowest value of  $369.96 \text{ W/m}^2$ . The lower thermal conductivity and density of the CHP sample may contribute to the lower heat flux. Materials with a higher U-value lose more heat, whereas those with a lower U-value lose less heat. According to the test results, the CHP sample had the lowest U-value, indicating the highest resistance (Table 6.4). Compared to the reference sample wall, the CHP, SDP, and ESP sample walls had a thermal resistance improvement of around 48%, 35%, and 16%, respectively.

**Table 6.3:** Last 24 hours average test results and coefficient of variation (% in parenthesis) of the different wall samples.

Measurements	Wall ID			
	REF	E-40	S-b-7.5	C-7.5
Average surface temperature (hot side) (°C)	37.32 (0.90)	37.30 (0.85)	37.40 (0.99)	37.46 (1.06)
Average surface temperature (cold side) (°C)	13.44 (0.77)	13.51 (0.51)	13.32 (0.58)	13.42 (0.73)
Average relative humidity (hot side) (%)	41.29 (9.67)	36.84 (6.28)	40.27 (8.39)	39.09 (8.36)
Average relative humidity (cold side) (%)	15.35 (4.74)	15.50 (3.50)	15.33 (5.60)	14.62 (5.80)
Average heat flux ( $\text{W/m}^2$ )	548.165 (1.93)	470.414 (2.77)	407.534 (2.36)	369.958 (3.21)

**Table 6.4:** Calculated U-values and R-values of the different wall samples.

Wall ID	U-value (W/m <sup>2</sup> K)	R-value (m <sup>2</sup> K/W)
REF	1.845	0.542
E-40	1.584	0.631
S-b-7.5	1.371	0.730
C-7.5	1.245	0.804

**Figure 6.8:** Heat fluxes measured across all wall samples (72 hours).

In Figure 6.9, the experimental U-value results of different wall constructions are compared to the findings of several studies in the literature (Callejas et al., 2017; Chowdhury and Neogi, 2019; Ojerinde, 2020; Teixeira et al., 2020; Krstić et al., 2021). Due to the different thicknesses of the experimented walls and since the U-value is highly dependent on the thickness of the wall, the apparent thermal conductivity values of the walls are calculated by multiplying the U-value by the thickness of the wall to

have a better comparison of their thermal efficiency (Douzane et al., 2016). It should be noted that relatively few experiments have been conducted and published in the literature so far.

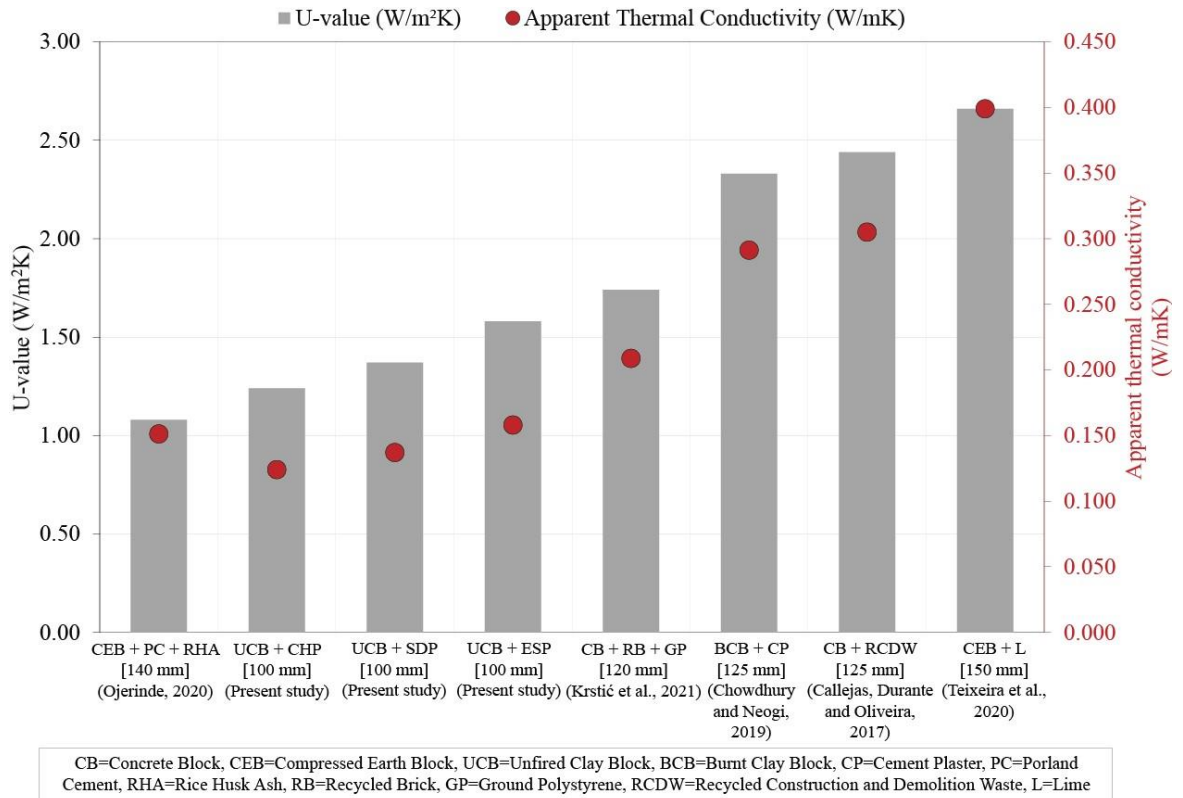


**Figure 6.9:** Comparison of thermal properties of different walls with literature.

Ojerinde (2020) observed that 10% to 30% rice husk ash addition as a partial replacement for Portland cement in compressed earth brick production decreased the U-value from 1.076 W/m<sup>2</sup>K to 1.086 W/m<sup>2</sup>K. In another study, Teixeira et al. (2020) found a U-value of 2.66 W/m<sup>2</sup>K using 7% lime in the compressed earth brick wall. Krstić et al. (2021) used two methods (heat flow and temperature based) to measure the in-situ U-value of a hollow concrete masonry block wall made with recycled crushed brick waste and ground polystyrene. According to the study, U-values for the wall without any insulation ranged from 1.740 W/m<sup>2</sup>K to 1.782 W/m<sup>2</sup>K for the heat flow method, while for the temperature-based method, the U-value was 1.363 W/m<sup>2</sup>K. In the case of a burnt clay brick wall with cement plaster using the guarded hot box method, Chowdhury and Neogi (2019) reported that the U-value ranged from 2.326 W/m<sup>2</sup>K to 2.488 W/m<sup>2</sup>K. Callejas et al. (2017) also used an adapted hot-box method to determine the thermal

properties of concrete blocks with recycled construction and demolition waste. Based on the results obtained, the block was found to have a U-value of between 2.439 W/m<sup>2</sup>K and 3.030 W/m<sup>2</sup>K in the solid area. After reviewing the experimental results described in the literature and based on the findings of the analyses, it can be concluded that coconut husk and sawdust have great potential for improving the thermal properties of unfired clay brick.

## 6.4 Summary of the Chapter

This chapter aimed to investigate the thermal properties of the produced clay blocks. The properties measured include thermal conductivity, volumetric heat capacity, specific heat capacity, thermal diffusivity, and thermal effusivity. Furthermore, the thermal efficiency of the produced walls was evaluated using an adapted hot box method in which the two surfaces of the wall were exposed to hot and cold temperatures, and the heat flow across the wall was measured concurrently.

The following conclusions can be drawn from the test results:

- The thermal properties tests of individual samples showed that the thermal conductivity of the different samples decreased with increasing waste percentages, and there is a direct relationship between thermal conductivity and density, with lower-density samples having lower conductivity. The lowest conductivity value was obtained for the 10% CHP sample (0.172 W/mK), followed by the 10% SDP-b sample (0.185 W/mK) and the 50% ESP sample (0.299 W/mK). Moreover, volumetric heat capacity, thermal diffusivity, and effusivity decreased, while the specific heat capacity of the samples increased with the addition of agro-wastes.
- The test results of the wall samples revealed that the coconut husk, sawdust, and eggshell sample walls outperformed the reference sample wall in terms of thermal resistance, with improvements of around 48%, 35%, and 16%, respectively. The wall composed of 7.5% coconut husk samples had the lowest heat flow because of its lightweight nature. Also, there was a higher air void content inside the samples, which reduced the heat transfer between the hot and cold environments.

## *Chapter 7*    **EVALUATION OF INDOOR THERMAL COMFORT (NUMERICAL SIMULATION)**

### **7.1 Introduction**

This chapter aims at assessing in detail the different thermophysical properties of building wall materials affecting the indoor thermal environment and energy efficiency of buildings in tropical climates (in the summer and winter) by conducting simplified simulation analyses using the Integrated Environmental Solutions Virtual Environment (IES-VE) programme. This study first developed the conditions for simulation analyses and then addressed selected findings by comparing the thermal responses of the materials to moderate outdoor temperatures and their energy-saving potential. While energy consumption estimation for a complete operational building is a complex method by which the performance of the wall materials cannot be properly defined, this simplistic simulation approach can guide the designers in conducting a preliminary analysis of the different building wall materials to select the best thermally efficient solution. The simulation procedure, the physical modelling of the space, and the data used as inputs for the simulation are discussed in this chapter. This chapter also presents the results of the simulation analyses on the reduction of indoor temperature fluctuations and energy consumption of the space.

### **7.2 Integrated Environmental Solutions Virtual Environment (IES-VE) Software**

Building simulation software tools are mostly used by building designers and engineers to explore various design alternatives under varying climatic conditions, internal gains, building envelope characteristics, building geometry, HVAC system specifications, operation schedules, and control strategies, etc. This type of software can perform energy analysis and estimate the energy requirements for both the heating and cooling of a

building on an hourly, daily, or monthly basis using dynamic thermal simulation models, which are mathematical representations of the thermal processes occurring in a building. This present work used the IES-VE software, which complies with several national and international standards (IES-VE, 2020). IES-VE is a user-friendly, dynamic simulation software based on architectural drawings. Many researchers have proven the efficiency of this software by validating the numerical results against experimental data (Ben and Steemers, 2014; Ji et al., 2014; Moran et al., 2014; Tong et al., 2018; Ji et al., 2019).

IES-VE's ApacheSim Thermal Application is a dynamic thermal simulation programme that is based on first-principles mathematical modelling of the heat transfer processes occurring inside and around a space. ApacheSim assumes that the conduction of each building element is unidirectional, and the thermophysical properties ( $\lambda$ ,  $\rho$  and  $C_p$ ) of each layer of the element are uniform within the layer. Under these assumptions, the following Equation (7.1) can be formulated:

$$\partial^2 T / \partial x^2 = \frac{\rho C_p}{\lambda} \partial T / \partial t \quad (7.1)$$

A finite-difference approach is considered in ApacheSim to solve the heat differentiation equation. In this approach, the element is replaced with a finite number of discrete nodes at which the temperature is calculated. By considering this spatial discretisation, Equation (7.2) can be written as follows:

$$\frac{T_{n-1} - 2T_n + T_{n+1}}{\delta_n^2} = -(\rho C_p / \lambda) \partial T / \partial t \quad (7.2)$$

Where  $T_n$  is the temperature ( $^{\circ}\text{C}$ ) at a node  $n$  and  $\delta_n$  is the local node spacing (m).

In the layers, the nodes are distributed properly to ensure accurate modelling of the heat transfer and storage characteristics for a selected time step. This process is based on constraints imposed on the Fourier number:

$$F = (\lambda / \rho C_p) \Delta / \delta_n^2 \quad (7.3)$$

where  $\Delta$  is the simulation time-step (s).

The temperature-time derivative ( $\partial T/\partial t$ ) at the present time is expressed by Equation (7.4):

$$\dot{T}_n^j = (T_n^{j+1} - T_n^j) / \Delta \quad (7.4)$$

where  $T_n^j$  is the temperature ( $^{\circ}\text{C}$ ) and  $\dot{T}_n^j$  is the time derivative of temperature (K/s) at node  $n$  and time-step  $j$ .

The energy demand for heating and cooling for a space or zone is calculated according to Equation (7.5) and Equation (7.6), respectively:

$$Q_{NH} = Q_{L,H} - (\eta_{G,H} \times Q_{G,H}) \quad (7.5)$$

subject to,  $Q_{NH} \geq 0$ ,  $\gamma_H \leq 2.5$  and  $\theta_i > \theta_e$  (otherwise,  $Q_{NH} = 0.0$ )

$$Q_{NC} = Q_{G,C} - (\eta_{L,C} \times Q_{L,C}) \quad (7.6)$$

subject to  $Q_{NC} \geq 0$ ,  $\lambda_c \leq 2.5$  and (otherwise,  $Q_{NC} = 0.0$ )

where  $Q_{NH}$  and  $Q_{NC}$  are the building zone energy demand for heating and cooling (MJ),  $Q_{L,H}$  and  $Q_{L,C}$  are the total heat transfer (losses) for the heating and cooling mode (MJ),  $Q_{G,H}$  and  $v$  are the total heat sources (gains) for the heating and cooling mode (MJ),  $\eta_{G,H}$  and  $\eta_{L,C}$  are the dimensionless gain utilisation factor (a function of mainly the gain-loss ratio and the thermal inertia of the building zone),  $\gamma_H$  and  $\lambda_c$  are the dimensionless gain/loss ratio for the heating and cooling mode respectively.  $\theta_i$  is the indoor temperature ( $^{\circ}\text{C}$ ) which is the heating and cooling set-points,  $\theta_e$  is the outdoor temperature ( $^{\circ}\text{C}$ ) which is obtained from hourly weather data for the location.

Total heat transfer is determined by Equation (7.7) and Equation (7.8):

$$Q_L = Q_T + Q_V \quad (7.7)$$

where  $Q_L$  is the total heat transfer (MJ),  $Q_T$  is the total heat transfer by transmission (MJ), and  $Q_V$  is the total heat transfer by ventilation (MJ).

$$Q_G = Q_I + Q_S \quad (7.8)$$

where  $Q_G$  is the total heat sources (MJ),  $Q_I$  is the sum of internal heat sources over the given period (MJ), and  $Q_S$  is the sum of solar heat sources over the given period (MJ) (IES-VE, 2011; SBEM, 2018).

### 7.3 Physical Model and Simulation Conditions

In IES-VE, a space of 12 m × 6 m × 6 m (length × width × height) (Figure 7.1) was modelled (elongated axis aligned east-west) to evaluate the indoor air temperature and annual energy consumption for different wall materials. The space was modelled without windows, and when running the simulation, all sources of internal heat gain and heating/cooling systems were excluded. However, 0.25 air changes per hour of infiltration rate was included to indicate natural air leakage through the envelope of the space. On the other hand, in the case of the energy calculation, for the cooling and heating periods, the maximum temperature was set to 23 °C and 19 °C, respectively, following the thermal comfort criteria. The study considered the weather data of the capital city of Dhaka, Bangladesh (23.8103°N, 90.4125°E), which features a sub-tropical monsoon climate (Khatun et al., 2016). Figure 7.2 presents the 10-year average maximum, mean, and minimum monthly air temperatures, and Figure 7.3 shows the relative humidity and precipitation data of Dhaka from the Bangladesh Meteorological Department (Bangladesh Meteorological Department, 2018). The hourly weather data of Dhaka, SunCast solar radiation, and MacroFlo for the natural infiltration were linked to ApacheSim, and the simulation period was set for the entire year. Though this type of building does not exist in reality, this approach was considered to provide a clear assessment of the envelope materials' thermal performance under dynamic weather conditions. The basic thermophysical properties of the materials (thermal conductivity, density, and specific heat capacity) from Chapter 6 were used for the simulation (see Table 6.2). The typical hottest (22 April) and coldest (06 January) days from the weather data record of the preceding year were considered for the analysis.

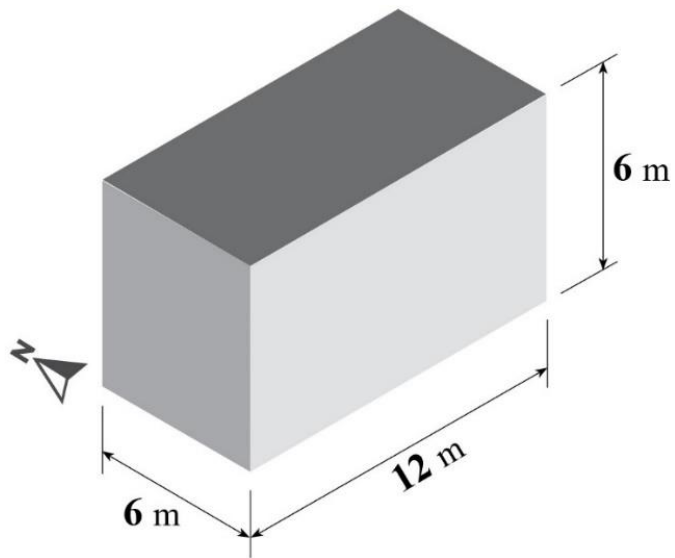


**Figure 7.1:** Building geometry.

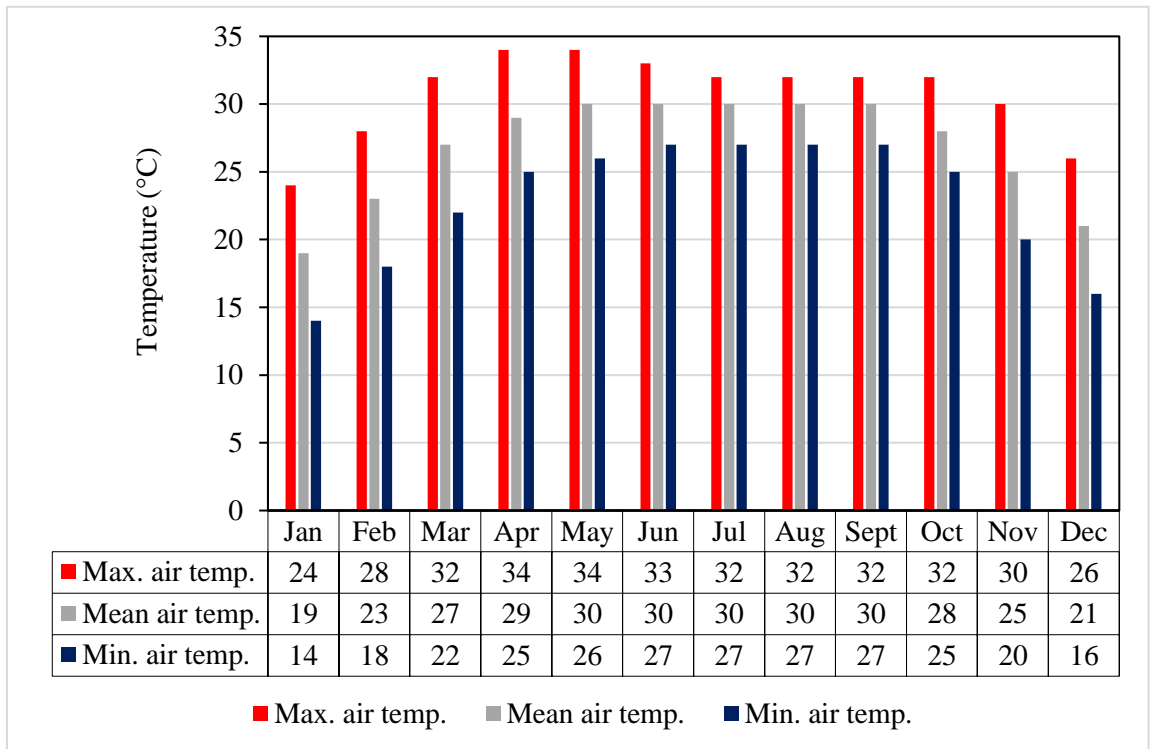


**Figure 7.2:** 10-year (2005-2015) average of maximum, mean, and minimum monthly air temperatures of the capital city of Bangladesh, Dhaka (Bangladesh Meteorological Department, 2018).

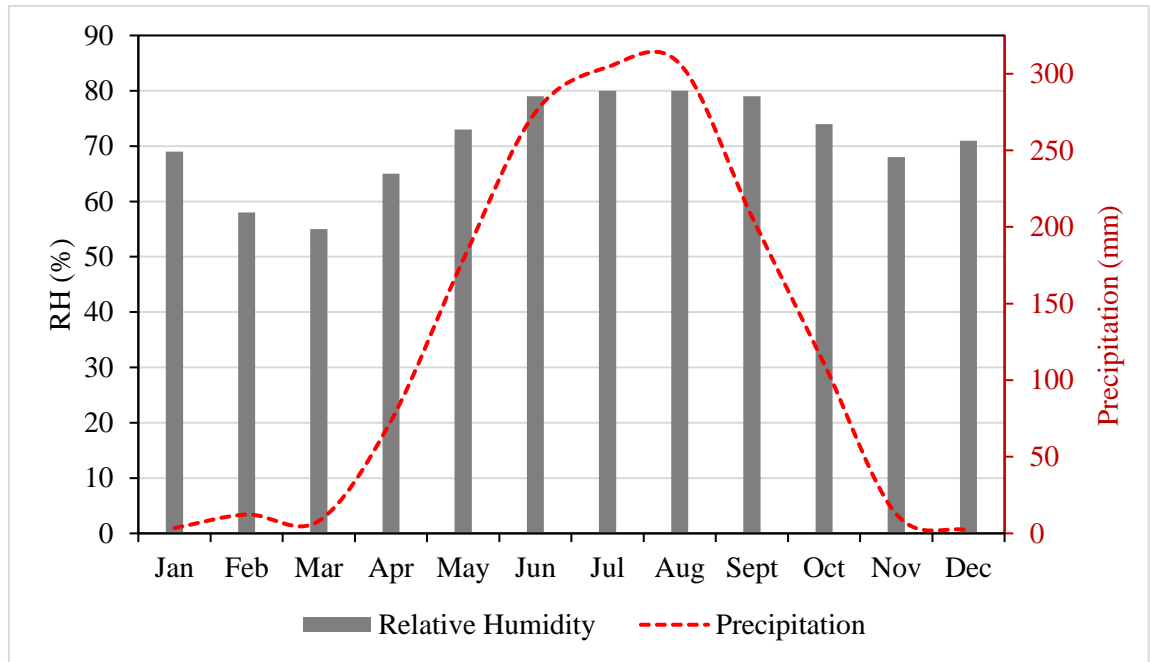


**Figure 7.3:** 10-year (2005-2015) average relative humidity and rainfall of the capital city of Bangladesh, Dhaka (Bangladesh Meteorological Department, 2018).

## 7.4 Simulation Phases

The simulation analyses were performed under the following two phases:

### 7.4.1 Phase 01: Different Wall Materials

This phase involved modelling and simulating the space separately with conventional materials as well as newly developed agro-wastes incorporated unfired earth blocks to evaluate their performance. The thickness (100 mm) of the walls was considered equal to laboratory investigation (Chapter 6), and for analysis, only the wall materials were altered, keeping all other elements unchanged. Table 7.1 presents the thermophysical properties of different wall materials used as input data for the simulation analyses. The properties of the compressed stabilised earth block (CSEB), hand-moulded burnt clay brick (HBCB), machine-moulded burnt clay brick (MBCB), and concrete brick (CB) were taken from the study of Rawal et al. (2020).

**Table 7.1:** Average values and coefficient of variation (% in parenthesis) of thermophysical properties of different materials used for simulation.

Materials	Density, $\rho$ (kg/m <sup>3</sup> )	Thermal conductivity, $\lambda$ (W/mK)	Specific heat capacity, $C_p$ (J/kgK)
Compressed stabilised earth block (CSEB) (Rawal et al., 2020)	1630	0.588	908.30
Hand-moulded burnt clay brick (HBCB) (Rawal et al., 2020)	1599	0.485	907.80
Machine-moulded burnt clay brick (MBCB) (Rawal et al., 2020)	1737	0.505	946.80
Concrete brick (CB) (Rawal et al., 2020)	2122	1.546	920.00
REF	2090.96 (0.32)	0.361 (0.14)	794.75 (0.12)
E-40	1845.32 (0.18)	0.305 (0.14)	842.13 (0.04)
S-b-7.5	1638.64 (0.09)	0.206 (0.41)	865.39 (0.28)
C-7.5	1552.52 (0.27)	0.195 (0.47)	886.20 (0.08)

#### ***7.4.2 Phase 02: Different Thicknesses of the Wall***

This simulation phase was designed to evaluate the effect of wall thickness variations on TL and DF. Therefore, in this phase, the space was modelled with different thicknesses (100 mm to 400 mm) of the wall material that performed best in the first phase of the simulation study.

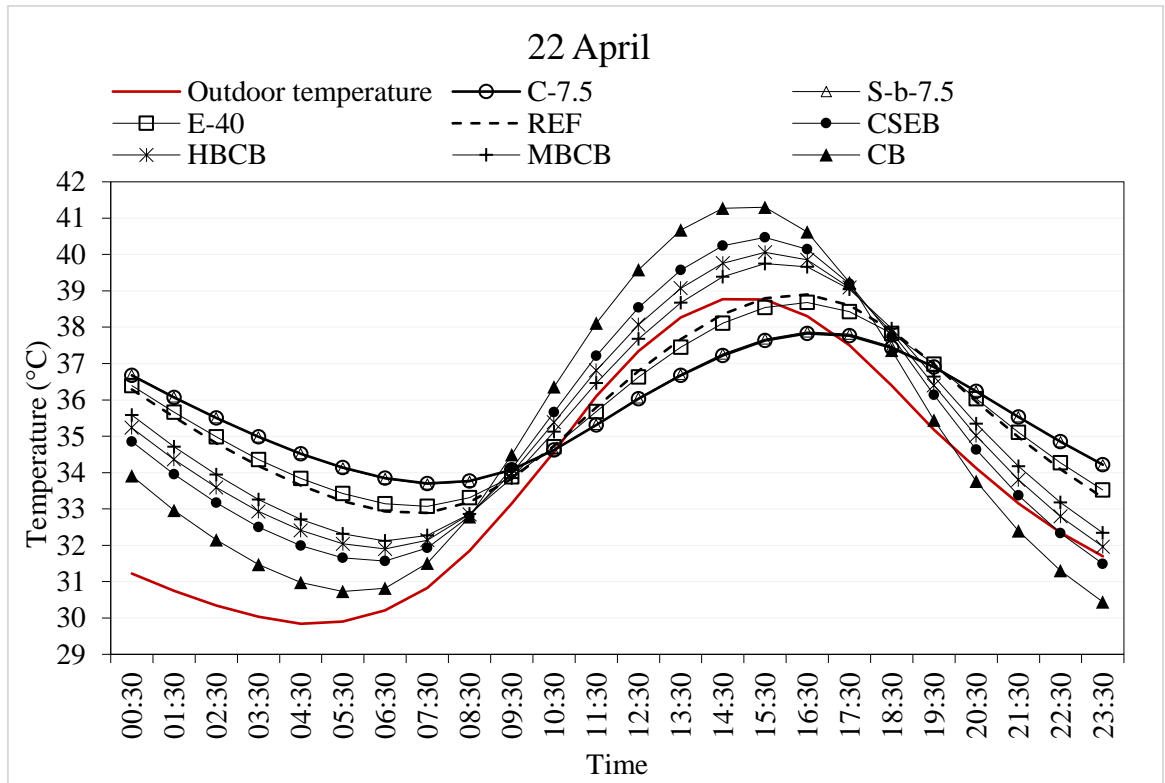
### **7.5 Results and Discussions**

#### ***7.5.3 Effects of Materials' Thermophysical Properties***

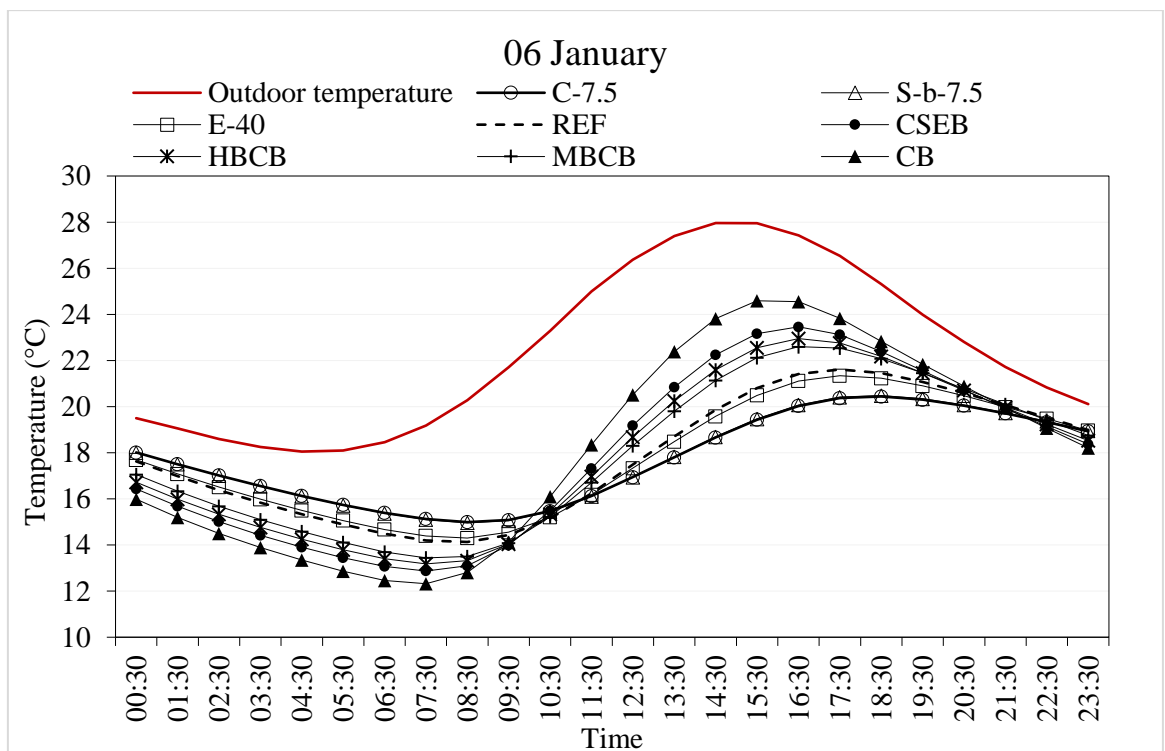
Countries in tropical zones experience a wider diurnal temperature range than countries in colder zones. The indoor temperature fluctuations in a building increase with an increase in diurnal temperature differences, which results in thermal instability.

Therefore, in hot climates, buildings should be evaluated for changes in indoor temperatures to minimise the daily variations, thus reducing the cooling load demand and ensuring a comfortable indoor environment (Rathore et al., 2020). Consequently, in this section, materials' ability to dampen the indoor temperature fluctuation was assessed and compared based on their basic thermal properties, including density ( $\rho$ ), thermal conductivity ( $\lambda$ ), specific heat capacity ( $C_p$ ), thermal diffusivity ( $\alpha$ ), thermal transmittance (U-value), and derived thermal properties such as time lag (TL) and decrement factor (DF). Furthermore, the yearly energy consumption was analysed for each wall construction and compared to reach a conclusion.

Figure 7.4 illustrates the outdoor and indoor air temperatures of the space during the summer (22 April) and winter (06 January) days. It also demonstrates that the outdoor air temperature fluctuation is high, with a maximum temperature of about 38.77 °C and a minimum of about 29.84 °C. According to the figure, the indoor air temperature of the reference wall construction responded rapidly to the outdoor temperature variations, followed by the eggshell (E-40), sawdust (S-b-7.5), and coconut husk (C-7.5) walls. The maximum indoor temperature for the reference wall construction was 38.90 °C and a minimum of 32.89 °C, therefore having a temperature swing of 6.01 °C. However, the temperature swing was found comparatively less for the eggshell wall (5.61 °C), whereas for the sawdust (4.19 °C) and coconut husk (4.13 °C) walls it was even lower. As the wall thickness remained equal for all the materials, this variation in temperature swing occurred due to the higher thermal conductivity value of the reference wall (0.361 W/mK) than the eggshell (0.305 W/mK), sawdust (0.206 W/mK), and coconut husk (0.195 W/mK) walls. Besides, the insignificant indoor temperature swing of the coconut husk and sawdust walls was due to their low thermal conductivity and high specific heat capacity. Also, it can be observed that, after mid-summer days, the indoor air temperature of the reference wall construction became higher than the outdoor temperature. This may occur since the space was modelled without windows and no natural ventilation or air conditioning systems were considered for the analysis (Zhu et al., 2015).



(a)



(b)

**Figure 7.4:** Outdoor and indoor temperatures for four different wall material constructions: (a) summer day and (b) winter day.

The thermal diffusivity values of coconut husk, sawdust, eggshell, and reference walls were calculated as  $0.142 \times 10^{-6} \text{ m}^2/\text{s}$ ,  $0.145 \times 10^{-6} \text{ m}^2/\text{s}$ ,  $0.196 \times 10^{-6} \text{ m}^2/\text{s}$ , and  $0.217 \times 10^{-6} \text{ m}^2/\text{s}$ , respectively, using Equation (2.1). Besides, the DF of these walls was determined (for the summer day) as 0.46, 0.47, 0.63, and 0.67, respectively, by Equation (2.3). Moreover, Figure 7.5 shows that the TL for the coconut husk and sawdust walls was comparatively higher (2 hours) than the eggshell wall (1.50 hours), while the reference wall had the lowest TL (1.25 hours). This reveals that materials with a higher thermal diffusivity and a higher DF take less time to reach thermal equilibrium with the outdoor temperature. Furthermore, due to a lower U-value ( $1.24 \text{ W/m}^2\text{K}$ ), the coconut husk wall had the lowest yearly energy consumption (14.90 MWh), followed by the sawdust (15.10 MWh) and eggshell (17.70 MWh) walls. On the other hand, the reference wall with a greater U-value ( $1.85 \text{ W/m}^2\text{K}$ ) had the highest yearly energy consumption (18.90 MWh) (Figure 7.6). Additionally, all developed materials performed better than the conventional materials.

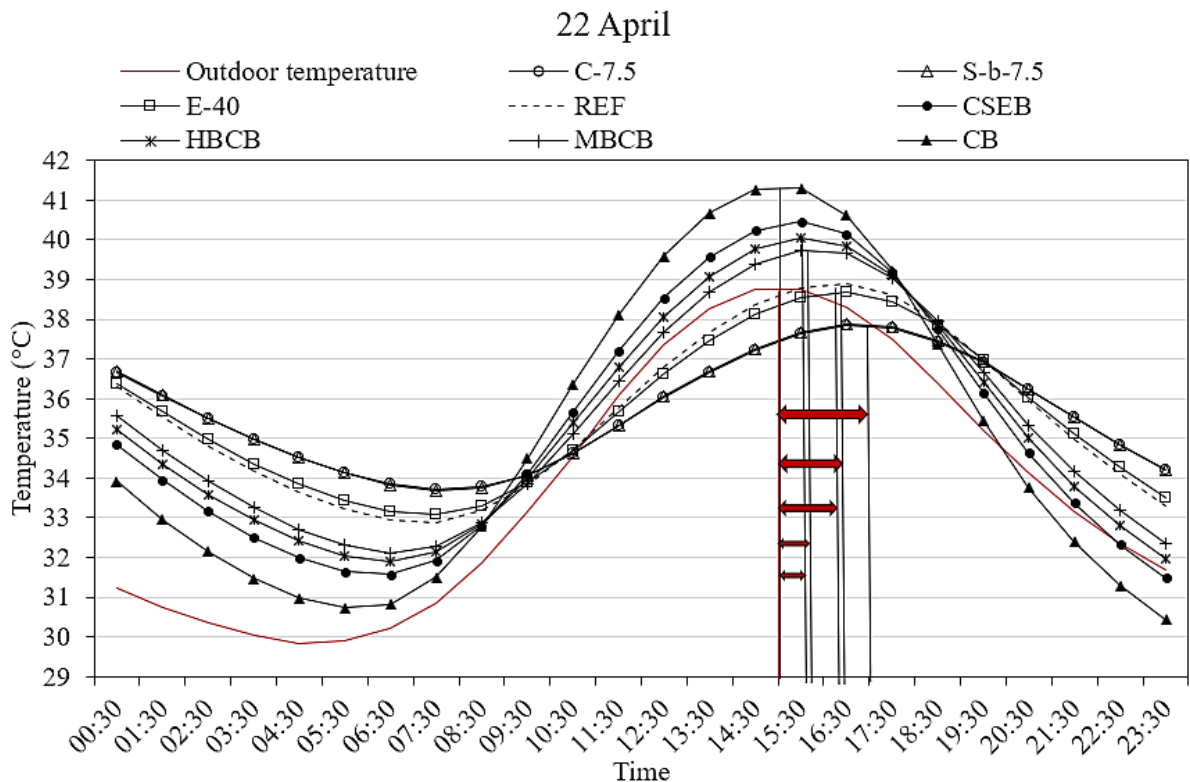


**Figure 7.5:** Time lag for different wall constructions (summer day).

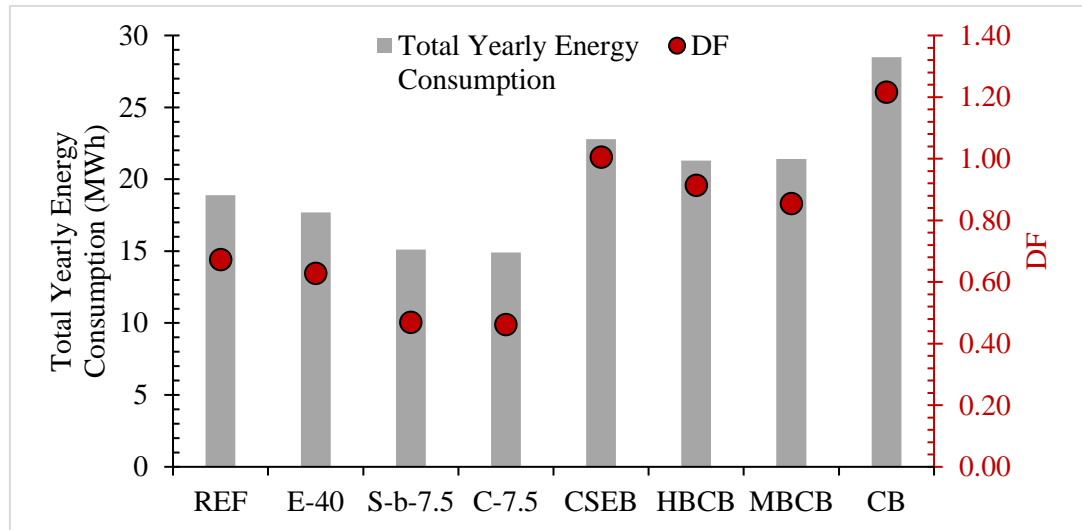


**Figure 7.6:** Yearly energy consumption and DF of different wall constructions.

#### 7.5.4 Effects of Wall Thickness Variation

The phase 1 simulation results revealed that the coconut husk wall (C-7.5) performed better than the other wall samples. Therefore, C-7.5 wall construction was further assessed in the phase 2 simulation by varying its thickness. From Table 7.2, it can be observed that the thermal mass for the thickness of 100 mm C-7.5 wall was 60.90 kJ/m<sup>2</sup>K, whereas the thermal mass of 200 mm, 300 mm, and 400 mm walls was similar to 97.45 kJ/m<sup>2</sup>K. It has been presented that temperature variations penetrate up to around 100 mm into the wall material within 24 hours, depending on the material type and the heat transfer rate (Braham et al., 2001; Perez Fernandez, 2012). In Apachesim, the boundary of the building is calculated as the internal horizontal dimensions between halfway through the thickness of the zone walls. As a result, after increasing the thickness of the wall above 200 mm the thermal mass value remains constant (Anđelković et al., 2012; SBEM, 2018). The simulation results of the space with different thicknesses of the C-7.5 wall revealed that as the thickness increased from 100 mm to 250 mm, the U-values of the walls decreased from 1.47 W/m<sup>2</sup>K to 0.69 W/m<sup>2</sup>K and DF declined from 0.46 to 0.03 (Table 7.2). On the other hand, TL increased from 2 hours to 6.50 hours with increasing wall thickness (Figure 7.7). This indicates that walls with a lower DF and a higher TL have a higher potential to dampen the heat flow from one surface to the other (Figure 7.8), which complies with the experimental results of El

Fgaier et al. (2016). Also, the larger the thickness of the wall, the lower the yearly energy consumption (Table 7.2).

**Table 7.2:** Derived thermal properties and yearly energy consumption of different wall thicknesses of C-7.5 wall construction.

Wall thickness (mm)	Thermal mass (kJ/m <sup>2</sup> k)	U-value (W/m <sup>2</sup> K)	R-value (m <sup>2</sup> K/W)	DF (Summer day)	Yearly Energy Consumption (MWh)
100	68.79	1.47	0.51	0.46	14.90
150	103.19	1.07	0.76	0.23	12.50
200	137.58	0.84	1.02	0.09	11.30
250	137.58	0.69	1.27	0.03	10.50

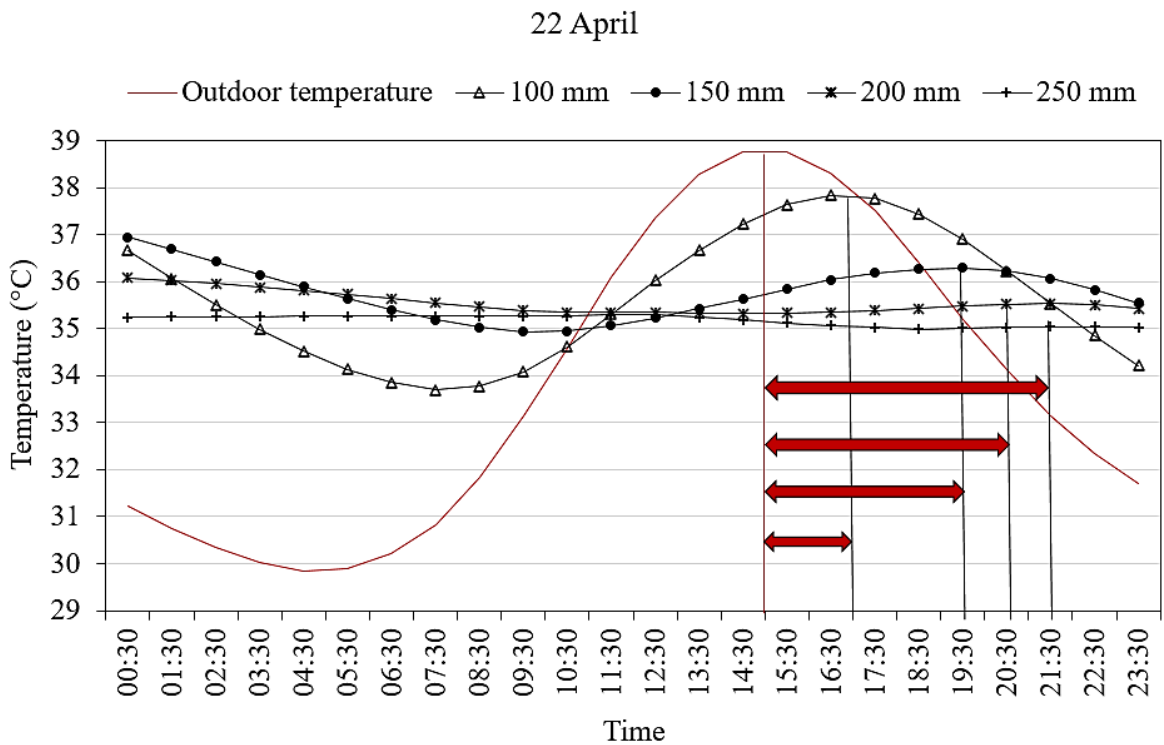
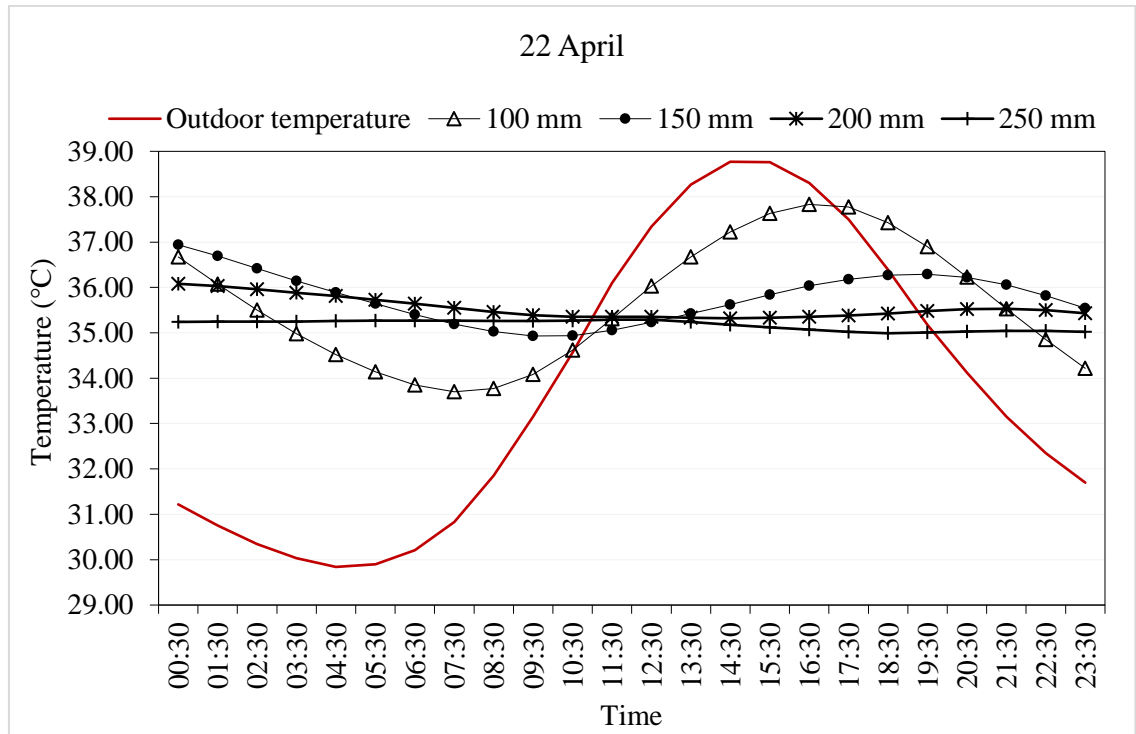
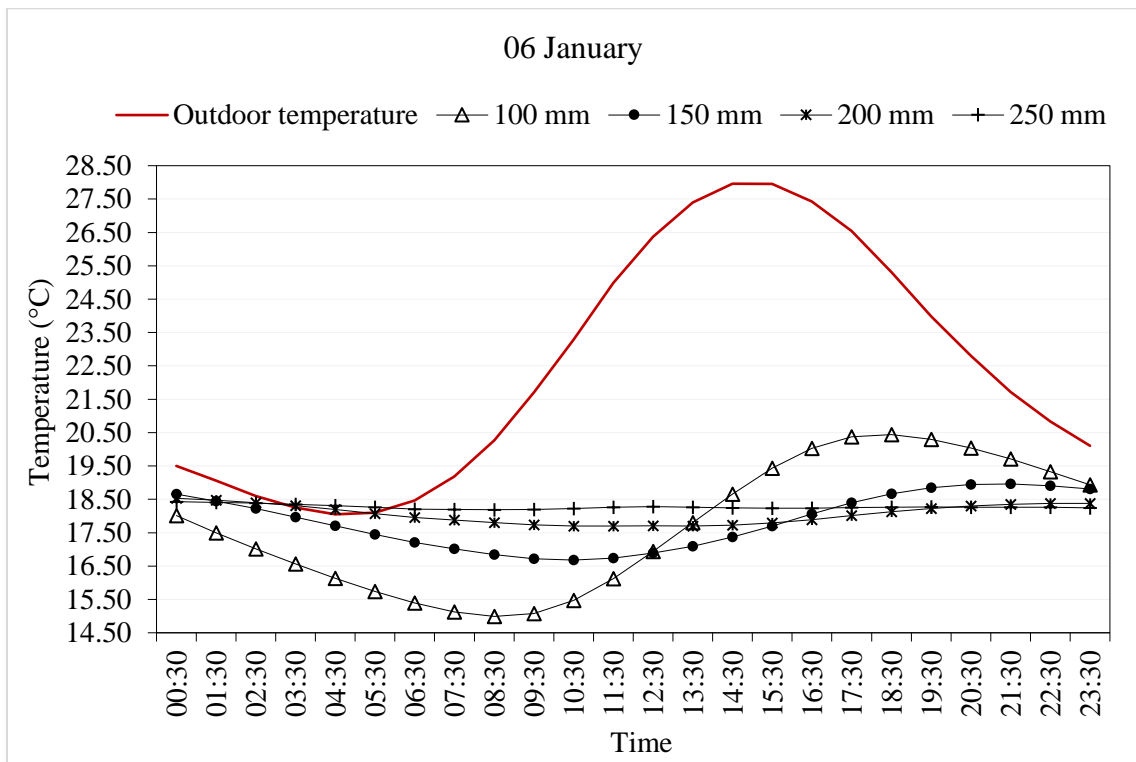


**Figure 7.7:** TL for different thicknesses of C-7.5 wall construction (summer day).



(a)



(b)

**Figure 7.8:** Outdoor and indoor temperatures for different thicknesses of C-7.5 wall construction: a) summer day and (b) winter day.

## 7.6 Summary of the Chapter

In this part of the study, numerical computer simulation was conducted to assess the dynamic thermal performance of the developed materials using IES-VE software. This section of the work presents the computer-based simulation of different wall materials under tropical climate conditions to understand in detail the dynamic thermal and energy performances of the wall materials. Although the models represented situations that were not under real building operation conditions, this approach was considered to accurately assess the thermal responses of the envelope wall materials.

The main conclusions that can be drawn from the simulation studies are as follows:

- The rate of heat transfer into the building highly depends on the thermophysical properties of the wall materials. It was observed that the material's capability to dampen the indoor temperature fluctuation is inversely proportional to the U-value and thermal diffusivity. The simulation results revealed that the coconut husk wall had the lowest decrement factor (0.46), followed by sawdust (0.47), eggshell (0.63), and reference (0.67) walls. Furthermore, compared to the reference (1.25 hours) and eggshell (1.50 hours) walls, the coconut husk and sawdust walls showed a longer (2 hours) time lag. Also, the yearly energy consumption of the coconut husk wall (14.90 MWh) was relatively lower than the sawdust (15.10 MWh), eggshell (17.70 MWh), and reference (18.90 MWh) walls.
- In addition, the analysis was extended by varying the thickness of the coconut husk wall. The results showed that with the increase in thickness, the decrement factor decreased from 0.46 to 0.03, whereas the time lag increased from 2 hours to 6.50 hours, indicating improved thermal resistance. Moreover, the yearly energy consumption decreased from 14.90 MWh to 10.50 MWh as wall thickness increased.

This simplified simulation approach may guide the designers in assessing the effects of various thermophysical properties of wall materials on indoor thermal comfort and energy efficiency of tropical buildings during the preliminary design process. It may also help to select the best solution for a building to match its functional requirements. For example, a wall with a high heat storage capacity but a low thermal diffusivity would be

ideal for spaces that are used for a long period, whereas a wall with a low heat storage capacity would be preferred for spaces that are used for a limited time in a day (Lotfabadi and Hançer, 2019).

## *Chapter 8*    **CONCLUSIONS AND FUTURE WORK**

### **8.1 Introduction**

This chapter summarises the research findings and limitations of the research as well as making some recommendations that can be considered important for future work.

### **8.2 Conclusions**

This research aims to utilise agro-wastes as an alternative raw material to enhance the performance of unfired clay blocks. Therefore, the results of this work would provide intriguing additional data to support the evaluation of the potential use of agro-wastes namely eggshell, sawdust, coconut husk, and walnut shell in the manufacturing of unfired clay blocks. Moreover, the utilisation of these agro-wastes in the production of sustainable construction materials would contribute to a feasible solution to the waste management problem. The study investigated the different properties of produced clay blocks with a focus on improving thermal comfort in tropical climates. The assessments were conducted using laboratory experiments and numerical computer thermal simulations. The following points are summarised based on the results of the laboratory experiments and numerical simulation work, which are directly related to the objectives of the study:

- The characterisation of different raw materials used for this research was presented in Chapter 3. Although the properties of the materials varied depending on their type, the findings indicated that these materials are suitable for producing clay blocks, as reported by several authors in Chapter 2. The findings revealed that eggshell had a high concentration of calcium oxide and other materials contained cellulose as the major element. Microscopic images showed that eggshell had irregular, stone-like shaped particles. On the other hand, coconut husk and sawdust had porous and rough surfaces, whereas walnut shell displayed a very rigid and thick structure.
- The results of the experimental studies on the physico-mechanical properties of agro-

wastes blended samples were described in Chapter 4. The results showed that when clay, eggshell, and water were mixed, cementitious compounds were formed as a result of the pozzolanic reaction of the clay minerals with the high calcium concentration in the eggshell, significantly enhancing the properties of the samples. However, there was no reaction when clay was mixed with sawdust, coconut husk, or walnut shell, limiting the benefits of their utilisation. Furthermore, it was also found that the walnut shell addition negatively influenced the strength of the samples.

- The tests for the durability properties of clay blocks were explained in Chapter 5. The findings demonstrated that the erosion resistance of the agro-wastes blended samples improved over the reference sample. The erosion rate decreased as the eggshell percentage increased in the mixture, while for other agro-wastes, increasing the content resulted in an increase in the erosion rate.
- The results of the experimental investigation on the thermal properties of agro-wastes incorporated clay blocks were reported in Chapter 6. The results indicated that as waste percentages increased, thermal conductivity values steadily decreased. Besides, coconut husk and sawdust samples had lower conductivity than eggshell samples. This may be attributed to the air-filled cellular porous structures of coconut husk and sawdust particles. Moreover, according to the test results of wall samples, the coconut husk wall had the highest thermal resistance, followed by the sawdust and eggshell walls, while the reference wall had the lowest resistance.
- The dynamic thermal simulation analyses were conducted to assess the thermal performance of wall materials under tropical climate conditions and provide additional support for laboratory thermal test results. The results of the simulation analyses were presented in Chapter 7. It was found that the thermal performance of building envelopes constructed with unfired earth blocks (of a given thickness) improved by reducing indoor temperature fluctuations and lowering total energy consumption due to the reduction in load. The simulation analyses were extended by altering wall thickness, where the results showed that the higher the wall thickness, the lower the fluctuations in the indoor temperature.

This study examined the properties of raw materials as well as the physico-mechanical,

durability, and thermal properties of produced clay blocks. The findings suggested that the incorporation of agro-wastes into clay blocks improved their properties, making them suitable for use as building construction material. The unfired clay blocks developed in this study can contribute to enhancing sustainability in building construction by addressing the three pillars of sustainable development (environmental, social, and economic). The simple production process of unfired clay blocks using local agro-waste materials offers low embodied energy, which lessens their environmental impact. Also, they are biodegradable and recyclable materials with a “cradle-to-cradle” life cycle. Apart from the environmental benefits, the utilisation of local resources provides socioeconomic benefits, such as cutting building costs and supporting local economies by paying for materials and labour locally.

### **8.3 Limitations of Research**

- This study experienced several disruptions during the time of investigation due to the COVID-19 pandemic. The inadequate supply of raw materials and restrictions on working hours had an impact on the sample number and size examined. In this study, for the evaluation of physico-mechanical properties, three prism samples (160 mm × 40 mm × 40 mm) were produced and tested for each mix composition. On the other hand, thermal and durability properties were examined by producing cube (100 mm × 100 mm × 100 mm) and full-scale brick samples (215 mm × 102 mm × 65 mm). The tested samples for thermal and durability properties were two and one, respectively. However, in most of the previous studies, it was recommended that larger scale sample manufacturing and at least three samples be tested to obtain satisfactory results.
- Moreover, only sawdust was investigated for different particle sizes, and other materials were not considered because of their limited supply.
- Furthermore, due to time and resource constraints, it was not possible to conduct the in-situ measurement of the thermal performance of the materials.

## 8.4 Future Work

Though this present study investigated several properties related to unfired clay block production incorporating agro-wastes, there is still a lot of work to be done in this area. Following are some recommendations for further research based on this present study:

- The hand compaction procedure was employed in this study to imitate the traditional rural brick-making process. However, higher strength levels are likely to be obtained by further enhancing the sample density (Dormohamadi and Rahimnia, 2020). Therefore, mechanical compaction in a controlled manner without affecting the thermal properties of the samples may be investigated. Furthermore, future research can investigate the properties of agro-wastes stabilised samples using different types of clay or soil.
- In this work, small walls were tested in the laboratory to determine the thermal characteristics of ago-wastes stabilised unfired clay blocks. In addition, computer simulations were run under dynamic weather conditions to evaluate their thermal performance. Future research might employ in-situ performance measurement of wall materials to arrive at a more realistic conclusion.
- Along with thermal comfort, indoor air quality is another key element of IEQ, which is directly related to the occupants' health. Under suitable environmental conditions, mold may grow on biological material, and mold development should be prevented since its emissions can cause health concerns. Mold and fungus are more likely to grow if the material's surface is moist and humid. In tropical climates, high humidity is one of the common features, resulting from the huge amount of rain. Therefore, it is necessary to undertake a mold growth investigation in agro-wastes blended samples to thoroughly analyse the IEQ in this region.
- The environmental effects of agro-wastes stabilised unfired clay blocks, such as life cycle, carbon emissions, and embodied energy might be investigated since these are among the most important factors to consider when evaluating the environmental performance of the building. Additionally, the cost of manufacturing the agro-wastes incorporated unfired clay blocks may be evaluated.

---

## References

---

- Aarcha, S., Ameena Shirin, N.S., Suryalekshmi, K.S., Rasheed, T. and Harindranath, S. (2019) Partial Replacement of Cement with Brick Powder and Egg Shell Powder in Concrete. *International Journal of Innovative Research in Science, Engineering and Technology*, 8 (6). [http://www.ijirset.com/upload/2019/june/38\\_Partial.pdf](http://www.ijirset.com/upload/2019/june/38_Partial.pdf)
- Abanto, G.A., Karkri, M., Lefebvre, G., Horn, M., Solis, J.L. and Gómez, M.M. (2017) Thermal properties of adobe employed in Peruvian rural areas: Experimental results and numerical simulation of a traditional bio-composite material. *Case Studies in Construction Materials*, 6, 177-191. <https://doi.org/10.1016/j.cscm.2017.02.001>
- Abid, R., Kamoun, N., Jamoussi, F. and El Feki, H. (2021) Fabrication and properties of compressed earth brick from local Tunisian raw materials. *Boletín de la Sociedad Española de Cerámica y Vidrio*. <https://doi.org/10.1016/j.bsecv.2021.02.001>
- ABNT-NBR 8492 (1984) *Tijolo maciço de solo-cimento-Determinação da resistência à compressão e da absorção de água (Massive earth cement bricks-determination of compressive strength and water absorption)[in Portuguese]*. Rio de Janeiro, Brazil: Brazilian National Standards Organization.
- Achenza, M. and Fenu, L. (2006) On earth stabilization with natural polymers for earth masonry construction. *Materials and Structures*, 39 (1), 21-27. <https://doi.org/10.1617/s11527-005-9000-0>
- Adamczyk, J. and Dylewski, R. (2017) The impact of thermal insulation investments on sustainability in the construction sector. *Renewable and Sustainable Energy Reviews*, 80, 421-429. <https://doi.org/10.1016/j.rser.2017.05.173>
- Adogla, F., Yalley, P.P.K. and Arkoh, M. (2016) Improving compressed laterite bricks using powdered eggshells. *The International Journal of Engineering and Science (IJES)*, 5 (4), 65-70. <http://www.theijes.com/papers/v5-i4/K0504071075.pdf>
- Afolayan, J.O., Oriola, F.O.P., Moses, G. and Sani, J.E. (2017) Investigating the effect of eggshell ash on the properties of sandcrete block. *International Journal of Civil Engineering, Construction and Estate Management*, 5 (3), 43-54. <https://www.eajournals.org/wp-content/uploads/Investigating-the-Effect-of-Eggshell-Ash-on-the-Properties-of-Sandcrete-Block.pdf>
- Agamuthu, P. (2009) *Challenges and opportunities in agro-waste management: An Asian perspective. Inaugural meeting of first regional 3R forum in Asia*: 11-12.
- Ahmad, J., Majdi, A., Al-Fakih, A., Deifalla, A.F., Althoey, F., El Ouni, M.H. and El-Shorbagy, M.A. (2022) Mechanical and Durability Performance of Coconut Fiber Reinforced Concrete: A State-of-the-Art Review. *Materials*, 15 (10), 3601. <https://doi.org/10.3390/ma15103601>
- Ajala, E.O., Eletta, O.A.A., Ajala, M.A. and Oyeniyi, S.K. (2018) Characterization and evaluation of chicken eggshell for use as a bio-resource. *Arid Zone Journal of Engineering, Technology and Environment*, 14 (1), 26-40. <https://www.azojete.com.ng/index.php/azojete/article/view/95>
- Akhtar, K., Khan, S.A., Khan, S.B. and Asiri, A.M. (2018) Scanning electron microscopy: principle and applications in nanomaterials characterization. In: Sharma, S. K. (ed.) *Handbook of Materials Characterization*. 1st ed. Switzerland: Springer International Publishing. pp. 113-145.
- Akhzouz, H., El Minor, H., Tatane, M. and Bendarma, A. (2021) Physical characterization of bio-composite CEB stabilized with Argan nut shell and cement. *Materials Today: Proceedings*, 36, 107-114. <https://doi.org/10.1016/j.matpr.2020.05.522>
- Akinyemi, A.B., Afolayan, J.O. and Oluwatobi, E.O. (2016) Some properties of composite corn cob and sawdust particle boards. *Construction and Building Materials*, 127, 436-441. <https://doi.org/10.1016/j.conbuildmat.2016.10.040>
- Al-Fakih, A., Mohammed, B.S., Liew, M.S. and Nikbakht, E. (2019) Incorporation of waste materials in

the manufacture of masonry bricks: An update review. *Journal of Building Engineering*, 21, 37-54. <https://doi.org/10.1016/j.jobe.2018.09.023>

Ali, M., Liu, A., Sou, H. and Chou, N. (2012) Mechanical and dynamic properties of coconut fibre reinforced concrete. *Construction and Building Materials*, 30, 814-825. <https://doi.org/10.1016/j.conbuildmat.2011.12.068>

Alzaidy, M.N.J. (2019) Experimental study for stabilizing clayey soil with eggshell powder and plastic wastes. *IOP Conference Series: Materials Science and Engineering*, 518 (2). <https://doi.org/10.1088/1757-899X/518/2/022008>

Amaral, M.C., Siqueira, F.B., Destefani, A.Z. and Holanda, J.N.F. (2013) Soil–cement bricks incorporated with eggshell waste. *Proceedings of the Institution of Civil Engineers-Waste and Resource Management*, 166 (3), 137-141. <https://doi.org/10.1680/warm.12.00024>

Amaral, R.E.C., Brito, J., Buckman, M., Drake, E., Ilatova, E., Rice, P., Sabbagh, C., Voronkin, S. and Abraham, Y.S. (2020) Waste management and operational energy for sustainable buildings: a review. *Sustainability*, 12 (13). <https://doi.org/10.3390/su12135337>

Amina, L.B., Joshua, A.A. and Musa, L.S. (2018) Enhancing the Thermophysical Properties of Rammed Earth by Stabilizing with Corn Husk Ash. In: Sayigh, A. (ed.) *Sustainable Building for a Cleaner Environment*. Switzerland: Springer International Publishing, pp. 405-413.

Amu, O.O., Fajobi, A.B. and Oke, B.O. (2005) Effect of eggshell powder on the stabilizing potential of lime on an expansive clay soil. *Research Journal of Agriculture and Biological Sciences*, 1 (1), 80-84. <http://www.aensiweb.net/AENSIWEB/rjabs/rjabs/80-84.pdf>

Amziane, S. and Sonebi, M. (2016) Overview on Biobased Building Material made with plant aggregate. *RILEM Technical Letters*, 1, 31-38. <https://doi.org/10.21809/rilemtechlett.2016.9>

Andelković, B.V., Stojanović, B.V., Stojiljković, M.M., Janevski, J.N. and Stojanović, M.B. (2012) Thermal mass impact on energy performance of a low, medium and heavy mass building in Belgrade. *Thermal Science*, 16 (suppl. 2), 447-459. <https://doi.org/10.2298/TSCI120409182A>

Antreich, S.J., Xiao, N., Huss, J.C., Horbelt, N., Eder, M., Weinkamer, R. and Gierlinger, N. (2019) The Puzzle of the Walnut Shell: A Novel Cell Type with Interlocked Packing. *Advanced Science*, 6 (16). <https://doi.org/10.1002/advs.201900644>

Anysz, H. and Narloch, P. (2019) Designing the composition of cement stabilized rammed earth using artificial neural networks. *Materials*, 12 (9). <https://doi.org/10.3390/ma12091396>

Aprianti S, E. (2017) A huge number of artificial waste material can be supplementary cementitious material (SCM) for concrete production—a review part II. *Journal of Cleaner Production*, 142, 4178-4194. <https://doi.org/10.1016/j.jclepro.2015.12.115>

Aramide, F.O. (2012) Production and characterization of porous insulating fired bricks from Ifon clay with varied sawdust admixture. *Journal of Minerals and Materials Characterization and Engineering*, 11 (10), 970-975. <https://doi.org/10.4236/jmmce.2012.1110097>

Araya-Letelier, G., Antico, F., Burbano-Garcia, C., Concha-Riedel, J., Norambuena-Contreras, J., Concha, J. and Flores, E.S. (2021) Experimental evaluation of adobe mixtures reinforced with jute fibers. *Construction and Building Materials*, 276. <https://doi.org/10.1016/j.conbuildmat.2020.122127>

Araya-Letelier, G., Concha-Riedel, J., Antico, F.C., Valdés, C. and Cáceres, G. (2018) Influence of natural fiber dosage and length on adobe mixes damage-mechanical behavior. *Construction and Building Materials*, 174, 645-655. <https://doi.org/10.1016/j.conbuildmat.2018.04.151>

Arooz, F.R. and Halwatura, R.U. (2018) Mud-concrete block (MCB): mix design & durability characteristics. *Case Studies in Construction Materials*, 8, 39-50. <https://doi.org/10.1016/j.cscm.2017.12.004>

Arzate-Vázquez, I., Méndez-Méndez, J.V., Flores-Johnson, E.A., Nicolás-Bermúdez, J., Chanona-Pérez, J.J. and Santiago-Cortés, E. (2019) Study of the porosity of calcified chicken eggshell using atomic force microscopy and image processing. *Micron*, 118, 50-57. <https://doi.org/10.1016/j.micron.2018.12.008>

Asan, H. (2006) Numerical computation of time lags and decrement factors for different building materials. *Building and Environment*, 41, 615-620. <https://doi.org/10.1016/j.buildenv.2005.02.020>

Asasutjarit, C., Hirunlabh, J., Khedari, J., Charoenvai, S., Zeghmati, B. and Shin, U.C. (2007) Development of coconut coir-based lightweight cement board. *Construction and Building Materials*, 21 (2), 277-288. <https://doi.org/10.1016/j.conbuildmat.2005.08.028>

Ascione, F., Bianco, N., De Masi, R.F., Mauro, G.M. and Vanoli, G.P. (2015) Design of the building envelope: A novel multi-objective approach for the optimization of energy performance and thermal comfort. *Sustainability*, 7 (8), 10809-10836. <https://doi.org/10.3390/su70810809>

Asdrubali, F. and Baldinelli, G. (2011) Thermal transmittance measurements with the hot box method: Calibration, experimental procedures, and uncertainty analyses of three different approaches. *Energy and Buildings*, 43 (7), 1618-1626. <https://doi.org/10.1016/j.enbuild.2011.03.005>

Ashiq, P.T. and Kumar, A. (2019) Experimental Investigation of Bricks Using Lithomargic Clay, Fly Ash and Egg Shells and Cement Blocks with Egg Shells. *International Journal of Scientific & Engineering Research*, 10 (3). <https://www.ijser.org/researchpaper/EXPERIMENTAL-INVESITIGATION-OF-BRICKS-USING-LITHOMARGIC-CLAY-FLY-ASH-AND-EGG-SHELLS-AND-CEMENT-BLOCKS-WITH-EGG-SHELLS.pdf>

Ashour, T., Korjenic, A., Korjenic, S. and Wu, W. (2015) Thermal conductivity of unfired earth bricks reinforced by agricultural wastes with cement and gypsum. *Energy and Buildings*, 104, 139-146. <https://doi.org/10.1016/j.enbuild.2015.07.016>

ASHRAE Standard 55 (2010) *Thermal environmental conditions for human occupancy*. Atlanta: American Society of Heating, Refrigerating and Air Conditioning Engineers.

ASTM C62 (2005) *Standard Specification for Building Brick (Solid Masonry Units Made From Clay or Shale)*. West Conshohocken, PA: ASTM International.

ASTM C618-9 (2005) *Standard Specification for Coal Fly Ash and Raw or Calcined Natural Pozzolan for Use in Concrete*. West Conshohocken, PA: ASTM International.

ASTM D422-63 (2002) *Standard Test Method for Particle-Size Analysis of Soils*. West Conshohocken, PA: ASTM International.

ASTM D698 (2012) *Standard Test Methods for Laboratory Compaction Characteristics of Soil Using Standard Effort (12,400 ft-lbf/ft<sup>3</sup> (600 kN-m/m<sup>3</sup>))*. West Conshohocken, PA: ASTM International.

ASTM D5334 (2008) *Standard Test Method for determination of thermal conductivity of soil and soft rock by thermal needle probe procedure*. West Conshohocken, PA: ASTM International.

Atiki, E., Taallah, B., Feia, S., Almeasar, K.S. and Guettala, A. (2021) Effects of Incorporating Date Palm Waste as a Thermal Insulating Material on the Physical Properties and Mechanical Behavior of Compressed Earth Block. *Journal of Natural Fibers*, 1-18. <https://doi.org/10.1080/15440478.2021.1967831>

Atoyebi, O.D., Ajamu, S.O., Odeyemi, S.O., Ojo, D.J. and Ramonu, J.A.L. (2021) Strength Evaluation of Aluminium Fibre Reinforced Particle Board made from Sawdust and Waste Glass. *IOP Conference Series: Materials Science and Engineering*, 1036. <https://doi.org/10.1088/1757-899X/1036/1/01204>

Auroville Earth Institute. (2009) *Building with Earth, Technique Overview* [online] Available at: [http://www.earthauroville.com/world\\_techniques\\_introduction\\_en.php](http://www.earthauroville.com/world_techniques_introduction_en.php) [Accessed: 10 January 2021]

- Ayodele, A.L., Oketope, O.M. and Olatunde, O.S. (2019) Effect of sawdust ash and eggshell ash on selected engineering properties of lateralized bricks for low cost housing. *Nigerian Journal of Technology*, 38 (2), 278-282. <https://doi.org/10.4314/njt.v38i2.1>
- Ayrilmis, N., Kaymakci, A. and Ozdemir, F. (2013) Physical, mechanical, and thermal properties of polypropylene composites filled with walnut shell flour. *Journal of Industrial and Engineering Chemistry*, 19 (3), 908-914. <https://doi.org/10.1016/j.jiec.2012.11.006>
- Azhar, S., Carlton, W.A., Olsen, D. and Ahmad, I. (2011) Building information modeling for sustainable design and LEED® rating analysis. *Automation in Construction*, 20 (2), 217-224. <https://doi.org/10.1016/j.autcon.2010.09.019>
- Babé, C., Kidmo, D.K., Tom, A., Mvondo, R.R.N., Boum, R.B.E. and Djongyang, N. (2020) Thermomechanical characterization and durability of adobes reinforced with millet waste fibers (sorghum bicolor). *Case Studies in Construction Materials*, 13. <https://doi.org/10.1016/j.cscm.2020.e00422>
- Babé, C., Kidmo, D.K., Tom, A., Mvondo, R.R.N., Kola, B. and Djongyang, N. (2021) Effect of neem (Azadirachta Indica) fibers on mechanical, thermal and durability properties of adobe bricks. *Energy Reports*, 7, 686-698. <https://doi.org/10.1016/j.egypr.2021.07.085>
- Badea, N. (2015) *Design for micro-combined cooling, heating and power systems: Stirling engines and renewable power systems*. London: Springer London.
- Baiden, B.K. and Asante, C.K.O. (2004) Effects of orientation and compaction methods of manufacture on strength properties of sandcrete blocks. *Construction and Building Materials*, 18 (10), 717-725. <https://doi.org/10.1016/j.conbuildmat.2004.04.032>
- Bangladesh Meteorological Department. (2018) [online] Available at: [www.bmd.gov.bd](http://www.bmd.gov.bd) [Accessed: 22 May 2021]
- Barcelo, L., Kline, J., Walenta, G. and Gartner, E. (2014) Cement and carbon emissions. *Materials and Structures*, 47 (6), 1055-1065. <https://doi.org/10.1617/s11527-013-0114-5>
- Ben, H. and Steemers, K. (2014) Energy retrofit and occupant behaviour in protected housing: A case study of the Brunswick Centre in London. *Energy and Buildings*, 80, 120-130. <https://doi.org/10.1016/j.enbuild.2014.05.019>
- Benkhadda, N. and Khaldoun, A. (2019) *Effective Unfired Clay Bricks with Natural Additives*, Al Akhawayn University, Morocco. <http://www.aui.ma/sse-capstone-repository/pdf/spring-2019/UNFIRED%20CLAY%20BRICKS%20WITH%20ADDITIVES-WOOL.pdf>.
- Benslimane, N. and Biara, R.W. (2019) The urban sustainable structure of the vernacular city and its modern transformation: A case study of the popular architecture in the saharian Region. *Energy Procedia*, 157, 1241-1252. <https://doi.org/10.1016/j.egypro.2018.11.290>
- Bhuvaneshwari, S., Thyagaraj, T., Robinson, R.G. and Gandhi, S.R. (2010) Alternative Technique to Induce Faster Lime Stabilization Reaction in Deeper Expansive Strata. *Indian Geotechnical Conference (IGC-2010)*, Mumbai, India, December 16-18.
- Binici, H., Aksogan, O. and Shah, T. (2005) Investigation of fibre reinforced mud brick as a building material. *Construction and Building Materials*, 19 (4), 313-318. <https://doi.org/10.1016/j.conbuildmat.2004.07.013>
- Blondet, M. and Garcia, G.V. (2004) Earthquake resistant earthen buildings. *13th World Conference on Earthquake Engineering* Vancouver, B.C., Canada, August 1-6.
- Borrelli, E. (1999) Porosity. In: (ed.) *Conservation of Architectural Heritage, Historic Structures and Materials*. Rome, Italy: Rome : ICCROM.

Bouhicha, M., Aouissi, F. and Kenai, S. (2005) Performance of composite soil reinforced with barley straw. *Cement and Concrete Composites*, 27 (5), 617-621. <https://doi.org/10.1016/j.cemconcomp.2004.09.013>

Braham, D., Barnard, N. and Jaunzens, D. (2001) *BRE Digest 454 Part 1: Thermal mass in office buildings: An introduction*. Bracknell, UK: Building Research Establishment.

Broitman, D., Raviv, O., Ayalon, O. and Kan, I. (2018) Designing an agricultural vegetative waste-management system under uncertain prices of treatment-technology output products. *Waste Management*, 75, 37-43. <https://doi.org/10.1016/j.wasman.2018.01.041>

Brundtland, G.H. (1987) *Our Common Future: Report of the World Commission on Environment and Development* [online]

Available at: [https://gat04-live-1517c8a4486c41609369c68f30c8-aa81074.divio-media.org/filer\\_public/6f/85/6f854236-56ab-4b42-810f-606d215c0499/cd\\_9127\\_extract\\_from\\_our\\_common\\_future\\_brundtland\\_report\\_1987\\_foreword\\_chpt\\_2.pdf](https://gat04-live-1517c8a4486c41609369c68f30c8-aa81074.divio-media.org/filer_public/6f/85/6f854236-56ab-4b42-810f-606d215c0499/cd_9127_extract_from_our_common_future_brundtland_report_1987_foreword_chpt_2.pdf)  
[Accessed: 12 April 2021]

Brunklaus, B. and Riise, E. (2018) Bio-based Materials Within the Circular Economy: Opportunities and Challenges. In: Benetto, E., Gericke, K. and Guiton, M. (ed.) *Designing Sustainable Technologies, Products and Policies*. Switzerland: Springer Nature. pp. 43-47.

Bruno, A.W., Gallipoli, D., Perlot, C. and Kallel, H. (2020) Thermal performance of fired and unfired earth bricks walls. *Journal of Building Engineering*, 28. <https://doi.org/10.1016/j.jobe.2019.101017>

BS 1377-2 (1990) *Methods of test for soils for civil engineering purpose-Part 2: Classification Tests*. London: British Standards Institution.

BS EN 771-1 (2003) *Specification for masonry units-Part 1: Clay masonry units*. London: British Standards Institution.

BS EN 772-14 (2002) *Methods of test for masonry units-Part 14: Determination of moisture movement of aggregate concrete and manufactured stone masonry units*. London: British Standards Institution.

BS EN 1015-18 (2002) *Methods of test for mortar for masonry-Part 18: Determination of water absorption coefficient due to capillary action of hardened mortar*. London: British Standards Institution.

BS EN 1015-11 (2019) *Methods of test for mortar for masonry-Part 11: Determination of flexural and compressive strength of hardened mortar*. London: British Standards Institution.

BS EN 1097-6 (2013) *Tests for mechanical and physical properties of aggregates. Determination of particle density and water absorption*. London: British Standards Institution.

BS EN ISO 6946 (2017) *Building components and building elements-Thermal resistance and thermal transmittance-Calculation methods*. London: British Standards Institution.

BS ISO 9869-1 (2014) *Thermal insulation-Building elements-In-situ measurement of thermal resistance and thermal transmittance-Part 1: Heat flow meter method*. London: British Standards Institution.

Buratti, C., Belloni, E., Lunghi, L., Borri, A., Castori, G. and Corradi, M. (2016) Mechanical characterization and thermal conductivity measurements using of a new 'small hot-box' apparatus: innovative insulating reinforced coatings analysis. *Journal of Building Engineering*, 7, 63-70. <https://doi.org/10.1016/j.jobe.2016.05.005>

Cabeza, L.F., Barreneche, C., Miro, L., Martínez, M., Fernandez, A.I. and Urge-Vorsatz, D. (2013) Affordable construction towards sustainable buildings: review on embodied energy in building materials. *Current Opinion in Environmental Sustainability*, 5 (2), 229-236. <https://doi.org/10.1016/j.cosust.2013.05.005>

- Callejas, I.J.A., Durante, L.C. and Oliveira, A.S.D. (2017) Thermal resistance and conductivity of recycled construction and demolition waste (RCDW) concrete blocks. *REM-International Engineering Journal*, 70 (2), 167-173. <https://doi.org/10.1590/0370-44672015700048>
- Carlile, W.R., Raviv, M. and Prasad, M. (2019) Organic Soilless Media Components. In: Raviv, M., Lieth, H. and Bar-Tal, A. (ed.) *Soilless Culture: Theory and Practice*. 2nd ed.: Academic Press. pp. 303-378.
- Chambers, J.R., Zaheer, K., Akhtar, H. and Abdel-Aal, E.-S.M. (2017) Chicken eggs. In: Hester, P. Y. (ed.) *Egg Innovations and Strategies for Improvements*. Academic press. pp. 1-9.
- Chan, C.-M. (2011) Effect of natural fibres inclusion in clay bricks: Physico-mechanical properties. *International Journal of Civil and Environmental Engineering*, 3 (1), 51-57. <https://citeseerx.ist.psu.edu/viewdoc/download?doi=10.1.1.1082.1024&rep=rep1&type=pdf>
- Charai, M., Mezrhab, A. and Moga, L. (2022) A structural wall incorporating biosourced earth for summer thermal comfort improvement: Hygrothermal characterization and building simulation using calibrated PMV-PPD model. *Building and Environment*, 212. <https://doi.org/10.1016/j.buildenv.2022.108842>
- Charai, M., Sghiouri, H., Mezrhab, A., Karkri, M., Elhammouti, K. and Nasri, H. (2020) Thermal performance and characterization of a sawdust-clay composite material. *Procedia Manufacturing*, 46, 690-697. <https://doi.org/10.1016/j.promfg.2020.03.098>
- Charis, G., Danha, G. and Muzenda, E. (2019) A review of timber waste utilization: Challenges and opportunities in Zimbabwe. *Procedia Manufacturing*, 35, 419-429. <https://doi.org/10.1016/j.promfg.2019.07.005>
- Chastas, P., Theodosiou, T. and Bikas, D. (2016) Embodied energy in residential buildings-towards the nearly zero energy building: A literature review. *Building and Environment*, 105, 267-282. <https://doi.org/10.1016/j.buildenv.2016.05.040>
- Chauhan, P., El Hajjar, A., Prime, N. and Plé, O. (2019) Unsaturated behavior of rammed earth: Experimentation towards numerical modelling. *Construction and Building Materials*, 227. <https://doi.org/10.1016/j.conbuildmat.2019.08.027>
- Chel, A. and Kaushik, G. (2018) Renewable energy technologies for sustainable development of energy efficient building. *Alexandria Engineering Journal*, 57 (2), 655-669. <https://doi.org/10.1016/j.aej.2017.02.027>
- Chemani, B. and Chemani, H. (2012) Effect of adding sawdust on mechanical-physical properties of ceramic bricks to obtain lightweight building material. *International Journal of Mechanical, Aerospace, Industrial, Mechatronic and Manufacturing Engineering*, 6 (11), 2521-2525. <https://doi.org/10.5281/zenodo.1077395>
- Chemani, H. and Chemani, B. (2013) Valorization of wood sawdust in making porous clay brick. *Scientific Research and Essays*, 8 (15), 609-614. <https://doi.org/10.5897/SRE12.608>
- Chen, X., Li, X., He, Z., Hou, Z., Xu, G., Yang, N. and Zheng, J. (2019) Comparative study of eggshell antibacterial effectivity in precocial and altricial birds using *Escherichia coli*. *PloS One*, 14 (7). <https://doi.org/10.1371/journal.pone.0220054>
- Cheng, W., Liu, G. and Chen, L. (2017) Pet Fiber Reinforced Wet-Mix Shotcrete with Walnut Shell as Replaced Aggregate. *Applied Sciences*, 7 (4), 345. <https://doi.org/10.3390/app7040345>
- Choi, D.S. and Ko, M.J. (2019) Analysis of Convergence Characteristics of Average Method Regulated by ISO 9869-1 for Evaluating In Situ Thermal Resistance and Thermal Transmittance of Opaque Exterior Walls. *Energies*, 12 (10). <https://doi.org/10.3390/en12101989>

- Chowdhury, D. and Neogi, S. (2019) Thermal performance evaluation of traditional walls and roof used in tropical climate using guarded hot box. *Construction and Building Materials*, 218, 73-89. <https://doi.org/10.1016/j.conbuildmat.2019.05.032>
- Chowdhury, S., Ahmed, K.S. and Hamada, Y. (2015) Thermal performance of building envelope of ready-made garments (RMG) factories in Dhaka, Bangladesh. *Energy and Buildings*, 107, 144-154. <https://doi.org/10.1016/j.enbuild.2015.08.014>
- Chung, L.L.P., Wong, Y.C. and Arulrajah, A. (2021) The Application of Spent Coffee Grounds and Tea Wastes as Additives in Alkali-Activated Bricks. *Waste and Biomass Valorization*, 12, 6273–6291. <https://doi.org/10.1007/s12649-021-01453-7>
- Cid-Falceto, J., Mazarrón, F.R. and Cañas, I. (2012) Assessment of compressed earth blocks made in Spain: International durability tests. *Construction and Building Materials*, 37, 738-745. <https://doi.org/10.1016/j.conbuildmat.2012.08.019>
- CID-GCBNMBC-91-1 (1991) *New Mexico Adobe and Rammed Earth Building Code*. Santa Fe, New Mexico: General Construction Bureau, Regulation & Licensing Department.
- Corasaniti, S., Potenza, M., Coppa, P. and Bovesecchi, G. (2020) Comparison of different approaches to evaluate the equivalent thermal diffusivity of building walls under dynamic conditions. *International Journal of Thermal Sciences*, 150. <https://doi.org/10.1016/j.ijthermalsci.2019.106232>
- Costa, C., Cerqueira, Â., Rocha, F. and Velosa, A. (2018) The sustainability of adobe construction: past to future. *International Journal of Architectural Heritage*, 13 (5). <https://doi.org/10.1080/15583058.2018.1459954>
- Cultrone, G., Aurrekoetxea, I., Casado, C. and Arizzi, A. (2020) Sawdust recycling in the production of lightweight bricks: How the amount of additive and the firing temperature influence the physical properties of the bricks. *Construction and Building Materials*, 235. <https://doi.org/10.1016/j.conbuildmat.2019.117436>
- Członka, S., Strąkowska, A. and Kairytė, A. (2020) Effect of walnut shells and silanized walnut shells on the mechanical and thermal properties of rigid polyurethane foams. *Polymer Testing*, 87. <https://doi.org/10.1016/j.polymertesting.2020.106534>
- Da Silva, C.F., Stefanowski, B., Maskell, D., Ormondroyd, G.A., Ansell, M.P., Dengel, A.C. and Ball, R.J. (2017) Improvement of indoor air quality by MDF panels containing walnut shells. *Building and Environment*, 123, 427-436. <https://doi.org/10.1016/j.buildenv.2017.07.015>
- Danja, I.I., Li, X. and Dalibi, S.G. (2017) Vernacular architecture of northern Nigeria in the light of sustainability. *IOP Conference Series: Earth and Environmental Science*, 63. <https://doi.org/10.1088/1755-1315/63/1/012034>
- Danso, H. (2016) Influence of compacting rate on the properties of compressed earth blocks. *Advances in Materials Science and Engineering*, 2016. <https://doi.org/10.1155/2016/8780368>
- Danso, H. (2017) Improving water resistance of compressed earth blocks enhanced with different natural fibres. *The Open Construction & Building Technology Journal*, 11 (1). <https://doi.org/10.2174/1874836801711010433>
- Danso, H., Martinson, B., Ali, M. and Mant, C. (2015a) Performance characteristics of enhanced soil blocks: a quantitative review. *Building Research & Information*, 43 (2), 253-262. <https://doi.org/10.1080/09613218.2014.933293>
- Danso, H., Martinson, D.B., Ali, M. and Williams, J.B. (2015b) Physical, mechanical and durability properties of soil building blocks reinforced with natural fibres. *Construction and Building Materials*, 101, 797-809. <https://doi.org/10.1016/j.conbuildmat.2015.10.069>
- Day, T., Doige, C. and Young, J. (2010) The concept of 'heat' in physical geography. *Geography*, 95 (1),

33-37. <https://doi.org/10.1080/00167487.2010.12094280>

Dayaratne, R. (2018) Toward sustainable development: Lessons from vernacular settlements of Sri Lanka. *Frontiers of Architectural Research*, 7 (3), 334-346. <https://doi.org/10.1016/j.foar.2018.04.002>

De Castrillo, M.C., Ioannou, I. and Philokyprou, M. (2021) Reproduction of traditional adobes using varying percentage contents of straw and sawdust. *Construction and Building Materials*, 294. <https://doi.org/10.1016/j.conbuildmat.2021.123516>

Demezhko, D.Y. (2011) Measurements of the thermal effusivity of solid materials by the contact method. *Instruments and Experimental Techniques*, 54 (6), 867-871. <https://link.springer.com/content/pdf/10.1134/S0020441211050113.pdf>

Demir, I. (2006) An investigation on the production of construction brick with processed waste tea. *Building and Environment*, 41 (9), 1274-1278. <https://doi.org/10.1016/j.buildenv.2005.05.004>

Demir, I. (2008) Effect of organic residues addition on the technological properties of clay bricks. *Waste Management*, 28 (3), 622-627. <https://doi.org/10.1016/j.wasman.2007.03.019>

Ding, G.K.C. (2014) Life cycle assessment (LCA) of sustainable building materials: an overview. *Eco-efficient Construction and Building Materials*, 38-62. <https://doi.org/10.1533/9780857097729.1.38>

Dixit, M.K., Culp, C.H. and Fernández-Solís, J.L. (2013) System boundary for embodied energy in buildings: A conceptual model for definition. *Renewable and Sustainable Energy Reviews*, 21, 153-164. <https://doi.org/10.1016/j.rser.2012.12.037>

Dixit, M.K., Fernández-Solís, J.L., Lavy, S. and Culp, C.H. (2010) Identification of parameters for embodied energy measurement: A literature review. *Energy and Buildings*, 42 (8), 1238-1247. <https://doi.org/10.1016/j.enbuild.2010.02.016>

Dong, X., Soebarto, V. and Griffith, M. (2015) Design optimization of insulated cavity rammed earth walls for houses in Australia. *Energy and Buildings*, 86, 852-863. <https://doi.org/10.1016/j.enbuild.2014.11.014>

Douzane, O., Promis, G., Roucoult, J.M., Le, A.D.T. and Langlet, T. (2016) Hygrothermal performance of a straw bale building: In situ and laboratory investigations. *Journal of Building Engineering*, 8, 91-98. <https://doi.org/10.1016/j.jobe.2016.10.002>

Dove, C. (2014) The development of unfired earth bricks using seaweed biopolymers. In: Brebbia, C. A. and Pulselli, R. M. (ed.) *Eco-Architecture V: Harmonisation between Architecture and Nature*. UK: WIT Press. pp. 219-230.

El Azhary, K., Chihab, Y., Mansour, M., Laaroussi, N. and Garoum, M. (2017) Energy efficiency and thermal properties of the composite material clay-straw. *Energy Procedia*, 141, 160-164. <https://doi.org/10.1016/j.egypro.2017.11.030>

El Fgaier, F., Lafhaj, Z., Antczak, E. and Chapiseau, C. (2016) Dynamic thermal performance of three types of unfired earth bricks. *Applied Thermal Engineering*, 93, 377-383. <https://doi.org/10.1016/j.applthermaleng.2015.09.009>

El Fgaier, F., Lafhaj, Z., Brachelet, F., Antczak, E. and Chapiseau, C. (2015) Thermal performance of unfired clay bricks used in construction in the north of France: Case study. *Case Studies in Construction Materials*, 3, 102-111. <https://doi.org/10.1016/j.cscm.2015.09.001>

Eslami, A., Mohammadi, H. and Banadaki, H.M. (2022) Palm fiber as a natural reinforcement for improving the properties of traditional adobe bricks. *Construction and Building Materials*, 325. <https://doi.org/10.1016/j.conbuildmat.2022.126808>

Evangelisti, L., Guattari, C., Gori, P. and Vollaro, R.D.L. (2015) In situ thermal transmittance measurements for investigating differences between wall models and actual building performance.

*Sustainability*, 7 (8), 10388-10398. <https://doi.org/10.3390/su70810388>

Fadele, O.A. and Ata, O. (2018) Water absorption properties of sawdust lignin stabilised compressed laterite bricks. *Case Studies in Construction Materials*, 9. <https://doi.org/10.1016/j.cscm.2018.e00187>

FAO. (2020) *FAOSTAT Data* [online]

Available at: [https://www.fao.org/faostat/en/#rankings/countries\\_by\\_commodity](https://www.fao.org/faostat/en/#rankings/countries_by_commodity)

[Accessed: 12 April 2021]

Faridi, H. and Arabhosseini, A. (2018) Application of eggshell wastes as valuable and utilizable products: A review. *Research in Agricultural Engineering*, 64 (2), 104-114. <https://doi.org/10.17221/6/2017-RAE>

Feeley, K.J. and Stroud, J.T. (2018) Where on Earth are the "tropics"? *Frontiers of Biogeography*, 10 (1-2). <https://doi.org/10.21425/F5FBG38649>

Fernandes, J., Mateus, R. and Bragança, L. (2014) The potential of vernacular materials to the sustainable building design. In: Correia, M., Carlos, G. and Rocha, S. (ed.) *Vernacular Heritage and Earthen Architecture: Contributions for Sustainable Development*. London, UK: CRC Press. pp. 623–629.

Fernandez-Lopez, J., Aleta, N. and Alia, R. (2002) Forest genetic resources conservation of *Juglans regia* L. In: Turok, J., Eriksson, G., Russell, K. and Borelli, S. (ed.) *Noble Hardwoods Network: Fourth and Fifth Meetings*. Rome, Italy: IPGRI. pp. 38-43.

Fernea, R., Manea, D.L., Tămaş-Gavrea, D.R. and Roşca, I.C. (2019) Hemp-clay building materials-An investigation on acoustic, thermal and mechanical properties. *Procedia Manufacturing*, 32, 216-223. <https://doi.org/10.1016/j.promfg.2019.02.205>

Fleck, N., Amlı, H., Dhanak, V. and Ahmed, W. (2021) Characterization techniques in energy generation and storage. In: Ahmed, W., Booth, M. and Nourafkan, E. (ed.) *Emerging Nanotechnologies for Renewable Energy*. Elsevier. pp. 259-285.

Fleming, D. and Temyer, J. (2009) Surface preparation: Practices, equipment, and standards through 25 years. *Journal of Protective Coatings & Linings*, 56-63. <https://www.proquest.com/docview/235956524/fulltext/30253EF962A34ECAQ/1?accountid=12118>

Fouchal, F., Gouny, F., Maillard, P., Ulmet, L. and Rossignol, S. (2015) Experimental evaluation of hydric performances of masonry walls made of earth bricks, geopolymer and wooden frame. *Building and Environment*, 87, 234-243. <https://doi.org/10.1016/j.buildenv.2015.01.036>

Franzoni, E. (2011) Materials selection for green buildings: which tools for engineers and architects?. *Procedia Engineering*, 21, 883-890. <https://doi.org/10.1016/j.proeng.2011.11.2090>

Freire, A.L.F., de Araújo Júnior, C.P., de Freitas Rosa, M., de Almeida Neto, J.A. and de Figueirêdo, M.C.B. (2017) Environmental assessment of bioproducts in development stage: Thea case of fiberboards made from coconut residues. *Journal of Cleaner Production*, 153, 230-241. <https://doi.org/10.1016/j.jclepro.2017.03.100>

Frencham, G.J. (1982) The Performance of Earth Buildings. *School of Architecture, Deakin University, Australia*.

Frontczak, M. and Wargocki, P. (2011) Literature survey on how different factors influence human comfort in indoor environments. *Building and Environment*, 46 (4), 922-937. <https://doi.org/10.1016/j.buildenv.2010.10.021>

Galán-Marín, C., Rivera-Gómez, C. and Bradley, F. (2013) Ultrasonic, molecular and mechanical testing diagnostics in natural fibre reinforced, polymer-stabilized earth blocks. *International Journal of Polymer Science*, 2013. <https://doi.org/10.1155/2013/130582>

Galán-Marín, C., Rivera-Gómez, C. and Petric, J. (2010) Clay-based composite stabilized with natural polymer and fibre. *Construction and Building Materials*, 24 (8), 1462-1468.

<https://doi.org/10.1016/j.conbuildmat.2010.01.008>

Ganga, G., Nsongo, T., Elega, H., Mabila, B., Tatsiete, T.T. and Nzonzolo (2014) Effect of incorporation of chips and wood dust mahogany on mechanical and acoustic behavior of brick clay. *Journal of Building Construction and Planning Research*, 2 (3), 198-208. <https://doi.org/10.4236/jbcpr.2014.23018>

Gaspar, K., Casals, M. and Gangoells, M. (2016) A comparison of standardized calculation methods for in situ measurements of façades U-value. *Energy and Buildings*, 130, 592-599. <https://doi.org/10.1016/j.enbuild.2016.08.072>

Gaspar, K., Casals, M. and Gangoells, M. (2018a) In situ measurement of façades with a low U-value: Avoiding deviations. *Energy and Buildings*, 170, 61-73. <https://doi.org/10.1016/j.enbuild.2018.04.012>

Gaspar, K., Casals, M. and Gangoells, M. (2018b) Review of criteria for determining HFM minimum test duration. *Energy and Buildings*, 176, 360-370. <https://doi.org/10.1016/j.enbuild.2018.07.049>

Ghani, A.N.A. (2014) Experimental Research Methods for Students in Built Environment and Engineering. *MATEC Web of Conferences*, 10. <https://doi.org/10.1051/mateconf/20141001001>

Ghavami, K., Toledo Filho, R.D. and Barbosa, N.P. (1999) Behaviour of composite soil reinforced with natural fibres. *Cement and Concrete Composites*, 21 (1), 39-48. [https://doi.org/10.1016/S0958-9465\(98\)00033-X](https://doi.org/10.1016/S0958-9465(98)00033-X)

Ghimire, A. and Maharjan, S. (2019) Experimental Analysis on the Properties of Concrete Brick With Partial Replacement of Sand by Saw Dust and Partial Replacement of Coarse Aggregate by Expanded Polystyrene. *Journal of Advanced College of Engineering and Management*, 5, 27-36. <https://doi.org/10.3126/jacem.v5i0.26674>

Giroudon, M., Laborel-Préneron, A., Aubert, J.-E. and Magniont, C. (2019) Comparison of barley and lavender straws as bioaggregates in earth bricks. *Construction and Building Materials*, 202, 254-265. <https://doi.org/10.1016/j.conbuildmat.2018.12.126>

Givoni, B. (1976) *Man, Climate and Architecture*. 2nd ed. London, UK: Applied Science Publishers.

Glass, J. (2012) The state of sustainability reporting in the construction sector. *Smart and Sustainable Built Environment*, 1 (1), 87-104.

Goh, C.S., Chong, H.-Y., Jack, L. and Faris, A.F.M. (2020) Revisiting triple bottom line within the context of sustainable construction: A systematic review. *Journal of Cleaner Production*, 252, 119884. <https://doi.org/10.1016/j.jclepro.2019.119884>

González, M.J. and Navarro, J.G. (2006) Assessment of the decrease of CO2 emissions in the construction field through the selection of materials: Practical case study of three houses of low environmental impact. *Building and Environment*, 41 (7), 902-909. <https://doi.org/10.1016/j.buildenv.2005.04.006>

Goodbun, J. (2016) Mud and Modernity. *ARENA Journal of Architectural Research*, 1 (1). <https://doi.org/10.5334/ajar.6>

Goodman-Elgar, M. (2008) The devolution of mudbrick: ethnoarchaeology of abandoned earthen dwellings in the Bolivian Andes. *Journal of Archaeological Science*, 35 (12), 3057-3071. <https://doi.org/10.1016/j.jas.2008.05.015>

Gope, P.C., Singh, V.K. and Rao, D.K. (2015) Mode I fracture toughness of bio-fiber and bio-shell particle reinforced epoxy bio-composites. *Journal of Reinforced Plastics and Composites*, 34 (13), 1075-1089. <https://doi.org/10.1177%2F0731684415586277>

Gorantla, K.K., Shaik, S. and Puttaranga Settee, A.B.T. (2016) Simulation of various wall and window glass material for energy efficient building design. *Key Engineering Materials*, 692, 9-16.

<https://doi.org/10.4028/www.scientific.net/KEM.692.9>

Gou, S., Nik, V.M., Scartezzini, J.-L., Zhao, Q. and Li, Z. (2018) Passive design optimization of newly-built residential buildings in Shanghai for improving indoor thermal comfort while reducing building energy demand. *Energy and Buildings*, 169, 484-506. <https://doi.org/10.1016/j.enbuild.2017.09.095>

Gou, Z. and Xie, X. (2017) Evolving green building: triple bottom line or regenerative design? *Journal of Cleaner Production*, 153, 600-607. <https://doi.org/10.1016/j.jclepro.2016.02.077>

Gowthaman, S., Nakashima, K. and Kawasaki, S. (2018) A state-of-the-art review on soil reinforcement technology using natural plant fiber materials: Past findings, present trends and future directions. *Materials*, 11 (4). <https://doi.org/10.3390/ma11040553>

Gregory, K., Moghtaderi, B., Sugo, H. and Page, A. (2008) Effect of thermal mass on the thermal performance of various Australian residential constructions systems. *Energy and Buildings*, 40 (4), 459-465. <https://doi.org/10.1016/j.enbuild.2007.04.001>

Guettatfi, L., Hamouine, A., Himouri, K. and Labbaci, B. (2021) Mechanical and Water Durability Properties of Adobes Stabilized with White Cement, Quicklime and Date Palm Fibers. *International Journal of Architectural Heritage*. <https://doi.org/10.1080/15583058.2021.1959675>

Gunawardana, S.A.A., Galkanda, H.H., Halwatura, R.U. and Jayasinghe, G.Y. (2021) Investigation of rain surface erosion and bonding strength of different wall care putty materials along with different walling materials. *Journal of Building Engineering*, 34. <https://doi.org/10.1016/j.jobe.2020.101872>

Gupta, V., Chai, H.K., Lu, Y. and Chaudhary, S. (2020) A state of the art review to enhance the industrial scale waste utilization in sustainable unfired bricks. *Construction and Building Materials*, 254. <https://doi.org/10.1016/j.conbuildmat.2020.119220>

Gürü, M., Atar, M. and Yıldırım, R. (2008) Production of polymer matrix composite particleboard from walnut shell and improvement of its requirements. *Materials & Design*, 29 (1), 284-287. <https://doi.org/10.1016/j.matdes.2006.10.023>

Hall, C. and Hamilton, A. (2015) Porosity–density relations in stone and brick materials. *Materials and Structures*, 48, 1265-1271. <https://doi.org/10.1617/s11527-013-0231-1>

Hall, C. and Hoff, W.D. (2021) *Water Transport in Brick, Stone and Concrete*. 3rd ed. London, UK: CRC Press.

Hamada, H.M., Tayeh, B.A., Al-Attar, A., Yahaya, F.M., Muthusamy, K. and Humada, A.M. (2020) The present state of the use of eggshell powder in concrete: A review. *Journal of Building Engineering*, 32. <https://doi.org/10.1016/j.jobe.2020.101583>

Hamzah, M.H., Deraman, R. and Saman, N.S.M. (2017) Investigating the effectiveness of using agricultural wastes from empty fruit bunch (EFB), coconut fibre (CF) and sugarcane baggasse (SB) to produce low thermal conductivity clay bricks. *AIP Conference Proceedings*, 1901 (1). <https://doi.org/10.1063/1.5010470>

Han, H., Wang, S., Rakita, M., Wang, Y., Han, Q. and Xu, Q. (2018) Effect of ultrasound-assisted extraction of phenolic compounds on the characteristics of walnut shells. *Food and Nutrition Sciences*, 9 (8), 1034-1045. <https://doi.org/10.4236/fns.2018.98076>

Harish, S., Michael, D.P., Bensely, A., Lal, D.M. and Rajadurai, A. (2009) Mechanical property evaluation of natural fiber coir composite. *Materials Characterization*, 60 (1), 44-49. <https://doi.org/10.1016/j.matchar.2008.07.001>

Harries, K.A. and Sharma, B. (2019) *Nonconventional and vernacular construction materials: Characterisation, properties and applications*. Cambridge, UK: Woodhead Publishing.

Hassan, M.A., Yami, A.M., Raji, A. and Ngala, M.J. (2014) Effects of sawdust and rice husk additives on

properties of local refractory clay. *The International Journal of Engineering and Science*, 3 (8), 40-44. <http://www.theijes.com/papers/v3-i8/Version-2/E0382040044.pdf>

He, K., Zhang, J. and Zeng, Y. (2019) Knowledge domain and emerging trends of agricultural waste management in the field of social science: A scientometric review. *Science of The Total Environment*, 670, 236-244. <https://doi.org/10.1016/j.scitotenv.2019.03.184>

Heath, A., Walker, P., Fourie, C. and Lawrence, M. (2009) Compressive strength of extruded unfired clay masonry units. *Proceedings of the Institution of Civil Engineers-Construction Materials*, 162 (3), 105-112. <http://dx.doi.org/10.1680/coma.2009.162.3.105>

Heathcote, K.A. (1995) Durability of earthwall buildings. *Construction and Building Materials*, 9 (3), 185-189. [https://doi.org/10.1016/0950-0618\(95\)00035-E](https://doi.org/10.1016/0950-0618(95)00035-E)

Heathcote, K.A. (2002) *An investigation into the erodibility of earth wall units*. Doctoral dissertation, University of Sydney, Australia. <https://opus.lib.uts.edu.au/bitstream/10453/20153/2020/02Whole.pdf>.

Hejazi, S.M., Sheikhzadeh, M., Abtahi, S.M. and Zadhoush, A. (2012) A simple review of soil reinforcement by using natural and synthetic fibers. *Construction and Building Materials*, 30, 100-116. <https://doi.org/10.1016/j.conbuildmat.2011.11.045>

Hekimoğlu, G., Sarı, A., Kar, T., Keleş, S., Kaygusuz, K., Tyagi, V.V., Sharma, R.K., Al-Ahmed, A., Al-Sulaiman, F.A. and Saleh, T.A. (2021) Walnut shell derived bio-carbon/methyl palmitate as novel composite phase change material with enhanced thermal energy storage properties. *Journal of Energy Storage*, 35. <https://doi.org/10.1016/j.est.2021.102288>

Hilal, N., Ali, T.K.M. and Tayeh, B.A. (2020) Properties of environmental concrete that contains crushed walnut shell as partial replacement for aggregates. *Arabian Journal of Geosciences*, 13 (812). <https://doi.org/10.1007/s12517-020-05733-9>

Horisawa, S., Sunagawa, M., Tamai, Y., Matsuoka, Y., Miura, T. and Terazawa, M. (1999) Biodegradation of nonlignocellulosic substances II: physical and chemical properties of sawdust before and after use as artificial soil. *Journal of Wood Science*, 45, 492-497. <https://jwoodscience.springeropen.com/articles/10.1007/BF00538959>

Hsieh, C. and Wu, I. (2012) Applying building information modelling in evaluating building energy performance. *Gerontechnology*, 11 (2). <https://doi.org/10.4017/gt.2012.11.02.227.00>

Husain, M.S., Ahmad, A., Huda, S. and Asim, M. (2017) Cost optimization of concrete by replacing fine aggregate with walnut shell powder. *International Journal of Civil Engineering and Technology*, 8 (3), 82-89. <http://www.iaeme.com/IJCIET/issues.asp?JType=IJCIET&VType=8&IType=3>

Huynh, T.P., Hwang, C.L., Lin, K.L. and Ngo, S.H. (2017) Effect of residual rice husk ash on mechanical-microstructural properties and thermal conductivity of sodium-hydroxide-activated bricks. *Environmental Progress & Sustainable Energy*, 37 (5), 1647-1656. <https://doi.org/10.1002/ep.12848>

Ibn-Mohammed, T., Greenough, R., Taylor, S., Ozawa-Meida, L. and Acquaye, A. (2013) Operational vs. embodied emissions in buildings—A review of current trends. *Energy and Buildings*, 66, 232-245. <https://doi.org/10.1016/j.enbuild.2013.07.026>

IES-VE. (2011) *IES-VE User Guide, ApacheSim Calculation Methods* [online]

Available at:

<http://www.iesve.com/downloads/help/Thermal/Reference/ApacheSimCalculationMethods.pdf>

[Accessed: 10 June 2020]

Integrated Environmental Solutions Virtual Environment. (2020).

Available at: <https://iesve.com/>

[Accessed: 12 June 2020]

Ige, O. and Danso, H. (2022) Experimental Characterization of Adobe Bricks Stabilized with Rice Husk

and Lime for Sustainable Construction. *Journal of Materials in Civil Engineering*, 34 (2). [https://doi.org/https://doi.org/10.1061/\(ASCE\)MT.1943-5533.0004059](https://doi.org/https://doi.org/10.1061/(ASCE)MT.1943-5533.0004059)

IS: 1725 (1982) *Specification for Soil Based Blocks Used in General Building Construction*. New Delhi: Bureau of Indian Standards.

Islam, M.S. and Iwashita, K. (2010) Earthquake resistance of adobe reinforced by low cost traditional materials. *Journal of Natural Disaster Science*, 32 (1). <https://doi.org/10.2328/jnds.32.1>

Jannat, N., Hussien, A., Abdullah, B. and Cotgrave, A. (2020) Application of agro and non-agro waste materials for unfired earth blocks construction: A review. *Construction and Building Materials*, 254. <https://doi.org/10.1016/j.conbuildmat.2020.119346>

Jayasinghe, C. and Kamaladasa, N. (2007) Compressive strength characteristics of cement stabilized rammed earth walls. *Construction and Building Materials*, 21 (11), 1971-1976. <https://doi.org/10.1016/j.conbuildmat.2006.05.049>

Jeanjean, A., Olives, R. and Py, X. (2013) Selection criteria of thermal mass materials for low-energy building construction applied to conventional and alternative materials. *Energy and Buildings*, 63, 36-48. <https://doi.org/10.1016/j.enbuild.2013.03.047>

Jesudass, A., Harish, K., Ram, S.S. and Riyas, S.M. (2021) Earthen blocks with Synthetic Fibres-A Review. *IOP Conference Series: Materials Science and Engineering*, 1145. <https://doi.org/10.1088/1757-899X/1145/1/012158>

Jha, A.K. and Sivapullaiah, P.V. (2015) Mechanism of improvement in the strength and volume change behavior of lime stabilized soil. *Engineering Geology*, 198, 53-64. <https://doi.org/10.1016/j.enggeo.2015.08.020>

Ji, Y., Fitton, R., Swan, W. and Webster, P. (2014) Assessing overheating of the UK existing dwellings-A case study of replica Victorian end terrace house. *Building and Environment*, 77. <https://doi.org/10.1016/j.buildenv.2014.03.012>

Ji, Y., Lee, A. and Swan, W. (2019) Building dynamic thermal model calibration using the Energy House facility at Salford. *Energy and Buildings*, 191, 224-234. <https://doi.org/10.1016/j.enbuild.2019.03.001>

Jokhio, G.A., Mohsin, S.M.S. and Gul, Y. (2018) Two-fold sustainability-Adobe with sawdust as partial sand replacement. *IOP Conference Series: Materials Science and Engineering*, 342. <https://doi.org/10.1088/1757-899X/342/1/012069>

Jones, D. and Brischke, C. (2017) *Performance of bio-based building materials*. Cambridge, UK: Woodhead Publishing.

Jörchel, S. (2019) Modern Earth Building-the Current State of Earth Building from a German Perspective. *IOP Conference Series: Earth and Environmental Science* 290. <https://doi.org/10.1088/1755-1315/290/1/012018>

Kadir, A.A., Mohd Zulkifly, S.N., Al Bakri, M.M.A. and Sarani, N.A. (2016) The utilization of coconut fibre into fired clay brick. *Key Engineering Materials*, 673, 213-222. <https://doi.org/10.4028/www.scientific.net/KEM.673.213>

Kamal, I., Sherwani, A.F., Ali, A., Khalid, A., Saadi, I. and Harbi, A. (2017) Walnut shell for partial replacement of fine aggregate in concrete: modeling and optimization. *Journal of Civil Engineering Research*, 7 (4), 109-119. <https://doi.org/10.5923/j.jce.20170704.01>

Kandula, R., Sanaka, S.P., Prasad A V, R. and Konireddy, H.R. (2022) Thermo-physical and Fire Properties of Natural Fiber Composites for Energy Saving Applications. *Journal of Natural Fibers*. <https://doi.org/10.1080/15440478.2022.2044964>

Kanna, G.V. and Dhanalakshmi, G. (2018) Experimental Investigations on Bricks with the replacement of

Coconut Fibre. *International Research Journal of Engineering and Technology*, 5 (2), 199-204. <https://www.irjet.net/archives/V5/i2/IRJET-V5I248.pdf>

Karimpour, M., Belusko, M., Xing, K. and Bruno, F. (2014) Minimising the life cycle energy of buildings: Review and analysis. *Building and Environment*, 73, 106-114. <https://doi.org/10.1016/j.buildenv.2013.11.019>

Karrech, A., Strazzeri, V. and Elchalakani, M. (2021) Improved thermal insulation of cement stabilised rammed earth embedding lightweight aggregates. *Construction and Building Materials*, 268. <https://doi.org/10.1016/j.conbuildmat.2020.121075>

Kasinikota, P. and Tripura, D.D. (2022) Prediction of physical-mechanical properties of hollow interlocking compressed unstabilized and stabilized earth blocks at different moisture conditions using ultrasonic pulse velocity. *Journal of Building Engineering*, 48. <https://doi.org/10.1016/j.jobe.2021.103961>

Kazmi, S.M.S., Munir, M.J., Patnaikuni, I., Wu, Y.-F. and Fawad, U. (2018) Thermal performance enhancement of eco-friendly bricks incorporating agro-wastes. *Energy and Buildings*, 158, 1117-1129. <https://doi.org/10.1016/j.enbuild.2017.10.056>

Ketta, M. and Tůmová, E. (2016) Eggshell structure, measurements, and quality-affecting factors in laying hens: a review. *Czech Journal of Animal Science*, 61 (7), 299-309. <https://doi.org/10.17221/46/2015-CJAS>

Khanjanzadeh, H., Pirayesh, H. and Sepahvand, S. (2014) Influence of walnut shell as filler on mechanical and physical properties of MDF improved by nano-SiO<sub>2</sub>. *Journal of the Indian Academy of Wood Science*, 11 (1), 15-20. <https://doi.org/10.1007/s13196-014-0111-5>

Khatun, M.A., Rashid, M.B. and Hygen, H.O. (2016) *Climate of Bangladesh, MET Report* [online] Available at: [https://www.met.no/publikasjoner/met-report/met-report-2016/\\_attachment/download/b50e3f06-4485-4f34-b642-0a1e86f12c7d:a483b63367b0f087f3bd9410e135a5e0837d1927/MET-report-08-2016.pdf](https://www.met.no/publikasjoner/met-report/met-report-2016/_attachment/download/b50e3f06-4485-4f34-b642-0a1e86f12c7d:a483b63367b0f087f3bd9410e135a5e0837d1927/MET-report-08-2016.pdf) [Accessed: 12 August 2021]

Khedari, J., Charoenvai, S. and Hirunlabh, J. (2003) New insulating particleboards from durian peel and coconut coir. *Building and Environment*, 38 (3), 435-441. [https://doi.org/10.1016/S0360-1323\(02\)00030-6](https://doi.org/10.1016/S0360-1323(02)00030-6)

Khedari, J., Suttisonk, B., Pratinthong, N. and Hirunlabh, J. (2001) New lightweight composite construction materials with low thermal conductivity. *Cement and Concrete Composites*, 23 (1), 65-70. [https://doi.org/10.1016/S0958-9465\(00\)00072-X](https://doi.org/10.1016/S0958-9465(00)00072-X)

Khedari, J., Watsanasathaporn, P. and Hirunlabh, J. (2005) Development of fibre-based soil-cement block with low thermal conductivity. *Cement and Concrete Composites*, 27, 111-116. <https://doi.org/10.1016/j.cemconcomp.2004.02.042>

Khoudja, D., Taallah, B., Izemmouren, O., Aggoun, S., Herihiri, O. and Guettala, A. (2021) Mechanical and thermophysical properties of raw earth bricks incorporating date palm waste. *Construction and Building Materials*, 270. <https://doi.org/10.1016/j.conbuildmat.2020.121824>

Kim, M., Kang, S.-H., Hong, S.-G. and Moon, J. (2019) Influence of effective water-to-cement ratios on internal damage and salt scaling of concrete with superabsorbent polymer. *Materials*, 12 (23). <https://doi.org/10.3390/ma12233863>

King'Ori, A.M. (2011) A review of the uses of poultry eggshells and shell membranes. *International Journal of Poultry Science*, 10 (11), 908-912. <https://doi.org/10.3923/ijps.2011.908.912>

Kiprop, J. (2017) *WorldAtlas* [online] Available at: <https://www.worldatlas.com/articles/what-is-a-tropical-climate.html> [Accessed: 15 April 2020]

- Kirilenko, A.P. and Sedjo, R.A. (2007) Climate change impacts on forestry. *Proceedings of the National Academy of Sciences*, 104 (50), 19697-19702. <https://doi.org/10.1073/pnas.0701424104>
- Kisilewicz, T. (2019) On the role of external walls in the reduction of energy demand and the mitigation of human thermal discomfort. *Sustainability*, 11 (4). <https://doi.org/10.3390/su11041061>
- Kontoleon, K.J. and Bikas, D.K. (2007) The effect of south wall's outdoor absorption coefficient on time lag, decrement factor and temperature variations. *Energy and Buildings*, 39 (9), 1011-1018. <https://doi.org/10.1016/j.enbuild.2006.11.006>
- Kosseva, M.R. (2016) Waste from fruit wine production. In: Kosseva, M. R., Joshi, V. K. and Panesar, P. S. (ed.) *Science and Technology of Fruit Wine Production*. First ed.: Academic Press. pp. 557-598.
- Kottek, M., Grieser, J., Beck, C., Rudolf, B. and Rubel, F. (2006) World map of the Köppen-Geiger climate classification updated. *Meteorologische Zeitschrift*, 15 (3), 259-263. <https://doi.org/10.1127/0941-2948/2006/0130>
- Koutous, A. and Hilali, E. (2021) Reinforcing rammed earth with plant fibers: A case study. *Case Studies in Construction Materials*, 14. <https://doi.org/10.1016/j.cscm.2021.e00514>
- Krstić, H., Miličević, I., Markulak, D. and Domazetović, M. (2021) Thermal Performance Assessment of a Wall Made of Lightweight Concrete Blocks with Recycled Brick and Ground Polystyrene. *Buildings*, 11 (12). <https://doi.org/10.3390/buildings11120584>
- Kulshreshtha, Y., Mota, N.J.A., Jagadish, K.S., Bredenoord, J., Vardon, P.J., Van Loosdrecht, M.C.M. and Jonkers, H.M. (2020) The potential and current status of earthen material for low-cost housing in rural India. *Construction and Building Materials*, 247. <https://doi.org/10.1016/j.conbuildmat.2020.118615>
- Kumar, A. and P Singh, O. (2013) Advances in the building materials for thermal comfort and energy saving. *Recent Patents on Engineering*, 7 (3), 220-232. <https://www.ingentaconnect.com/content/ben/eng/2013/00000007/00000003/art00006>
- Kumar, N. and Barbato, M. (2022) Effects of sugarcane bagasse fibers on the properties of compressed and stabilized earth blocks. *Construction and Building Materials*, 315. <https://doi.org/10.1016/j.conbuildmat.2021.125552>
- La Scala Jr, N., Boleli, I.C., Ribeiro, L.T., Freitas, D. and Macari, M. (2000) Pore size distribution in chicken eggs as determined by mercury porosimetry. *Brazilian Journal of Poultry Science*, 2 (2), 177-181. <https://doi.org/10.1590/S1516-635X2000000200007>
- Laborel-Préneron, A., Aubert, J.E., Magniont, C., Maillard, P. and Poirier, C. (2017) Effect of plant aggregates on mechanical properties of earth bricks. *Journal of Materials in Civil Engineering*, 29 (12). [https://doi.org/10.1061/\(ASCE\)MT.1943-5533.0002096](https://doi.org/10.1061/(ASCE)MT.1943-5533.0002096)
- Laborel-Préneron, A., Aubert, J.E., Magniont, C., Tribout, C. and Bertron, A. (2016) Plant aggregates and fibers in earth construction materials: A review. *Construction and Building Materials*, 111, 719-734. <https://doi.org/10.1016/j.conbuildmat.2016.02.119>
- Laborel-Préneron, A., Faria, P., Aubert, J.E. and Magniont, C. (2021) Assessment of Durability of Bio-based Earth Composites. *Recent Progress in Materials*, 3 (2). <https://doi.org/10.21926/rpm.2102016>
- Laborel-Préneron, A., Magniont, C. and Aubert, J.E. (2018) Hygrothermal properties of unfired earth bricks: effect of barley straw, hemp shiv and corn cob addition. *Energy and Buildings*, 178, 265-278. <https://doi.org/10.1016/j.enbuild.2018.08.021>
- Lachowicz, H., Wróblewska, H., Wojtan, R. and Sajdak, M. (2019) The effect of tree age on the chemical composition of the wood of silver birch (*Betula pendula* Roth.) in Poland. *Wood Science and Technology*, 53, 1135-1155. <https://doi.org/10.1007/s00226-019-01121->
- Laibi, A.B., Poullain, P., Leklou, N., Gomina, M. and Sohounhloúé, D.K.C. (2018) Influence of the kenaf

fiber length on the mechanical and thermal properties of Compressed Earth Blocks (CEB). *KSCE Journal of Civil Engineering*, 22 (2), 785-793. <https://doi.org/10.1007/s12205-017-1968-9>

Lakshmi, S.M., Sasikala, S., Padmavathi, V., Priya, S. and Saranya, V. (2018) Utilization of Coconut Coir Fibre For Improving Subgrade Strength Characteristics Of Clayey Sand. *International Journal of Inovative Research in Science Engineering and Technology*, 5 (4), 2873-2878. <https://www.irjet.net/archives/V5/i4/IRJET-V5I4635.pdf>

Lamrani, M., Mansour, M., Laaroussi, N. and Khalfaoui, M. (2019) Thermal study of clay bricks reinforced by three ecological materials in south of morocco. *Energy Procedia*, 156, 273-277. <https://doi.org/10.1016/j.egypro.2018.11.141>

Latawiec, R., Woyciechowski, P. and Kowalski, K.J. (2018) Sustainable concrete performance-CO<sub>2</sub>-emission. *Environments*, 5 (2). <https://doi.org/10.3390/environments5020027>

Latha, P.K., Darshana, Y. and Venugopal, V. (2015) Role of building material in thermal comfort in tropical climates—A review. *Journal of Building Engineering*, 3, 104-113. <https://doi.org/10.1016/j.jobe.2015.06.003>

Latif, A.M.A. and Rasoul, Z.M.R.A. (2009) Correlation between the compressive strength of concrete and ultrasonic pulse velocity; investigation and interpretation. *Journal of Kerbala University*, 5 (1), 17-29. [https://www.iraqjournals.com/article\\_46652\\_0.html](https://www.iraqjournals.com/article_46652_0.html)

Lekshmi, M.S., Vishnudas, S. and Nair, D.G. (2017) An investigation on the potential of mud as sustainable building material in the context of Kerala. *International Journal of Energy Technology and Policy*, 13 (1-2), 107-122. <https://www.inderscienceonline.com/doi/abs/10.1504/IJETP.2017.080621>

Lima, S.A., Varum, H., Sales, A. and Neto, V.F. (2012) Analysis of the mechanical properties of compressed earth block masonry using the sugarcane bagasse ash. *Construction and Building Materials*, 35, 829-837. <https://doi.org/10.1016/j.conbuildmat.2012.04.127>

Limami, H., Manssouri, I., Cherkaoui, K. and Khaldoun, A. (2021) Mechanical and physicochemical performances of reinforced unfired clay bricks with recycled Typha-fibers waste as a construction material additive. *Cleaner Engineering and Technology*, 2. <https://doi.org/10.1016/j.clet.2020.100037>

Lin, H., Liu, F.Y., Lourenço, S.D.N., Schwantes, G., Trumpf, S., Holohan, D. and Beckett, C.T.S. (2021) Stabilization of an earthen material with Tung oil: compaction, strength and hydrophobic enhancement. *Construction and Building Materials*, 290. <https://doi.org/10.1016/j.conbuildmat.2021.123213>

Lizana, J., Chacartegui, R., Barrios-Padura, A. and Valverde, J.M. (2017) Advances in thermal energy storage materials and their applications towards zero energy buildings: A critical review. *Applied Energy*, 203, 219-239. <https://doi.org/10.1016/j.apenergy.2017.06.008>

Lopez, Y.M., Paes, J.B., Gustavo, D., Gonçalves, F.G., Méndez, F.C. and Nantet, A.C.T. (2020) Production of wood-plastic composites using cedrela odorata sawdust waste and recycled thermoplastics mixture from post-consumer products - A sustainable approach for cleaner production in Cuba. *Journal of Cleaner Production*, 244. <https://doi.org/10.1016/j.jclepro.2019.118723>

Lotfabadi, P. and Hançer, P. (2019) A comparative study of traditional and contemporary building envelope construction techniques in terms of thermal comfort and energy efficiency in hot and humid climates. *Sustainability*, 11 (13). <https://doi.org/10.3390/su11133582>

Lu, J., Wang, K. and Qu, M.L. (2020) Experimental determination on the capillary water absorption coefficient of porous building materials: A comparison between the intermittent and continuous absorption tests. *Journal of Building Engineering*, 28. <https://doi.org/10.1016/j.jobe.2019.101091>

Lu, X. and Memari, A.M. (2018) Comparative study of Hot Box Test Method using laboratory evaluation of thermal properties of a given building envelope system type. *Energy and Buildings*, 178, 130-139. <https://doi.org/10.1016/j.enbuild.2018.08.044>

- Lu, X. and Memari, A.M. (2022) Comparison of the Experimental Measurement Methods for Building Envelope Thermal Transmittance. *Buildings*, 12 (3), 282. <https://doi.org/10.3390/buildings12030282>
- Madhumathi, A., Vishnupriya, J. and Vignesh, S. (2014) Sustainability of traditional rural mud houses in Tamilnadu, India: An analysis related to thermal comfort. *Journal of Multidisciplinary Engineering Science and Technology*, 1 (5), 302-311. <http://www.jmest.org/wp-content/uploads/JMESTN42350265.pdf>
- Mageswari, M. and Vidivelli, B. (2009) The use of sawdust ash as fine aggregate replacement in concrete. *Journal of Environmental Research and Development*, 3 (3), 720-726.
- Mahlia, T.M.I., Taufiq, B.N., Ismail and Masjuki, H.H. (2007) Correlation between thermal conductivity and the thickness of selected insulation materials for building wall. *Energy and Buildings*, 39 (2), 182-187. <https://doi.org/10.1016/j.enbuild.2006.06.002>
- Martín-del-Río, J.J., Canivell, J. and Falcon, R.M. (2020) abid *Construction and Building Materials*, 242. <https://doi.org/10.1016/j.conbuildmat.2020.118060>
- Martínez, M.L., Labuckas, D.O., Lamarque, A.L. and Maestri, D.M. (2010) Walnut (*Juglans regia* L.): genetic resources, chemistry, by-products. *Journal of the Science of Food and Agriculture*, 90 (12), 1959-1967. <https://doi.org/10.1002/jsfa.4059>
- Martinez, R.G. (2017) Hygrothermal assessment of a prefabricated timber-frame construction based in hemp. *Procedia Environmental Sciences*, 38, 729-736. <https://doi.org/10.1016/j.proenv.2017.03.155>
- Masuka, S., Gwenzi, W. and Rukuni, T. (2018) Development, engineering properties and potential applications of unfired earth bricks reinforced by coal fly ash, lime and wood aggregates. *Journal of Building Engineering*, 18, 312-320. <https://doi.org/10.1016/j.jobe.2018.03.010>
- Mazraeh, H.M. and Pazhouhanfar, M. (2018) Effects of vernacular architecture structure on urban sustainability case study: Qeshm Island, Iran. *Frontiers of Architectural Research*, 7 (1), 11-24. <https://doi.org/10.1016/j.foar.2017.06.006>
- Medjelekh, D., Ulmet, L., Abdou, S. and Dubois, F. (2016) A field study of thermal and hygric inertia and its effects on indoor thermal comfort: Characterization of travertine stone envelope. *Building and Environment*, 106, 57-77. <https://doi.org/10.1016/j.buildenv.2016.06.010>
- Medvey, B. and Dobszay, G. (2020) Durability of Stabilized Earthen Constructions: A Review. *Geotechnical and Geological Engineering*, 38 (3), 2403-2425. <https://link.springer.com/content/pdf/10.1007/s10706-020-01208-6.pdf>
- Mellaikhafi, A., Ouakarouch, M., Benallel, A., Tilioua, A., Ettakni, M., Babaoui, A., Garoum, M. and Hamdi, M.A.A. (2021) Characterization and thermal performance assessment of earthen adobes and walls additive with different date palm fibers. *Case Studies in Construction Materials*, 15. <https://doi.org/10.1016/j.cscm.2021.e00693>
- Memarian, S., Kari, B.M., Asadi, S. and Fayaz, R. (2020) Building Envelope Thermal Mass and Its Effect on Spring and the Autumn Seasonal Transition Period. *Journal of Architectural Engineering*, 26 (2). [https://doi.org/10.1061/\(ASCE\)AE.1943-5568.0000391](https://doi.org/10.1061/(ASCE)AE.1943-5568.0000391)
- Meng, X., Luo, T., Gao, Y., Zhang, L., Shen, Q. and Long, E. (2017) A new simple method to measure wall thermal transmittance in situ and its adaptability analysis. *Applied Thermal Engineering*, 122, 747-757. <https://doi.org/10.1016/j.applthermaleng.2017.05.074>
- Millogo, Y., Hajjaji, M. and Ouedraogo, R. (2008) Microstructure and physical properties of lime-clayey adobe bricks. *Construction and Building Materials*, 22 (12), 2386-2392. <https://doi.org/10.1016/j.conbuildmat.2007.09.002>
- Millogo, Y., Morel, J.C., Aubert, J.E. and Ghavami, K. (2014) Experimental analysis of Pressed Adobe Blocks reinforced with *Hibiscus cannabinus* fibers. *Construction and Building Materials*, 52, 71-78.

<https://doi.org/10.1016/j.conbuildmat.2013.10.094>

Mirón, S., Wendonly, B., Gutiérrez, R., Salvador, R., Orozco, M. and Eugenia, M. (2017) Alternative material for load-bearing wall with addition of walnut shell. Waste Reduction. *3rd International Congress on Sustainable Construction and Eco-Efficient Solutions*, Seville, Spain, March 27-29.

Mirski, R., Derkowski, A., Dziurka, D., Wieruszewski, M. and Dukarska, D. (2020a) Effects of chip type on the properties of chip-sawdust boards glued with polymeric diphenyl methane diisocyanate. *Materials*, 13 (6). <https://doi.org/10.3390/ma13061329>

Mirski, R., Dukarska, D., Derkowski, A., Czarnecki, R. and Dziurka, D. (2020b) By-products of sawmill industry as raw materials for manufacture of chip-sawdust boards. *Journal of Building Engineering*, 32. <https://doi.org/10.1016/j.jobe.2020.101460>

Mittal, A., Teotia, M., Soni, R.K. and Mittal, J. (2016) Applications of egg shell and egg shell membrane as adsorbents: a review. *Journal of Molecular Liquids*, 223, 376-387. <https://doi.org/10.1016/j.molliq.2016.08.065>

Mohamed, A.E.M.K. (2013) Improvement of swelling clay properties using hay fibers. *Construction and Building Materials*, 38, 242-247. <https://doi.org/10.1016/j.conbuildmat.2012.08.031>

Mohammad, S. and Shea, A. (2013) Performance evaluation of modern building thermal envelope designs in the semi-arid continental climate of Tehran. *Buildings*, 3 (4), 674-688. <https://doi.org/10.3390/buildings3040674>

Mohammed, A. and Abdullah, A. (2018) Scanning electron microscopy (SEM): A review. *HERVEX 2018 : 24th International Conference on Hydraulics, Pneumatics, Sealing Elements, Fine Mechanics, Tools, Specific Electronic Equipment & Mechatronics*, Băile Govora, Romania, November 7-9.

Mohebbi, L. and Kazemi, E. (2014) Explaining the Role of Material in Vernacular Architecture and its Comparison with Modern Materials Architecture and Utilizing Nanotechnology. *The SIJ Transactions on Advances in Space Research & Earth Exploration*, 2 (4). <https://pdfs.semanticscholar.org/c33f/04037c7d5355eb48c74bccaf87bddba4bd8bc.pdf>

Monteiro, H., Fernandez, J.E. and Freire, F. (2016) Comparative life-cycle energy analysis of a new and an existing house: The significance of occupant's habits, building systems and embodied energy. *Sustainable Cities and Society*, 26, 507-518. <https://doi.org/10.1016/j.scs.2016.06.002>

Moorey, P.R.S. (1999) *Ancient Mesopotamian materials and industries: the archaeological evidence*. Indiana, United States: Eisenbrauns.

Moran, F., Blight, T., Natarajan, S. and Shea, A. (2014) The use of Passive House Planning Package to reduce energy use and CO<sub>2</sub> emissions in historic dwellings. *Energy and Buildings*, 75, 216-227. <https://doi.org/10.1016/j.enbuild.2013.12.043>

Morgan, R.P.C. and Rickson, R.J. (2003) *Slope stabilization and erosion control: a bioengineering approach*. London, UK: Taylor & Francis.

Morton, T. (2008) *Earth masonry: Design and construction guidelines*. Berkshire, UK: IHS BRE Press.

Mostafa, M. and Uddin, N. (2015) Effect of banana fibers on the compressive and flexural strength of compressed earth blocks. *Buildings*, 5 (1), 282-296. <https://doi.org/10.3390/buildings5010282>

Mostafa, M. and Uddin, N. (2016) Experimental analysis of Compressed Earth Block (CEB) with banana fibers resisting flexural and compression forces. *Case Studies in Construction Materials*, 5, 53-63. <https://doi.org/10.1016/j.cscm.2016.07.001>

Motealleh, P., Zolfaghari, M. and Parsaee, M. (2018) Investigating climate responsive solutions in vernacular architecture of Bushehr city. *HBRC Journal*, 14 (2), 215-223. <https://doi.org/10.1016/j.hbrj.2016.08.001>

- Muazu, A.G. and Alibaba, H.Z. (2017) The use of Traditional Building Materials in Modern Methods of Construction (A Case Study of Northern Nigeria). *International Journal of Engineering Science Technology and Research*, 2 (6), 30-40. <http://www.ijestr.com/asset/images/uploads/15140408341854.pdf>
- Muheise-Araalia, D. and Pavia, S. (2021) Properties of unfired, illitic-clay bricks for sustainable construction. *Construction and Building Materials*, 268. <https://doi.org/10.1016/j.conbuildmat.2020.121118>
- Muntohar, A.S. (2011) Engineering characteristics of the compressed-stabilized earth brick. *Construction and Building Materials*, 25 (11), 4215-4220. <https://doi.org/10.1016/j.conbuildmat.2011.04.061>
- Murillo, C.G., Walker, P.J. and Ansell, M.P. (2005) Henequen fibres for reinforcement of unfired earth blocks. *The Eleventh International Conference for Renewable Resources and Plant Biotechnology (NAROSSA)*, Poznan, Poland, June 6-7.
- Muthuraj, R., Lacoste, C., Lacroix, P. and Bergeret, A. (2019) Sustainable thermal insulation biocomposites from rice husk, wheat husk, wood fibers and textile waste fibers: Elaboration and performances evaluation. *Industrial Crops and Products*, 135, 238-245. <https://doi.org/10.1016/j.indcrop.2019.04.053>
- Mwango, A. and Kambole, C. (2019) Engineering Characteristics and Potential Increased Utilisation of Sawdust Composites in Construction-A Review. *Journal of Building Construction and Planning Research*, 7 (3), 59-88. <https://doi.org/10.4236/jbcpr.2019.73005>
- Mydin, M.A.O., Rozlan, N.A. and Ganesan, S. (2015) Experimental study on the mechanical properties of coconut fibre reinforced lightweight foamed concrete. *Journal of Materials and Environmental Science*, 6 (2), 407-411. <https://citeseerx.ist.psu.edu/viewdoc/download?doi=10.1.1.719.8431&rep=rep1&type=pdf>
- Nagaraj, G. (2009) *Oilseeds: properties, processing, products and procedures*. Delhi, India: New India Publishing.
- Namango, S.S. (2006) *Development of Cost Effective Earthen Building Material for Housing Wall Construction: Investigations Into the Properties of Compressed Earth Blocks Stabilized with Sisal Vegetable Fibres, Cassava Powder and Cement Compositions*. Doctoral dissertation, Brandenburg University of Technology Cottbus, Germany. [https://opus4.kobv.de/opus4btu/frontdoor/deliver/index/docId/6/file/diss\\_saul.pdf](https://opus4.kobv.de/opus4btu/frontdoor/deliver/index/docId/6/file/diss_saul.pdf).
- Nath, A.J., Lal, R. and Das, A.K. (2018) Fired bricks: CO<sub>2</sub> emission and food insecurity. *Global Challenges*, 2 (4). <https://doi.org/10.1002/gch2.201700115>
- Nayak, J.K. and Prajapati, J.A. (2006) *Handbook on energy conscious buildings*. New Delhi: Solar Energy Centre, Ministry of Non-conventional Energy Sources, Government of India.
- Ndagi, A., Umar, A.A., Hejazi, F. and Jaafar, M.S. (2019) Non-destructive assessment of concrete deterioration by ultrasonic pulse velocity: A review. *IOP Conference Series: Earth and Environmental Science*, 357. <https://doi.org/10.1088/1755-1315/357/1/012015>
- NF XP P13-901 (2001) *Blocs de terre comprimée pour murs et cloisons: définitions-Spécifications-Méthodes d'essais-Conditions de réception [in French]*. Paris, France : Association Française de Normalisation (AFNOR).
- Ngayakamo, B.H., Bello, A. and Onwualu, A.P. (2020) Development of eco-friendly fired clay bricks incorporated with granite and eggshell wastes. *Environmental Challenges*, 1. <https://doi.org/10.1016/j.envc.2020.100006>
- Nguyen, A.T., Truong, N.S.H., Rockwood, D. and Le, A.D.T. (2019) Studies on sustainable features of vernacular architecture in different regions across the world: A comprehensive synthesis and evaluation. *Frontiers of Architectural Research*, 8 (4), 535-548. <https://doi.org/10.1016/j.foar.2019.07.006>

Nitin, S. and Singh, V.K. (2013) Mechanical behavior of walnut reinforced composite. *Journal of Materials and Environmental Science*, 4 (2), 238. [https://www.jmaterenvironsci.com/Document/vol4/vol4\\_N2/29-JMES-328-2012-Nitin.pdf](https://www.jmaterenvironsci.com/Document/vol4/vol4_N2/29-JMES-328-2012-Nitin.pdf)

NMX-C-404-ONNCCE (2005) *Industria de la construcción-mampostería-bloques, tabiques o ladrillos y tabicones para uso estructural-especificaciones y métodos de ensayo (Building industry-masonry-blocks or bricks for structural use-specifications and essay method) [in Spanish]*. Distrito Federal, México: Diario Oficial de la Federación.

Nowotna, A., Pietruszka, B. and Lisowski, P. (2019) Eco-friendly building materials. *IOP Conference Series: Earth and Environmental Science*.

Nshimiyimana, P., Miraucourt, D., Messan, A. and Courard, L. (2018) Calcium carbide residue and rice husk ash for improving the compressive strength of compressed earth blocks. *MRS Advances*, 3 (34-35), 2009-2014. <https://doi.org/10.1557/adv.2018.147>

NZS 4298 (1998) *Materials and Workmanship of Earth Buildings*. New Zealand: Standard New Zealand.

Obi, F.O., Ugwuishiwu, B.O. and Nwakaire, J.N. (2016) Agricultural waste concept, generation, utilization and management. *Nigerian Journal of Technology*, 35 (4), 957-964. <https://www.ajol.info/index.php/njt/article/view/145674>

Odeyemi, S.O., Akinpelu, M.A., Atoyebi, O.D. and Yahaya, R.T. (2017) Determination of load carrying capacity of clay bricks reinforced with straw. *International Journal of Sustainable Construction Engineering and Technology*, 8 (2), 57-65. <https://publisher.uthm.edu.my/ojs/index.php/IJSCET/article/view/1727>

Ogah, A.O. and James, T.U. (2018) Mechanical Behavior of Agricultural Waste Fibers Reinforced Vinyl Ester Bio-composites. *Asian Journal of Physical and Chemical Sciences*, 5 (1). <https://doi.org/10.9734/AJOPACS/2018/35841>

Ojerinde, A. (2020) *The use of Rice Husk Ash (RHA) as stabilizer in Compressed Earth Block (CEB) for affordable houses*. Doctoral dissertation, Cardiff University, UK <https://orca.cardiff.ac.uk/139200/>.

Ojo, E.B., Bello, K.O., Mustapha, K., Teixeira, R.S., Santos, S.F. and Savastano Jr, H. (2019) Effects of fibre reinforcements on properties of extruded alkali activated earthen building materials. *Construction and Building Materials*, 227. <https://doi.org/10.1016/j.conbuildmat.2019.116778>

Okunade, E.A. (2008) The effect of wood ash and sawdust admixtures on the engineering properties of a burnt laterite-clay brick. *Journal of Applied Sciences*, 8 (6), 1042-1048. <https://doi.org/10.3923/jas.2008.1042.1048>

Olarewaju, A.J., Balogun, M.O. and Akinlolu, S.O. (2011) Suitability of eggshell stabilized lateritic soil as subgrade material for road construction. *Electronic Journal of Geotechnical Engineering*, 16, 899-908. <https://eprints.ums.edu.my/id/eprint/4959/>

Omer, M.A.B. and Noguchi, T. (2020) A conceptual framework for understanding the contribution of building materials in the achievement of Sustainable Development Goals (SDGs). *Sustainable Cities and Society*, 52. <https://doi.org/10.1016/j.scs.2019.101869>

Onyelowe, K.C. and Okafor, F.O. (2012) A comparative review of soil modification methods. *ARPJ Journal of Earth Sciences*, 1 (2). <http://citeseerx.ist.psu.edu/viewdoc/download?doi=10.1.1.1067.704&rep=rep1&type=pdf>

Orelma, H., Tanaka, A., Vuoriluoto, M., Khakalo, A. and Korpela, A. (2021) Manufacture of all-wood sawdust-based particle board using ionic liquid-facilitated fusion process. *Wood Science and Technology*, 55, 331-349. <https://doi.org/10.1007/s00226-021-01265-x>

Orue, A., Eceiza, A. and Arbelaiz, A. (2020) The use of alkali treated walnut shells as filler in plasticized

poly (lactic acid) matrix composites. *Industrial Crops and Products*, 145. <https://doi.org/10.1016/j.indcrop.2019.111993>

Oskouei, A.V., Afzali, M. and Madadipour, M. (2017) Experimental investigation on mud bricks reinforced with natural additives under compressive and tensile tests. *Construction and Building Materials*, 142, 137-147. <https://doi.org/10.1016/j.conbuildmat.2017.03.065>

Ouattara, S., Boffoue, M.O., Assande, A.A., Kouadio, K.C., Kouakou, C.H., Emeruwa, E. and Pasres (2016) Use of Vegetable Fibers as Reinforcement in the Structure of Compressed Ground Bricks: Influence of Sawdust on the Rheological Properties of Compressed Clay Brick. *American Journal of Materials Science and Engineering*, 4 (1), 13-19. <https://citeseerx.ist.psu.edu/viewdoc/download?doi=10.1.1.1057.3575&rep=rep1&type=pdf>

Ouedraogo, M., Dao, K., Millogo, Y., Aubert, J.E., Messan, A., Seynou, M., Zerbo, L. and Gomina, M. (2019) Physical, thermal and mechanical properties of adobes stabilized with fonio (*Digitaria exilis*) straw. *Journal of Building Engineering*, 23, 250-258. <https://doi.org/10.1016/j.jobe.2019.02.005>

Pacheco-Torgal, F. and Jalali, S. (2012) Earth construction: Lessons from the past for future eco-efficient construction. *Construction and Building Materials*, 29, 512-519. <https://doi.org/10.1016/j.conbuildmat.2011.10.054>

Pan, J., Zou, R. and Jin, F. (2017) Experimental study on specific heat of concrete at high temperatures and its influence on thermal energy storage. *Energies*, 10 (1). <https://doi.org/10.3390/en10010033>

Panyakaew, S. and Fotios, S. (2011) New thermal insulation boards made from coconut husk and bagasse. *Energy and Buildings*, 43 (7), 1732-1739. <https://doi.org/10.1016/j.enbuild.2011.03.015>

Papadakis, V.G. and Tsimas, S. (2002) Supplementary cementing materials in concrete: Part I: efficiency and design. *Cement and Concrete Research*, 32 (10), 1525-1532. [https://doi.org/10.1016/S0008-8846\(02\)00827-X](https://doi.org/10.1016/S0008-8846(02)00827-X)

Paraschiv, L.S., Acomi, N., Serban, A. and Paraschiv, S. (2020) A web application for analysis of heat transfer through building walls and calculation of optimal insulation thickness. *Energy Reports*, 6, 343-353. <https://doi.org/10.1016/j.egyr.2020.08.055>

Parisi, F., Asprone, D., Fenu, L. and Prota, A. (2015) Experimental characterization of Italian composite adobe bricks reinforced with straw fibers. *Composite Structures*, 122, 300-307. <https://doi.org/10.1016/j.compstruct.2014.11.060>

Parveen, S., Rana, S. and Fanguero, R. (2017) Macro-and nanodimensional plant fiber reinforcements for cementitious composites. In: Junior, H. S., Fiorelli, J. and Dos Santos, S. F. (ed.) *Sustainable and nonconventional construction materials using inorganic bonded fiber composites*. Woodhead Publishing. pp. 343-382.

Pásztor, Z. (2021) An overview of factors influencing thermal conductivity of building insulation materials. *Journal of Building Engineering*, 44, 102604. <https://doi.org/10.1016/j.jobe.2021.102604>

Pathirana, S., Rodrigo, A. and Halwatura, R. (2019) Effect of building shape, orientation, window to wall ratios and zones on energy efficiency and thermal comfort of naturally ventilated houses in tropical climate. *International Journal of Energy and Environmental Engineering*, 10, 107-120. <https://doi.org/10.1007/s40095-018-0295-3>

Pattanaik, L., Pattnaik, F., Saxena, D.K. and Naik, S.N. (2019) Biofuels from agricultural wastes. In: Basile, A. and Dalena, F. (ed.) *Second and Third Generation of Feedstocks: The Evolution of Biofuels*. Elsevier. pp. 103-142.

Paul, S.C., Mbewe, P.B.K., Kong, S.Y. and Šavija, B. (2019) Agricultural solid waste as source of supplementary cementitious materials in developing countries. *Materials*, 12 (7). <https://doi.org/10.3390/ma12071112>

- Peñaloza, D. (2017) *The role of biobased building materials in the climate impacts of construction: Effects of increased use of biobased materials in the Swedish building sector*. Doctoral dissertation, KTH Royal Institute of Technology, Sweden. <https://kth.diva-portal.org/smash/get/diva2:1096048/FULLTEXT01.pdf>.
- Penna, I. (2010) *Understanding the FAO's 'Wood Supply from Planted Forests' Projections*. 1 ed. University of Ballarat: Centre for Environmental Management.
- Perez Fernandez, N. (2012) *Therma performance of buildings with post-tensioned timber structure compared with concrete and steel alternatives*. Doctoral dissertation, University of Canterbury, UK. <https://core.ac.uk/download/pdf/35467597.pdf>.
- Petroudy, S.R.D. (2017) Physical and mechanical properties of natural fibers. In: Fan, M. and Fu, F. (ed.) *Advanced high strength natural fibre composites in construction*. Cambridge, UK: Woodhead Publishing. pp. 59-83.
- Pettersen, R.C. (1984) The chemical composition of wood. In: Rowell, R. (ed.) *The Chemistry of Solid Wood*. Washington, D.C.: ACS Publications. pp. 57-126.
- Philippe, F.X., Mahmoudi, Y., Cinq-Mars, D., Lefrançois, M., Moula, N., Palacios, J., Pelletier, F. and Godbout, S. (2020) Comparison of egg production, quality and composition in three production systems for laying hens. *Livestock Science*, 232. <https://doi.org/10.1016/j.livsci.2020.103917>
- Piani, T.L., Weerheijm, J., Peroni, M., Koene, L., Krabbenborg, D., Solomos, G. and Sluys, L.J. (2020) Dynamic behaviour of adobe bricks in compression: The role of fibres and water content at various loading rates. *Construction and Building Materials*, 230. <https://doi.org/10.1016/j.conbuildmat.2019.117038>
- Pickering, K.L., Efendy, M.G.A. and Le, T.M. (2016) A review of recent developments in natural fibre composites and their mechanical performance. *Composites Part A: Applied Science and Manufacturing*, 83, 98-112. <https://doi.org/10.1016/j.compositesa.2015.08.038>
- Pirayesh, H., Khanjanzadeh, H. and Salari, A. (2013) Effect of using walnut/almond shells on the physical, mechanical properties and formaldehyde emission of particleboard. *Composites Part B: Engineering*, 45 (1), 858-863. <https://doi.org/10.1016/j.compositesb.2012.05.008>
- Potter, D., Gao, F., Baggett, S., McKenna, J.R. and McGranahan, G.H. (2002) Defining the sources of Paradox: DNA sequence markers for North American walnut (*Juglans L.*) species and hybrids. *Scientia Horticulturae*, 94 (1-2), 157-170. [https://doi.org/10.1016/S0304-4238\(01\)00358-2](https://doi.org/10.1016/S0304-4238(01)00358-2)
- Prasad, K., Mathachan, N., James, P. and Justine, T.L. (2016) Effect of curing on soil stabilized with eggshell. *International Journal of Science and Technology & Engineering*, 2 (12), 259-264. <http://www.ijste.org/articles/IJSTE2112022.pdf>
- Praseeda, K.I., Reddy, B.V.V. and Mani, M. (2016) Embodied and operational energy of urban residential buildings in India. *Energy and Buildings*, 110, 211-219. <https://doi.org/10.1016/j.enbuild.2015.09.072>
- Purnomo, H. and Arini, S.W. (2019) Experimental Evaluation of Three Different Humidity Conditions to Physical and Mechanical Properties of Three Different Mixtures of Unfired Soil Bricks. *Makara Journal of Technology*, 23 (2), 92-102. <https://scholarhub.ui.ac.id/cgi/viewcontent.cgi?article=1377&context=mjt>
- Radivojević, A. and Đukanović, L. (2018) Material Aspect of Energy Performance and Thermal Comfort in Buildings. In: Konstantinou, T., Ignjatović, N. Č. and Zbašnik-Senegačnik, M. (ed.) *Energy: resources and building performance*. Delft, Netherlands: TU Delft Open. pp. 61-86.
- Rahmani-Sani, A., Singh, P., Raizada, P., Lima, E.C., Anastopoulos, I., Giannakoudakis, D.A., Sivamani, S., Dontsova, T.A. and Hosseini-Bandegharai, A. (2020) Use of chicken feather and eggshell to synthesize a novel magnetized activated carbon for sorption of heavy metal ions. *Bioresource Technology*, 297. <https://doi.org/10.1016/j.biortech.2019.122452>

- Ramesh, T., Prakash, R. and Shukla, K. (2010) Life cycle energy analysis of buildings: An overview. *Energy and Buildings*, 42 (10), 1592-1600. <https://doi.org/10.1016/j.enbuild.2010.05.007>
- Ramli, M., Kwan, W.H. and Abas, N.F. (2013) Strength and durability of coconut-fiber-reinforced concrete in aggressive environments. *Construction and Building Materials*, 38, 554-566. <https://doi.org/10.1016/j.conbuildmat.2012.09.002>
- Rashad, A.M. (2015) A brief on high-volume Class F fly ash as cement replacement-A guide for Civil Engineer. *International Journal of Sustainable Built Environment*, 4 (2), 278-306. <https://doi.org/10.1016/j.ijse.2015.10.002>
- Rathore, P.K.S., Shukla, S.K. and Gupta, N.K. (2020) Yearly analysis of peak temperature, thermal amplitude, time lag and decrement factor of a building envelope in tropical climate. *Journal of Building Engineering*, 31. <https://doi.org/10.1016/j.jobe.2020.101459>
- Rattanongphisat, W. and Rordprapat, W. (2014) Strategy for energy efficient buildings in tropical climate. *Energy Procedia*, 52, 10-17. <https://doi.org/10.1016/j.egypro.2014.07.049>
- Raut, A.N. and Gomez, C.P. (2017) Development of thermally efficient fibre-based eco-friendly brick reusing locally available waste materials. *Construction and Building Materials*, 133, 275-284. <https://doi.org/10.1016/j.conbuildmat.2016.12.055>
- Rawal, A., Shah, T. and Anand, S. (2010) Geotextiles: Production, properties and performance. *Textile Progress*, 42 (3), 181-226. <https://doi.org/10.1080/00405160903509803>
- Rawal, R., Maithel, S., Shukla, Y., Rana, S., Gowri, G., Patel, J. and Kumar, S. (2020) *Thermal performance of walling material and wall technology, Part-1* [online]  
Available at: [https://www.beepindia.org/wp-content/uploads/2020/08/Thermal-performance-of-walling-material-and-wall-Technology\\_Part-12\\_V2.pdf](https://www.beepindia.org/wp-content/uploads/2020/08/Thermal-performance-of-walling-material-and-wall-Technology_Part-12_V2.pdf)  
[Accessed: 10 July 2021]
- Rijal, H.B., Yoshida, H. and Umemiya, N. (2010) Seasonal and regional differences in neutral temperatures in Nepalese traditional vernacular houses. *Building and environment*, 45 (12), 2743-2753. <https://doi.org/10.1016/j.buildenv.2010.06.002>
- Riza, F.V., Rahman, I.A. and Zaidi, A.M.A. (2010) A brief review of compressed stabilized earth brick (CSEB). *2010 International Conference on Science and Social Research (CSSR 2010)* Kuala Lumpur, Malaysia, December 5-7.
- Rodriguez, C.M. and D'Alessandro, M. (2019) Indoor thermal comfort review: The tropics as the next frontier. *Urban Climate*, 29. <https://doi.org/10.1016/j.uclim.2019.100488>
- Rominiyi, O.L., Adaramola, B.A., Ikumapayi, O.M., Oginni, O.T. and Akinola, S.A. (2017) Potential Utilization of Sawdust in Energy, Manufacturing and Agricultural Industry; Waste to Wealth. *World Journal of Engineering and Technology*, 5 (03). <https://doi.org/10.4236/wjet.2017.53045>
- Sabbağ, N. and Uyanık, O. (2017) Prediction of reinforced concrete strength by ultrasonic velocities. *Journal of Applied Geophysics*, 141, 13-23. <https://doi.org/10.1016/j.jappgeo.2017.04.005>
- Sadeghifam, A.N., Marsono, A.K., Kiani, I., Isikdag, U., Bavafa, A.A. and Tabatabaee, S. (2016) Energy analysis of wall materials using building information modeling (BIM) of public buildings in the tropical climate countries. *Jurnal Teknologi*, 78 (10). <https://doi.org/10.11113/jt.v78.7591>
- Sadineni, S.B., Madala, S. and Boehm, R.F. (2011) Passive building energy savings: A review of building envelope components. *Renewable and Sustainable Energy Reviews*, 15 (8), 3617-3631. <https://doi.org/10.1016/j.rser.2011.07.014>
- Sahlol, D.G., Elbeltagi, E., Elzoughiby, M. and Abd Elrahman, M. (2021) Sustainable building materials assessment and selection using system dynamics. *Journal of Building Engineering*, 35. <https://doi.org/10.1016/j.jobe.2020.101978>

- Saint-Pierre, F., Philibert, A., Giroux, B. and Rivard, P. (2016) Concrete quality designation based on ultrasonic pulse velocity. *Construction and Building Materials*, 125, 1022-1027. <https://doi.org/10.1016/j.conbuildmat.2016.08.158>
- Salasinska, K., Barczewski, M., Górny, R. and Kloziński, A. (2018) Evaluation of highly filled epoxy composites modified with walnut shell waste filler. *Polymer Bulletin*, 75, 2511-2528. <https://doi.org/10.1007/s00289-017-2163-3>
- Salih, M.M., Osofero, A.I. and Imbabi, M.S. (2020) Critical review of recent development in fiber reinforced adobe bricks for sustainable construction. *Frontiers of Structural and Civil Engineering*, 14 (4), 839–854. <https://doi.org/10.1007/s11709-020-0630-7>
- Samuel, D.G.L., Dharmasastha, K., Nagendra, S.M.S. and Maiya, M.P. (2017) Thermal comfort in traditional buildings composed of local and modern construction materials. *International Journal of Sustainable Built Environment*, 6 (2), 463-475. <https://doi.org/10.1016/j.ijsbe.2017.08.001>
- Sandak, A., Sandak, J., Brzezicki, M. and Kutnar, A. (2019) *Bio-based building skin*. Singapore: Springer Nature.
- Sangma, S., Pohti, L. and Tripura, D.D. (2019) Size Effect of Fiber on Mechanical Properties of Mud Earth Blocks. In: Agnihotri, A. K., Reddy, K. R. and Bansal, A. (ed.) *Recycled Waste Materials*. Springer. pp. 119-125.
- Sarsari, N.A., Pourmousa, S. and Tajdini, A. (2016) Physical and mechanical properties of walnut shell flour-filled thermoplastic starch composites. *BioResources*, 11 (3), 6968-6983. <https://bioresources.cnr.ncsu.edu/resources/physical-and-mechanical-properties-of-walnut-shell-flour-filled-thermoplastic-starch-composites/>
- Savov, V., Mihajlova, J. and Grigorov, R. (2019) Selected physical and mechanical properties of combined wood based panels from wood fibers and sawdust. *Innovation in Woodworking Industry and Engineering Design* (2), 42-48. <https://inspectapedia.com/insulation/Wood-Based-Panel-Properties-Savov.pdf>
- Sayigh, A. (2019) *Sustainable Vernacular Architecture: How the Past Can Enrich the Future*. Springer, Cham.
- SBEM. (2018) *A Technical Manual for SBEM, UK Volume* [online]  
Available at: [https://www.uk-ncm.org.uk/filelibrary/SBEM-Technical-Manual\\_v5.2.g\\_20Nov15.pdf](https://www.uk-ncm.org.uk/filelibrary/SBEM-Technical-Manual_v5.2.g_20Nov15.pdf)  
[Accessed: 12 July 2020]
- Schiavoni, S., Bianchi, F. and Asdrubali, F. (2016) Insulation materials for the building sector: A review and comparative analysis. *Renewable and Sustainable Energy Reviews*, 62, 988-1011. <https://doi.org/10.1016/j.rser.2016.05.045>
- Schroeder, H. (2012) Modern earth building codes, standards and normative development. In: Hall, M. R., Lindsay, R. and Krayenhoff, M. (ed.) *Modern Earth Buildings: Materials, Engineering, Constructions and Applications*. Cambridge, UK: Woodhead Publishing. pp. 72-109.
- Serrano, S., Barreneche, C. and Cabeza, L.F. (2016) Use of by-products as additives in adobe bricks: Mechanical properties characterisation. *Construction and Building Materials*, 108, 105-111. <https://doi.org/10.1016/j.conbuildmat.2016.01.044>
- Shafiqh, P., Mahmud, H.B., Jumaat, M.Z.B., Ahmmad, R. and Bahri, S. (2014) Structural lightweight aggregate concrete using two types of waste from the palm oil industry as aggregate. *Journal of Cleaner Production*, 80, 187-196. <https://doi.org/10.1016/j.jclepro.2014.05.051>
- Sharma, V., Marwaha, B.M. and Vinayak, H.K. (2016) Enhancing durability of adobe by natural reinforcement for propagating sustainable mud housing. *International Journal of Sustainable Built Environment*, 5 (1), 141-155. <https://doi.org/10.1016/j.ijsbe.2016.03.004>

- Sharma, V., Vinayak, H.K. and Marwaha, B.M. (2015a) Enhancing compressive strength of soil using natural fibers. *Construction and Building Materials*, 93, 943-949. <https://doi.org/10.1016/j.conbuildmat.2015.05.065>
- Sharma, V., Vinayak, H.K. and Marwaha, B.M. (2015b) Enhancing sustainability of rural adobe houses of hills by addition of vernacular fiber reinforcement. *International Journal of Sustainable Built Environment*, 4 (2), 348-358. <https://doi.org/10.1016/j.ijbsbe.2015.07.002>
- Shaviv, E., Yezioro, A. and Capeluto, I.G. (2001) Thermal mass and night ventilation as passive cooling design strategy. *Renewable Energy*, 24 (3-4), 445-452. [https://doi.org/10.1016/S0960-1481\(01\)00027-1](https://doi.org/10.1016/S0960-1481(01)00027-1)
- Shubbar, A.A., Sadique, M., Kot, P. and Atherton, W. (2019) Future of clay-based construction materials-A review. *Construction and Building Materials*, 210, 172-187. <https://doi.org/10.1016/j.conbuildmat.2019.03.206>
- Shwetha, A., Dhananjaya, Shravana, K.S.M. and Ananda (2018) Ananda. Comparative study on calcium content in egg shells of different birds. *International Journal of Zoology Studies*, 3, 31-33. <http://www.zoologyjournals.com/archives/2018/vol3/issue4/3-4-18>
- Sidebotham, G. (2015) Heat Transfer Modes: Conduction, Convection, and Radiation. *Heat Transfer Modeling: An Inductive Approach*, 61-93. [https://link.springer.com/chapter/10.1007/978-3-319-14514-3\\_3](https://link.springer.com/chapter/10.1007/978-3-319-14514-3_3)
- Silva, L.C., Caldas, L.R., Paiva, R.L.M. and Filho, R.D.T. (2018) *Role of Bio-based Building Materials in Climate Change Mitigation: Special Report of the Brazilian Panel on Climate Change* [online] Available at: <https://drive.google.com/file/d/18fzyEAa1CIPSU7I9k-XWOEC6DNUiSV29/view> [Accessed: 12 July 2021]
- Singh, R.R. and Mittal, E.S. (2014) Improvement of local subgrade soil for road construction by the use of coconut coir fiber. *International Journal of Research in Engineering and Technology*, 3 (5), 707-711. <http://citeseerx.ist.psu.edu/viewdoc/download?doi=10.1.1.673.9620&rep=rep1&type=pdf>
- Sinka, M., Korjakins, A., Bajare, D., Zimele, Z. and Sahmenko, G. (2018) Bio-based construction panels for low carbon development. *Energy Procedia*, 147, 220-226. <https://doi.org/10.1016/j.egypro.2018.07.063>
- Sivakumar Babu, G.L. and Vasudevan, A.K. (2008) Strength and stiffness response of coir fiber-reinforced tropical soil. *Journal of Materials in Civil Engineering* 20 (9), 571-577. <https://ascelibrary.org/doi/pdf/10.1061/%28ASCE%290899-1561%282008%2920%3A9%28571%29>
- Sivapullaiah, P.V. and Jha, A.K. (2014) Gypsum induced strength behaviour of fly ash-lime stabilized expansive soil. *Geotechnical and Geological Engineering*, 32, 1261-1273. <https://doi.org/10.1007/s10706-014-9799-7>
- SLS 1382 (2009) *Specification for Compressed Stabilized Earth Blocks*. Colombo, Sri Lanka: Sri Lanka Standards Institution.
- Soares, N., Martins, C., Gonçalves, M., Santos, P., Da Silva, L.S. and Costa, J.J. (2019) Laboratory and in-situ non-destructive methods to evaluate the thermal transmittance and behavior of walls, windows, and construction elements with innovative materials: A review. *Energy and Buildings*, 182, 88-110. <https://doi.org/10.1016/j.enbuild.2018.10.021>
- Soebarto, V. (2009) Analysis of indoor performance of houses using rammed earth walls. *Eleventh International IBPSA Conference* Glasgow, Scotland July 27-30.
- Sousa, V. and Bogas, J.A. (2021) Comparison of energy consumption and carbon emissions from clinker and recycled cement production. *Journal of Cleaner Production*, 306. <https://doi.org/10.1016/j.jclepro.2021.127277>

- Souza, J.W.d.L., Jaques, N.G., Popp, M., Kolbe, J., Fook, M.V.L. and Wellen, R.M.R. (2019) Optimization of epoxy resin: an investigation of eggshell as a synergic filler. *Materials*, 12 (9). <https://doi.org/10.3390/ma12091489>
- Spiegel, R. and Meadows, D. (2010) *Green building materials: a guide to product selection and specification*. John Wiley & Sons.
- Srinivasan, A. and Viraraghavan, T. (2008) Removal of oil by walnut shell media. *Bioresource Technology*, 99 (17), 8217-8220. <https://doi.org/10.1016/j.biortech.2008.03.072>
- Stapulionienė, R., Vaitkus, S., Vėjelis, S. and Sankauskaitė, A. (2016) Investigation of thermal conductivity of natural fibres processed by different mechanical methods. *International Journal of Precision Engineering and Manufacturing*, 17 (10), 1371-1381. <https://doi.org/10.1007/s12541-016-0163-0>
- Statuto, D., Boichichio, M., Sica, C. and Picuno, P. (2018) Experimental development of clay bricks reinforced with agricultural by-products. *46th Symposium "Actual Tasks on Agricultural Engineering"*, Opatjia, Croatia, February 27-March 1.
- Stewart, M. (2021) *Surface Production Operations: Volume 5: Pressure Vessels, Heat Exchangers, and Aboveground Storage Tanks: Design, Construction, Inspection, and Testing*. Gulf Professional Publishing.
- Strzałkowski, J. and Garbalińska, H. (2018) Thermal simulation of building performance with different loadbearing materials. *IOP Conference Series: Materials Science and Engineering, Kraków*, 415. <https://doi.org/10.1088/1757-899X/415/1/012014>
- Subramanian, G.K.M., Balasubramanian, M. and Jeya Kumar, A.A. (2021) A Review on the Mechanical Properties of Natural Fiber Reinforced Compressed Earth Blocks. *Journal of Natural Fibers*. <https://doi.org/10.1080/15440478.2021.1958405>
- Šujanová, P., Rychtáriková, M., Sotto Mayor, T. and Hyder, A. (2019) A healthy, energy-efficient and comfortable indoor environment, a review. *Energies*, 12 (8). <https://doi.org/10.3390/en12081414>
- Suryanarayana, C. (2017) Microstructure: An Introduction. In: Prasad, N. E. and Wanhill, R. J. (ed.) *Aerospace Materials and Material Technologies*. Singapore: Springer. pp. 105-123.
- Syed, H., Nerella, R. and Madduru, S.R.C. (2020) Role of coconut coir fiber in concrete. *Materials Today: Proceedings*, 27, 1104-1110. <https://doi.org/10.1016/j.matpr.2020.01.477>
- Taallah, B. and Guettala, A. (2016) The mechanical and physical properties of compressed earth block stabilized with lime and filled with untreated and alkali-treated date palm fibers. *Construction and Building Materials*, 104, 52-62. <https://doi.org/10.1016/j.conbuildmat.2015.12.007>
- Taallah, B., Guettala, A., Guettala, S. and Kriker, A. (2014) Mechanical properties and hygroscopicity behavior of compressed earth block filled by date palm fibers. *Construction and Building Materials*, 59, 161-168. <https://doi.org/10.1016/j.conbuildmat.2014.02.058>
- Tangboriboon, N., Moonsri, S., Netthip, A. and Sirivat, A. (2016) Innovation of Embedding Eggshell to Enhance Physical-Mechanical-Thermal Properties in Fired Clay Bricks via Extrusion Process *MATEC Web of Conferences*, 78. <https://doi.org/10.1051/mateconf/20167801003>
- Tatane, M., Akhzouz, H., Elminor, H. and Feddaoui, M.b. (2018a) Thermal, Mechanical and Physical Behavior of Compressed Earth Blocks Loads by Natural Wastes. *International Journal of Civil Engineering and Technology*, 9, 1353-1368. [https://www.researchgate.net/publication/326187477\\_THERMAL\\_MECHANICAL\\_AND\\_PHYSICAL\\_BEHAVIOR\\_OF\\_COMPRESSED\\_EARTH\\_BLOCKS\\_LOADS\\_BY\\_NATURAL\\_WASTES](https://www.researchgate.net/publication/326187477_THERMAL_MECHANICAL_AND_PHYSICAL_BEHAVIOR_OF_COMPRESSED_EARTH_BLOCKS_LOADS_BY_NATURAL_WASTES)
- Tatane, M., Elminor, H., Ayeb, M., Lacherai, A., Feddaoui, M., Nouh, F.A. and Boukhattem, L. (2018b) Effect of argan nut shell powder on thermal and mechanical behavior of compressed earth blocks.

*International Journal of Applied Engineering Research*, 13 (7), 4740-4750.  
[https://www.iaeme.com/MasterAdmin/Journal\\_uploads/IJCIET/VOLUME\\_9\\_ISSUE\\_6/IJCIET\\_09\\_06\\_152.pdf](https://www.iaeme.com/MasterAdmin/Journal_uploads/IJCIET/VOLUME_9_ISSUE_6/IJCIET_09_06_152.pdf)

Tawasil, D.N.b., Aminudin, E., Lim, N.H.A.S., Soh, N.M.Z.N., Leng, P.C., Ling, G.H.T. and Ahmad, M.H. (2021) Coconut Fibre and Sawdust as Green Building Materials: A Laboratory Assessment on Physical and Mechanical Properties of Particleboards. *Buildings*, 11 (6).  
<https://doi.org/10.3390/buildings11060256>

Teixeira, E.R., Machado, G., P Junior, A.d., Guarnier, C., Fernandes, J., Silva, S.M. and Mateus, R. (2020) Mechanical and thermal performance characterisation of compressed earth blocks. *Energies*, 13 (11). <https://doi.org/10.3390/en13112978>

Thanushan, K. and Sathiparan, N. (2022) Mechanical performance and durability of banana fibre and coconut coir reinforced cement stabilized soil blocks. *Materialia*, 21.  
<https://doi.org/10.1016/j.mtla.2021.101309>

Thanushan, K., Yogananth, Y., Sangeeth, P., Coonghe, J.G. and Sathiparan, N. (2019) Strength and Durability Characteristics of Coconut Fibre Reinforced Earth Cement Blocks. *Journal of Natural Fibers*, 18 (6), 773-788. <https://doi.org/10.1080/15440478.2019.1652220>

The International Nut and Dried Fruit Council Foundation (INC) (2020) *Nuts & Dried Fruits Statistical Yearbook*.

Thiffault, E., Barrette, J., Blanchet, P., Nguyen, Q.N. and Adjalle, K. (2019) Optimizing quality of wood pellets made of hardwood processing residues. *Forests*, 10 (7). <https://doi.org/10.3390/f10070607>

Thormark, C. (2006) The effect of material choice on the total energy need and recycling potential of a building. *Building and Environment*, 41 (8), 1019-1026. <https://doi.org/10.1016/j.buildenv.2005.04.026>

Tiuc, A.E., Nemeş, O., Vermeşan, H. and Toma, A.C. (2019) New sound absorbent composite materials based on sawdust and polyurethane foam. *Composites Part B: Engineering*, 165, 120-130.  
<https://doi.org/10.1016/j.compositesb.2018.11.103>

Tong, J.C.K., Tse, J.M.Y. and Jones, P.J. (2018) Development of thermal evaluation tool for detached houses in Mongolia. *Energy and Buildings*, 173, 81-90. <https://doi.org/10.1016/j.enbuild.2018.05.026>

Tornay, N., Schoetter, R., Bonhomme, M., Faraut, S. and Masson, V. (2017) GENIUS: A methodology to define a detailed description of buildings for urban climate and building energy consumption simulations. *Urban Climate*, 20, 75-93. <https://doi.org/10.1016/j.uclim.2017.03.002>

Tran, K.Q., Satomi, T. and Takahashi, H. (2018) Improvement of mechanical behavior of cemented soil reinforced with waste cornsilk fibers. *Construction and Building Materials*, 178, 204-210.  
<https://doi.org/10.1016/j.conbuildmat.2018.05.104>

TS 2514 (1977) *Adobe Blocks and Production Methods [in Turkish]*. Ankara, Turkey: Turkish Standards Institute.

Turco, C., Junior, A.C.P., Teixeira, E.R. and Mateus, R. (2021) Optimisation of Compressed Earth Blocks (CEBs) using natural origin materials: A systematic literature review. *Construction and Building Materials*, 309. <https://doi.org/10.1016/j.conbuildmat.2021.125140>

Türkmen, İ., Ekinci, E., Kantarcı, F. and Sarıcı, T. (2017) The mechanical and physical properties of unfired earth bricks stabilized with gypsum and Elazığ Ferrochrome slag. *International Journal of Sustainable Built Environment*, 6 (2), 565-573. <https://doi.org/10.1016/j.ijbsbe.2017.12.003>

Udawattha, C., De Silva, D.E., Galkanda, H. and Halwatura, R. (2018) Performance of natural polymers for stabilizing earth blocks. *Materialia*, 2, 23-32. <https://doi.org/10.1016/j.mtla.2018.07.019>

Udawattha, C. and Halwatura, R. (2016) Thermal performance and structural cooling analysis of brick,

cement block, and mud concrete block. *Advances in Building Energy Research*, 12 (2), 150-163. <https://doi.org/10.1080/17512549.2016.1257438>

Uzun, B.B. and Yaman, E. (2017) Pyrolysis kinetics of walnut shell and waste polyolefins using thermogravimetric analysis. *Journal of the Energy Institute*, 90 (6), 825-837. <https://doi.org/10.1016/j.joei.2016.09.001>

Valero, L.R., Sasso, V.F. and Vicioso, E.P. (2019) In situ assessment of superficial moisture condition in façades of historic building using non-destructive techniques. *Case Studies in Construction Materials*, 10. <https://doi.org/10.1016/j.cscm.2019.e00228>

Van Damme, H. and Houben, H. (2018) Earth concrete. Stabilization revisited. *Cement and Concrete Research*, 114, 90-102. <https://doi.org/10.1016/j.cemconres.2017.02.035>

Vega, P., Juan, A., Guerra, M.I., Morán, J.M., Aguado, P.J. and Llamas, B. (2011) Mechanical characterisation of traditional adobes from the north of Spain. *Construction and Building Materials*, 25 (7), 3020-3023. <https://doi.org/10.1016/j.conbuildmat.2011.02.003>

Venkatesan, B., Lijina, V.J., Kannan, V. and Dhevasenaa, P.R. (2021) Partial replacement of fine aggregate by steel slag and coarse aggregate by walnut shell in concrete. *Materials Today: Proceedings*, 37, 1761-1766. <https://doi.org/10.1016/j.matpr.2020.07.361>

Verbeke, S. and Audenaert, A. (2018) Thermal inertia in buildings: A review of impacts across climate and building use. *Renewable and Sustainable Energy Reviews*, 82, 2300-2318. <https://doi.org/10.1016/j.rser.2017.08.083>

Vilane, B.R.T. (2010) Assessment of stabilisation of adobes by confined compression tests. *Biosystems Engineering*, 106, 551-558. <https://doi.org/10.1016/j.biosystemseng.2010.06.008>

Villamizar, M.C.N., Araque, V.S., Reyes, C.A.R. and Silva, R.S. (2012) Effect of the addition of coal-ash and cassava peels on the engineering properties of compressed earth blocks. *Construction and Building Materials*, 36, 276-286. <https://doi.org/10.1016/j.conbuildmat.2012.04.056>

Vincelas, F.F.C., Ghislain, T. and Robert, T. (2017) Effects of the type of building materials on the thermal behavior of building in the hot dry climates: A case study of Maroua city, Cameroon. *International Journal of Innovative Science, Engineering & Technology*, 4 (3). [https://ijiset.com/vol4/v4s3/IJISSET\\_V4\\_I03\\_01.pdf](https://ijiset.com/vol4/v4s3/IJISSET_V4_I03_01.pdf)

Vishwakarma, V. and Uthaman, S. (2020) Environmental impact of sustainable green concrete. In: Liew, M. S., Nguyen-Tri, P., Nguyen, T. A. and Kakooei, S. (ed.) *Smart Nanoconcretes and Cement-Based Materials: Properties, Modelling and Applications*. Elsevier. pp. 241-255.

Vodounon, N.A., Kanali, C. and Mwero, J. (2018) Compressive and flexural strengths of cement stabilized earth bricks reinforced with treated and untreated pineapple leaves fibres. *Open Journal of Composite Materials*, 8 (4), 145-160. <https://doi.org/10.4236/ojcm.2018.84012>

Vyncke, J., Kupers, L. and Denies, N. (2018) Earth as Building Material-an overview of RILEM activities and recent Innovations in Geotechnics. *MATEC Web of Conferences* 149. <https://doi.org/10.1051/mateconf/201814902001>

Waheed, M., Butt, M.S., Shehzad, A., Adzahan, N.M., Shabbir, M.A., Suleria, H.A.R. and Aadil, R.M. (2019) Eggshell calcium: A cheap alternative to expensive supplements. *Trends in Food Science & Technology*, 91, 219-230. <https://doi.org/10.1016/j.tifs.2019.07.021>

Waheed, M., Yousaf, M., Shehzad, A., Inam-Ur-Raheem, M., Khan, M.K.I., Khan, M.R., Ahmad, N. and Aadil, R.M. (2020) Channelling eggshell waste to valuable and utilizable products: a comprehensive review. *Trends in Food Science & Technology*. <https://doi.org/10.1016/j.tifs.2020.10.009>

Walia, S., Singh, G. and Singh, H. (2015) Effect of eggshell powder and stone dust on compaction characteristics and CBR value of clayey soil. *Proceedings of 50th Indian Geotechnical Conference*, Pune,

Maharashtra, India, December 17-19.

Walker, P., Keable, R., Martin, J. and Maniatidis, V. (2005) *Rammed Earth: Design and Construction Guidelines*. BREPress

Walker, P.J. (1995) Strength, durability and shrinkage characteristics of cement stabilised soil blocks. *Cement and Concrete Composites*, 17 (4), 301-310. [https://doi.org/10.1016/0958-9465\(95\)00019-9](https://doi.org/10.1016/0958-9465(95)00019-9)

Wang, W. and Huang, G. (2009) Characterisation and utilization of natural coconut fibres composites. *Materials & Design*, 30 (7), 2741-2744. <https://doi.org/10.1016/j.matdes.2008.11.002>

Wang, Z., Zhao, C., Zhang, Y., Hua, B. and Lu, X. (2019) Study on Strength Characteristics of Straw (EPS Particles)-Sparse Sludge Unburned Brick. *IOP Conference Series: Materials Science and Engineering*, 490 (3). <https://doi.org/10.1088/1757-899X/490/3/032005>

Watson, D. (1983) *Climatic Design: Energy-Efficient Building Principles and Practices*. NY, USA: McGraw Hill Higher Education.

Windapo, A. and Ogunsanmi, O. (2014) Construction sector views of sustainable building materials. *Proceedings of the institution of civil engineers-engineering sustainability*.

Wojtacha-Rychter, K., Kucharski, P. and Smolinski, A. (2021) Conventional and Alternative Sources of Thermal Energy in the Production of Cement-An Impact on CO<sub>2</sub> Emission. *Energies*, 14 (6). <https://doi.org/10.3390/en14061539>

Wonorahardjo, S., Sutjahja, I.M., Mardiyati, Y., Andoni, H., Thomas, D., Achsani, R.A. and Steven, S. (2020) Characterising thermal behaviour of buildings and its effect on urban heat island in tropical areas. *International Journal of Energy and Environmental Engineering*, 11, 129-142. <https://doi.org/10.1007/s40095-019-00317-0>

Xiao, N., Bock, P., Antreich, S.J., Staedler, Y.M., Schönerberger, J. and Gierlinger, N. (2020) From the soft to the hard: changes in microchemistry during cell wall maturation of walnut shells. *Frontiers in Plant Science*, 11. <https://doi.org/10.3389/fpls.2020.00466>

Yang, L., Yan, H. and Lam, J.C. (2014) Thermal comfort and building energy consumption implications—a review. *Applied Energy*, 115, 164-173. <https://doi.org/10.1016/j.apenergy.2013.10.062>

Yttrup, P.J., Diviny, K. and Sottile, F. (1981) Development of a drip test for the erodability of mud bricks. *School of Architecture, Deakin University*.

Zahedi, M., Pirayesh, H., Khanjanzadeh, H. and Tabar, M.M. (2013) Organo-modified montmorillonite reinforced walnut shell/polypropylene composites. *Materials & Design*, 51, 803-809. <https://doi.org/10.1016/j.matdes.2013.05.007>

Zak, P., Ashour, T., Korjenic, A., Korjenic, S. and Wu, W. (2016) The influence of natural reinforcement fibers, gypsum and cement on compressive strength of earth bricks materials. *Construction and Building Materials*, 106, 179-188. <https://doi.org/10.1016/j.conbuildmat.2015.12.031>

Zeghari, K., Gounni, A., Louahlia, H., Marion, M., Boutouil, M., Goodhew, S. and Streif, F. (2021) Novel Dual Walling Cob Building: Dynamic Thermal Performance. *Energies*, 14 (22). <https://doi.org/10.3390/en14227663>

Zhang, L., Yang, L., Jelle, B.P., Wang, Y. and Gustavsen, A. (2018a) Hygrothermal properties of compressed earthen bricks. *Construction and Building Materials*, 162, 576-583. <https://doi.org/10.1016/j.conbuildmat.2017.11.163>

Zhang, Q., Li, Y., Yu, C., Qi, J., Yang, C., Cheng, B. and Liang, S. (2020) Global timber harvest footprints of nations and virtual timber trade flows. *Journal of Cleaner Production*, 250. <https://doi.org/10.1016/j.jclepro.2019.119503>

- Zhang, Y., Li, N., Dong, L. and Lang, M. (2017) Study on modern application of traditional building materials based on geographical background. *UIA 2017 Seoul World Architects Congress* Seoul, South Korea, September 3-10.
- Zhang, Z., Wong, Y.C., Arulrajah, A. and Horpibulsuk, S. (2018b) A review of studies on bricks using alternative materials and approaches. *Construction and Building Materials*, 188, 1101-1118. <https://doi.org/10.1016/j.conbuildmat.2018.08.152>
- Zhao, D., Qian, X., Gu, X., Jajja, S.A. and Yang, R. (2016) Measurement techniques for thermal conductivity and interfacial thermal conductance of bulk and thin film materials. *Journal of Electronic Packaging*, 138 (4). <https://doi.org/10.1115/1.4034605>
- Zhao, S., Niu, J., Yun, L., Liu, K., Wang, S., Wen, J., Wang, H. and Zhang, Z. (2019a) The Relationship among the Structural, Cellular, and Physical Properties of Walnut Shells. *HortScience*, 54 (2), 275-281. <https://doi.org/10.21273/HORTSCI13381-18>
- Zhao, X., Mofid, S.A., Al Hulayel, M.R., Saxe, G.W., Jelle, B.P. and Yang, R. (2019b) Reduced-scale hot box method for thermal characterization of window insulation materials. *Applied Thermal Engineering*, 160. <https://doi.org/10.1016/j.applthermaleng.2019.114026>
- Zheng, K., Cho, Y.K., Wang, C. and Li, H. (2016) Noninvasive Residential Building Envelope R-Value Measurement Method Based on Interfacial Thermal Resistance. *Journal of Architectural Engineering*, 22 (4). <https://ascelibrary.org/doi/epdf/10.1061/%28ASCE%29AE.1943-5568.0000182>
- Zhu, L., Hurt, R., Correia, D. and Boehm, R. (2009) Detailed energy saving performance analyses on thermal mass walls demonstrated in a zero energy house. *Energy And Buildings*, 41 (3), 303-310. <https://doi.org/10.1016/j.enbuild.2008.10.003>
- Zhu, Z., Jin, X., Li, Q. and Meng, Q. (2015) Experimental study on the thermal performance of ventilation wall with cladding panels in hot and humid area. *Procedia Engineering*, 121, 410-414. <https://doi.org/10.1016/j.proeng.2015.08.1086>
- Zou, S., Li, H., Wang, S., Jiang, R., Zou, J., Zhang, X., Liu, L. and Zhang, G. (2020) Experimental research on an innovative sawdust biomass-based insulation material for buildings. *Journal of Cleaner Production*, 260. <https://doi.org/10.1016/j.jclepro.2020.121029>
- Zuo, J. and Zhao, Z.-Y. (2014) Green building research—current status and future agenda: A review. *Renewable and Sustainable Energy Reviews*, 30, 271-281. <https://doi.org/10.1016/j.rser.2013.10.021>

## Appendices

**Appendix A:** Physical properties tests results of stabilised clay blocks.

Mix ID	Density (kg/m <sup>3</sup> )	Av. density (kg/m <sup>3</sup> )	SD	CV (%)	Capillary water absorption coefficient (kg/m <sup>2</sup> .min <sup>0.5</sup> )	Av. capillary water absorption coefficient (kg/m <sup>2</sup> .min <sup>0.5</sup> )	SD	CV (%)	Linear shrinkage (%)	Av. linear shrinkage (%)	SD	CV (%)
REF-1	2084.48				0.173				8.05			
REF-2	2090.39	2090.96	6.78	0.32	0.178	0.178	0.005	2.81	8.08	8.07	0.02	0.26
REF-3	2098.01				0.183				8.09			
E-10-1	1974.16				0.171				6.92			
E-10-2	1975.71	1975.78	1.65	0.08	0.176	0.174	0.003	1.52	6.93	6.92	0.01	0.14
E-10-3	1977.45				0.175				6.91			
E-20-1	1924.96				0.169				6.23			
E-20-2	1917.19	1921.58	3.98	0.21	0.166	0.164	0.006	3.46	6.21	6.23	0.02	0.32
E-20-3	1922.60				0.158				6.25			
E-30-1	1882.45				0.160				5.97			
E-30-2	1880.22	1880.72	1.54	0.08	0.156	0.159	0.002	1.46	6.05	5.98	0.06	0.95
E-30-3	1879.49				0.160				5.94			
E-40-1	1847.50				0.151				5.84			
E-40-2	1841.52	1845.32	3.30	0.18	0.150	0.151	0.001	0.38	5.85	5.83	0.03	0.45
E-40-3	1846.93				0.151				5.80			

Appendix A: Physical properties tests results of stabilised clay blocks (continued).

Mix ID	Density (kg/m <sup>3</sup> )	Av. density (kg/m <sup>3</sup> )	SD	CV (%)	Capillary water absorption coefficient (kg/m <sup>2</sup> .min <sup>0.5</sup> )	Av. capillary water absorption coefficient (kg/m <sup>2</sup> .min <sup>0.5</sup> )	SD	CV (%)	Linear shrinkage (%)	Av. linear shrinkage (%)	SD	CV (%)
E-50-1	1786.94				0.161				5.58			
E-50-2	1793.34	1791.04	3.56	0.20	0.168	0.162	0.006	3.44	5.63	5.61	0.03	0.47
E-50-3	1792.84				0.157				5.62			
S-a-2.5-1	1861.99				0.200				6.19			
S-a-2.5-2	1860.95	1860.64	1.52	0.08	0.198	0.200	0.002	1.00	6.15	6.15	0.04	0.57
S-a-2.5-2	1858.99				0.202				6.12			
S-a-5-1	1796.09				0.223				6.33			
S-a-5-2	1794.63	1794.61	1.49	0.08	0.218	0.220	0.003	1.14	6.41	6.38	0.04	0.68
S-a-5-3	1793.11				0.220				6.40			
S-a-7.5-1	1707.95				0.228				6.53			
S-a-7.5-2	1705.45	1706.64	1.25	0.07	0.233	0.229	0.004	1.57	6.60	6.56	0.04	0.58
S-a-7.5-3	1706.53				0.226				6.54			
S-a-10-1	1610.73				0.235				7.25			
S-a-10-2	1611.88	1611.19	0.61	0.04	0.241	0.238	0.003	1.26	7.30	7.24	0.07	0.91
S-a-10-3	1610.94				0.238				7.17			
S-b-2.5-1	1837.11				0.197				6.19			
S-b-2.5-2	1838.52	1837.05	1.50	0.08	0.186	0.190	0.006	3.20	5.82	6.05	0.20	3.28
S-b-2.5-2	1835.52				0.187				6.13			

Appendix A: Physical properties tests results of stabilised clay blocks (continued).

Mix ID	Density (kg/m <sup>3</sup> )	Av. density (kg/m <sup>3</sup> )	SD	CV (%)	Capillary water absorption coefficient (kg/m <sup>2</sup> .min <sup>0.5</sup> )	Av. capillary water absorption coefficient (kg/m <sup>2</sup> .min <sup>0.5</sup> )	SD	CV (%)	Linear shrinkage (%)	Av. linear shrinkage (%)	SD	CV (%)
S-b-5-1	1734.93				0.210				5.87			
S-b-5-2	1738.34	1735.85	2.17	0.13	0.203	0.206	0.004	1.75	5.85	5.84	0.04	0.62
S-b-5-3	1734.30				0.205				5.80			
S-b-7.5-1	1637.42				0.209				5.64			
S-b-7.5-2	1638.34	1638.64	1.39	0.09	0.225	0.219	0.009	3.89	5.60	5.64	0.05	0.80
S-b-7.5-3	1640.16				0.222				5.69			
S-b-10-1	1476.55				0.224				5.53			
S-b-10-2	1475.93	1476.38	0.40	0.03	0.230	0.225	0.004	1.85	5.54	5.53	0.01	0.10
S-b-10-3	1476.67				0.222				5.53			
S-c-2.5-1	1775.93				0.193				6.05			
S-c-2.5-2	1784.21	1781.39	4.73	0.27	0.186	0.187	0.005	2.74	5.95	5.99	0.05	0.88
S-c-2.5-2	1784.02				0.183				5.97			
S-c-5-1	1679.01				0.199				5.46			
S-c-5-2	1678.90	1678.26	1.21	0.07	0.205	0.198	0.008	4.09	5.50	5.47	0.04	0.64
S-c-5-3	1676.86				0.189				5.43			
S-c-7.5-1	1588.10				0.200				4.93			
S-c-7.5-2	1586.10	1586.33	1.67	0.11	0.217	0.209	0.009	4.09	5.03	4.94	0.08	1.64
S-c-7.5-3	1584.79				0.210				4.87			

Appendix A: Physical properties tests results of stabilised clay blocks (continued).

Mix ID	Density (kg/m <sup>3</sup> )	Av. density (kg/m <sup>3</sup> )	SD	CV (%)	Capillary water absorption coefficient (kg/m <sup>2</sup> .min <sup>0.5</sup> )	Av. capillary water absorption coefficient (kg/m <sup>2</sup> .min <sup>0.5</sup> )	SD	CV (%)	Linear shrinkage (%)	Av. linear shrinkage (%)	SD	CV (%)
S-c-10-1	1423.84				0.227				4.50			
S-c-10-2	1423.55	1422.07	2.82	0.20	0.220	0.222	0.004	1.82	4.47	4.47	0.03	0.67
S-c-10-3	1418.82				0.220				4.44			
C-2.5-1	1728.92				0.223				8.04			
C-2.5-2	1726.44	1725.44	4.07	0.24	0.230	0.226	0.004	1.60	8.04	8.18	0.24	2.89
C-2.5-2	1720.96				0.225				8.45			
C-5-1	1635.89				0.232				8.53			
C-5-2	1636.93	1638.79	4.14	0.25	0.245	0.238	0.007	2.80	8.45	8.48	0.05	0.54
C-5-3	1643.53				0.236				8.45			
C-7.5-1	1551.95				0.243				8.91			
C-7.5-2	1548.63	1552.52	4.21	0.27	0.238	0.244	0.006	2.47	9.01	8.96	0.05	0.57
C-7.5-3	1556.99				0.250				8.94			
C-10-1	1380.70				0.258				12.32			
C-10-2	1381.49	1381.24	0.47	0.03	0.256	0.258	0.003	0.97	12.31	12.29	0.04	0.35
C-10-3	1381.52				0.261				12.24			
W-5-1	1894.15				0.178				6.94			
W-5-2	1895.14	1896.33	2.96	0.16	0.175	0.176	0.002	0.87	6.97	6.96	0.02	0.25
W-5-3	1899.70				0.176				6.97			

Appendix A: Physical properties tests results of stabilised clay blocks (continued).

Mix ID	Density (kg/m <sup>3</sup> )	Av. density (kg/m <sup>3</sup> )	SD	CV (%)	Capillary water absorption coefficient (kg/m <sup>2</sup> .min <sup>0.5</sup> )	Av. capillary water absorption coefficient (kg/m <sup>2</sup> .min <sup>0.5</sup> )	SD	CV (%)	Linear shrinkage (%)	Av. linear shrinkage (%)	SD	CV (%)
W-10-1	1810.68				0.170				6.42			
W-10-2	1809.30	1808.05	3.43	0.19	0.173	0.172	0.002	0.89	6.36	6.36	0.06	0.94
W-10-3	1804.17				0.172				6.30			
W-15-1	1698.04				0.166				5.36			
W-15-2	1713.02	1707.81	8.47	0.50	0.168	0.166	0.002	1.20	5.49	5.45	0.07	1.38
W-15-3	1712.37				0.164				5.49			
W-20-1	1643.44				0.161				4.42			
W-20-2	1642.57	1643.91	1.63	0.10	0.163	0.161	0.002	0.95	4.47	4.49	0.08	1.82
W-20-3	1645.72				0.160				4.58			
ES-b-2.5/10-1	1794.18				0.163				5.89			
ES-b-2.5/10-2	1788.29	1792.37	3.54	0.20	0.156	0.160	0.004	2.20	5.90	5.90	0.01	0.10
ES-b-2.5/10-3	1794.65				0.160				5.90			
ES-b-2.5/20-1	1720.91				0.170				5.38			
ES-b-2.5/20-2	1714.65	1718.63	3.45	0.20	0.168	0.175	0.010	5.97	5.35	5.36	0.02	0.28
ES-b-2.5/20-3	1720.31				0.187				5.36			
ES-b-2.5/30-1	1650.15				0.180				5.14			
ES-b-2.5/30-2	1643.96	1649.57	5.34	0.32	0.196	0.188	0.008	4.26	5.11	5.13	0.02	0.34
ES-b-2.5/30-3	1654.60				0.189				5.14			

Appendix A: Physical properties tests results of stabilised clay blocks (continued).

Mix ID	Density (kg/m <sup>3</sup> )	Av. density (kg/m <sup>3</sup> )	SD	CV (%)	Capillary water absorption coefficient (kg/m <sup>2</sup> .min <sup>0.5</sup> )	Av. capillary water absorption coefficient (kg/m <sup>2</sup> .min <sup>0.5</sup> )	SD	CV (%)	Linear shrinkage (%)	Av. linear shrinkage (%)	SD	CV (%)
EC-2.5/10-1	1672.09				0.181				8.12			
EC-2.5/10-2	1678.52	1675.35	3.22	0.19	0.185	0.185	0.004	2.16	8.08	8.08	0.04	0.43
EC-2.5/10-3	1675.45				0.189				8.05			
EC-2.5/20-1	1602.25				0.206				7.72			
EC-2.5/20-2	1602.08	1601.49	1.17	0.07	0.195	0.200	0.006	2.78	7.69	7.70	0.02	0.22
EC-2.5/20-3	1600.15				0.199				7.69			
EC-2.5/30-1	1531.01				0.212				7.33			
EC-2.5/30-2	1537.06	1535.55	4.00	0.26	0.221	0.214	0.006	2.92	7.51	7.40	0.09	1.28
EC-2.5/30-3	1538.57				0.209				7.37			
EW-5/10-1	1805.81				0.170				6.58			
EW-5/10-2	1817.78	1810.88	6.19	0.34	0.169	0.169	0.002	0.91	6.68	6.60	0.07	1.09
EW-5/10-3	1809.06				0.167				6.54			
EW-5/20-1	1751.93				0.162				5.99			
EW-5/20-2	1753.89	1755.07	3.86	0.22	0.162	0.163	0.001	0.71	5.84	5.90	0.08	1.38
EW-5/20-3	1759.38				0.164				5.86			
EW-5/30-1	1690.06				0.156				5.13			
EW-5/30-2	1676.60	1682.90	6.77	0.40	0.160	0.158	0.002	1.27	5.12	5.11	0.03	0.52
EW-5/30-3	1682.05				0.158				5.08			

**Appendix B: Mechanical properties tests results of stabilised clay blocks.**

Mix ID	Flexural strength (FS)						Air-dried Compressive strength (CS)						Oven-dried Compressive strength (CS)					
	Rupture Force (N)	Strength (MPa)	Av. FS (MPa)	SD	CV (%)	% increase/decrease in FS	Force (kN)	Stress (MPa)	Av. CS (MPa)	SD	CV (%)	% increase/decrease in CS	Force (kN)	Stress (MPa)	Av. CS (MPa)	SD	CV (%)	% increase/decrease in CS
REF-1	453	1.38					6.00	3.74					8.30	5.20				
REF-2	497	1.53	1.52	0.14	8.90	-	6.30	3.95	4.06	0.39	9.53	-	8.60	5.38	5.40	0.22	4.00	-
REF-3	535	1.65					7.20	4.49					9.00	5.63				
E-10-1	553	1.63					7.00	4.36					9.30	5.65				
E-10-2	578	1.70	1.68	0.04	2.59	10.53	7.40	4.62	4.54	0.16	3.44	11.82	9.90	6.19	6.02	0.32	5.33	11.48
E-10-3	580	1.71					7.40	4.64					9.90	6.22				
E-20-1	662	1.92					7.70	4.80					10.30	6.45				
E-20-2	691	2.01	1.99	0.06	2.95	30.92	7.70	4.83	4.88	0.11	2.33	20.20	10.60	6.61	6.57	0.11	1.67	21.67
E-20-3	698	2.03					8.10	5.01					10.70	6.66				
E-30-1	712	2.05					8.30	5.19					10.60	6.58				
E-30-2	748	2.16	2.12	0.06	2.87	45.39	8.20	5.11	5.24	0.16	3.07	29.06	10.70	6.68	6.67	0.09	1.35	23.52
E-30-3	750	2.15					8.70	5.42					10.80	6.76				
E-40-1	773	2.21					9.00	5.60					11.00	6.89				
E-40-2	792	2.25	2.24	0.03	1.36	47.37	9.10	5.68	5.68	0.08	1.32	39.90	11.00	6.89	6.92	0.05	0.67	28.15
E-40-3	798	2.27					9.20	5.75					11.20	6.97				
E-50-1	633	1.76					7.50	4.70					9.70	6.09				
E-50-2	656	1.83	1.81	0.04	2.41	19.08	7.60	4.77	4.77	0.07	1.36	17.49	10.20	6.40	6.36	0.26	4.04	17.78
E-50-3	661	1.84					7.70	4.83					10.50	6.60				

Appendix B: Mechanical properties tests results of stabilised clay blocks (continued).

Mix ID	Flexural strength (FS)						Air-dried Compressive strength (CS)						Oven-dried Compressive strength (CS)					
	Rupture Force (N)	Strength (MPa)	Av. FS (MPa)	SD	CV (%)	% increase/decrease in FS	Force (kN)	Stress (MPa)	Av. CS (MPa)	SD	CV (%)	% increase/decrease in CS	Force (kN)	Stress (MPa)	Av. CS (MPa)	SD	CV (%)	% increase/decrease in CS
S-a-2.5-1	593	1.68					6.50	4.03					8.50	5.32				
S-a-2.5-2	590	1.66	1.69	0.04	2.13	11.18	6.60	4.08	4.09	0.06	1.47	0.66	8.80	5.47	5.44	0.10	1.91	0.68
S-a-2.5-2	611	1.73					6.60	4.15					8.80	5.52				
S-a-5-1	537	1.55					6.00	3.77					7.90	4.95				
S-a-5-2	543	1.56	1.57	0.02	1.33	3.29	6.10	3.79	3.81	0.05	1.39	-6.16	8.00	5.01	5.03	0.09	1.82	-6.85
S-a-5-3	551	1.59					6.20	3.87					8.20	5.13				
S-a-7.5-1	486	1.42					5.60	3.51					7.40	4.64				
S-a-7.5-2	502	1.48	1.46	0.03	2.21	-3.95	5.70	3.56	3.55	0.04	1.14	-12.48	8.20	5.08	4.95	0.27	5.45	-8.33
S-a-7.5-3	503	1.47					5.70	3.59					8.20	5.13				
S-a-10-1	401	1.20					5.00	3.15					7.30	4.54				
S-a-10-2	415	1.24	1.26	0.07	5.72	-17.11	5.40	3.38	3.33	0.16	4.83	-17.98	7.30	4.57	4.58	0.05	1.12	-15.12
S-a-10-3	448	1.34					5.50	3.46					7.40	4.64				
S-b-2.5-1	690	1.97					7.30	4.54					10.00	6.22				
S-b-2.5-2	698	2.01	2.00	0.03	1.52	31.58	7.60	4.77	4.74	0.18	3.85	16.67	10.10	6.30	6.28	0.05	0.84	16.30
S-b-2.5-2	715	2.03					7.80	4.90					10.10	6.32				
S-b-5-1	640	1.82					6.80	4.26					9.00	5.63				
S-b-5-2	659	1.87	1.86	0.04	2.17	22.37	6.90	4.28	4.29	0.04	0.84	5.67	9.40	5.86	5.82	0.17	2.91	7.72
S-b-5-3	669	1.90					6.90	4.33					9.50	5.96				
S-b-7.5-1	581	1.64					6.60	4.13					8.50	5.32				
S-b-7.5-2	585	1.64	1.65	0.03	1.74	8.55	6.60	4.15	4.15	0.03	0.61	2.30	9.10	5.70	5.58	0.23	4.09	3.40
S-b-7.5-3	603	1.69					6.70	4.18					9.20	5.73				

Appendix B: Mechanical properties tests results of stabilised clay blocks (continued).

Mix ID	Flexural strength (FS)						Air-dried Compressive strength (CS)						Oven-dried Compressive strength (CS)					
	Rupture Force (N)	Strength (MPa)	Av. FS (MPa)	SD	CV (%)	% increase/decrease in FS	Force (kN)	Stress (MPa)	Av. CS (MPa)	SD	CV (%)	% increase/decrease in CS	Force (kN)	Stress (MPa)	Av. CS (MPa)	SD	CV (%)	% increase/decrease in CS
S-b-10-1	488	1.33					5.50	3.43					7.10	4.41				
S-b-10-2	498	1.36	1.36	0.04	2.58	-10.53	5.70	3.56	3.53	0.09	2.52	-13.05	7.80	4.85	4.74	0.29	6.07	-12.28
S-b-10-3	512	1.40					5.90	3.60					7.90	4.95				
S-c-2.5-1	573	1.59					5.80	3.59					8.30	5.16				
S-c-2.5-2	582	1.61	1.63	0.06	3.59	7.24	6.30	3.95	3.90	0.28	7.28	-4.02	8.30	5.21	5.23	0.04	0.78	-3.24
S-c-2.5-2	613	1.70					6.60	4.15					8.40	5.24				
S-c-5-1	515	1.41					5.40	3.41					7.30	4.59				
S-c-5-2	534	1.47	1.45	0.04	2.61	-4.61	5.60	3.46	3.45	0.04	1.05	-15.02	7.50	4.70	4.68	0.08	1.75	-13.33
S-c-5-3	539	1.48					5.60	3.48					7.60	4.75				
S-c-7.5-1	469	1.27					5.20	3.25					6.60	4.13				
S-c-7.5-2	474	1.29	1.28	0.01	0.90	-15.79	5.30	3.28	3.28	0.03	0.77	-19.29	7.10	4.41	4.35	0.20	4.62	-19.38
S-c-7.5-3	476	1.29					5.30	3.30					7.20	4.52				
S-c-10-1	377	1.01					4.90	3.07					6.20	3.90				
S-c-10-2	383	1.03	1.05	0.06	5.56	-30.92	5.10	3.20	3.17	0.09	2.69	-22.00	6.90	4.31	4.19	0.25	6.02	-22.41
S-c-10-3	418	1.12					5.20	3.23					7.00	4.36				
C-2.5-1	691	2.08					7.50	4.70					10.00	6.27				
C-2.5-2	708	2.14	2.14	0.05	2.36	40.79	7.60	4.72	4.78	0.13	2.66	17.73	10.40	6.48	6.49	0.23	3.55	20.19
C-2.5-2	721	2.18					7.90	4.93					10.80	6.73				
C-5-1	635	1.94					7.20	4.52					9.50	5.96				
C-5-2	654	1.99	1.99	0.05	2.27	30.92	7.30	4.59	4.58	0.05	1.12	12.81	10.10	6.30	6.22	0.23	3.71	15.19
C-5-3	668	2.03					7.40	4.62					10.20	6.40				

Appendix B: Mechanical properties tests results of stabilised clay blocks (continued).

Mix ID	Flexural strength (FS)						Air-dried Compressive strength (CS)						Oven-dried Compressive strength (CS)					
	Rupture Force (N)	Strength (MPa)	Av. FS (MPa)	SD	CV (%)	% increase/decrease in FS	Force (kN)	Stress (MPa)	Av. CS (MPa)	SD	CV (%)	% increase/decrease in CS	Force (kN)	Stress (MPa)	Av. CS (MPa)	SD	CV (%)	% increase/decrease in CS
C-7.5-1	545	1.69					7.00	4.36					9.20	5.73				
C-7.5-2	548	1.70	1.70	0.01	0.34	11.84	7.10	4.44	4.42	0.05	1.20	8.87	9.40	5.83	5.83	0.10	1.72	7.96
C-7.5-3	551	1.70					7.10	4.46					9.50	5.93				
C-10-1	431	1.54					6.60	4.13					9.00	5.60				
C-10-2	446	1.58	1.57	0.03	1.94	3.29	6.70	4.18	4.18	0.05	1.20	2.96	9.00	5.63	5.64	0.04	0.72	4.44
C-10-3	450	1.60					6.80	4.23					9.10	5.68				
W-5-1	486	1.35					5.80	3.64					8.10	5.03				
W-5-2	510	1.43	1.46	0.13	8.74	-3.98	6.10	3.79	3.83	0.21	5.42	-5.75	8.20	5.11	5.09	0.05	1.04	-5.74
W-5-3	567	1.60					6.50	4.05					8.20	5.13				
W-10-1	347	0.96					5.30	3.30					7.30	4.59				
W-10-2	365	1.01	1.02	0.07	6.43	-32.84	5.40	3.35	3.39	0.11	3.24	-16.58	7.40	4.62	4.63	0.04	0.87	-14.32
W-10-3	396	1.09					5.60	3.51					7.50	4.67				
W-15-1	228	0.60					4.70	2.94					5.10	3.17				
W-15-2	248	0.65	0.67	0.08	12.22	-55.74	5.10	3.17	3.12	0.16	5.16	-23.15	6.00	3.77	3.59	0.36	10.08	-33.58
W-15-3	288	0.76					5.20	3.25					6.10	3.82				
W-20-1	175	0.45					4.30	2.63					5.00	3.10				
W-20-2	193	0.50	0.49	0.04	7.36	-67.83	4.30	2.66	2.68	0.06	2.12	-34.07	5.50	3.46	3.36	0.22	6.66	-37.84
W-20-3	200	0.52					4.40	2.74					5.60	3.51				
ES-b-2.5/10-1	578	1.68					6.60	4.15					9.00	5.65				
ES-b-2.5/10-2	583	1.69	1.70	0.03	1.56	11.84	6.90	4.31	4.35	0.22	5.12	7.14	9.20	5.75	5.82	0.21	3.67	7.78
ES-b-2.5/10-3	596	1.73					7.40	4.59					9.70	6.06				

Appendix B: Mechanical properties tests results of stabilised clay blocks (continued).

Mix ID	Flexural strength (FS)						Air-dried Compressive strength (CS)						Oven-dried Compressive strength (CS)					
	Rupture Force (N)	Strength (MPa)	Av. FS (MPa)	SD	CV (%)	% increase/decrease in FS	Force (kN)	Stress (MPa)	Av. CS (MPa)	SD	CV (%)	% increase/decrease in CS	Force (kN)	Stress (MPa)	Av. CS (MPa)	SD	CV (%)	% increase/decrease in CS
ES-b-2.5/20-1	529	1.51					6.50	4.03					8.70	5.40				
ES-b-2.5/20-2	548	1.55	1.55	0.05	2.90	2.63	6.50	4.08	4.07	0.04	0.89	0.25	8.70	5.42	5.44	0.05	0.97	0.74
ES-b-2.5/20-3	563	1.60					6.60	4.10					8.90	5.50				
ES-b-2.5/30-1	504	1.42					6.20	3.84					8.30	5.16				
ES-b-2.5/30-2	510	1.43	1.44	0.03	1.84	-6.58	6.20	3.87	3.89	0.07	1.75	-4.19	8.30	5.19	5.19	0.03	0.49	-3.89
ES-b-2.5/30-3	522	1.47					6.40	3.97					8.30	5.21				
EC-2.5/10-1	573	1.70					6.90	4.28					9.50	5.91				
EC-2.5/10-2	600	1.81	1.78	0.07	4.13	17.11	7.10	4.40	4.49	0.27	6.06	10.59	9.60	6.01	6.02	0.12	1.92	11.48
EC-2.5/10-3	612	1.84					7.70	4.80					9.80	6.14				
EC-2.5/20-1	553	1.61					6.40	4.03					8.70	5.42				
EC-2.5/20-2	560	1.62	1.62	0.02	0.94	7.24	6.60	4.13	4.10	0.06	1.41	0.99	9.00	5.57	5.54	0.11	1.95	2.59
EC-2.5/20-3	563	1.64					6.60	4.13					9.00	5.63				
EC-2.5/30-1	445	1.28					6.20	3.84					8.30	5.20				
EC-2.5/30-2	547	1.56	1.47	0.16	11.20	-3.29	6.20	3.90	3.91	0.08	2.07	-3.69	8.30	5.20	5.21	0.01	0.22	-3.52
EC-2.5/30-3	548	1.57					6.40	4.00					8.30	5.22				
EW-5/10-1	486	1.40					5.90	3.64					7.80	4.90				
EW-5/10-2	487	1.41	1.42	0.02	1.47	-6.87	6.00	3.74	3.76	0.13	3.49	-7.39	7.90	4.93	4.95	0.07	1.37	-8.27
EW-5/10-3	498	1.44					6.20	3.90					8.10	5.03				
EW-5/20-1	444	1.26					5.10	3.20					6.40	4.03				
EW-5/20-2	453	1.28	1.28	0.03	1.96	-15.67	5.20	3.25	3.30	0.14	4.18	-18.64	7.40	4.64	4.53	0.46	10.13	-16.05
EW-5/20-3	460	1.31					5.50	3.46					7.90	4.93				

*Appendix B: Mechanical properties tests results of stabilised clay blocks (continued).*

Mix ID	Flexural strength (FS)						Air-dried Compressive strength (CS)						Oven-dried Compressive strength (CS)					
	Rupture Force (N)	Strength (MPa)	Av. FS (MPa)	SD	CV (%)	% increase/decrease in FS	Force (kN)	Stress (MPa)	Av. CS (MPa)	SD	CV (%)	% increase/decrease in CS	Force (kN)	Stress (MPa)	Av. CS (MPa)	SD	CV (%)	% increase/decrease in CS
EW-5/30-1	270	0.76					4.70	2.92					5.20	3.23				
EW-5/30-2	288	0.81	0.83	0.08	9.98	-45.57	4.80	2.97	2.98	0.06	2.02	-26.68	5.30	3.28	3.37	0.21	6.12	-37.53
EW-5/30-3	328	0.92					4.90	3.04					5.80	3.61				

**Appendix C: UPV test results of stabilised clay blocks.**

<b>Mix ID</b>	<b>Direction</b>	<b>Velocity (m/s)</b>	<b>Average velocity (m/s)</b>
REF	L	1099	1257.67
	W	1291	
	H	1383	
E-10	L	1278	1263.00
	W	1286	
	H	1225	
E-20	L	1308	1361.33
	W	1361	
	H	1415	
E-30	L	1380	1420.00
	W	1418	
	H	1462	
E-40	L	1405	1453.33
	W	1431	
	H	1524	
E-50	L	1360	1350.67
	W	1346	
	H	1346	
S-b-2.5	L	1447	1560.33
	W	1448	
	H	1786	
S-b-5	L	1404	1464.33
	W	1397	
	H	1592	
S-b-7.5	L	1349	1381.67
	W	1340	
	H	1456	
S-b-10	L	1297	1318.33
	W	1294	
	H	1364	
C-2.5	L	1357	1384.67
	W	1304	
	H	1493	
C-5	L	1294	1293.67
	W	1262	
	H	1325	

*Appendix C: UPV test results of stabilised clay blocks (continued).*

<b>Mix ID</b>	<b>Direction</b>	<b>Velocity (m/s)</b>	<b>Average velocity (m/s)</b>
C-7.5	L	1173	1193.67
	W	1194	
	H	1214	
C-10	L	1114	1123.00
	W	1098	
	H	1157	
ES-b-2.5/10	L	1285	1337.67
	W	1353	
	H	1375	
ES-b-2.5/20	L	1259	1313.67
	W	1331	
	H	1351	
ES-b--2.5/30	L	1219	1247.67
	W	1300	
	H	1224	
EC-2.5/10	L	1298	1267.00
	W	1285	
	H	1218	
EC-2.5/20	L	1201	1183.33
	W	1203	
	H	1146	
EC-2.5/30	L	1175	1130.33
	W	1122	
	H	1094	

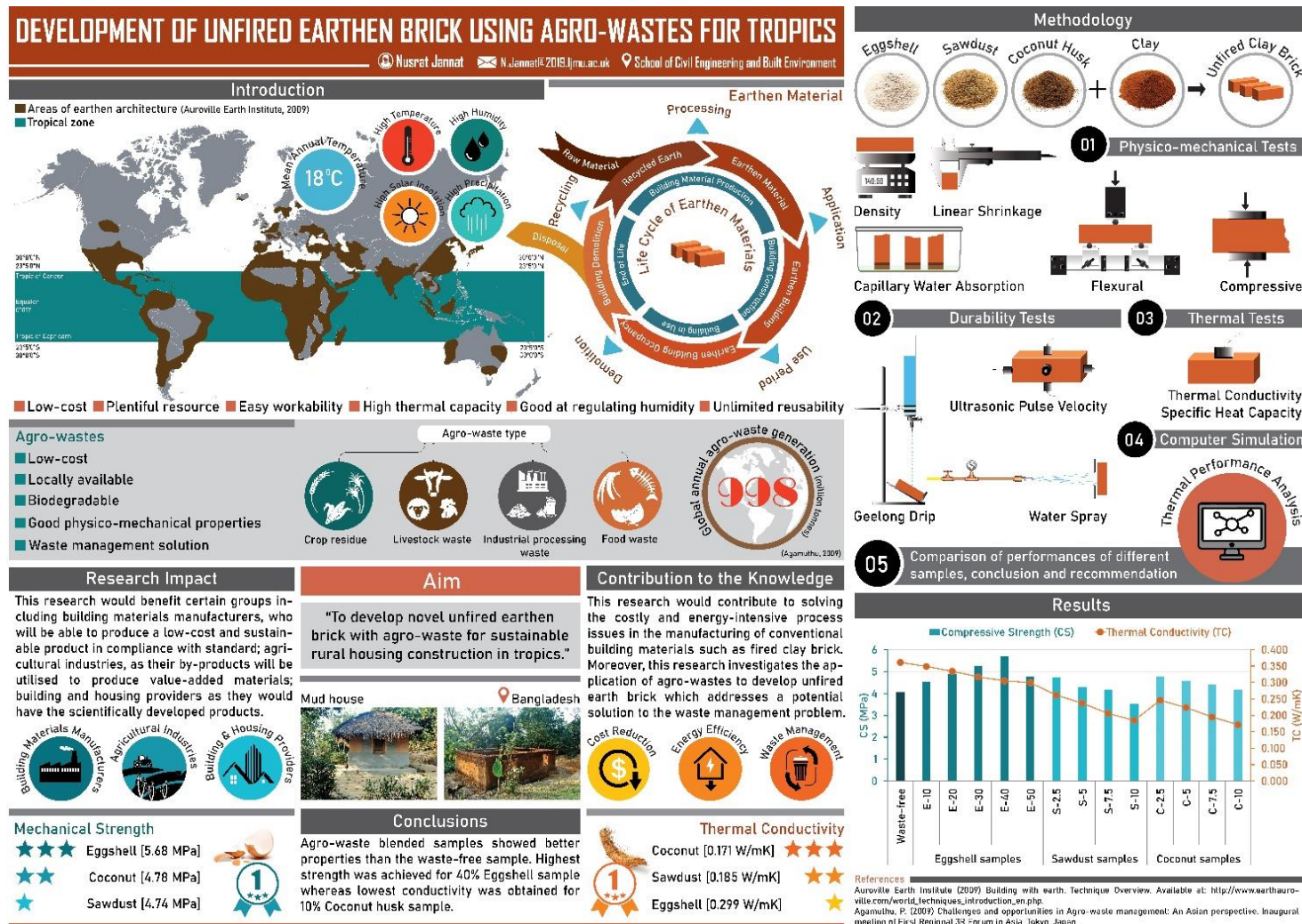
**Appendix D: Water spray test results of stabilised clay blocks.**

<b>Mix ID</b>	<b>Erosion</b>			
	<b>15 min (mm)</b>	<b>30 min (mm)</b>	<b>45 min (mm)</b>	<b>60 min (mm)</b>
REF	18.54	27.10	37.64	44.94
E-10	14.75	25.47	33.19	39.45
E-20	14.79	25.12	30.63	36.52
E-30	12.91	20.53	29.57	35.92
E-40	9.06	20.24	23.54	30.88
E-50	14.48	23.82	33.00	38.47
S-b-2.5	10.58	16.34	20.47	22.46
S-b-5	11.63	16.83	20.81	25.95
S-b-7.5	12.04	17.58	21.05	27.71
S-b-10	17.20	21.43	25.95	28.68
C-2.5	14.71	21.30	26.60	32.56
C-5	16.65	22.84	28.63	33.49
C-7.5	17.61	24.30	30.53	38.78
C-10	22.04	26.00	34.79	40.63
ES-b-2.5/10	13.22	20.21	28.50	33.05
ES-b-2.5/20	16.38	21.28	28.07	35.91
ES-b-2.5/30	18.04	26.99	31.33	36.79
EC-2.5/10	10.98	20.93	33.10	38.84
EC-2.5/20	16.10	23.56	34.83	40.09
EC-2.5/30	17.60	29.45	36.80	40.38

**Appendix E:** Thermal properties tests results of stabilised clay blocks.

Sample ID	Thermal conductivity, $\lambda$ (W/mK)		Volumetric heat capacity, $\rho C_p \times 10^{-6}$ (J/m <sup>3</sup> K)	
	Measurement 1	Measurement 2	Measurement 1	Measurement 2
REF	0.361	0.362	1.658	1.666
E-10	0.349	0.349	1.595	1.587
E-20	0.334	0.334	1.572	1.577
E-30	0.318	0.316	1.567	1.562
E-40	0.306	0.305	1.557	1.551
E-50	0.300	0.299	1.532	1.538
S-b-2.5	0.261	0.262	1.511	1.517
S-b-5	0.238	0.237	1.471	1.478
S-b-7.5	0.206	0.205	1.422	1.414
S-b-10	0.184	0.185	1.359	1.350
C-2.5	0.246	0.246	1.469	1.460
C-5	0.224	0.223	1.405	1.412
C-7.5	0.194	0.196	1.380	1.371
C-10	0.171	0.172	1.300	1.309

**Appendix F: Posters on the development of agro-wastes incorporated unfired earthen material to improve indoor thermal comfort in tropics.**

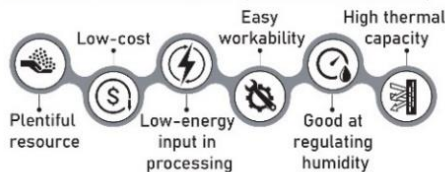


## Introduction

### Why Earth?



■ Areas of earthen architecture (Auroville Earth Institute 2009)



### Why Stabilisation?

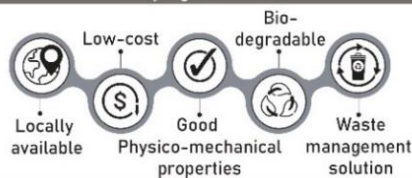
To overcome the drawbacks of earthen materials

### Drawbacks

- ▶ Excessive water absorption causing cracks
- ▶ Deterioration by frequent wetting & drying
- ▶ Low strength
- ▶ Massive wall thickness
- ▶ Low resistance to abrasion

Earthen materials

### Why Agro-wastes?



# DEVELOPMENT OF BIO-BASED EARTHEN MATERIAL TO IMPROVE INDOOR THERMAL COMFORT IN TROPICS

Nusrat Jannat

N.Jannat@2019.ijmu.ac.uk

Earthen architecture in developing countries



“When the indoor thermal conditions are not controlled by mechanical means, the materials affect the temperatures of both the indoor air and surfaces and thus have a very pronounced effect on the occupant comfort. Even when control is used, in the form of heating or air-conditioning for instance, the thermophysical properties of the materials used determine the amount of heating or cooling which is provided and also the temperature of the internal surfaces (radiant temperature). Therefore, even in these circumstances, the materials have an effect on the comfort of the occupants, as well as on the economical efficiency of the control systems (Givoni, 1976).”

## Methodology

Selected agro-wastes



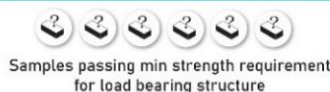
### 1 Characterisation of raw materials



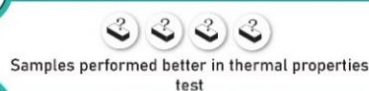
### 2 Sample preparation



### 3 Physical & Mechanical properties tests



### 4 Thermal properties tests



### 5 Simulation analysis

Comparison of performances of different samples, conclusion and recommendation

## Aim

“To develop novel bio-based earthen material for sustainable rural housing construction in tropics.”

## Research Impact

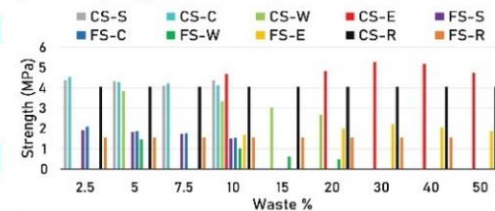
This research would be supportive of particular groups including:



## Preliminary tests (Mechanical strength tests)



Samples in moulds Flexural strength test Compressive strength test  
FS=Flexural strength; CS=Compressive strength; R=Reference sample (Waste-free); E=Eggshell; S=Sawdust; C=Coconut husk; W=Walnut shell



## Conclusions

Eggshell, Sawdust and Coconut husk addition improved the strength while Walnut shell decreased the strength compared to the Reference sample.



References  
Auroville Earth Institute (2009) Building with earth. Technique Overview. Available at: [http://www.earthauroville.com/world\\_techniques\\_introduction\\_en.php](http://www.earthauroville.com/world_techniques_introduction_en.php)  
Givoni, B. (1976) Man, Climate and Architecture. Applied Science Publishers, Ltd., London.  
Agamuthu, P. (2009) Challenges and opportunities in Agro-waste management: An Asian perspective. Inaugural meeting of First Regional 3R Forum in Asia, Tokyo, Japan.

# THE DOCTORAL ACADEMY

## Poster Competition 2022 Mid-Later Stage Category Winner

Nusrat Jannat



Professor Keith George  
Pro-Vice Chancellor for Research,  
Scholarship and Knowledge Transfer



Professor Julie Sheldon  
Dean, The Doctoral Academy



# THE DOCTORAL ACADEMY



## Poster Competition later-stage PGR category Winner 2021

**Nusrat Jannat**



Professor Ian G Campbell  
Vice-Chancellor and Chief Executive



Professor Keith George  
Pro-Vice Chancellor for Research,  
Scholarship and Knowledge Transfer



Professor Julie Sheldon  
Dean, The Doctoral Academy



## Development of bio-based unfired earthen material to improve indoor thermal comfort in tropics

Nusrat Jannat\*, Rafal Latif Al-Mufti\*, Badr Abdullah\*, Allison Cotgrave\*, Asel Hussien\*

\*School of Civil Engineering and Built Environment, Liverpool John Moores University, Byrom Street, Liverpool, L3 3AF, UK

\*Department of Architectural Engineering, University of Sharjah, Sharjah, United Arab Emirates

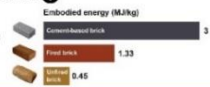
### Abstract

Indoor environment quality (IEQ) is one of the major health concerns in the world. Among various variables of IEQ, thermal comfort is a key component that is influenced by the design techniques and materials used in building. Hence, it has become a priority to find ways to improve IEQ by using environmentally friendly building materials. The production process of conventional building materials like concrete and fired brick, consumes a high amount of energy which has a negative effect on the environment. On the other hand, local materials such as earth can be a good option for building construction because of its availability as well as low environmental impact. Over many years, scientists have introduced various additives into the earthen matrix in order to enhance its performance. At the same time, in developing countries, waste disposal from the agricultural sector raises another serious concern. However, recent studies have presented that these wastes have a high potential to be used in manufacturing building materials on account of their good physico-mechanical properties. The proposed work aims at using agricultural wastes (Sawdust, Eggshell, Coconut husk and Walnut shell) to produce unfired earthen blocks with improved properties. The laboratory tests will be conducted to measure the physical, mechanical, durability and thermal properties of the waste incorporated unfired earthen blocks. Furthermore, results acquired from the laboratory tests will be used for indoor climate simulation to make a clear evaluation of the performance of the developed materials when exposed to dynamic weather conditions. Finally, the study will propose the most suitable material composition which will perform better in the studied climatic zone meeting the applicability, compatibility and actual requirements.

### INTRODUCTION

#### Why unfired earthen materials?

- Plentiful resource
- Low-cost
- Low energy input in processing
- Easy workability
- Good at regulating humidity
- High thermal capacity
- Unlimited reusability



### PROBLEM STATEMENT

#### Why stabilisation?

##### Drawbacks

- Excessive water absorption causing cracks
- Deterioration by frequent wetting & drying
- Low strength
- Massive wall thickness
- Low resistance to abrasion

##### Earthen materials



“When the indoor thermal conditions are not controlled by mechanical means, the materials affect the temperatures of both the indoor air and surfaces and thus have a very pronounced effect on the occupant comfort. Even when control is used, in the form of heating or air-conditioning for instance, the thermophysical properties of the materials used determine the amount of heating or cooling which is provided and also the temperature of the internal surfaces (radiant temperature). Therefore, even in these circumstances, the materials have an effect on the comfort of the occupants, as well as on the economical efficiency of the control systems (Gleason, 1970)”

#### Why agro-waste?

- Locally available
- Low-cost
- Biodegradable
- Good physico-mechanical properties
- Solution to waste management problem

### AIM

To develop novel bio-based unfired earthen material for sustainable rural housing construction in tropics.

### METHODOLOGY

1. Characterisation of raw materials
  - Clay
  - Particle size
  - Chemical composition
  - Morphology
2. Specimens preparation
  - Clay
  - Stabilisers
3. Physical & Mechanical properties tests
  - Samples passing through requirement for load bearing structure
4. Durability tests
  - Samples performed better in durability test
5. Thermal properties tests
  - Samples performed better in thermal properties test
6. Simulation analysis
  - Comparison of performance of different samples
  - Conclusion and recommendation

### Standards for unfired brick

Standard	Compressive strength	Flexural strength
Sri Lankan Standard: SLS 1362	2.80 MPa	-
New Mexico Earthen Building Code	2.06 MPa	0.35 MPa
New Zealand Standard: NZS 04299	1.30 MPa	0.25 MPa

### Selected agro-wastes

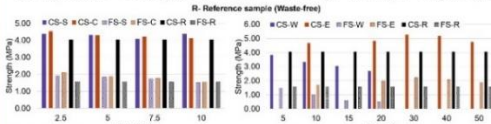


### PRELIMINARY TESTS

#### Flexural Strength (FS) & Compressive Strength (CS)



R- Reference sample (Waste-free)



### CONCLUSIONS

- Preliminary test results reveal that all the samples meet the minimum strength requirement of the standards (1.30-2.80 MPa).
- Except the samples with Walnut shell (W), samples containing Eggshell (E), Sawdust (S) and Coconut Husk (C) showed higher strength than the waste-free sample (CS-R, FS-R).
- The highest strength was achieved at 30% Eggshell content.

### RESEARCH IMPACT

This research would be supportive of particular groups including:



### REFERENCES

American Earth Institute (2009) Building with earth. Technical Overview. Available at: [http://www.earthinstitute.com/earth\\_techniques\\_123001\\_01\\_01.pdf](http://www.earthinstitute.com/earth_techniques_123001_01_01.pdf)

Gleason, B. (1976) Man, Climate and Architecture. 2nd ed. Applied Science Publishers, Ltd, London.

Faculty of Engineering & Technology

The Award for Best Potential Impact  
First Place  
at Postgraduate Research Day 2021  
is awarded to:

**Nusrat Jannat**

Signed: Faculty PVC *N. Jannat* 19<sup>th</sup> May 2021  
Dated

Article

# Thermophysical Properties of Sawdust and Coconut Coir Dust Incorporated Unfired Clay Blocks

Nusrat Jannat <sup>1,2,\*</sup> , Jeff Cullen <sup>1</sup>, Badr Abdullah <sup>1</sup> , Rafal Latif Al-Mufti <sup>1</sup> and Karyono Karyono <sup>1,3</sup> 

<sup>1</sup> School of Civil Engineering & Built Environment, Liverpool John Moores University, Byrom Street, Liverpool L3 3AF, UK

<sup>2</sup> Department of Architecture, Chittagong University of Engineering & Technology, Chattogram 4349, Bangladesh

<sup>3</sup> Faculty of Engineering and Informatics, Universitas Multimedia Nusantara, Scientia Garden, Gading Serpong, Tangerang 15810, Indonesia

\* Correspondence: n.jannat@2019.ljmu.ac.uk

**Abstract:** Sawdust and coconut coir dust are agro-wastes/by-products which are suitable for use as raw materials to manufacture unfired clay blocks due to their excellent physical and mechanical properties. A limited number of studies have been conducted on the utilisation of these agro-wastes in clay block production, and they have mostly been devoted to investigating the physico-mechanical properties, with less attention given to the thermal properties. Moreover, the majority of the studies have used chemical binders (cement and lime) in combination with agro-waste, thus increasing the carbon footprint and embodied energy of the samples. Furthermore, no research has been performed on the thermal performance of these agro-wastes when incorporated into clay blocks at the wall scale. Therefore, to address these limitations, the present study developed unfired clay blocks incorporating sawdust and coconut coir dust (0, 2.5, 5, and 7.5% by weight), without the use of chemical binders, and evaluated their thermal performance, both at the individual and wall scales. The experiments were divided into two phases. In the first phase, individual sample blocks were tested for basic thermal properties. Based on the results of the first phase, small walls with dimensions of 310 mm × 215 mm × 100 mm were built in the second phase, using the best performing mixture from each waste type, and these were assessed for thermal performance using an adapted hot box method. The thermal performance of the walls was evaluated by measuring the heat transfer rate from hot to cold environments and comparing the results to the reference wall. The results showed that thermal conductivity decreased from 0.36 W/mK for the reference sample, to 0.19 W/mK for the 7.5% coconut coir dust sample, and 0.21 W/mK for the 7.5% sawdust sample, indicating an improvement in thermal insulation. Furthermore, the coconut coir dust and sawdust sample walls showed a thermal resistance improvement of around 48% and 35%, respectively, over the reference sample wall. Consequently, the findings of this study will provide additional essential information that will help in assessing the prospective applications of sawdust and coconut coir dust as the insulating material for manufacturing unfired clay blocks.

**Keywords:** agro-wastes; clay blocks; thermal; unfired; wall



**Citation:** Jannat, N.; Cullen, J.; Abdullah, B.; Latif Al-Mufti, R.; Karyono, K. Thermophysical Properties of Sawdust and Coconut Coir Dust Incorporated Unfired Clay Blocks. *Constr. Mater.* **2022**, *2*, 234–257. <https://doi.org/10.3390/constrmater2040016>

Received: 25 August 2022

Accepted: 28 September 2022

Published: 8 October 2022

**Publisher's Note:** MDPI stays neutral with regard to jurisdictional claims in published maps and institutional affiliations.



Copyright © 2022 by the authors. Licensee MDPI, Basel, Switzerland. This article is an open access article distributed under the terms and conditions of the Creative Commons Attribution (CC BY) license (<https://creativecommons.org/licenses/by/4.0/>).

## 1. Introduction

The tropics survey report [1] states that over half of the world's population will be residing in tropical regions by 2050, resulting in a considerable rise in demand for indoor thermal comfort. The high temperatures and high humidity features of tropical climates necessitate the development of high thermal resistance building technologies to improve thermal comfort in residential housing. Since the Intergovernmental Panel on Climate Change [2] predicts an increase in global mean surface air temperature of +1.3 to +4.5 °C by the end of the twenty-first century, thermal comfort improvement in this

Article

# Eggshell and Walnut Shell in Unburnt Clay Blocks

Nusrat Jannat <sup>1,\*</sup>, Rafal Latif Al-Mufti <sup>1</sup> and Aseel Hussien <sup>2</sup>

<sup>1</sup> School of Civil Engineering & Built Environment, Liverpool John Moores University, Liverpool L3 3AF, UK; r.a.latifalmufti@ljmu.ac.uk

<sup>2</sup> Department of Architectural Engineering, University of Sharjah, Sharjah 341246, United Arab Emirates; ahussien@sharjah.ac.ae

\* Correspondence: n.jannat@2019.ljmu.ac.uk

**Abstract:** Agricultural residues/by-products have become a popular choice for the manufacturing of building materials due to their cost-effectiveness and environmental friendliness, making them a viable option for achieving sustainability in the construction sector. This study addresses the utilisation of two agro-wastes, i.e., eggshell and walnut shell, in the manufacture of unburnt clay blocks. The experiments were carried out on three series of samples in which first eggshell (10–50%) and walnut shell (5–20%) were incorporated individually and then combined (5% walnut, 10–30% eggshell) in the mixture to assess their influences on the physical and mechanical properties of the unburnt clay blocks. This study performed the following tests: Density, capillary water absorption, linear shrinkage, flexural and compressive strength. The results indicated that eggshell enhanced the strength relative to the control sample when the materials were employed individually, but walnut shell lowered it. Moreover, combining the two materials in the mixer reduced the strength of the samples even further. Nevertheless, the inclusion of the waste materials decreased the density, capillary water absorption coefficient and linear shrinkage of the samples. The findings indicate that eggshell has great potential for unburnt clay block manufacture. However, walnut shell integration needs further research.

**Keywords:** clay blocks; eggshell; mechanical properties; physical properties; unburnt; walnut shell



Citation: Jannat, N.;

Latif Al-Mufti, R.; Hussien, A.

Eggshell and Walnut Shell in Unburnt Clay Blocks. *CivilEng* **2022**, *3*, 263–276. <https://doi.org/10.3390/civileng3020016>

Academic Editor: Aires Camões

Received: 24 February 2022

Accepted: 25 March 2022

Published: 1 April 2022

**Publisher's Note:** MDPI stays neutral with regard to jurisdictional claims in published maps and institutional affiliations.



Copyright: © 2022 by the authors. Licensee MDPI, Basel, Switzerland. This article is an open access article distributed under the terms and conditions of the Creative Commons Attribution (CC BY) license (<https://creativecommons.org/licenses/by/4.0/>).

## 1. Introduction

It is well acknowledged that the application of building materials has a substantial influence on the environment because of embodied energy and the challenges of disposal of particular materials. Hence, new approaches for the manufacture of building materials are essential. One approach for lowering the negative environmental effect of building materials and reducing the consumption of material resources is to utilise the waste materials to manufacture building materials. Agricultural industries produce a large amount of wastes and by-products that can be an important source of raw materials for different industrial sectors, including building material construction. Walnut shell is an agricultural residue/by-product that is either burnt or disposed of in landfills. According to the report, worldwide walnut production reached around 965,400 tonnes in 2019 [1] and given that the shell accounts for almost 67% of the total fruit weight, this equates to 646,818 tonnes of walnut shells per year [2,3]. Figure 1 shows the leading walnut-producing countries [4]. The hydrophobic elements (lignin, 50.3%) in walnut shells are more abundant than hygroscopic materials (cellulose (23.9%) and hemicellulose (22.4%)) [5,6]. The lower water absorption, higher strength and bio-resistance characteristics of walnut shell have made it popular in the building construction industry. Studies have been conducted using walnut shell in the production of bio-composite [7–13], particleboard [14,15], MDF panels [16,17] and as an aggregate substitute in concrete [18–22]. However, the use of walnut shells in the production of unburnt clay brick is rarely mentioned in the literature. Mirón et al. [23] used different percentages of walnut shell (5–20%) to develop compressed earth blocks in two series of experiments. One series



ELSEVIER

Contents lists available at ScienceDirect

## Construction and Building Materials

journal homepage: [www.elsevier.com/locate/conbuildmat](http://www.elsevier.com/locate/conbuildmat)

## Influences of agro-wastes on the physico-mechanical and durability properties of unfired clay blocks

Nusrat Jannat<sup>a,c,\*</sup>, Rafal Latif Al-Mufti<sup>a</sup>, Aseel Hussien<sup>b</sup>, Badr Abdullah<sup>a</sup>, Alison Cotgrave<sup>a</sup>

<sup>a</sup> School of Civil Engineering & Built Environment, Liverpool John Moores University, Byrom Street, Liverpool L3 3AF, United Kingdom

<sup>b</sup> Department of Architectural Engineering, University of Sharjah, Sharjah 341246, United Arab Emirates

<sup>c</sup> Department of Architecture, Chittagong University of Engineering & Technology, Chattogram 4349, Bangladesh

## ARTICLE INFO

**Keywords:**  
 Agro-wastes  
 Durability properties  
 Mechanical properties  
 Physical properties  
 Unfired clay blocks

## ABSTRACT

The increasing demand for construction materials along with the challenge of waste management has necessitated the development of sustainable materials utilising wastes properly. Therefore, this research examines the utilisation of various agricultural wastes, such as Eggshell Powder (ESP), Sawdust Powder (SDP) and Coconut Husk Powder (CHP), in the production of unfired clay blocks. Samples were made with various percentages of wastes: 10–50% of dry wt. of clay for ESP and 2.5–10% for SDP and CHP. In this study, the physico-mechanical and durability properties of unfired clay blocks were investigated by conducting density, linear shrinkage, capillary water absorption, flexural strength, compressive strength, ultrasonic pulse velocity test, drip test and water spray test. The tests were carried out in two phases, with the first phase including the individual integration of waste in the mixture and the second phase combining ESP (10–30%) with the optimum SDP (2.5%) and CHP (2.5%). The test results show that when the additives were used individually, the 40% ESP samples performed the best whereas for SDP and CHP 2.5% content showed better performance. Contrarily, the samples' overall characteristics deteriorated when ESP, SDP, and CHP were used together. Nevertheless, all the samples met the strength requirement of the standards and passed the durability tests. The results of this study might be useful in assessing the potential of ESP, SDP and CHP for the production of unfired clay blocks as well as finding a feasible solution to the waste management problem.

### 1. Introduction

Currently, a new awareness of the application of sustainable and healthy materials in the construction sector is emerging in both developing and developed countries. The manufacturing processes of conventional building materials like concrete and fired earth bricks are not only expensive but also has negative environmental effects such as excessive energy demand and greenhouse gas emissions [1–3]. On the other hand, unfired earthen materials require approximately 99% less energy for the manufacturing process compared to concrete [4] and have less embodied energy (0.45 MJ/kg) than fired earth bricks (3 MJ/kg) [5]. There are also many other benefits for unfired earthen building materials, including regionally available raw materials, easy-to-construct, cost-effective, good hygrothermal properties and ease of recycling with minimum environmental effects [6–8]. Hence, unfired earthen materials are gaining growing attention as natural sustainable materials for building construction. However, there are some

disadvantages associated with earthen structures such as poor mechanical and durability properties as well as regular repair [9–12]. Consequently, researchers have experimented with different additives and stabilisation techniques to enhance its properties and a substantial number of studies on this issue have been published in recent decades [13–15]. These investigations indicate that different stabilisers impart strength and durability to earthen materials to different extents depending on the chemical compositions and physico-mechanical properties of individual stabiliser. Researchers have suggested many kinds of man-made stabilisers such as cement, lime, plastic waste, synthetic fibre etc. to improve the performance of the earthen materials [16–20]. Cement, though, is a source of CO<sub>2</sub> emissions from these stabilisers, is the most commonly used one [21–23]. The use of man-made stabilisers, on the other hand, lowers the “green” aspects of earthen materials by increasing embodied energy levels and reducing the recycling potential of demolished wastes. To overcome this, the utilisation of natural materials such as agricultural residues for earth stabilisation is

\* Corresponding author at: School of Civil Engineering & Built Environment, Liverpool John Moores University, Byrom Street, Liverpool L3 3AF, United Kingdom.  
 E-mail address: [n.jannat@2019.ljmu.ac.uk](mailto:n.jannat@2019.ljmu.ac.uk) (N. Jannat).

<https://doi.org/10.1016/j.conbuildmat.2021.126011>

Received 20 October 2021; Received in revised form 19 November 2021; Accepted 3 December 2021

Available online 11 December 2021

0950-0618/© 2021 Elsevier Ltd. All rights reserved.

Article

# Influence of Sawdust Particle Sizes on the Physico-Mechanical Properties of Unfired Clay Blocks

Nusrat Jannat <sup>1,\*</sup>, Rafal Latif Al-Mufti <sup>1</sup>, Aseel Hussien <sup>2</sup>, Badr Abdullah <sup>1</sup>  and Alison Cotgrave <sup>1</sup>

<sup>1</sup> School of Civil Engineering & Built Environment, Liverpool John Moores University, Byrom Street, Liverpool L3 3AF, UK; R.A.LatifAlMufti@ljmu.ac.uk (R.L.A.-M.); B.M.Abdullah@ljmu.ac.uk (B.A.); A.J.Cotgrave@ljmu.ac.uk (A.C.)

<sup>2</sup> Department of Architectural Engineering, University of Sharjah, Sharjah 341246, United Arab Emirates; ahussien@sharjah.ac.ae

\* Correspondence: N.Jannat@2019.ljmu.ac.uk

**Abstract:** Sawdust, which is a waste/by-product of the wood/timber industry, can be utilised as a valuable raw material in building material production due to its abundance and low cost. However, the application of sawdust in the manufacture of unfired clay blocks has received little investigation. Furthermore, the impact of different sawdust particle sizes on the properties of unfired clay blocks has not been studied. Therefore, this study screened sawdust at three different particle sizes: SP-a ( $212 \mu\text{m} < x < 300 \mu\text{m}$ ), SP-b ( $425 \mu\text{m} < x < 600 \mu\text{m}$ ) and SP-c ( $1.18 \text{mm} < x < 2.00 \text{mm}$ ), to examine their effects on the physical and mechanical properties of unfired clay blocks. The density, linear shrinkage, capillary water absorption and flexural and compressive strengths were among the tests performed. Different sawdust percentages, i.e., 2.5%, 5%, 7.5% and 10% of the total weight of the clay, were considered. The tests results show that when sawdust was added to the mixture, the density of the samples reduced for all particle sizes. However, the linear shrinkage increased in SP-a samples but decreased in the other two particle size samples as the sawdust percentage increased from 2.5% to 10%. On the other hand, the capillary water absorption coefficient increased while the strength decreased with increasing sawdust content for all three groups. The highest compressive strength (CS) and flexural strength (FS) were achieved at 2.5% of sawdust content. Furthermore, it was observed that SP-b (CS—4.74 MPa, FS—2.00 MPa) samples showed the highest strength followed by SP-a (CS—4.09 MPa, FS—1.69 MPa) and SP-c (CS—3.90 MPa, FS—1.63 MPa) samples. Consequently, good-quality unfired clay blocks can be manufactured using sawdust up to 2.5% with particle sizes ranging between 600 and 425  $\mu\text{m}$ .

**Keywords:** wood by-products; sawdust; particle size; clay blocks; unfired



**Citation:** Jannat, N.; Latif Al-Mufti, R.; Hussien, A.; Abdullah, B.; Cotgrave, A. Influence of Sawdust Particle Sizes on the Physico-Mechanical Properties of Unfired Clay Blocks. *Designs* **2021**, *5*, 57. <https://doi.org/10.3390/designs5030057>

Academic Editor: Tiago Ribeiro

Received: 14 August 2021

Accepted: 13 September 2021

Published: 14 September 2021

**Publisher's Note:** MDPI stays neutral with regard to jurisdictional claims in published maps and institutional affiliations.



**Copyright:** © 2021 by the authors. Licensee MDPI, Basel, Switzerland. This article is an open access article distributed under the terms and conditions of the Creative Commons Attribution (CC BY) license (<https://creativecommons.org/licenses/by/4.0/>).

## 1. Introduction

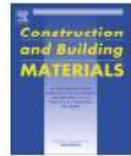
Currently, there is a great interest in adopting alternative sustainable building materials in the construction industry, and researchers have been engaged in manufacturing novel building materials utilising different wastes/by-products. In this context, the social, economic and environmental sustainability of earthen building materials enhanced with agricultural wastes/by-products has become apparent. These materials require less energy to process and offer good technical characteristics. Sawdust is considered as a waste material which is a by-product of the wood/timber industry and produced by the cutting, sawing or grinding of timber. Every year, sawmills produce huge volumes of sawdust [1,2] (Figure 1). According to one report, the average annual growth rate of the global wood harvest was 0.20% between 1990 and 2015 [3], and the FAO estimates a 55% increase in the potential industrial roundwood supply by 2030 [4]. As a result, the timber industry is becoming more concerned about the cost-effective disposal of sawdust as the bulk of it is burned off, polluting the environment [5–7]. Sawdust, on the other hand, can be used as a valuable raw material in a variety of industries due to its abundance



Contents lists available at ScienceDirect

# Construction and Building Materials

journal homepage: [www.elsevier.com/locate/conbuildmat](http://www.elsevier.com/locate/conbuildmat)



## Review

### Utilisation of nut shell wastes in brick, mortar and concrete: A review

Nusrat Jannat<sup>a,c,\*</sup>, Rafal Latif Al-Mufti<sup>a</sup>, Aseel Hussien<sup>b</sup>, Badr Abdullah<sup>a</sup>, Alison Cotgrave<sup>a</sup>



<sup>a</sup> School of Civil Engineering & Built Environment, Liverpool John Moores University, Byrom Street, Liverpool L3 3AF, United Kingdom

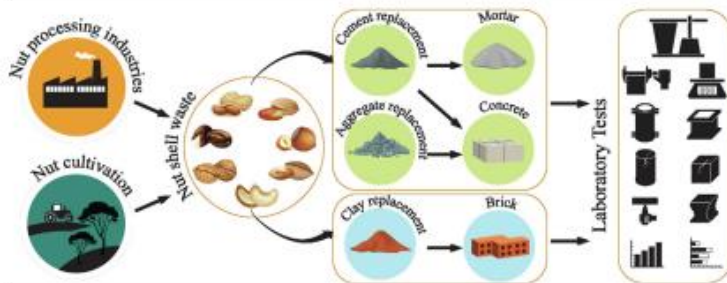
<sup>b</sup> Department of Architectural Engineering, University of Sharjah, Sharjah, United Arab Emirates

<sup>c</sup> Department of Architecture, Chittagong University of Engineering & Technology, Chattogram 4349, Bangladesh

#### HIGHLIGHTS

- Utilisation of nut shell wastes in brick, mortar and concrete is reviewed.
- Different properties of the developed materials are discussed.
- Findings are compared with related standards.
- Further investigations on the durability and thermal properties are required.

#### GRAPHICAL ABSTRACT



#### ARTICLE INFO

##### Article history:

Received 27 December 2020  
 Received in revised form 23 March 2021  
 Accepted 30 April 2021  
 Available online 11 May 2021

##### Keywords:

Brick  
 Concrete  
 Mortar  
 Nut shell waste  
 Replacement

#### ABSTRACT

Currently, growing activities in the construction sector have resulted in a rapid depletion of natural resources for building material production. On the other hand, agricultural industries generate a huge amount of residues/by-products every year around the world creating environmental concerns since most of these residues are burnt or disposed to the landfill. However, several current studies have presented the potential application of agricultural wastes in building material production owing to good physical and mechanical properties. Moreover, utilisation of such waste materials can contribute to reducing environmental impacts by proving alternative waste management strategies worldwide. This paper reviews some of the nut shell wastes (Argan nut, Brazil nut, Cashew nut, Groundnut, Hazelnut, Pistachio, Shea nut and Walnut) for the production of three groups of materials i.e. brick, mortar and concrete. Different properties of brick, mortar and concrete when admixed with nut shell wastes are discussed and compared with related standards. The review of literature exhibited an obvious potential of the nut shell waste as a partial replacement of conventional materials since most of the developed materials comply with the standards. However, a lack of studies on durability and thermal properties is observed. Besides, existing studies are inadequate to ascertain the potentiality of these wastes for reuse in building materials production. Therefore, extensive research is required to enhance the existing knowledge in this domain to achieve sustainable objectives in the construction industry.

© 2021 Elsevier Ltd. All rights reserved.

\* Corresponding author at: School of Civil Engineering & Built Environment, Liverpool John Moores University, Byrom Street, Liverpool L3 3AF, United Kingdom.

E-mail addresses: [N.Jannat@2019.ljmu.ac.uk](mailto:N.Jannat@2019.ljmu.ac.uk), [nusrat\\_arch0715@gmail.com](mailto:nusrat_arch0715@gmail.com) (N. Jannat), [R.A.LatifAlMufti@ljmu.ac.uk](mailto:R.A.LatifAlMufti@ljmu.ac.uk) (R. Latif Al-Mufti), [ahussien@sharjah.ac.ae](mailto:ahussien@sharjah.ac.ae) (A. Hussien), [B.M.Abdullah@ljmu.ac.uk](mailto:B.M.Abdullah@ljmu.ac.uk) (B. Abdullah), [A.J.Cotgrave@ljmu.ac.uk](mailto:A.J.Cotgrave@ljmu.ac.uk) (A. Cotgrave).

<https://doi.org/10.1016/j.conbuildmat.2021.123546>  
 0950-0618/© 2021 Elsevier Ltd. All rights reserved.

Article

# A Comparative Simulation Study of the Thermal Performances of the Building Envelope Wall Materials in the Tropics

Nusrat Jannat <sup>\*</sup>, Aseel Hussien, Badr Abdullah  and Alison Cotgrave

Department of Built Environment, Liverpool John Moores University, Liverpool L3 3AF, UK; A.Hussien@ljmu.ac.uk (A.H.); B.M.Abdullah@ljmu.ac.uk (B.A.); A.J.Cotgrave@ljmu.ac.uk (A.C.)

<sup>\*</sup> Correspondence: N.Jannat@2019.ljmu.ac.uk

Received: 14 May 2020; Accepted: 12 June 2020; Published: 15 June 2020



**Abstract:** The building walls which form the major part of the building envelope thermally interact with the changing surrounding environment throughout the day influencing the indoor thermal comfort of the space. This paper aims at assessing in detail the different aspects (thermophysical properties, thickness, exposure to solar heat gain, etc.) of opaque building wall materials affecting the indoor thermal environment and energy efficiency of the buildings in tropical climate (in the summer and winter days) by conducting simplified simulation analysis using the Integrated Environmental Solutions Virtual Environment (IES-VE) program. Besides, the thermal efficiency of a number of selected wall materials with different thermal properties and wall configurations was analysed to determine the most optimal option for the studied climate. This study first developed the conditions for parametric simulation analysis and then addressed selected findings by comparing the thermal responses of the materials to moderate outdoor temperature and energy-saving potential. While energy consumption estimation for a complete operational building is a complex method by which the performance of the wall materials cannot be properly defined, as a result, this simplistic simulation approach can guide the designers to preliminary analyse the different building wall materials in order to select the best thermal efficiency solution.

**Keywords:** dynamic simulation; energy performance; thermal comfort; tropics; wall materials

## 1. Introduction

Indoor environment quality is one of the major health concerns in the world as people spend about 80–90% of their time at home or other public indoor environments [1]. Thermal comfort is a key variable of indoor environment quality which is influenced by the design techniques and materials used in building [2,3]. According to how materials respond to the climate, the human settlement environment on earth can be categorised into the heat preservation priority and heat insulation priority climate zones. In the heat preservation priority climate, building materials are used to prevent the external heat gain (hot zone) or internal heat loss (cold zone) since there is a wide disparity between the indoor and outdoor temperatures. On the other hand, heat insulation priority climate zone consists of the tropical and subtropical regions where high humidity, temperatures, and solar radiation are the major stresses. Therefore, materials in this area are mainly used for solving the sun shading and heat insulation [4,5]. According to the State of the Tropics survey, about 50% of the world's inhabitants would live in the tropical regions before 2050 and consequently the demand for indoor thermal comfort in this region is increasing dramatically [6]. Currently, most of the tropical developing countries are facing difficulties in achieving indoor thermal comfort in the absence of mechanical control because of inappropriate building design. Besides, limited access to energy resources (energy poverty) is another



## Review

## Application of agro and non-agro waste materials for unfired earth blocks construction: A review



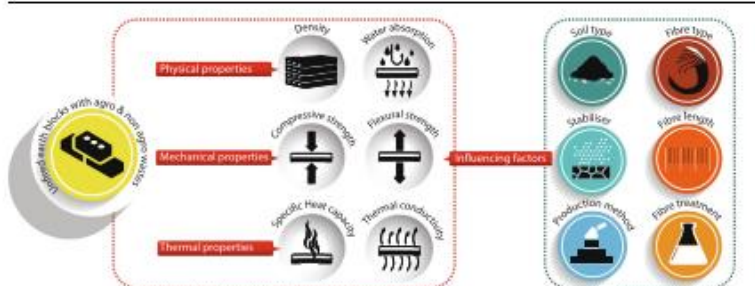
Nusrat Jannat\*, Aseel Hussien, Badr Abdullah, Alison Cotgrave

Built Environment and Sustainable Technologies (BEST) Research Institute, Department of Built Environment, Liverpool John Moores University, Byram Street, Liverpool L3 3AF, UK

## HIGHLIGHTS

- Application of agro and non-agro wastes in unfired earth blocks is reviewed.
- Physico-mechanical and thermal properties of the composites are discussed.
- Test results are compared with relevant standards.
- Further studies on the development of guidelines and standards are required.

## GRAPHICAL ABSTRACT



## ARTICLE INFO

## Article history:

Received 28 January 2020  
 Received in revised form 21 March 2020  
 Accepted 24 April 2020  
 Available online 30 April 2020

## Keywords:

Agro waste  
 Earth block  
 Non-agro waste  
 Sustainability  
 Unfired

## ABSTRACT

The production process of conventional building materials consumes a high amount of energy which has a negative impact on the environment. The use of locally available materials and upgradation of traditional techniques can be a good option for sustainable development. Consequently, earth has attracted the attention of the researchers as a building construction material for its availability and lower environmental impact. On the other hand, in developing countries waste disposal from the agricultural and industrial sectors raises another serious concern. The scientists have introduced such waste additives into the earth matrix to improve its performance. Therefore, the present paper reviews the state-of-the-art of research on the effects of these various agro and non-agro wastes in the production of unfired earth blocks. This study is divided into three sections: The first section outlines the different types of waste materials and earth blocks considered in the selected papers. The second part deals in depth with the test results of the different properties (density, water absorption, compressive strength, flexural strength and thermal conductivity) of unfired earth blocks containing waste materials. The last section analyses and compares the results with the current earth-building construction standards. The literature survey presents that the waste materials have a clear potential to partly replace earth by complying with certain requirements. Moreover, the application of such wastes for the development of building construction materials provides a solution that decreases energy usage as well as contributes to effective waste management. Future research on establishing guidelines and standards for the development and production of these sustainable unfired earth building materials is recommended.

© 2020 Elsevier Ltd. All rights reserved.

\* Corresponding author.

E-mail addresses: [N.Jannat@2019.ljmu.ac.uk](mailto:N.Jannat@2019.ljmu.ac.uk) (N. Jannat), [A.Hussien@ljmu.ac.uk](mailto:A.Hussien@ljmu.ac.uk) (A. Hussien), [B.M.Abdullah@ljmu.ac.uk](mailto:B.M.Abdullah@ljmu.ac.uk) (B. Abdullah), [A.J.Cotgrave@ljmu.ac.uk](mailto:A.J.Cotgrave@ljmu.ac.uk) (A. Cotgrave).

<https://doi.org/10.1016/j.conbuildmat.2020.119346>  
 0950-0618/© 2020 Elsevier Ltd. All rights reserved.